When nanomedicines meet tropical diseases
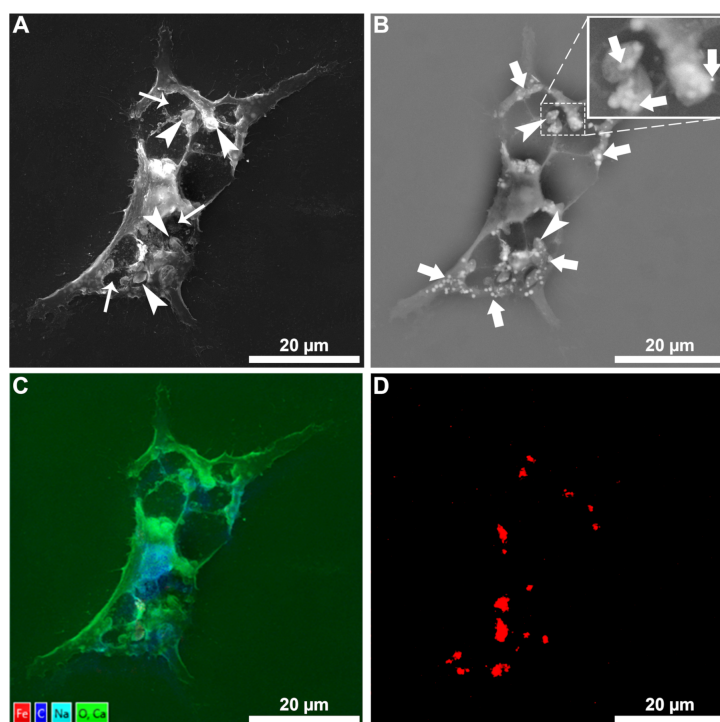
Edited by Eder Lilia Romero, Fabio Rocha Formiga and Katrien Van Bocxlaer

When nanomedicines meet tropical diseases

Eder Lilia Romero[1], Katrien Van Bocxlaer[2] and Fabio Rocha Formiga[*3,4]

Editorial

Address:
[1]Nanomedicine Research and Development Centre (NARD), Science and Technology Department, National University of Quilmes, Roque Saenz Peña 352, B1876 Bernal, Provincia de Buenos Aires, Argentina, [2]Skin Research Centre, Hull York Medical School, York Biomedical Research Institute, University of York, York YO10 5DD, UK, [3]Aggeu Magalhães Institute, Oswaldo Cruz Foundation (FIOCRUZ), 50670-420, Recife, PE, Brazil and [4]Faculty of Medical Sciences, University of Pernambuco (UPE), 52171-011, Recife, PE, Brazil

Email:
Fabio Rocha Formiga[*] - fabio.formiga@fiocruz.br

* Corresponding author

In May 2021, the World Health Assembly from the World Health Organization (WHO) decided to officially recognize January 30th as the World Neglected Tropical Diseases Day. This initiative was done to call the attention of everyone, including health authorities, leaders, and communities to unite, act, and eradicate neglected tropical diseases (NTDs). According to the WHO, NTDs primarily affect the most vulnerable populations, where clean water availability, sanitation, and access to health care are inadequate in low- and middle-income countries of Africa, Asia, and Latin America. These pathologies affect over one billion people worldwide and are responsible for thousands of preventable deaths. Caused mostly by viruses, bacteria, parasites, fungi, and toxins, NTDs can blind, disable, and disfigure people. These diseases can also affect the ability of a person to stay in school, earn a living, or even be accepted by the community due to disease-related stigma.

The WHO has updated the list of NTDs to include leishmaniasis, malaria, sleeping sickness, filariasis, snakebite envenoming, and Chagas disease. In addition, emerging diseases such as dengue, chikungunya, and zika infections are also considered NTDs. Historically, NTDs have long been overlooked in the global health agenda, attracting little attention and low funding. Currently, there are few tools available to diagnose and treat those diseases. However, apart from the symbolism behind the World Neglected Tropical Diseases Day, research initiatives fighting NTDs have been conducted over the last years, paving the way for the development of new programs for prevention, diagnosis, and treatment of NTDs. A number of institutions and research groups have dedicated their notable work to investigating vaccines, diagnostics, and medicines to prevent, diagnose, and treat NTDs.

The field in which nanomaterials are used for diagnosing, monitoring, controlling, preventing, and treating diseases is called "nanomedicine" [1]. Potentially beneficial properties of nanomedicines include enhanced drug solubility, improved bioavailability, targeted drug delivery, longer half-life, and

reduced toxicity. This thematic issue covers pre-clinical research employing chemotherapeutic or prophylactic nanomedicines against NTDs in a concise article collection. Among the articles, an interesting strategy to improve the bioavailability of benzonidazole towards Chagas disease has been presented by Muraca and colleagues, who reported a stable and safe nanostructured lipid formulation with potential effects against *Trypanosoma cruzi* [2]. In turn, Morilla and collaborators presented a critical review on nanomedicines and Chagas disease, highlighting the potential of oral nanocrystals and parenteral nano-immunostimulants to treat this NTD [3].

Moving to leishmaniases, Verçoza et al. evaluated the therapeutic potential of green superparamagnetic iron oxide nanoparticles (SPIONs) for treating cutaneous lesions caused by *Leishmania amazonensis.* The selectivity index for intracellular amastigotes was more than 240 times higher compared to that of current prescribed drugs to treat the disease, making SPIONs strong candidates for a new therapeutic approach against leishmaniasis [4]. Dourado and collaborators, who showed the therapeutic potential of curcumin-loaded nanocarriers, have also focused their review on these vector-borne NTDs [5].

With an emphasis on the treatment of schistosomiasis using nanoparticles, Carvalho and colleagues provided a comprehensive review on the field. Herein, the authors have accessed different databases, finding inorganic and polymeric nanoparticles as the most investigated nanosystems towards schistosomiasis, an acute and chronic parasitic NTD caused by blood-feeding nematodes of the genus *Schistosoma* [6].

Another important contribution to this thematic issue focused on development of nanoemulsions containing plant-based insecticides for vector control. In this work, Duarte and colleagues developed and characterized nanoemulsions encapsulating monoterpenes, which exhibited significant lethality against third-instar *Aedes aegypti* larvae [7]. This warrants further investigation on eco-friendly insecticides to fight *Aedes aegypti*, the primary vector of dengue, zika, and chikungunya.

Overall, this article collection was conceived to be an original literature resource converging nanomedicine and NTDs. All high-quality contributions emphasized the design and applications of nanomaterials as potential solutions for these diseases. We thank all the authors for submitting their articles. Meanwhile, we hope scientists, health authorities, and communities continue to fight against NTDs. And, who knows, maybe we will have a day to celebrate the cure or effective control of these diseases, promoting life quality for vulnerable populations.

Eder Lilia Romero, Katrien Van Bocxlaer and Fabio Rocha Formiga

Bernal, York and Recife, June 2024

Author Contributions

Eder Lilia Romero: conceptualization; writing – review & editing. Katrien Van Bocxlaer: conceptualization; writing – review & editing. Fabio Rocha Formiga: conceptualization; writing – original draft; writing – review & editing.

ORCID® iDs

Fabio Rocha Formiga - https://orcid.org/0000-0003-1553-0533

Data Availability Statement

Data sharing is not applicable as no new data was generated or analyzed in this study.

References

1. Zhao, Q.; Cheng, N.; Sun, X.; Yan, L.; Li, W. *Front. Bioeng. Biotechnol.* **2023**, *11*, 1219054. doi:10.3389/fbioe.2023.1219054
2. Muraca, G.; Ruiz, M. E.; Gambaro, R. C.; Scioli-Montoto, S.; Sbaraglini, M. L.; Padula, G.; Cisneros, J. S.; Chain, C. Y.; Álvarez, V. A.; Huck-Iriart, C.; Castro, G. R.; Piñero, M. B.; Marchetto, M. I.; Alba Soto, C.; Islan, G. A.; Talevi, A. *Beilstein J. Nanotechnol.* **2023**, *14*, 804–818. doi:10.3762/bjnano.14.66
3. Morilla, M. J.; Ghosal, K.; Romero, E. L. *Beilstein J. Nanotechnol.* **2024**, *15*, 333–349. doi:10.3762/bjnano.15.30
4. Verçoza, B. R. F.; Bernardo, R. R.; de Oliveira, L. A. S.; Rodrigues, J. C. F. *Beilstein J. Nanotechnol.* **2023**, *14*, 893–903. doi:10.3762/bjnano.14.73
5. Dourado, D.; Silva Medeiros, T.; do Nascimento Alencar, É.; Matos Sales, E.; Formiga, F. R. *Beilstein J. Nanotechnol.* **2024**, *15*, 37–50. doi:10.3762/bjnano.15.4
6. Carvalho, L.; Sarcinelli, M.; Patrício, B. *Beilstein J. Nanotechnol.* **2024**, *15*, 13–25. doi:10.3762/bjnano.15.2
7. Duarte, J. L.; Di Filippo, L. D.; de Faria Mota Oliveira, A. E. M.; Sábio, R. M.; Marena, G. D.; Bauab, T. M.; Duque, C.; Corbel, V.; Chorilli, M. *Beilstein J. Nanotechnol.* **2024**, *15*, 104–114. doi:10.3762/bjnano.15.10

Nanostructured lipid carriers containing benznidazole: physicochemical, biopharmaceutical and cellular in vitro studies

Giuliana Muraca, María Esperanza Ruiz, Rocío C. Gambaro, Sebastián Scioli-Montoto, María Laura Sbaraglini, Gisel Padula, José Sebastián Cisneros, Cecilia Yamil Chain, Vera A. Álvarez, Cristián Huck-Iriart, Guillermo R. Castro, María Belén Piñero, Matias Ildebrando Marchetto, Catalina Alba Soto, Germán A. Islan[*] and Alan Talevi[*]

Abstract

Chagas disease is a neglected endemic disease prevalent in Latin American countries, affecting around 8 million people. The first-line treatment, benznidazole (BNZ), is effective in the acute stage of the disease but has limited efficacy in the chronic stage, possibly because current treatment regimens do not eradicate transiently dormant *Trypanosoma cruzi* amastigotes. Nanostructured lipid carriers (NLC) appear to be a promising approach for delivering pharmaceutical active ingredients as they can have a positive impact on bioavailability by modifying the absorption, distribution, and elimination of the drug. In this study, BNZ was successfully loaded into nanocarriers composed of myristyl myristate/Crodamol oil/poloxamer 188 prepared by ultrasonication. A stable NLC formulation was obtained, with ≈80% encapsulation efficiency (%EE) and a biphasic drug release profile with an initial burst release followed by a prolonged phase. The hydrodynamic average diameter and zeta potential of NLC obtained by dynamic light scattering were approximately 150 nm and −13 mV, respectively, while spherical and well-distributed nanoparticles were observed by transmission electron microscopy. Fourier-transform infrared spectroscopy, differential scanning calorimetry, thermogravimetric analysis, and small-angle X-ray scattering analyses of the nanoparticles indicated that BNZ might be dispersed in the nanoparticle matrix in an amorphous state. The mean size, zeta potential, polydispersity index, and %EE of the formulation remained stable for at least six months. The hemolytic effect of the nanoparticles was insignificant compared to that of the positive lysis control. The nanoparticle formulation exhibited similar performance in vitro against *T. cruzi* compared to free BNZ. No formulation-related cytotoxic effects were observed on either Vero or CHO cells. Moreover, BNZ showed a 50% reduction in CHO cell

viability at 125 µg/mL, whereas NLC-BNZ and non-loaded NLC did not exert a significant effect on cell viability at the same concentration. These results show potential for the development of new nanomedicines against *T. cruzi*.

Introduction

Chagas disease is a neglected disease endemic to Latin America, affecting around 8 million people and causing 2000 deaths per year, according to the World Health Organization [1]. Currently, this health problem is not restricted to Latin American countries, as it has spread to non-endemic regions such as the United States and Europe [2,3]. It is caused by the hemoflagellate protozoan *Trypanosoma cruzi*, whose life cycle involves transitioning from non-flagellated multiplicative intracellular forms (amastigotes) to blood-circulating non-multiplicative forms (trypomastigotes). It is mainly transmitted by an insect vector of the Triatominae subfamily, although other modes of transmission (blood transfusion, organ transplant, and congenital transmission) have gained importance over the last decades. It is characterized by two stages: acute, and chronic. During the acute stage, which lasts up to two months after infection, the patients might present or mild, nonspecific, or no symptoms. This phase is followed by a chronic stage where parasites can be primarily found inside specific tissues. Decades after infection, signs and symptoms of damage to target organs, mainly the heart, gastrointestinal tract, and brain appear in 20–30% of chronically infected individuals [1,4].

Currently, two drugs have been approved for the treatment of Chagas disease: benznidazole (BNZ) and nifurtimox. The first-line treatment, BNZ, is a nitroimidazole that generates radical intermediates via the reduction of its nitro group, which covalently bind to macromolecules under aerobic and anaerobic conditions [5]. Cure rates are high when BNZ is administered during the acute phase [6]; however, in the chronic stage the cure rate is estimated to be less than 10% [7]. Some authors differ about this percentage owing to the variability in sensibility of the tests that are used to establish cure criteria [8,9]. BNZ is associated with a variety of adverse reactions including allergic dermatitis, hypersensitivity syndrome, gastric pain, anorexia, insomnia, vomiting, which ultimately lead to withdrawal in 12–18% of the patients [10]. Additionally, the BENEFIT (Benznidazole Evaluation for Interrupting Trypanosomiasis) trial could not prove that the standard treatment with BNZ can prevent disease progression [11].

BNZ has been classified as a class IV drug (low solubility, low permeability) in the Biopharmaceutics Classification System (BCS) [12]. It has an apparent volume of distribution (V_d) of 0.56 L/kg, and reactive products of its metabolism [13]. Such V_d and low permeability values across biological barriers could result in difficulties for BNZ to reach intracellular amastigotes.

The encapsulation of BNZ within nanoscale pharmaceutical carriers has been proposed as a strategy to reduce toxicity and improve efficacy [13]. Incorporation of drugs into nanoscale vehicles could result in changes in its absorption, distribution, metabolism, and excretion, which in turn could translate into improved efficacy and diminished BNZ toxicity. For example, BNZ-loaded nanoparticles could accumulate in the site of inflammation delivering the drug in the surroundings of their molecular target. In addition, nanocarriers may pass through the cell membrane via endocytosis to avoid BNZ efflux via the P-glycoprotein efflux pump [14-16], thus delivering the drug more efficiently. Many developments have been made in the past years resulting in lipid formulations such as liposomes, solid lipid nanoparticles (SLNs), and nanoemulsions, which increased the apparent solubility of BNZ and its efficacy against parasites [17]. Remarkably, oil-in-water nanoemulsions improved the trypanocidal activity against trypomastigotes compared to that of the free drug [18]. Among the aforementioned nanosystems, SLNs have recently gained special attention owing to their biocompatibility properties, biodegradability, relatively easy surface and composition modification, and efficacy in loading and delivering active principles [19]. SLNs comprise a lipid core, solid at 25 °C, stabilized by steric effects with a surfactant. The addition of small amounts of a liquid lipid at 25 °C leads to the improvement of SLNs in terms of sustained drug release and encapsulation efficiency (EE%), enabling the development of nanostructured lipid carriers (NLC) [20].

Here, we resort to NLC encapsulating BNZ, describing the preparation, physicochemical and biopharmaceutical characterization, and in vitro evaluation against *T. cruzi* intracellular and blood circulating forms. Interestingly, our formulation achieves a higher cumulative release and considerable higher activity against amastigotes compared to previously reported BNZ-loaded NLCs. Moreover, we report the dose-response intrinsic activity of myristyl myristate, a relatively common constituent of NLCs, against *T. cruzi*, which might be of future interest to other researchers working in the field.

Results and Discussion
Formulation and physicochemical characterization of NLC-BNZ
Nanoparticle formulations were prepared by the ultrasonication method and named as NLC-BNZ or NLC-VEHICLE, in that

order, depending on whether they contained BNZ or not. Stable homogeneous formulations were prepared. The encapsulation efficiency of NLC-BNZ was considerably high for the lipid formulations, reaching approx. 80%. The theoretical drug loading was 2.5%. Our results were in concordance with the encapsulation results of a previous study by Vinuesa et al., involving different types of nanoparticles and BNZ, including SLN and NLC [21]. The NLC-BNZ formulation was analyzed using transmission electron microscopy (TEM) to confirm the presence of nanoparticles showing a spherical morphology and a narrow distribution of sizes (Figure 1). Image analysis through ImageJ [22] software showed a mean particle size of 150 ± 13 nm.

Accordingly, the hydrodynamic diameter of the nanoparticles measured by dynamic light scattering (DLS) was in the 100–200 nm range (≈150 nm), with a moderate distribution of sizes as indicated by a polydispersity index (PdI) of 0.204. The zeta potential (ζ) was measured by Doppler anemometry, and it was found to be around −13 mV.

Differential scanning calorimetry (DSC) and thermogravimetric analysis (TGA) were performed to determine the thermal stability and melting/recrystallization processes of the components after drug encapsulation. Overlaid DSC thermograms are shown in Figure 2, whereas the melting temperature (T_m), the enthalpy of fusion (ΔH_f), and crystallinity index (CI) are presented in Table 1. Whereas BNZ showed an endothermic peak at its melting point (191.2 °C) [23], the formulation

showed two endothermic peaks in the range of 40–50 °C, which could be referred to the melting points of the lipid and the surfactant, respectively. This suggests that no other endothermic changes occur to the formulation constituents or its load during the high-energy sonication procedure. A peak matching the phase transition peak of BNZ did not appear in the nanoparticle thermogram, indicating that BNZ was dispersed within the lipid matrix [24]. Correlating with the lower enthalpy of fusion, the CI (%) value of the nanoparticles was lower than that of the bulk myristyl myristate. Lipid molecules could be less ordered in the nanoparticles than in the bulk material, considering the disarrangement caused by the incorporation of the drug and the surfactant. For that reason, it might require less energy to melt in comparison to the pure crystalline substance [25].

Thermogravimetric curves of myristyl myristate, poloxamer 188, and BNZ showed one thermal degradation process, whereas NLC-BNZ and NLC-VEHICLE presented two events (Figure 3). That was also observed in the derivative curves. The weight loss process for the lipid started at 180 °C and finished at 320 °C. The poloxamer 188 thermogram showed a decomposition process starting at 300 °C and ending at 410 °C, and BNZ degradation occurred in the 190–300 °C range. Considering these processes, nanoparticle thermal behavior might be attributed first to lipid degradation, and second to poloxamer weight loss.

The attenuated total reflection Fourier-transform infrared spectroscopy (ATR-FTIR) technique was used to analyze the nano-
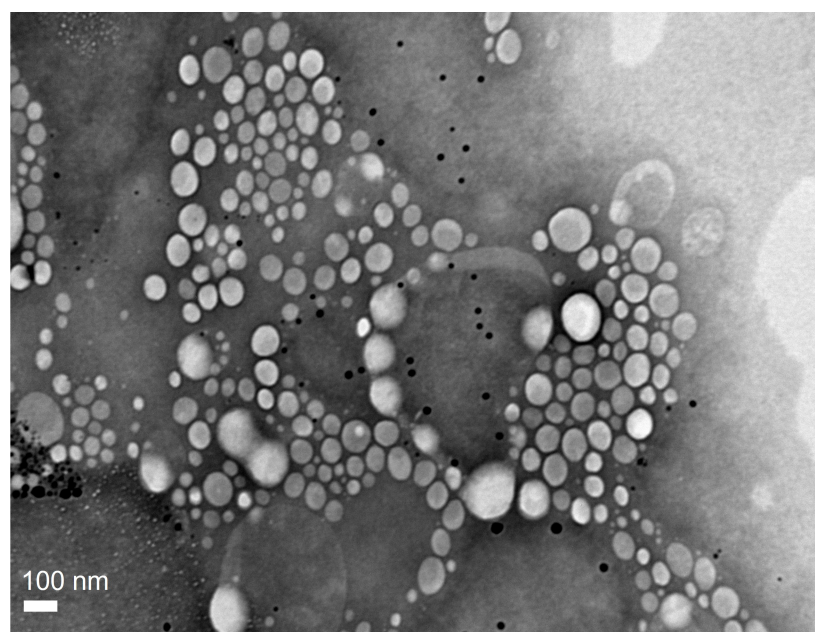
Figure 1: TEM image of NLC-BNZ.
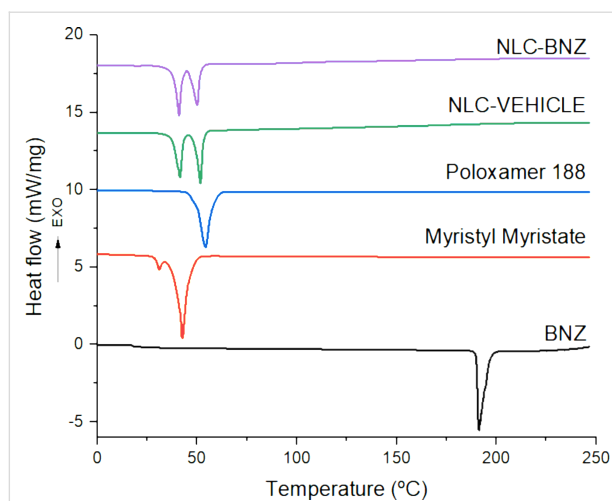
Figure 2: DSC thermograms of BNZ, myristyl myristate, poloxamer 188, NLC VEHICLE, and NLC-BNZ.

Table 1: Thermal properties of benznidazole (BNZ), myristyl myristate, poloxamer 188, and nanoparticles (NLC-VEHICLE and NLC-BNZ). Abbreviations: T_m, melting temperature; ΔH_f, fusion enthalpy; CI (%), crystallinity index.

Sample	T_m (°C)	ΔH_f (j/g)	CI (%)
BNZ	191.2	142.3	100
myristyl myristate	42.9	239.4	100
poloxamer 188	54.2	148.8	100
NLC-VEHICLE	41.4–51.7	61.1	12.7
NLC-BNZ	40.9–50.0	59.4	12.4

amide (1500–1400 cm^{-1} is also the absorption range of the C=C in the benzyl group), 1357 cm^{-1} to the symmetric vibration of R–NO$_2$, and 1141 cm^{-1} to C–N in the imidazole ring [26]. Myristyl myristate displayed peaks at 2913 and 2848 cm^{-1} corresponding to C–H of alkane, 1731–1184 cm^{-1} to C=O and C–O stretching of ester groups, respectively. The peak at 1467 cm^{-1} was associated with the deforming vibrations of the C–H of alkanes [27]. The characteristic peaks of poloxamer 188 were at 3600 cm^{-1} relative to the O–H stretching, the intense peak at 2873 cm^{-1} corresponding to C–H stretching of alkanes, another intense peak at 1105 cm^{-1} to the symmetric stretching of C–O–C, and 964–833 cm^{-1} to asymmetrical and symmetrical stretching of C–C–O, respectively [28]. The NLC-BNZ spectra showed myristyl myristate and poloxamer characteristic peaks (overlapping of the most intense peaks in the 3000 cm^{-1} region – 2910 cm^{-1}, 2883 cm^{-1}, and 2854 cm^{-1} – due to the presence of the lipid and surfactant). In contrast, the spectra did
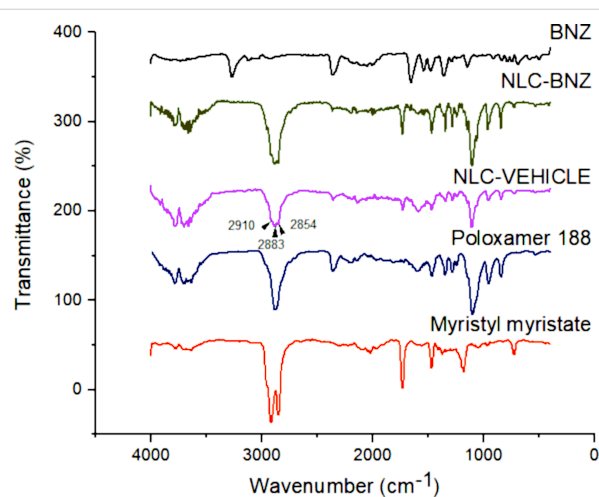
Figure 4: ATR-FTIR spectra of BNZ, myristyl myristate, poloxamer 188, NLC VEHICLE, and NLC-BNZ.

particle surface composition and determine the possible interactions among the formulation components (Figure 4). The BNZ spectrum presented its characteristic peaks at 3264 cm^{-1} corresponding to N–H in the secondary amide bond, 1652 cm^{-1} to C=O in the amide, 1523–1400 cm^{-1} to N–H flexion in the

Figure 3: Thermogravimetric (A) and derivative thermogravimetric (B) curves of BNZ, myristyl myristate, poloxamer 188, NLC-VEHICLE, and NLC-BNZ.

not show peaks that could be linked to BNZ, suggesting that drug molecules were not on the nanoparticle surface but rather dispersed into the lipid matrix [24].

Structural analysis was performed by selecting different angular regions from the small-angle X-ray scattering (SAXS) and wide-angle X-ray scattering (WAXS) patterns. The WAXS patterns (Figure 5) showed contributions of diffraction peaks from BNZ, myristyl myristate, and NLC. The nanostructured lipid carriers showed contributions from both the isolated myristyl myristate and additional Bragg peaks at 19.1° and 23.3° corresponding to the copolymer. This indicates that there was phase segregation, most likely a core–shell structure with the lipidic phase inside and the hydrophilic part of the copolymer in the outer part of the NLC. Myristyl myristate major peak positions expressed in terms of $d_{spacing}$ were 4.1 and 3.8 Å, corresponding to a family of the β' polymorph [29] and did not change after NLC synthesis or BNZ addition. Furthermore, there were no contributions from the crystalline phase of BNZ within NLC because of its small quantity or to dissolution inside the NLC.

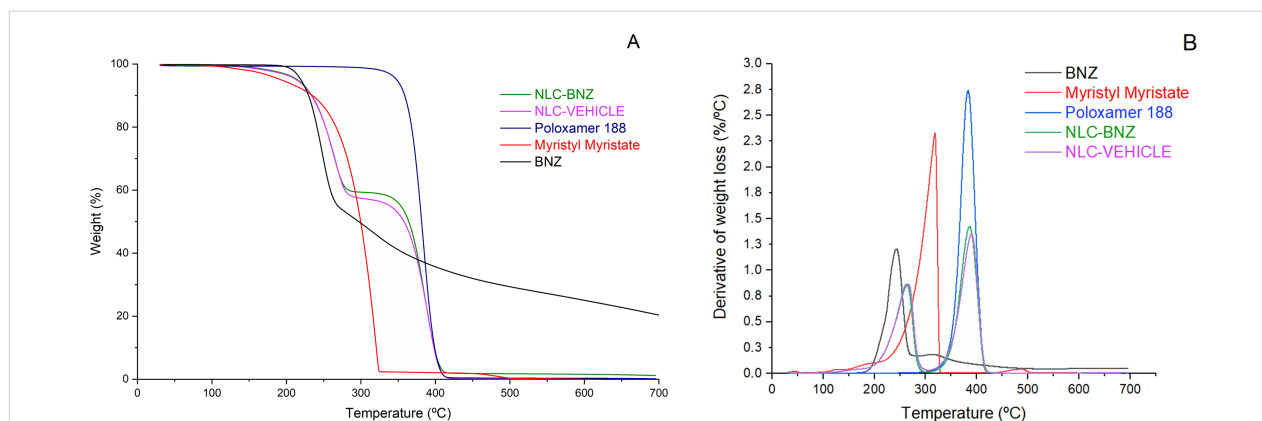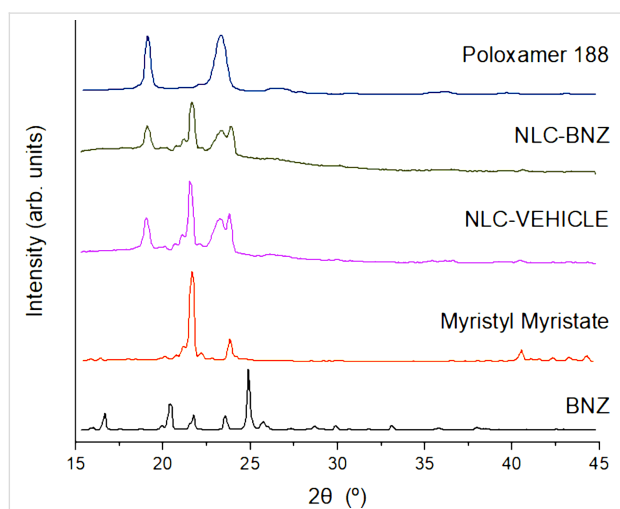**Figure 5:** WAXS patterns for BNZ, myristyl myristate, poloxamer 188, NLC-VEHICLE, and NLC-BNZ.

The long period Bragg diffraction peaks for Myristyl myristate could be observed in SAXS patterns at the *q* range between 0.15 and 0.2 Å^{-1} (Figure 6). Bare myristyl myristate confirmed the presence of a β' polymorph with long period $d_{spacing}$ of 3.99 (001) and 3.47 nm (002), while in the NLC only the 3.47 nm of $d_{spacing}$ peak remains. Also, in the NLC systems, the main Bragg peak was wider, attributed to a nanosized crystal effect where the estimated crystallite average sizes were 94 ± 5 nm and 101 ± 5 nm for NLC-VEHICLE and NLC-BNZ, respectively, using the Scherrer approximation. However, a broadening of the lower part of the main peak in the NLC-BNZ samples sug-
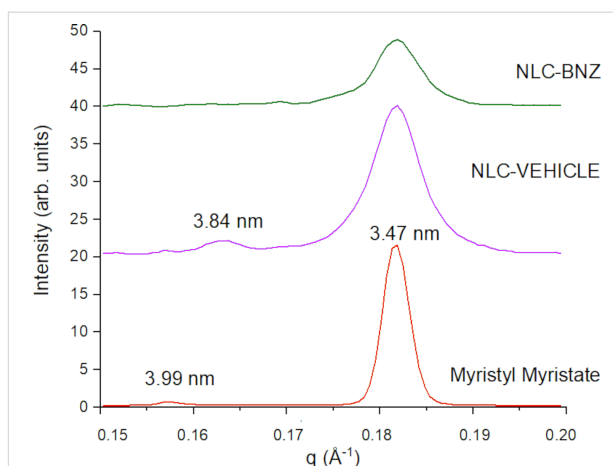
Figure 6: SAXS patterns for samples with myristyl myristate in their composition.

gests defects in the structure, probably due to the inclusion of BNZ in the formulation. At smaller angles, the copolymer on the surface exhibited a lamellar-like structure [30]. The Lorentz/Kratky plot (q^2I vs q) is shown in Figure 7, where the peaks of NLC and NLC-BNZ remained at the same position, independently of the presence of the BNZ load. The linear correlation function was obtained by using the following transformation (Equation 1) [31,32]:

$$K(z) = \frac{\int_0^\infty I_{norm}(q) q^2 \cos(qz) \, dq}{\int_0^\infty I_{norm}(q) q^2 \, dq} \tag{1}$$

where I_{norm} is the normalized intensity after removing the myristyl myristate (i.e., MM) contribution: $I_{norm} = I_{NLC}(q) - I_{background} - c(I_{MM}(q) - I_{background})$, c being a constant or weighted proportionality between phases. From this transformation the lamellar period obtained from the first maximum of the oscillation was 12.6 nm for both systems (Figure 7). In contrast with amphiphilic low-weight loading, BNZ is a lipophilic molecule that did not change the structure of the copolymer. Thus, it is proposed to be dissolved in the core of the lipidic nanoparticle.

Drug release and physical stability

The release profiles (Figure 8) showed that 78% of the free drug was dissolved in the first 15 min of the experiment. In contrast, during the first 15 min only about 12% of the drug was released from the NLC formulation. An initial burst release was observed, followed by a sustained release. This phenomenon could be explained in part by considering the presence of free drug molecules in the formulation (around 20% of the initial drug load) and in part by the release of drug molecules located
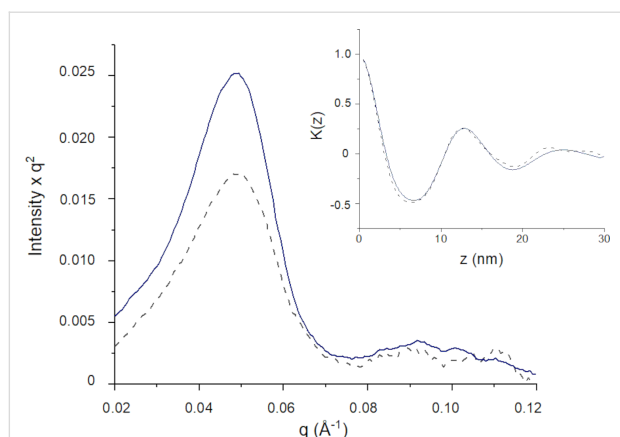
Figure 7: Lorentz/Kratky plot for SAXS patterns of NLC-VEHICLE (continuous line) and NLC-BNZ (dashed line). The inset corresponds to the linear correlation transformation for lamellar systems.

near the surface of the NLC, which rapidly diffuse out of the vehicle. The slow increase of the drug concentration in the release medium observed after the initial stage could be attributed to the gradual release of drug molecules from the matrix core, where the drug is mainly located according to X-ray diffraction (XRD) results [33]. Remarkably, although our NLC possess a comparatively lower drug load, the maximal accumulated drug release is higher than that of similar systems previously reported [21].

Figure 8: In vitro release profile of free BNZ and NLC-BNZ for 24 hours. The inset graph shows the release profiles during the first three hours.

The in vitro release data were fitted to different mathematical models. The model that best adjusted the data was the Korsmeyer–Peppas model followed by a first-order model (Supporting Information File 1, Table S1). The Korsmeyer–Peppas model, also called power law, was initially used

to describe drug release in polymeric systems where the two predominant mechanisms were relaxation of the polymer chains and diffusio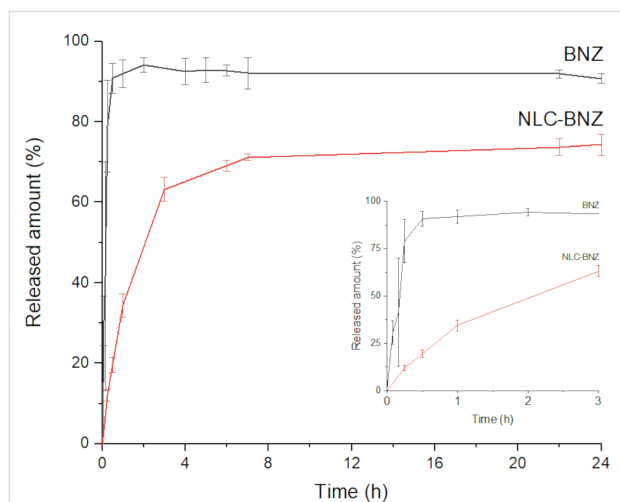n. In this model (Equation 2), M_t/M_∞ is the fraction dissolved, K is a constant that incorporates structural and geometrical information, and the exponent n is the diffusional or transport exponent, that provides information about the release mechanism. However, it can also be viewed as a generalization for the explanation of two different drug release mechanisms that could coexist [34]. The mechanism that dominates the release can be inferred through the value of the release exponent n. For spherical systems, n will take a value of 0.43 for drug release governed by Fickian diffusion, a value of 1 for zero-order release, and intermediate values for intermediate behavior, often regarded as anomalous transport. In our case, the estimated value of n was 0.56, suggesting mixed release mechanisms at play with a strong contribution of diffusion. As in our case there is no polymer relaxation involved, it may be hypothesized that the burst effect could be slightly affecting the global kinetics of the process [35]. Although this description has its limitations, it has been widely used to describe drug release from similar lipidic formulations [35-38].

$$\frac{M_t}{M_\infty} = Kt^n \qquad (2)$$

The mean particle size, PdI, zeta potential, and encapsulation efficiency were selected as parameters to follow the physical stability of the nanoparticle dispersion for six months under the selected storage conditions (refrigerator at 4 °C) (Figure 9). Based on these results, the formulation could be stored at 4 °C for at least three months without losing its initial properties in terms of size; polydispersity and encapsulation efficiency values remained unaltered during the storage period, and the zeta potential parameter started at −10 mV and ended up at −15 mV after six months. Dynamic light scattering analysis of the formulations revealed nanoparticles with a hydrodynamic diameter in the 100−200 nm range (≈50 nm) starting at 146 nm and slightly increasing in the third month up to 155 nm. The Z-average parameter was chosen to report the nanoparticles size. The size values were consistent with the TEM image analysis. The zeta potential (ζ) was measured by Doppler anemometry and operated as a report of the formulation surface characteristics. The surface charges required to achieve a good dispersion of nanoparticles stabilized by electrostatic repulsion are around ±30 mV [39]. The ζ value of our formulation was ≈14 mV. Although this value is not optimal for stabilization by electrostatic repulsion, it still contributes with a positive aspect, as high-negative ζ values may impede cellular uptake [40]. On the other hand, it was observed that the nanoparticulated systems remained stable after six months with no precipitation. This suggests that in this case the stabilization is not achieved
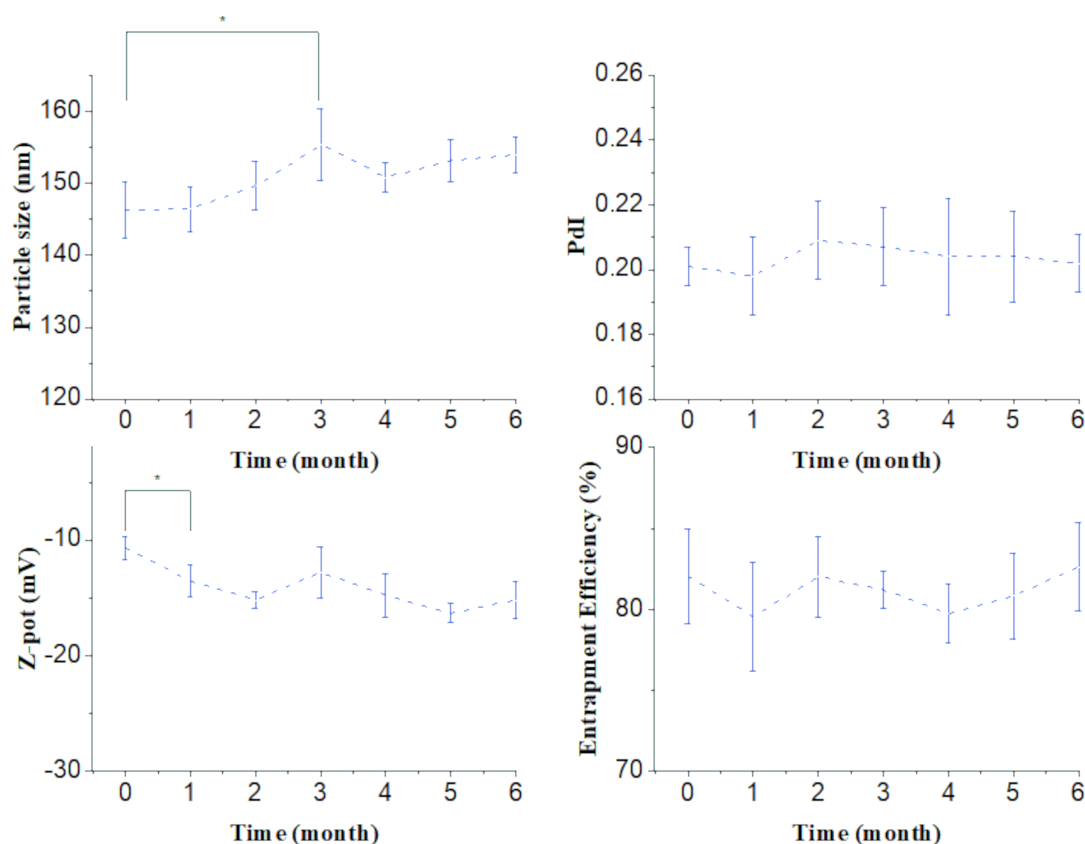
Figure 9: Followed-up of relevant physical parameters of the formulation for up to six months to test its stability under the selected storage conditions (refrigerator at 4 °C), * = *p* < 0.05.

by means of surface charge alone, but also by the steric repulsion after adding a non-ionic surfactant [41].

Cytotoxicity and hemolytic activity

Cytotoxicity assays using the tetrazolium 3-[4,5-dimethyl-thiazol-2-yl]-2,5-diphenyltetrazolium bromide salt method (MTT) showed that Chinese hamster ovary cells (CHO) viability was affected by BNZ concentration in a dose-dependent manner (Figure 10). Interestingly, the cell viability for NLC-VEHICLE or NLC-BNZ at the same tested concentrations of free BNZ resulted in values above 80% in all cases, suggesting a decreased cytotoxic effect. That decrease in toxicity generated by NLC-BNZ, in comparison with free BNZ, could be attributed to the release profile of BNZ from NLC, exposing cells to lower doses of BNZ during the first stages of cellular division. This is a remarkable result, as toxic effects of BZN are a major cause of treatment discontinuation in the clinical setting [42]. Additionally, cytotoxicity was evaluated in the Vero cell line by flow cytometry, where the percentage of dead cells labeled with propidium iodide (PI, Supporting Information File 1, Figure S2) was measured. Neither the drug-loaded or unloaded NLCs elicited significant toxicity in Vero cells.
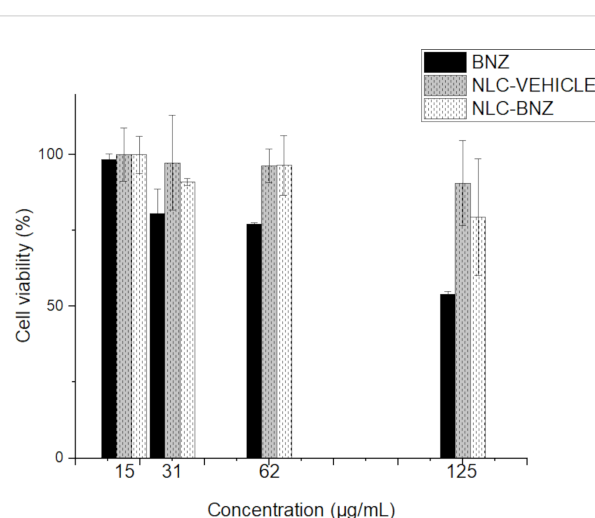
Figure 10: Cell cytotoxicity in CHO cells treated with free BNZ, NLC-VEHICLE, and NLC-BNZ.

As it is common to parenterally administer nanoparticle formulations, it is of interest to study the potential toxicity of pharmaceutical nanocarriers in blood cells. Most of the published

papers evaluated the hemolytic activity (HA) of nanoparticles after 2, 3, or 5 h of incubation [43-45]. The standard methods to test hemolytic activity of nanoparticles (ISO/TR 7406 or ASTM E2524-08 standard) established that biomaterials that induce a critical hemolytic ratio of <5% can be considered safe for biological applications [46]. In our study, it was observed no hemolytic effects for BNZ, NLC-VEHICLE, and NLC-BNZ at different concentrations after 3 and 24 h of incubation (data not shown). However, some hemolytic activity was observed for NLC-VEHICLE and NLC-BNZ after 48 h of incubation (Figure 11). Despite NLC-BNZ showed 4.8% HA at the highest concentration, the formulation could still be considered safe according to the regulations. In fact, hemolytic activity could be caused by several reasons, including the ageing of the blood sample after 48 h of incubation with the concomitant release of hemoglobin, but also by the presence of surfactants that could destabilized the erythrocyte membrane [47]. On the other hand, the differences between NLC-VEHICLE and NLC-BNZ, the latter exhibiting a higher HA, could be explained by adding the HA of the free drug to the effect of the vehicle on erythrocytes.

More studies would be necessary to investigate the effect of the composition, size, or porosity of these nanoparticles after a long term exposure to blood samples as was described for other type of nanoparticles [45]. Our results suggest that the reported NLC-BNZ formulations are hemocompatible [43].

In vitro antiparasitic activity

As shown in Figure 12A, free BNZ displayed a clear dose-dependent effect on *T. cruzi* trypomastigotes (with an EC_{50} of 6.07 μM), whereas the NLC-BNZ and NLC-VEHICLE also exhibited a dose-response behavior despite comparatively large variability across replicates. While for free BNZ the estimated EC_{50} value was 6.07 μM with similar reported values (6.04 μM [48]) for the same parasite classification (TcI), the NLC-BNZ presented a full trypanocidal effect at concentrations higher than 5 μM (10 μM). A similar observation was found for the empty particles (NLC-VEHICLE) suggesting that the formulation itself possesses intrinsic toxicity on *T. cruzi* trypomastigotes. A separate assay of the individual constituents of the formulations was thus performed, demonstrating that myristyl myristate, at a

Figure 11: Hemolytic activity (%) of BNZ, NLC-VEHICLE, and NLC-BNZ at three different concentrations. * = *p* < 0.05.

Figure 12: Dose-response effect of BNZ, NLC-BNZ, and NLC-VEHICLE (empty, non-loaded with BNZ) on *T. cruzi* trypomastigotes (A) and amastigotes (B). For NLC-VEHICLE, the assayed concentrations of empty NLC correspond to those that would contain the indicated concentration of BNZ. Dunnet's test was performed to identify significant differences against the control group. *$p < 0.05$, **$p < 0.01$.

relatively low concentration, has a negative effect on parasite viability (dose-response studies for myristyl myristate against amastigotes are shown in Supporting Information File 1). This may imply that myristyl myristate cannot be considered, in our case, as a pharmacol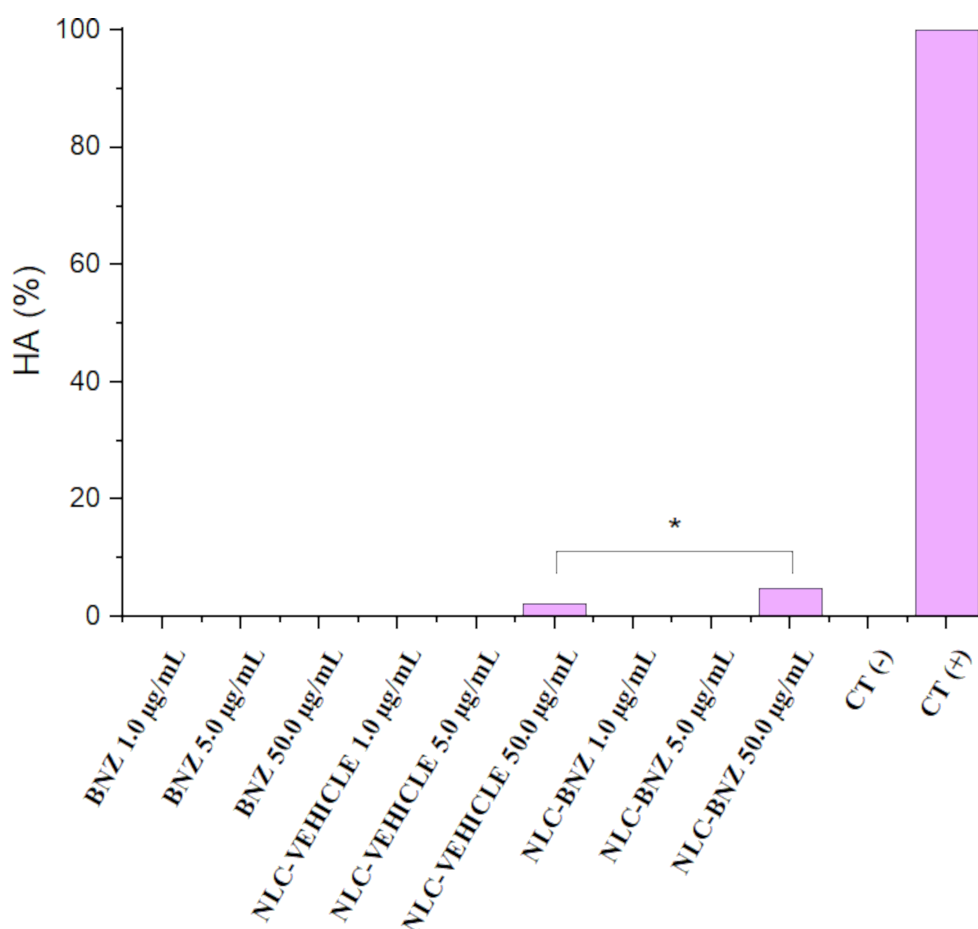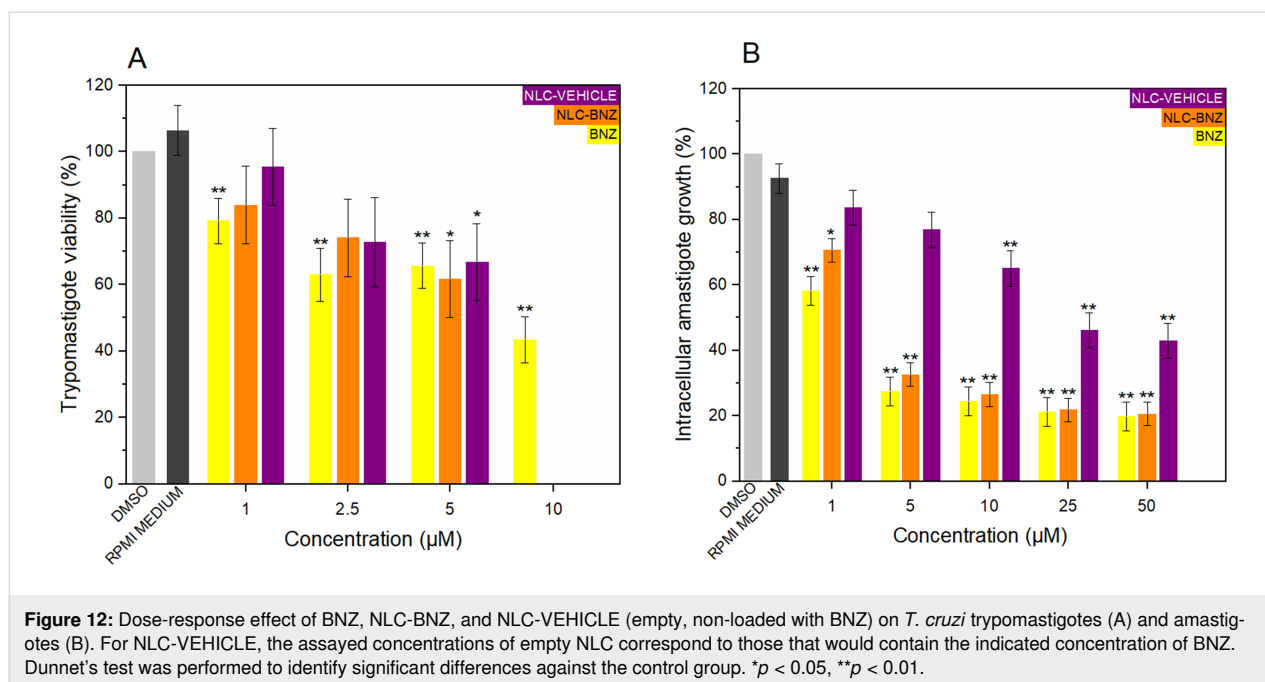ogically inert constituent in our formulation. Instead, it should be considered as a pharmaceutical active ingredient based on its intrinsic effects against *T. cruzi*.

The dose-response effects of BNZ, NLC-VEHICLE, and NLC-BNZ on *T. cruzi* amastigotes were also evaluated (Figure 12B), and the corresponding EC_{50} were calculated. Benznidazole and NLC-BNZ presented inhibition of the intracellular growth of the parasites even at the lowest concentration, with no significant differences observed between the treatments. Benznidazole and NLC-BNZ EC_{50} values were 3.15 and 3.33 μM, respectively. In agreement with the in vitro trypanocidal assay, NLC-VEHICLE also displayed intrinsic anti-amastigote activity with an EC_{50} value of 10.29 μM. This was unexpected, although not necessarily a negative outcome, having in mind that our formulation displayed reduced cytotoxicity against mammal cells. Isolated myristyl myristate lipid was also tested against amastigotes, showing a reduced amastigote density at effective concentrations (Supporting Information File 1, Figure S1). Neither P188 nor GTCC-LQ displayed any effect against trypomastigotes or amastigotes up to 50 μM. Of note, the more efficacious NLC encapsulating BNZ previously reported in the literature [21] had an EC_{50} against amastigotes of 17.6 μM. The higher efficacy of our system may be explained by a higher maximal drug release and/or by the intrinsic activity of myristyl myristate, which adds to that of BNZ.

A hypothesis about the intrinsic toxicity of our nanoscale vehicle on *T. cruzi* may be linked to a modification of glycosylphosphatidylinositols (GPIs). Glycosylphosphatidylinositols are the main anchor complexes used by protozoans to bind to cell surface proteins. It covalently attaches to the C terminus of a protein connecting it to the outer leaflet of the lipid bilayer [49]. *Trypanosoma brucei* predominant membrane protein variant surface glycoprotein (VSG), which is involved in parasite host immune system evasion, is anchored by a GPI that requires myristate for its synthesis. Analogs of myristate have shown toxicity towards the parasite [50]. *T. cruzi* trypomastigotes connect mucin (a surface molecule implicated in parasite virulence) to the membrane through a GPI which is synthesized exclusively with a C16 fatty acid [51], though a C14 fatty acid incorporation could be toxic to the parasite. Experiments in *T. brucei* indicated that the specificity of fatty acid incorporation depends on chain length [52]. The lipid in our formulation is an ester of fatty acids that could hypothetically interrupt the anchoring of mucin to the lipid bilayer in *T. cruzi,* thus rendering the parasites non-viable. However, further studies are required to test this hypothesis.

Conclusion

Among the spectra of nanoformulations encapsulating BNZ that exist to date, the nanoparticles presented in this work might be considered a novelty in terms of the lipid and manufacturing technique of choice. We achieve physical stability for at least six months with acceptable particle size, PdI, and EE%. Complementary to these results, TEM images showed a spherical configuration. Thermal and crystallographic experiments indi-

cated that BNZ was dispersed into the lipid matrix. The formulations showed a sustained drug release profile for 24 h, achieving a maximal accumulated release above 74% during 24 h. The release profile was adequately fitted to the Korsmeyer–Peppas model with an estimated release exponent of 0.56, suggesting a mixed mechanism of release with a dominant Fickian behavior. In vitro experiments on *T. cruzi* trypomastigotes and amastigotes showed similar performances against the intracellular form of the parasite when comparing encapsulated and free BNZ. Surprisingly, the empty nanoparticles exhibited activity against the parasite, which was later attributed to one of the constituents of the formulation, myristyl myristate. This may explain why our formulations exhibited increased performance against *T. cruzi* compared with other previously reported BNZ-loaded NLC. It would be interesting to study the effect of other lipids on the parasite to optimize the efficacy of the formulations based on a potential additive or synergistic effect of BNZ and the formulation itself. Remarkably, the cytotoxicity effect on host cells was lower for the BNZ-loaded nanoparticles compared to that of the free drug, showing a possible benefit for the use of our formulation.

Experimental
Materials
Benznidazole (Lot #MKCD5602, purity ≥ 97%) and Kolliphor®P188 (poloxamer 188) were purchased from Sigma-Aldrich. Myristyl myristate (Crodamol™ MM, melting range = 36–40 °C), and the oil (Crodamol™ GTCC-LQ, a mixture of fully saturated triglycerides, melting point = −5 °C) were kindly donated by Croda Argentina. All reagents used in the preparation and analysis of the formulations were of analytical grade and were obtained from different commercially available sources.

Formulation of benznidazole-loaded nanostructured lipid carriers
BNZ-loaded NLCs were obtained via ultrasonication as previously described in Scioli-Montoto et al. (2022) [53]. Solid myristyl myristate (2% w/v, 400 mg) was melted in a water bath at 60–70 °C. The oil (40 μL) was added to the melted lipid phase simultaneously with BNZ (10 mg). The aqueous phase was prepared by dissolving 600 mg (3% w/v) of poloxamer 188 (poly(ethylene glycol)-block-poly(propylene glycol)block-poly(ethylene glycol)) in 20 mL of ultrapure water (Milli-Q®, Millipore, Ma., USA) and was preheated at the same temperature as the melted lipid in the water bath. After 30 min of thermostatization, the aqueous solution was poured over the lipid phase, and ultrasonication was carried out for 20 min at an 80% amplitude using an ultrasonic processor (130 Watts, Cole-Parmer, USA) equipped with a 6 mm titanium tip. After the sonication process, NLC-BNZ were obtained by leaving the hot

suspension to cool to room temperature. The remaining volume was then measured.

Measurement of the encapsulation efficiency
Concentration of the free drug in the dispersion medium was measured to calculate the encapsulation efficiency (EE%). For this, 500 μL of the formulation was placed in Microcon® centrifugation filters (MWCO = 10000, Merck Millipore, Billerica, MA, USA) and centrifuged at 10000 rpm for 15 min. The amount of BNZ was estimated by performing a high-performance liquid chromatography (HPLC) analysis of the filtrate. Considering the initial amount of BNZ added to the formulation, the EE% was calculated as follows:

$$ EE\left(\%\right) = \frac{M_0 - \left(C_{\text{free}} \cdot V_{\text{f}}\right)}{M_0} \times 100 \qquad (3) $$

where M_0 is the initial amount of BNZ added to the formulation, C_{free} is the drug concentration of the filtrate (i.e., the free drug concentration) in μg/mL, and V_{f} is the volume after ultrasonication (mL).

The theoretical drug loading (DL%) was calculated as follows:

$$ \text{DL}\left(\%\right) = \frac{\text{Mass of drug incorporated}\ \left(\text{mg}\right)}{\text{Lipid mass}\ \left(\text{mg}\right)} \times 100 \qquad (4) $$

HPLC analysis of benznidazole
Chromatographic separation was achieved by HPLC (Gilson SAS, Villiers-Le-Bel, France) via UV detection. A Platinum EPS C8 (150 mm × 4.6 mm, 5 μm, Grace™, Columbia, MD, USA) column was used; the mobile phase consisted of a mixture of methanol and 0.02% phosphoric acid solution (60:40) for a final pH of 2.5. The system was operated isocratically at a 1.0 mL/min flow rate and the detection was performed at 324 nm. The volume of injection was 20 μL.

In vitro benznidazole release assay
The release of BNZ from the nanoparticles was performed in a rotating paddle apparatus (Vision Classic 6, Hanson Research, Chatsworth, CA, USA) at 75 rpm using 500 mL of KH_2PO_4 buffer (pH 6.8) as the dissolution medium. The bath temperature was set at 37.0 ± 0.5 °C. A volume of 5 mL of each formulation was placed in a pre-hydrated dialysis membrane (MWCO 10 kDa) and submerged into the dissolution vessels. A solution of free BNZ at the same concentration was used as control. At 0, 5, 10, 15, and 30 min, and at 1, 2, 3, 4, 5, 6, 7, and 24 h, 1 mL

of the dissolution medium was taken from the vessel. Samples were analyzed by HPLC as described above. Experiments were performed in triplicate and the mean values were used for data analysis. The data were fitted to mathematical models of drug release (i.e., First order, Hopfenberg, Baker–Lonsdale, Korsmeyer–Peppas, and Hixon Crowell) via the DDSolver complement developed by Zhang et al. and available for Excel® [54]. The model that best fitted the data according to the goodness-of-fit measures (R^2, R^2-adj, MSE, and AIC) was chosen.

Particle size, zeta potential and polydispersion index

Nano ZS Zetasizer (Malvern Instruments Corp, Worcestershire, UK) was used to measure particle size distribution and mean diameter by DLS at 25 °C in polystyrene cuvettes with a thickness of 10 mm. The zeta potential was determined by Doppler anemometry using the previously described equipment. As an estimation of the distribution of particle sizes, the polydispersion index was determined. All experiments were carried out in triplicate, except for the particle size estimation, which was measured six times.

Physical stability

The mean particle size, PdI, zeta potential, and encapsulation efficiency were measured to assess the physical stability of the nanoparticle dispersion during storage at 4 °C protected from light. Physical parameters (e.g., particle size, PdI, zeta potential) were measured by DLS and EE% was measured by HPLC, once a month, during a six-month period.

Differential scanning calorimetry analysis

Thermal analysis of BNZ, myristyl myristate, poloxamer 188, and NLC-BNZ was performed by differential scanning calorimetry (DSC Q2000, TA Instruments, New Castle, DE, USA) under an inert atmosphere of dry nitrogen (50 mL·min^{-1}). A standard aluminum pan containing approximately 5 mg of the dry sample after freeze drying the formulations was used. Scans were run in the range from 0 to 250 °C at a heating rate of 10 °C/min.

The degree of crystallinity (% crystallinity index, CI) was calculated using the following equation [55]:

$$\mathrm{CI}\left(\%\right) = \frac{\Delta H_{\mathrm{NLC\ aqueous\ dispersion}}}{\Delta H_{\mathrm{bulk\ material}} \times \mathrm{Concentration}_{\mathrm{lipid\ phase}}} \times 100 \quad (5)$$

where ΔH_{NLC} and $\Delta H_{\mathrm{bulk\ material}}$ are the melting enthalpies (J·g^{-1}) of the NLC dispersion and the bulk lipid, respectively. The concentration of the lipid phase was 2%.

Thermogravimetric analysis

Thermogravimetric analysis was performed to assess the thermal stability of BNZ, myristyl myristate, poloxamer 188, and NLC-BNZ on a TGA Q500 apparatus (TA Instruments, New Castle, DE, USA). Freeze dried formulations of approximately 10 mg were accurately weighed in a platinum pan. Measurements were performed from room temperature to 600 °C at a heating rate of 10 °C/min under nitrogen atmosphere to avoid thermo-oxidative degradation.

Attenuated total reflection Fourier-transform infrared spectroscopy

Fourier-transform infrared spectroscopy spectra were obtained. The attenuated total reflection mode was used to record the spectra over the range of 400–4000 cm^{-1} at a resolution of 2 cm^{-1}.

Transmission electron microscopy

Transmission electron microscopy images were captured using a Jeol-1200 EX II-TEM microscope (Jeol, MA, USA). A drop (10 μL) of the nanoparticle dispersion previously diluted (1:10) with ultrapure water was spread onto a collodion-coated Cu grid (400 mesh). Excess liquid was drained with filter paper. A drop of phosphotungstic acid was added to the dispersion for contrast enhancement.

X-ray diffraction structural analysis

Small angle X-ray scattering/wide angle X-ray scattering measurements were performed using a XEUSS 2.0 equipment (XENOCS, France). Patterns were registered with two synchronous 2D photon-counting pixel X-ray detectors for SAXS Pilatus 200k (DECTRIS, Switzerland), and a Pilatus 100k (DECTRIS, Switzerland) placed 159 mm from the sample with a tilted angle of 36 °C for WAXS. The SAXS measurements were performed using two samples to detect distances, 1194 and 337 mm, to obtain a wide angular range. The scattering intensity, $I(q)$, was recorded by means of the scattering momentum transfer q, where $q = 4\pi/\lambda \sin(\theta)$, 2θ is the scattering angle and λ = 0.15419 nm is the weighted average of the X-ray wavelength of the Cu K$\alpha_{1,2}$ emission lines. Owing to the small beam size pointed at the sample (< 1 mm × 1 mm) smearing effects were not considered. The NLC samples were placed under vacuum between Kapton® tapes. The measurements were done in transmission mode. The SAXS/WAXS patterns were taken for 10 min each.

Cell toxicity assay on CHO cells

The viability of CHO cells was analyzed by the reduction of the tetrazolium salt to a formazan product (i.e., the MTT method). A 96-well polystyrene microplate containing 1×10^4 cells per well of CHO cells (obtained from the American Type Culture

Collection, Manassas, VA, USA) were cultured in Ham's F12 medium (Gibco BRL, Grand Island, NY, USA) supplemented with 10% fetal bovine serum (FBS, Notocor Laboratories, Cordoba, Argentina) and antibiotics (50 IU penicillin and 50 μg/mL streptomycin) (Bagó Laboratories, Buenos Aires, Argentina) in a humidified atmosphere with 5% CO_2. After 24 h, the cells were incubated with increasing concentrations of RPMI as control, BNZ, NLC-VEHICLE, and NLC-BNZ (0, 15, 31, 62, and 125 μg·mL^{-1}). The MTT reagent (5 mg·mL^{-1} in phosphate-buffered saline (PBS)) was then added for 3 h. Dimethyl sulfoxide (DMSO,100 μL per well) was added under agitation for 10 min to dissolve the MTT. The color was measured in a microplate reader (MultiskanTM GO spectrophotometer, Thermo Fisher Scientific) at 550 nm. The assays were performed in triplicate.

Cell toxicity assay on Vero cells
Cell viability was analyzed by flow cytometry as described in the "In vitro anti-amastigote effect" section after adding PI to obtain the percentage of dead cells following the incubation with the formulation of nanoparticles or the free drug.

Hemolytic effect
Hemolysis was assessed on 3 mL of a freshly drawn heparinized suspension of fresh human blood placed on a 6-well cell culture plate. Increasing concentrations of freshly prepared dilutions of the free drug and NLC-BNZ (1, 5, and 50 μg·mL^{-1}) were added to each well and incubated for 3, 24, and 48 h at 37 °C. Samples were then centrifuged for 5 minutes at 2500 rpm, and the absorbance of the supernatant was determined at 540 nm in a microplate reader (MultiskanTM GO spectrophotometer, Thermo Fisher Scientific). Triton X 100 (10%), saline solution, NLC-VEHICLE, and BNZ were used as the positive, negative, vehicle, and reference drug controls, respectively. The hemolytic activity was calculated as [56]:

$$HA\left(\%\right) = \frac{A_{540\,nm}\text{sample} - A_{540\,nm}\text{saline}}{A_{540\,nm}\text{Triton} - A_{540\,nm}\text{saline}} \times 100 \qquad (6)$$

where $A_{540\,nm}$sample represents the absorbance value of the sample, $A_{540\,nm}$Triton the absorbance value of the positive control, and $A_{540\,nm}$saline the absorbance value of the negative control.

The blood was obtained from the "Institute of Hemotherapy" in La Plata, Buenos Aires, Argentina as part of a formal agreement between the "Instituto de Genética Veterinaria (IGEVET, UNLP-CONICET La Plata)" and this institution. Also, this assay protocol was approved by the National University of La Plata Ethics Committee and it was developed in accordance with the principles proclaimed in the Universal Declaration of Human Rights of 1948, the ethical norms established by the Nuremberg Code of 1947, and the Declaration of Helsinki of 1964 and its successive amendments and clarifications. Special attention was paid to Patient Rights in their relationship with health professionals and institutions and the National Law 25326 on the Protection of Personal Data.

Parasites
The *T. cruzi* strain K98 (TcI, low virulence) was used. Tissue culture trypomastigotes were obtained from the supernatants of 2- to 3-day-old infected Vero cells (African green monkey kidney epithelial cells) maintained in RPMI-1640 medium supplemented with 10% FBS (Internegocios S.A, Argentina) at 37 °C in a 5% humidified CO_2 atmosphere. Amastigotes were obtained after infecting Vero cells at a multiplicity of infection (MOI) of 1:2.

In vitro anti-trypomastigote effect
A trypomastigote suspension (1×10^5 trypomastigotes per well) was co-cultured in a 96 well-plate with dilutions of both a solution of the free drug and of the nanoparticle formulations (concentration range = 1, 2.5, 5, and 10 μM) in RPMI-1640 supplemented with 5% FBS at 37 °C in 5% CO_2 atmosphere. The NLC-VEHICLE sample was tested using the same dilutions as the NLC-BNZ formulation. After 24 h of incubation, motile parasites were counted in a hemocytometer chamber under a light microscope. Controls consisted of RPMI-1640 supplemented with 5% FBS as well as RPMI-1640 with 0.1% of DMSO.

Results were expressed as mean viability of trypomastigotes (%) (regarding to RPMI-1640 + DMSO control). Experiments were performed in triplicate. The half maximal effective concentration (EC_{50}) against the trypomastigote form was determined from concentration-response curves fitted through a nonlinear regression on GraphPad Prism version 8.0.1 software (San Diego, CA, USA).

In vitro anti-amastigote effect
Vero cells were infected with the trypomastigote form of GFP-expressing *T. cruzi* (K98 strain) [57] at a multiplicity of infection (MOI) 1:2. After 24 h the cells were washed with PBS, trypsinized for 10 min, and seeded onto 96-well plates (5×10^4 cells/well). After the cells attached to the microplate (i.e., 2–3 h), increasing concentrations of freshly prepared dilutions of the formulations (1, 5, 10, 25, and 50 μM) or the free drug were added. After 72 h of treatment, the cells were harvested with a trypsin/EDTA solution and processed for flow cytometry analysis using a BD Biosciences FACSCANTO II Flow Cytometer (Franklin Lakes, NJ, USA). Propidium iodide (Sigma, St. Louis, USA) was added to the cell suspensions

(50 µg/mL) for 10 min, prior to analysis. In total, 20000 events were acquired for each sample. Data analysis was performed using the FlowJo[TM] software (FlowJo, LCC). The EC_{50} values were determined from dose-response curves fitted through a non-linear regression using GraphPad Prism version 8.0.1 software (San Diego, CA, USA). The experiments were performed in duplicates.

Statistical analysis

The normality of the variable distribution was assessed using the Shapiro–Wilk normality test. Comparisons of the means were performed by analysis of variance (ANOVA) followed by Tukey or Dunnet comparison tests. Statistical significance was set at $p < 0.05$.

Supporting Information

This file includes a summary of the goodness-of-fit measures that indicate how different mathematical models of drug release fit our experimental data.

Supporting Information File 1
Supplementary material.
[https://www.beilstein-journals.org/bjnano/content/supplementary/2190-4286-14-66-S1.pdf]

Acknowledgements

Authors
Giuliana Muraca[1], María Esperanza Ruiz[1], Rocío C. Gambaro[2], Sebastián Scioli-Montoto[1], María Laura Sbaraglini[1], Gisel Padula[2], José Sebastián Cisneros[3], Cecilia Yamil Chain[3], Vera Alvarez[4], Cristián Huck-Iriart[5,6], Guillermo Castro[7], María Belén Piñero[8], Matias Ildebrando Marchetto[8], Catalina Alba Soto[8], Germán A. Islan[9]* and Alan Talevi[1]*

Addresses
[1]Laboratorio de Investigación y Desarrollo de Bioactivos (LIDeB), Departamento de Ciencias Biológicas, Facultad de Ciencias Exactas, Universidad Nacional de La Plata, La Plata, Argentina, [2]Instituto de Genética Veterinaria (IGEVET, UNLP-CONICET La Plata), Facultad de Ciencias Veterinarias Universidad Nacional de La Plata (UNLP), La Plata, Argentina, [3]Instituto de Investigaciones Fisicoquímicas Teóricas y Aplicadas (CONICET-UNLP), La Plata, Buenos Aires, Argentina, [4]Grupo de Materiales Compuestos Termoplásticos (CoMP), Instituto de Investigaciones en Ciencia y Tecnología de Materiales (INTEMA), Facultad de Ingeniería, Universidad Nacional de Mar del Plata (UNMDP) – CONICET, Av. Colón 10850 (B7608FDQ), Mar del Plata, Buenos Aires, Argentina, [5]Laboratorio de Cristalografía Aplicada, Escuela de Ciencia y Tecnología, CONICET, Universidad Nacional de San Martín (UNSAM), Campus Miguelete, 25 de Mayo y Francia, San Martín B1650KNA, Buenos Aires, Argentina, [6]ALBA Synchrotron Light Source, Carrer de la Llum 2–26, Cerdanyola del Vallès, 08290 Barcelona, España, [7]Nanomedicine Research Unit (Nanomed), Federal University of ABC (UFABC), Santo André, SP, Brazil, [8]Instituto de Investigaciones en Microbiología y Parasitología Médica (IMPaM) - Consejo Nacional de Investigaciones Científicas y Técnicas - Universidad de Buenos Aires Departamento de Microbiología, Facultad de Medicina, Buenos Aires, Argentina and [9]Centro de Investigación y Desarrollo en Fermentaciones Industriales (CINDEFI), Laboratorio de Nanobiomateriales, Departamento de Química, Facultad de Ciencias Exactas, Universidad Nacional de La Plata (UNLP)-CONICET (CCT La Plata), Calle 47 y 115, (B1900AJI), La Plata, Buenos Aires, Argentina

ORCID® iDs
Giuliana Muraca - https://orcid.org/0000-0002-4785-8050
María Esperanza Ruiz - https://orcid.org/0000-0001-8617-667X
Sebastián Scioli-Montoto - https://orcid.org/0000-0003-3314-3406
María Laura Sbaraglini - https://orcid.org/0000-0002-4671-2658
José Sebastián Cisneros - https://orcid.org/0000-0001-7563-978X
Cecilia Yamil Chain - https://orcid.org/0000-0002-8234-0556
Vera A. Álvarez - https://orcid.org/0000-0002-4909-4592
Guillermo R. Castro - https://orcid.org/0000-0002-6187-7805
María Belén Piñero - https://orcid.org/0009-0004-4431-368X
Catalina Alba Soto - https://orcid.org/0000-0002-2724-0421
Alan Talevi - https://orcid.org/0000-0003-3178-826X

References

1. American trypanosomiasis, April 1, 2021. https://www.who.int/es/news-room/fact-sheets/detail/chagas-disease-%28american-trypanosomiasis%29 (accessed June 11, 2022).

2. Strasen, J.; Williams, T.; Ertl, G.; Zoller, T.; Stich, A.; Ritter, O. *Clin. Res. Cardiol.* **2014,** *103,* 1–10. doi:10.1007/s00392-013-0613-y

3. Lynn, M. K.; Bossak, B. H.; Sandifer, P. A.; Watson, A.; Nolan, M. S. *Acta Trop.* **2020,** *205,* 105361. doi:10.1016/j.actatropica.2020.105361

4. Nunes, M. C. P.; Beaton, A.; Acquatella, H.; Bern, C.; Bolger, A. F.; Echeverría, L. E.; Dutra, W. O.; Gascon, J.; Morillo, C. A.; Oliveira-Filho, J.; Ribeiro, A. L. P.; Marin-Neto, J. A. *Circulation* **2018,** *138,* e169–e209. doi:10.1161/cir.0000000000000599

5. Edwards, D. I. *J. Antimicrob. Chemother.* **1993,** *31,* 9–20. doi:10.1093/jac/31.1.9

6. Losada Galván, I.; Alonso-Padilla, J.; Cortés-Serra, N.; Alonso-Vega, C.; Gascón, J.; Pinazo, M. J. *Expert Rev. Anti-Infect. Ther.* **2021,** *19,* 547–556. doi:10.1080/14787210.2021.1834849

7. Prata, A. *Lancet Infect. Dis.* **2001,** *1,* 92–100. doi:10.1016/s1473-3099(01)00065-2

8. Sgambatti de Andrade, A. L. S.; Zicker, F.; de Oliveira, R. M.;
    Almeida e Silva, S.; Luquetti, A.; Travassos, L. R.; Almeida, I. C.;
    de Andrade, S. S.; Guimarães de Andrade, J.; Martelli, C. M. *Lancet*
    1996, *348,* 1407–1413. doi:10.1016/s0140-6736(96)04128-1

9. Krettli, A. U.; Cançado, J. R.; Brener, Z. *Mem. Inst. Oswaldo Cruz*
    1984, *79,* 157–164. doi:10.1590/s0074-02761984000500027

10. Frade, V. P.; Simões, N. S.; Couto, N. R. B.; Sanches, C.;
    Oliveira, C. D. L. *Rev. Inst. Med. Trop. Sao Paulo* **2020,** *62,* e52.
    doi:10.1590/s1678-9946202062052

11. Morillo, C. A.; Marin-Neto, J. A.; Avezum, A.; Sosa-Estani, S.;
    Rassi, A., Jr.; Rosas, F.; Villena, E.; Quiroz, R.; Bonilla, R.; Britto, C.;
    Guhl, F.; Velazquez, E.; Bonilla, L.; Meeks, B.; Rao-Melacini, P.;
    Pogue, J.; Mattos, A.; Lazdins, J.; Rassi, A.; Connolly, S. J.; Yusuf, S.
    N. Engl. J. Med. **2015,** *373,* 1295–1306. doi:10.1056/nejmoa1507574

12. Maximiano, F. P.; Costa, G. H. Y.; de Souza, J.;
    da Cunha-Filho, M. S. S. *Quim. Nova* **2010,** *33,* 1714–1719.
    doi:10.1590/s0100-40422010000800018

13. Morilla, M. J.; Romero, E. L. *Nanomedicine (London, U. K.)* **2015,** *10,*
    465–481. doi:10.2217/nnm.14.185

14. Arrúa, E. C.; Seremeta, K. P.; Bedogni, G. R.; Okulik, N. B.;
    Salomon, C. J. *Acta Trop.* **2019,** *198,* 105080.
    doi:10.1016/j.actatropica.2019.105080

15. Arrua, E. C.; Hartwig, O.; Loretz, B.; Goicoechea, H.; Murgia, X.;
    Lehr, C.-M.; Salomon, C. J. *Colloids Surf., B* **2022,** *217,* 112678.
    doi:10.1016/j.colsurfb.2022.112678

16. Rigalli, J. P.; Perdomo, V. G.; Luquita, M. G.; Villanueva, S. S. M.;
    Arias, A.; Theile, D.; Weiss, J.; Mottino, A. D.; Ruiz, M. L.;
    Catania, V. A. *PLoS Negl. Trop. Dis.* **2012,** *6,* e1951.
    doi:10.1371/journal.pntd.0001951

17. Muraca, G.; Berti, I. R.; Sbaraglini, M. L.; Fávaro, W. J.; Durán, N.;
    Castro, G. R.; Talevi, A. *Front. Chem. (Lausanne, Switz.)* **2020,** *8,*
    601151. doi:10.3389/fchem.2020.601151

18. Streck, L.; Sarmento, V. H. V.; de Menezes, R. P. R. P. B.;
    Fernandes-Pedrosa, M. F.; Martins, A. M. C.; da Silva-Júnior, A. A.
    Int. J. Pharm. **2019,** *555,* 36–48. doi:10.1016/j.ijpharm.2018.11.041

19. Scioli Montoto, S.; Sbaraglini, M. L.; Talevi, A.; Couyoupetrou, M.;
    Di Ianni, M.; Pesce, G. O.; Alvarez, V. A.; Bruno-Blanch, L. E.;
    Castro, G. R.; Ruiz, M. E.; Islan, G. A. *Colloids Surf., B* **2018,** *167,*
    73–81. doi:10.1016/j.colsurfb.2018.03.052

20. Müller, R. H.; Radtke, M.; Wissing, S. A. *Int. J. Pharm.* **2002,** *242,*
    121–128. doi:10.1016/s0378-5173(02)00180-1

21. Vinuesa, T.; Herráez, R.; Oliver, L.; Elizondo, E.; Acarregui, A.;
    Esquisabel, A.; Pedraz, J. L.; Ventosa, N.; Veciana, J.; Viñas, M.
    Am. J. Trop. Med. Hyg. **2017,** *97,* 1469–1476.
    doi:10.4269/ajtmh.17-0044

22. ImageJ. https://imagej.nih.gov/ij/index.html (accessed Sept 9, 2022).

23. Maximiano, F. P.; Novack, K. M.; Bahia, M. T.; de Sá-Barreto, L. L.;
    da Cunha-Filho, M. S. S. *J. Therm. Anal. Calorim.* **2011,** *106,* 819–824.
    doi:10.1007/s10973-011-1371-6

24. Islan, G. A.; Tornello, P. C.; Abraham, G. A.; Duran, N.; Castro, G. R.
    Colloids Surf., B **2016,** *143,* 168–176.
    doi:10.1016/j.colsurfb.2016.03.040

25. Hou, D.; Xie, C.; Huang, K.; Zhu, C. *Biomaterials* **2003,** *24,* 1781–1785.
    doi:10.1016/s0142-9612(02)00578-1

26. Espinosa, Y. R.; Galvis-Ovallos, F.; Maldonado Rozo, A. *J. Cienc. Ing.*
    2018, *10,* 32–38.
    https://jci.uniautonoma.edu.co/2018/2018-4.pdf

27. Nosal, H.; Moser, K.; Warzała, M.; Holzer, A.; Stańczyk, D.; Sabura, E.
    J. Polym. Environ. **2021,** *29,* 38–53. doi:10.1007/s10924-020-01841-5

28. Liu, Y.; Xu, Y.; Wu, M.; Fan, L.; He, C.; Wan, J.-B.; Li, P.; Chen, M.;
    Li, H. *Int. J. Nanomed.* **2016,** *11,* 3167–3178. doi:10.2147/ijn.s103556

29. Jenning, V.; Thünemann, A. F.; Gohla, S. H. *Int. J. Pharm.* **2000,** *199,*
    167–177. doi:10.1016/s0378-5173(00)00378-1

30. Ambrosi, M.; Raudino, M.; Diañez, I.; Martínez, I. *Eur. Polym. J.* **2019,**
    120, 109189. doi:10.1016/j.eurpolymj.2019.08.016

31. Rivas-Rojas, P. C.; Ollier, R. P.; Alvarez, V. A.; Huck-Iriart, C.
    J. Mater. Sci. **2021,** *56,* 5595–5608. doi:10.1007/s10853-020-05603-5

32. Nojima, S.; Terashima, Y.; Ashida, T. *Polymer* **1986,** *27,* 1007–1013.
    doi:10.1016/0032-3861(86)90064-9

33. Strategies to Modify the Drug Release from Pharmaceutical Systems |
    ScienceDirect.
    https://www.sciencedirect.com/book/9780081000922/strategies-to-mod
    ify-the-drug-release-from-pharmaceutical-systems (accessed Sept 9,
    2022).

34. 5 - Mathematical Models of Drug Release. In *Strategies to Modify the
    Drug Release from Pharmaceutical Systems;* Bruschi, M. L., Ed.;
    Woodhead Publishing, 2015; pp 63–86.
    doi:10.1016/b978-0-08-100092-2.00005-9

35. Öztürk, A. A.; Aygül, A.; Şenel, B. *J. Drug Delivery Sci. Technol.* **2019,**
    54, 101240. doi:10.1016/j.jddst.2019.101240

36. Gundogdu, E.; Demir, E.-S.; Ekinci, M.; Ozgenc, E.; Ilem-Ozdemir, D.;
    Senyigit, Z.; Gonzalez-Alvarez, I.; Bermejo, M. *Nanomaterials* **2022,**
    12, 250. doi:10.3390/nano12020250

37. Wu, K.-W.; Sweeney, C.; Dudhipala, N.; Lakhani, P.;
    Chaurasiya, N. D.; Tekwani, B. L.; Majumdar, S. *AAPS PharmSciTech*
    2021, *22,* 240. doi:10.1208/s12249-021-02108-5

38. Rehman, M.; Madni, A.; Ihsan, A.; Khan, W. S.; Khan, M. I.;
    Mahmood, M. A.; Ashfaq, M.; Bajwa, S. Z.; Shakir, I. *Int. J. Nanomed.*
    2015, *10,* 2805–2814. doi:10.2147/ijn.s67147

39. Kovačević, A. B.; Müller, R. H.; Savić, S. D.; Vuleta, G. M.; Keck, C. M.
    Colloids Surf., A **2014,** *444,* 15–25. doi:10.1016/j.colsurfa.2013.12.023

40. Bhattacharya, S.; Ahir, M.; Patra, P.; Mukherjee, S.; Ghosh, S.;
    Mazumdar, M.; Chattopadhyay, S.; Das, T.; Chattopadhyay, D.;
    Adhikary, A. *Biomaterials* **2015,** *51,* 91–107.
    doi:10.1016/j.biomaterials.2015.01.007

41. Scioli Montoto, S.; Muraca, G.; Ruiz, M. E. *Front. Mol. Biosci.* **2020,** *7,*
    587997. doi:10.3389/fmolb.2020.587997

42. Olivera, M. J.; Cucunubá, Z. M.; Valencia-Hernández, C. A.;
    Herazo, R.; Agreda-Rudenko, D.; Flórez, C.; Duque, S.; Nicholls, R. S.
    PLoS One **2017,** *12,* e0185033. doi:10.1371/journal.pone.0185033

43. Snima, K. S.; Jayakumar, R.; Unnikrishnan, A. G.; Nair, S. V.;
    Lakshmanan, V.-K. *Carbohydr. Polym.* **2012,** *89,* 1003–1007.
    doi:10.1016/j.carbpol.2012.04.050

44. Chen, L. Q.; Fang, L.; Ling, J.; Ding, C. Z.; Kang, B.; Huang, C. Z.
    Chem. Res. Toxicol. **2015,** *28,* 501–509. doi:10.1021/tx500479m

45. Lin, Y.-S.; Haynes, C. L. *J. Am. Chem. Soc.* **2010,** *132,* 4834–4842.
    doi:10.1021/ja910846q

46. Chinnaiyan, S. K.; Karthikeyan, D.; Gadela, V. R. *Pharm. Nanotechnol.*
    2018, *6,* 253–263. doi:10.2174/2211738507666181221142406

47. Dobrovolskaia, M. A.; Clogston, J. D.; Neun, B. W.; Hall, J. B.;
    Patri, A. K.; McNeil, S. E. *Nano Lett.* **2008,** *8,* 2180–2187.
    doi:10.1021/nl0805615

48. Revollo, S.; Oury, B.; Vela, A.; Tibayrenc, M.; Sereno, D. *Pathogens*
    2019, *8,* 197. doi:10.3390/pathogens8040197

49. Borges, A. R.; Link, F.; Engstler, M.; Jones, N. G. *Front. Cell Dev. Biol.*
    2021, *9,* 720536. doi:10.3389/fcell.2021.720536

50. Doering, T. L.; Lu, T.; Werbovetz, K. A.; Gokel, G. W.; Hart, G. W.;
    Gordon, J. I.; Englund, P. T. *Proc. Natl. Acad. Sci. U. S. A.* **1994,** *91,*
    9735–9739. doi:10.1073/pnas.91.21.9735

51. Lee, S. H.; Stephens, J. L.; Englund, P. T. *Nat. Rev. Microbiol.* **2007,** *5,* 287–297. doi:10.1038/nrmicro1617

52. Doering, T. L.; Raper, J.; Buxbaum, L. U.; Adams, S. P.; Gordon, J. I.; Hart, G. W.; Englund, P. T. *Science* **1991,** *252,* 1851–1854. doi:10.1126/science.1829548

53. Scioli-Montoto, S.; Sbaraglini, M. L.; Cisneros, J. S.; Chain, C. Y.; Ferretti, V.; León, I. E.; Alvarez, V. A.; Castro, G. R.; Islan, G. A.; Talevi, A.; Ruiz, M. E. *Front. Chem. (Lausanne, Switz.)* **2022,** *10,* 908386. doi:10.3389/fchem.2022.908386

54. Zhang, Y.; Huo, M.; Zhou, J.; Zou, A.; Li, W.; Yao, C.; Xie, S. *AAPS J.* **2010,** *12,* 263–271. doi:10.1208/s12248-010-9185-1

55. Teeranachaideekul, V.; Souto, E. B.; Müller, R. H.; Junyaprasert, V. B. *J. Microencapsulation* **2008,** *25,* 111–120. doi:10.1080/02652040701817762

56. Barrett, D.; Tanaka, A.; Harada, K.; Ohki, H.; Watabe, E.; Maki, K.; Ikeda, F. *Bioorg. Med. Chem. Lett.* **2001,** *11,* 479–482. doi:10.1016/s0960-894x(00)00705-8

57. Miranda, C. G.; Solana, M. E.; de los Angeles Curto, M.; Lammel, E. M.; Schijman, A. G.; Alba Soto, C. D. *Acta Trop.* **2015,** *152,* 8–16. doi:10.1016/j.actatropica.2015.08.004

License and Terms

Green SPIONs as a novel highly selective treatment for leishmaniasis: an in vitro study against *Leishmania amazonensis* intracellular amastigotes

Brunno R. F. Verçoza[1], Robson R. Bernardo[1,2], Luiz Augusto S. de Oliveira[1,2] and Juliany C. F. Rodrigues[*1]

Full Research Paper

Address:
[1]Núcleo Multidisciplinar de Pesquisas em Biologia, NUMPEX-Bio, Campus UFRJ Duque de Caxias Prof. Geraldo Cidade, Universidade Federal do Rio de Janeiro, Rodovia Washington Luiz, n. 19593, km 104.5, 25240-005, Duque de Caxias, RJ, Brasil and [2]Núcleo Multidisciplinar de Pesquisas em Nanotecnologia, NUMPEX-Nano, Campus UFRJ Duque de Caxias Prof. Geraldo Cidade, Universidade Federal do Rio de Janeiro, Rodovia Washington Luiz, n. 19593, km 104.5, 25240-005, Duque de Caxias, RJ, Brasil

Email:
Juliany C. F. Rodrigues[*] - juliany.rodrigues@caxias.ufrj.br

* Corresponding author

Abstract

The main goal of this work was to evaluate the therapeutic potential of green superparamagnetic iron oxide nanoparticles (SPIONs) produced with coconut water for treating cutaneous leishmaniasis caused by *Leishmania amazonensis*. Optical and electron microscopy techniques were used to evaluate the effects on cell proliferation, infectivity percentage, and ultrastructure. SPIONs were internalized by both parasite stages, randomly distributed in the cytosol and located mainly in membrane-bound compartments. The selectivity index for intracellular amastigotes was more than 240 times higher compared to current drugs used to treat the disease. The synthesized SPIONs showed promising activity against *Leishmania* and can be considered a strong candidate for a new therapeutic approach for treating leishmaniases.

Introduction

Leishmaniasis is one of the most important neglected diseases of chronic nature and remains a serious global health problem. A worrying increase has been observed in the number of leishmaniasis cases worldwide in recent decades. It is estimated that about 600 million people live in risk areas, and 0.6–1.2 million new leishmaniasis cases appear annually [1]. The treatment for

this disease involves using pentavalent antimonials, miltefosine, amphotericin B, paromomycin, or pentamidine. However, side effects of these drugs and an increased number of drug-resistant parasites have been reported [2-5]. These facts demonstrate the need to develop new treatments or alternatives that are safer, more effective, and more accessible to patients.

In this context, nanomedicine is one of the most promising branches of contemporary medicine, currently concentrating a large part of the scientific effort on the search for new treatments for different diseases. Its main objective is to develop therapies with higher specificity, effectiveness, and safety, as well as less toxicity [6]. One interesting class of nanomaterials in medicine are superparamagnetic iron oxide nanoparticles (SPIONs). SPIONs exhibit theranostic properties, that is, they can be used simultaneously for diagnosis and therapy. Thus, SPIONs have emerged as one of the best options for the development of new therapeutic methods. SPIONs offer several features such as good biocompatibility, degradability under moderate acid conditions, the ability for magnetic manipulation, the possibility of being used in magnetic resonance imaging, and the ability to generate controlled heat non-invasively when exposed to an alternating magnetic field [7,8]. In 2019, our group published an article describing a low-cost green synthesis of SPIONs using coconut water [9]. In this article, the ability of macrophages to uptake these SPIONs was evaluated, together with some physical and chemical characterizations. The synthesized green SPIONs are around 4 nm in diameter, are composed of pure nonstoichiometric magnetite, exhibit superparamagnetic behavior at room temperature, and are taken up by macrophages without being toxic for these mammalian cells [9].

The application of SPIONs in treating leishmaniasis has been studied by different groups over the past few years, showing promising and satisfactory results [10-13]; thus, using SPIONs to develop new topical treatments can mean a revolution. SPIONs could be used for topical application, associated with drugs and combined or not with thermotherapy by magnetic hyperthermia. Furthermore, the treatment can be applied to the localized cutaneous lesion, making the treatment more specific and less toxic to the patient. Thus, the main goal of this study is to evaluate the effects of green SPIONs against *Leishmania amazonensis* (*L. amazonensis*) in vitro.

Results
Uptake of SPIONs by *L. amazonensis* promastigotes and intracellular amastigotes
Bright-field optical microscopy of *L. amazonensis* promastigotes and intracellular amastigotes incubated with Prussian blue

revealed that both parasite stages can uptake the SPIONs (Figure 1). The arrows and arrowheads in Figure 1 show the characteristic blue stain that indicates the positive reaction between potassium ferrocyanide and ferrous compounds. In promastigotes (Figure 1A,B), the SPIONS are distributed throughout the cytosol. In contrast, in the intracellular amastigotes cultivated in macrophages, the SPIONs appear in the mammalian cytosol, inside the parasitophorous vacuole, and in the parasite cytosol (Figure 1C,D).

After the first microscopic analysis, scanning electron microscopy and chemical element mapping analysis were carried out to confirm the uptake of the SPIONs by *L. amazonensis* intracellular amastigotes after removing the plasma membrane to expose the cytoplasmic environment (Figure 2). Secondary electron imaging revealed intracellular amastigotes inside the parasitophorous vacuoles (Figure 2A). Backscattered electron imaging showed several small electron-lucent structures randomly distributed throughout the macrophage cytosol, inside the parasitophorous vacuoles (Figure 2B, arrows), and in the intracellular amastigotes (Figure 2B, arrowheads). The ferrous nature of the observed structures was assessed by chemical element mapping analysis using energy-dispersive X-ray spectroscopy (Figure 2C), confirming that the electron-lucent structures contain iron atoms (Figure 2D).

Transmission electron microscopy (TEM) was used to confirm the internalization of the SPIONs. First, promastigotes were treated with 100 µg/mL of SPIONs for 24 h (Figure 3A–C). TEM images confirmed the presence of SPION aggregates randomly distributed throughout the cytoplasm of the promastigotes (Figure 3A–C, arrowheads). The images suggest that these aggregates have different sizes. Furthermore, at high magnification, it is possible to observe that the SPIONS are frequently surrounded by membranes (Figure 3B, arrows). In addition, SPIONs were also observed inside the flagellar pocket (Figure 3C, arrowheads) and closely associated with the membrane.

The uptake of SPIONs was also observed in macrophages infected with *L. amazonensis* intracellular amastigotes after treatment with 100 µg/mL of SPIONs for 24 h (Figure 3D–F). The images confirmed the presence of SPION aggregates inside the macrophage cytosol, the parasitophorous vacuoles, and the intracellular amastigotes (Figure 3C,D, arrowheads). SPIONs were also observed inside the macrophages close to the parasitophorous vacuole membrane (Figure 3D, large arrow), sometimes appearing inside membrane-bound structures and exhibiting different sizes (Figure 3E, arrowheads). Some alterations in amastigote ultrastructure can also be observed, namely electron-lucent lipid bodies, a multivesicular body close to the Golgi
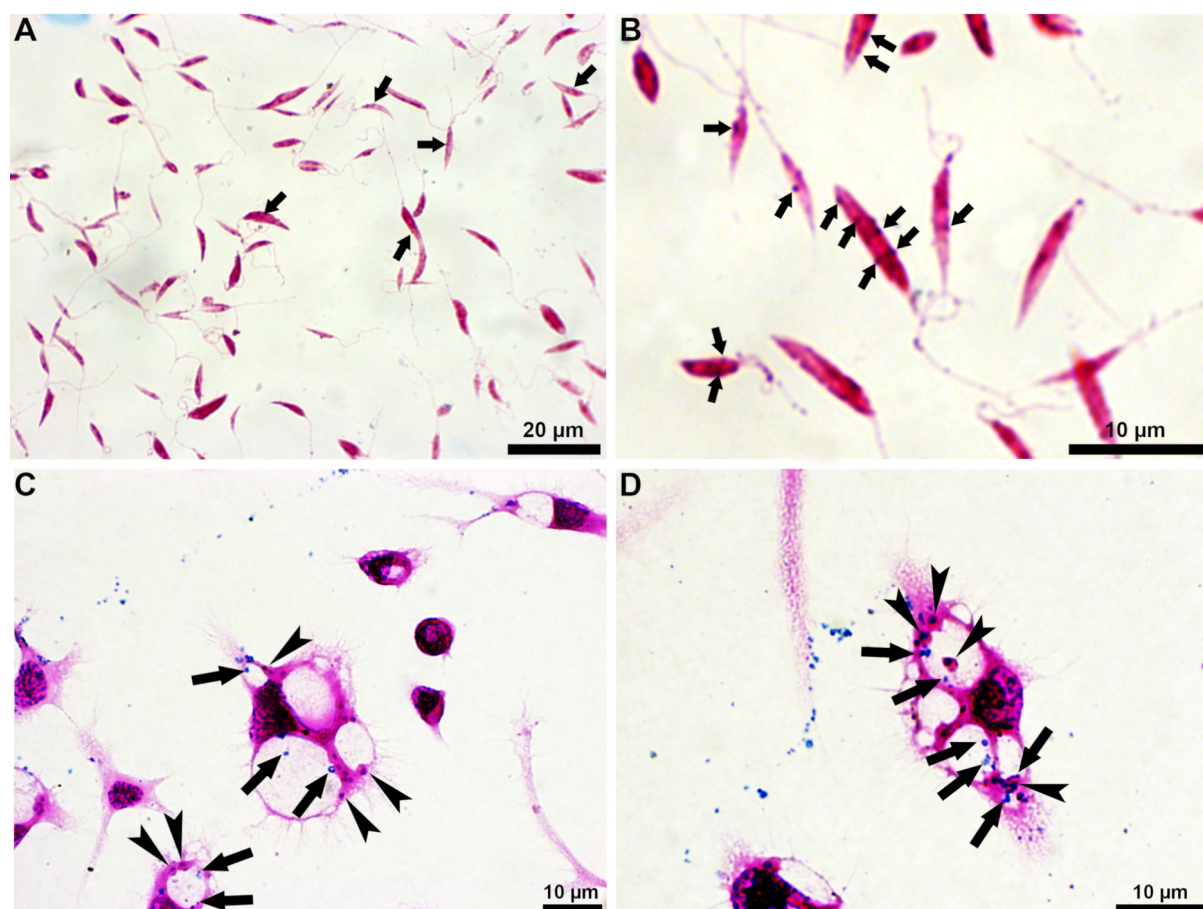
Figure 1: Bright-field optical microscopy of *L. amazonensis* promastigotes (A, B) and intracellular amastigotes (C, D) treated with 100 µg/mL of SPIONs for 24 h, after staining with Prussian blue (A–D). (A) The arrows indicate the blue stain characteristic for the reaction with ferrous compounds in the promastigote cytosol. (B) Digital magnification shows that SPIONs are randomly distributed throughout the cytosol. (C) In the case of macrophages infected with intracellular amastigotes, the SPIONs were observed inside the parasitophorous vacuoles. (D) Digital magnification shows the SPIONs (arrows) inside the macrophage cytosol, the parasitophorous vacuoles, and the amastigote cytosol (arrowheads).

complex, and endoplasmic reticulum profiles very close to organelles such as mitochondrion and glycosome. Higher magnification revealed that the SPION aggregates are constituted of small nanoparticles that appear associated with tiny filaments (Figure 3F, thin arrow).

Antiproliferative effects of SPIONs in *L. amazonensis* promastigotes and intracellular amastigotes

The analysis of the antiproliferative effects of SPIONs in *L. amazonensis* promastigotes showed that they could not alter the growth for any of the concentrations evaluated (Figure 4A). In contrast, the SPIONs were very active against intracellular amastigotes (Figure 4B). Furthermore, analysis of the growth curve shows a statistically significant reduction in the percentage of infection for all tested concentrations of SPIONs (1, 5, 10, 25, and 50 µg/mL) and treatment times (24, 48, and 72 h) when compared with the control of infected macrophages.

After the first 24 h of treatment, it was possible to observe a reduction in the percentage of infection of about 50% for a concentration of 1 µg/mL and of about 90% for 50 µg/mL of SPIONs. The data revealed a concentration-dependent effect, which increased within 48 and 72 h of treatment. The percentage of infection significantly reduces over time, indicating a time-dependent effect. The IC_{50} values were calculated for each treatment time and confirmed the results obtained (Figure 4B), that is, 1.206, 0.848, and 0.668 µg/mL for treatment times of 24, 48, and 72 h, respectively.

Evaluation of possible effects on the ultrastructure of *L. amazonensis* intracellular amastigotes

Transmission electron microscopy allowed us to analyze ultrastructural alterations induced by treating *L. amazonensis* intracellular amastigotes with 100 µg/mL of SPIONs for 24 h (Figure 5). The images revealed several alterations, namely
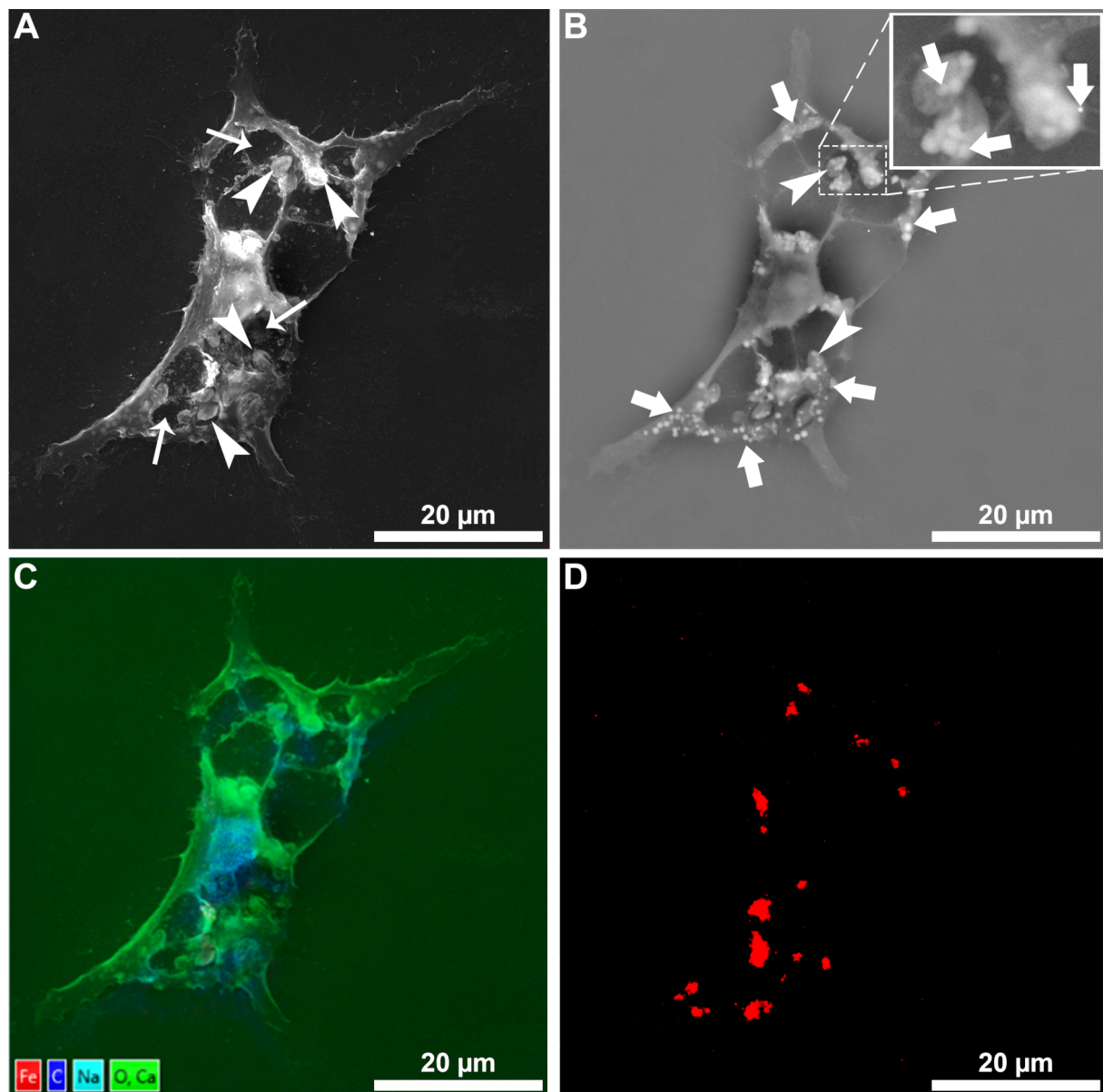
Figure 2: Scanning electron microscopy of macrophages infected with *L. amazonensis* intracellular amastigotes after treatment with 100 µg/mL SPIONs for 24 h. The plasma membrane was gently removed to observe the presence of nanoparticles inside the cells. Panel A shows infected macrophages with some amastigotes (arrowheads) inside the parasitophorous vacuoles (thin arrows). Panel B shows the same macrophage; however, the image was obtained by detecting backscattered electrons, revealing several electron-lucent aggregates (arrows). Digital magnification (highlighted rectangular area) showed electron-lucent aggregates even inside intracellular amastigotes (arrowheads). Panels C and D show the X-ray microanalysis mapping of infected macrophages, indicating the presence of iron in the cytosol (red color in Figure 2D).

(1) lipid bodies (Figure 5A–C, thin arrows), (2) cytoplasmic disorganization with many vacuoles, which may indicate activation of autophagic processes (Figure 5A–C, arrows), (3) myelin-like figures (Figure 5A, arrowhead), and (4) mitochondrial swelling (Figure 5C, star). Furthermore, in the intracellular amastigotes, there are membrane-bound compartments containing SPION aggregates and parasitophorous vacuoles containing cellular debris and dead amastigotes (Figure 5D, triangle).

Discussion

SPIONs represent a new approach to diagnosing and treating diseases, particularly when associated with magnetic hyperthermia, an emerging form of active treatment [14-18]. However, despite all their potential, the synthesis processes of the SPIONs are characterized by being expensive and toxic to humans and the environment [6]. In this scenario, our group demonstrated the therapeutic potential of low-cost biocompatible SPIONs produced by green synthesis [9]. The present study

Figure 3: Transmission electron microscopy of *L. amazonensis* promastigotes and intracellular amastigotes treated with 100 μg/mL of SPIONs for 24 h. Electron-dense aggregates of SPIONs (arrowheads) are randomly distributed in both developmental stages. (A) SPIONs (arrowheads) were observed in the promastigote cytosol, closely associated with endoplasmic reticulum profiles and lipid bodies. (B) High-magnification image with SPION aggregates (arrowheads) inside membrane-bound compartments (arrows). (C) SPIONs (arrowheads) are associated with thin filaments inside the flagellar pocket and in the cytosol closely associated with the flagellar pocket membrane. (D) In the macrophages infected with intracellular amastigotes, the SPIONs appear inside the parasitophorous vacuole and in the macrophage and parasite cytosol (arrowheads). In this image, it is also possible to observe the SPIONs surrounded by a membrane (arrows) and an aggregate close to the membrane of the parasitophorous vacuole (large arrow). (E, F) High-magnification images of intracellular amastigotes revealing SPIONs (arrowheads) inside membrane-bound compartments (arrows). The aggregates are formed by smaller individual nanoparticles (small arrow). Figure 3E also shows many lipid bodies, vacuoles, and a multivesicular structure, which are features typically found in treated parasites. F, flagellum; FP, flagellar pocket; LB, lipid body; M, mitochondrion; N, nucleus; and PV, parasitophorous vacuole.
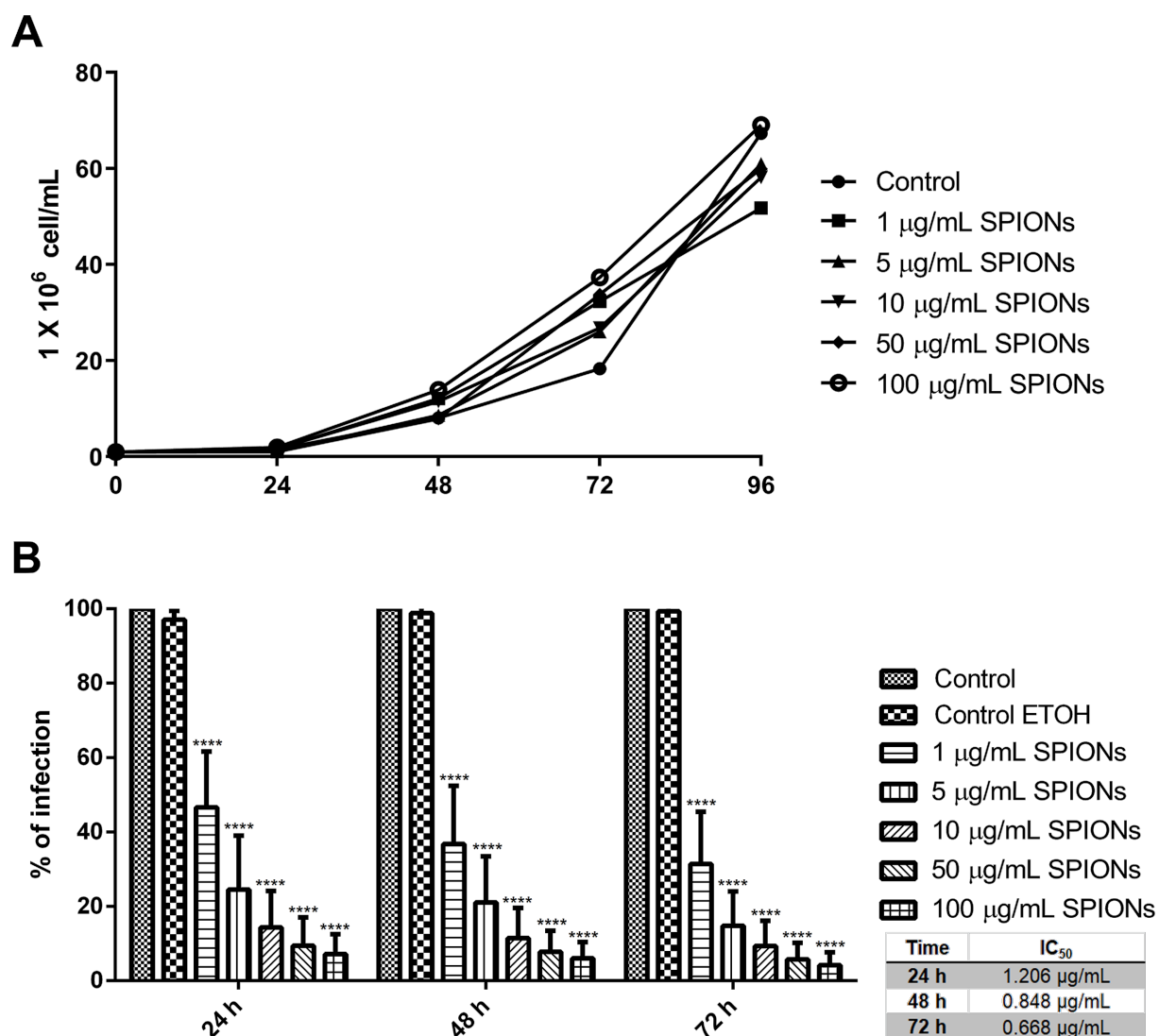
Figure 4: Analysis of the antiproliferative effect in *L. amazonensis* promastigotes and intracellular amastigotes treated with different concentrations of SPIONs. (A) Growth curve of *L. amazonensis* promastigotes; the SPIONs were added to the culture medium after 24 h of growth. (B) For intracellular amastigotes, infected macrophages were treated, and the percentage of infection was obtained for each treatment condition; the SPIONs were added to the infected macrophage culture after 24 h of infection. *P* values for panel B: **** *p* < 0.0001.

aimed to evaluate in vitro the therapeutic potential of SPIONs produced with coconut water to treat cutaneous leishmaniasis caused by *L. amazonensis*.

Microscopy techniques efficiently revealed the uptake and distribution of SPIONs in *L. amazonensis* promastigotes and intracellular amastigotes. The first analysis confirmed the uptake of SPIONs by macrophages, which was published previously by our group [9]. Furthermore, in the article here, the images revealed SPIONs inside the parasitophorous vacuole and in the cytosol of intracellular amastigotes. In addition, SPIONs were also observed randomly distributed throughout the cytosol of promastigotes, in the flagellar pocket, and inside membrane-

bound structures. It is the first time that superparamagnetic iron oxide nanoparticles SPIONs are observed inside the *Leishmania* spp and the parasitophorous vacuole. Chemical element mapping analysis by scanning electron microscopy confirmed the ferrous nature of the nanoparticle aggregates. These results prove the ability of both promastigotes and intracellular amastigotes to uptake SPIONs from the culture medium.

The acquisition of iron by *Leishmania* intracellular amastigotes that live inside mammalian host cells is important for cell differentiation and the pathogenesis of the disease [19-21]. Thus, it is possible to speculate that SPIONs use iron transport mechanisms to reach the parasitophorous vacuole and amastigote

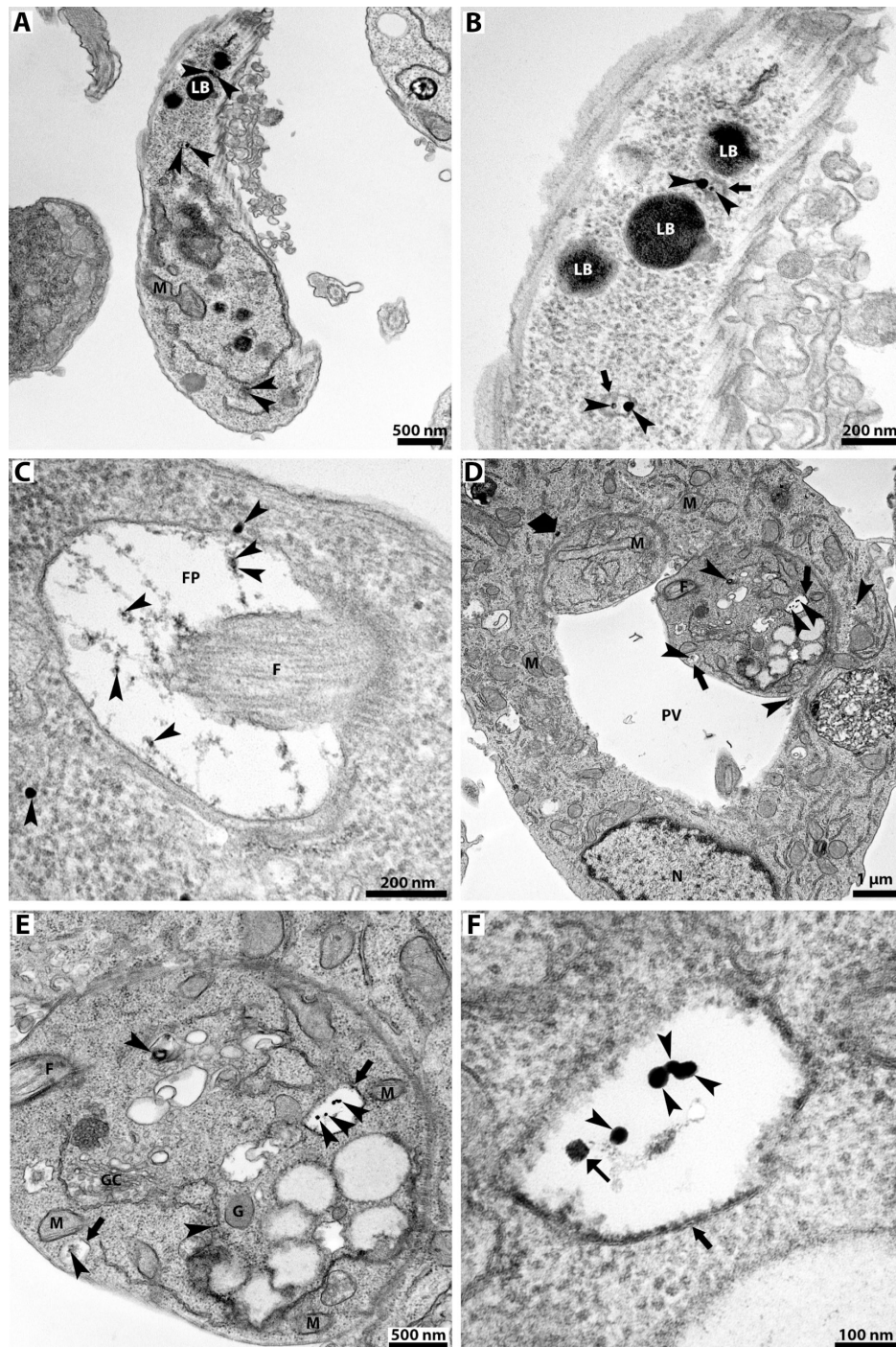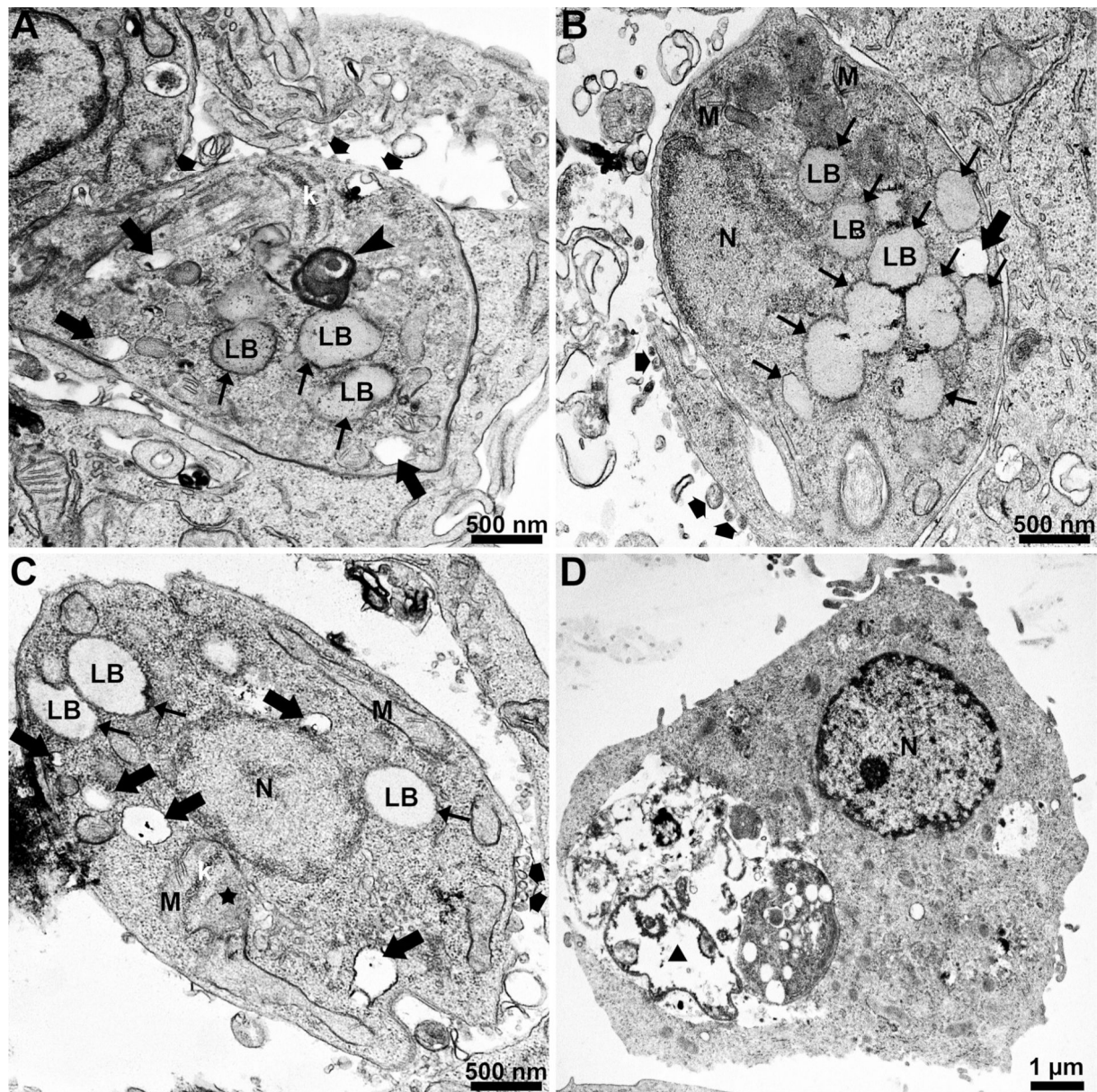**Figure 5:** Transmission electron microscopy of *L. amazonensis* intracellular amastigotes treated with 100 µg/mL of SPIONs for 24 h. Different ultra-structural changes were observed in intracellular amastigotes: (1) many lipid bodies (A–C, thin arrows), (2) increased secretion of extracellular vesicles (A–C, broad arrows), (3) intracellular vacuolization (A–C, arrows), (4) myelin-like figures (A, arrowhead), (5) mitochondrial swelling (C, star), and (6) destroyed amastigotes (D, triangle). F, flagellum; k, kinetoplast; LB, lipid body; M, mitochondrion; and N, nucleus.

cytosol [21]. However, further studies need to be carried out to confirm this hypothesis and to elucidate the mechanisms of SPION uptake in promastigotes and amastigotes.

We evaluated the antiproliferative effects of SPIONs in *L. amazonensis* promastigotes and intracellular amastigotes. Despite being internalized by promastigotes, SPIONs did not affect the cell proliferation of the parasites (Figure 4A). A completely different result was observed for intracellular amastig-

otes, where the reduction in the percentage of infection was very significant already with the lowest concentration of SPIONs used [1 µg/mL] (Figure 4B). The IC$_{50}$ values found for intracellular amastigotes during the treatment were 1.206, 0.848, and 0.668 µg/mL for treatment times of 24, 48 and 72 h, respectively. In a previous study published by our group, we analyzed the cytotoxicity of SPIONs against macrophages [9]. The results revealed no toxic effects up to a concentration of 300 µg/mL, indicating that SPIONs are well tolerated by

macrophages. Because CC_{50} values are difficult to calculate, we used GraphPad Prism software to estimate them. CC_{50} values are essential to calculate the selective index (SI), and both quantities are important to understand how effective the nanoparticles are against the parasite while being less toxic for mammalian cells (Table 1).

The SI revealed that the SPIONs were highly selective for *L. amazonensis* intracellular amastigotes (Table 1), presenting values significantly higher when compared with other compounds and drugs used to treat *Leishmania* sp. (Table 2) [22-27]. These data indicate a high selectivity index for SPIONs compared with current treatments, different from most compounds, drugs, and nanomaterials developed in the last decades.

During TEM analyses, we observed that intracellular amastigotes were undergoing substantial ultrastructural alterations (Figure 5) when treated with SPIONs. These alterations include (1) accumulation of lipid bodies, (2) intense intracellular vacuolization, (3) mitochondrial swelling, (4) myelin-like figures, and (5) cell death. The observed ultrastructural effects corroborate the significant antiproliferative effect found and give indications of the possible mechanisms of action of these nanoparticles, which may be closely associated with intracellular iron homeostasis.

Iron homeostasis has been extensively studied because of its essential role in maintaining the cellular functions of several cell types. It is well established that, in mammalian cells, iron in its free state can participate in the Haber–Weiss reaction, catalyzing the formation of highly reactive hydroxyl radicals

that lead to oxidative stress [28,29]. Thus, one of the possibilities for the observed antiproliferative effects could be the result of an imbalance in iron homeostasis with the consequent induction of oxidative stress and death of the parasites. However, further studies need to be carried out to confirm this hypothesis. In *Leishmania,* it is well known that available iron has an important influence on the homeostasis of reactive oxygen species [30]. Studies have already shown that iron excess in the diet of mice causes a decrease in the replication of *Leishmania* spp. in different tissues of infected animals due to the interaction with reactive oxygen and nitrogen species [31,32].

Several studies have shown the potential of using nanoparticles as a new method for treating leishmaniasis. However, only a few studies report the effects of using iron oxide nanoparticles [11,12,15,33-35]. Recently, the effects of magnetic iron oxide nanoparticles were demonstrated in *L. mexicana* axenic amastigotes. First, the amastigotes were treated with 200 µg/mL of magnetic nanoparticles. Subsequently, magnetic hyperthermia was applied using an alternating field of 30 mT with a frequency of 452 kHz for 40 min. The results showed that magnetic hyperthermia was efficient in killing *L. mexicana* axenic amastigotes [12]. Another study demonstrated the anti-*Leishmania* effect of magnetic nanoparticles synthesized by green chemistry in *L. major* promastigotes [35]. Finally, a study showed the effect in vitro and in vivo of amphotericin B encapsulated in magnetic iron oxide nanoparticles coated with glycine-rich peptides for treating visceral leishmaniasis caused by *L. donovani* [12]. All these studies demonstrated the potential gain of drug conjugation with magnetic nanoparticles for treating leishmaniasis.

Table 1: Estimated CC_{50} and SI obtained after the analysis of the macrophage cytotoxicity assay previously published in [9] using the GraphPad Prism software.

Time	Estimated cytotoxic concentration of 50% (CC_{50}) for macrophages	Estimated selective index (SI)
24 h	1271.5 µg/mL	1054
48 h	2250.6 µg/mL	2654
72 h	3420.0 µg/mL	5119

Table 2: Selectivity index values for different compounds and drugs studied and used for treating leishmaniasis.

Time	Compound	SI	Reference
24 h	amphotericin B	16	[26]
48 h	TC95	24	[23]
48 h	KH-TFMDI	81	[22]
72 h	itraconazole	103.17	[25]
72 h	ravuconazole	28.9	[24]
72 h	miltefosine	34.2	[27]

Conclusion

The use of SPIONs synthesized with coconut water to treat macrophages infected with *Leishmania amazonensis* intracellular amastigotes revealed a significant anti-*Leishmania* effect with a selectivity index more than 240 times higher than those of other currently used drugs. Furthermore, it was also observed that the SPIONs could be directed into the parasitophorous vacuoles of infected cells and parasites. Thus, this new nanomaterial is a promising new therapeutic alternative as (1) an active treatment agent because of its intrinsic properties, (2) a treatment agent associated with heating through alternating current magnetic fields, and (3) a drug carrier.

Finally, SPIONs can be considered a strong candidate for a new therapeutic approach to treating cutaneous leishmaniasis, that is, an accessible and low-cost topical treatment.

Experimental
SPIONs

The SPIONs used in the present study were synthesized as described in [9] (patent application registration BR 10 2020 015814 [36]). For assays, after synthesis and purification, the SPIONs were dispersed in a 70% ethanol solution (Merck, Germany). The maximum ethanol concentration in cultures did not exceed 0.5%, which did not interfere with cell growth. The nanoparticles used in the biological tests were stored at −20 °C.

Ethics committee for the use of laboratory animals

The assays that used mammalian macrophages and parasites from animal models were approved by the Ethics Committee for the Use of Laboratory Animals (CEUA) of the Centro de Ciências da Saúde from the Universidade Federal do Rio de Janeiro according to the Brazilian Federal Law (11794/2008, Decreto No. 6,899/2009). For the use of peritoneal macrophages resident in mice and the maintenance of *Leishmania amazonensis* species in Balb/C mice, the protocol number was UFRJ/CCS-142/21. Furthermore, all animals received human care according to the guide published by the Brazilian Society of Zootechnics of Laboratory and Council National Control of Animal Experimentation.

Cell culture

The immortalized murine macrophages RAW 264.7 were grown in 25 cm^2 bottles in RPMI 1640 medium (Cultilab, Brasil) supplemented with 2% sodium bicarbonate, 10% fetal bovine serum, and 100 U/mL penicillin. Cells were cultured at 37 °C in 5% CO$_2$ atmosphere, and the medium was changed three times a week; cells were passed when they reached confluence in the bottles. In addition, primary cultures of

murine macrophages were obtained from the peritoneal cavity of CF1 mice by washing with Hanks' balanced solution. Then, they were plated on coverslips in a 24-well culture plate and placed to adhere for 24 h at 37 °C in an atmosphere of 5% CO$_2$. For the microscopic analyses, macrophages were grown in 25 cm^2 bottles or on glass coverslips in 24-well plates; after 24 h of culture, they were treated for 24 h with different SPION concentrations. This study used the WHOM/BR/75/JOSEFA *Leishmania amazonensis* strain as a standard model for cutaneous leishmaniasis. The parasites were maintained according to previously published protocols [22].

Prussian blue staining

For staining with Prussian blue (Sigma-Aldrich, Germany), promastigote and intracellular amastigotes were treated with 100 µg/mL of SPIONs for 24 h. The promastigotes (control and treated cells) were washed in phosphate-buffered saline (PBS) pH 7.2 and adhered for 10 min on glass coverslips previously coated with poly-L-lysine (Sigma-Aldrich, Germany). The intracellular amastigotes were obtained after infection of RAW 264.7 macrophages at a ratio of ten parasites to one macrophage. After treatment, cells were washed in PBS pH 7.2, fixed, and dehydrated, as described in [9]. Finally, cells were observed using a DM2500 optical microscope (Leica Microsystem, Germany) in bright-field mode.

Electron microscopy analysis

Control and treated cells were washed in PBS pH 7.2, fixed, and post-fixed according to previously published protocols [23]. Then, cells were processed for scanning electron microscopy and chemical element mapping analysis as described in [9]. The micrographs were obtained using a TESCAN VEGA 3 LMU scanning electron microscope operating at 20 kV equipped with an OXFORD X-MaxN 20 mm^2 detector (Oxford Instruments, United Kingdom) for energy-dispersive X-ray spectroscopy. For transmission electron microscopy, after fixation, samples were dehydrated in increasing acetone concentrations and embedded in Epon. Ultrathin sections were obtained using a PT-PC PowerTome ultramicrotome (RMC Boeckeler, USA) stained with uranyl acetate and lead citrate and observed using a FEI TECNAI SPIRIT transmission electron microscope operating at 120 kV.

Antiproliferative effects of SPIONs in *Leishmania amazonensis* promastigotes and intracellular amastigotes

To evaluate the effect of the SPIONs on the growth of *L. amazonensis* promastigotes, cell density experiments were initiated with an inoculum of 1.0×10^6 parasites/mL in M199 culture medium supplemented with 10% fetal bovine serum and cultivated at 25 °C. After 24 h of growth, different concentra-

tions of SPIONs (1, 5, 10, 50, and 100 µg/mL) were added, and cells were cultured for 96 h. The cell density was calculated every 24 h by counting the number of cells in a Neubauer chamber using contrast-phase light microscopy. Besides, SPIONs were also evaluated against intracellular amastigotes, the clinically relevant stage of leishmaniasis. For this analysis, murine macrophages and parasites were obtained as previously published [23]. After 24 h of the initial infection, different concentrations of SPIONs (1, 5, 10, 25, and 50 µg/mL) were added, and the medium with the nanoparticles was changed every day for three days. The IC_{50} was calculated using the linear regression method defined in [37].

Statistical analysis

Statistical analysis was conducted using GraphPad Prism with one-way analysis of variance (ANOVA). The results were considered statistically significant for cases of $p \leq 0.05$ (*).

Acknowledgements

Funding

ORCID® iDs

Brunno R. F. Verçoza - https://orcid.org/0000-0001-6117-7879
Robson R. Bernardo - https://orcid.org/0000-0002-0035-5149
Luiz Augusto S. de Oliveira - https://orcid.org/0000-0002-4034-8365
Juliany C. F. Rodrigues - https://orcid.org/0000-0001-6807-8101

Preprint

A non-peer-reviewed version of this article has been previously published as a preprint: https://doi.org/10.3762/bxiv.2023.17.v1

References

1. World Health Organization (WHO). Disease factsheet 2019 – Leishmaniasis. 2019; https://www.who.int/news-room/fact-sheets/detail/leishmaniasis.

2. Chakravarty, J.; Sundar, S. *J. Global Infect. Dis.* **2010,** *2,* 167. doi:10.4103/0974-777x.62887

3. Croft, S. L.; Sundar, S.; Fairlamb, A. H. *Clin. Microbiol. Rev.* **2006,** *19,* 111–126. doi:10.1128/cmr.19.1.111-126.2006

4. Ponte-Sucre, A.; Padrón-Nieves, M., Eds. *Drug Resistance in Leishmania Parasites;* Springer International Publishing: Cham, Switzerland, 2018. doi:10.1007/978-3-319-74186-4

5. Khoo, S. H.; Bond, J.; Denning, D. W. *J. Antimicrob. Chemother.* **1994,** *33,* 203–213. doi:10.1093/jac/33.2.203

6. Bobo, D.; Robinson, K. J.; Islam, J.; Thurecht, K. J.; Corrie, S. R. *Pharm. Res.* **2016,** *33,* 2373–2387. doi:10.1007/s11095-016-1958-5

7. Barick, K. C.; Aslam, M.; Lin, Y.-P.; Bahadur, D.; Prasad, P. V.; Dravid, V. P. *J. Mater. Chem.* **2009,** *19,* 7023–7029. doi:10.1039/b911626e

8. Lee, J.-H.; Jang, J.-t.; Choi, J.-s.; Moon, S. H.; Noh, S.-h.; Kim, J.-w.; Kim, J.-G.; Kim, I.-S.; Park, K. I.; Cheon, J. *Nat. Nanotechnol.* **2011,** *6,* 418–422. doi:10.1038/nnano.2011.95

9. Verçoza, B. R. F.; Bernardo, R. R.; Pentón-Madrigal, A.; Sinnecker, J. P.; Rodrigues, J. C. F.; de Oliveira, L. A. S. *Nanomedicine (London, U. K.)* **2019,** *14,* 2293–2313. doi:10.2217/nnm-2018-0500

10. Abazari, R.; Mahjoub, A. R.; Molaie, S.; Ghaffarifar, F.; Ghasemi, E.; Slawin, A. M. Z.; Carpenter-Warren, C. L. *Ultrason. Sonochem.* **2018,** *43,* 248–261. doi:10.1016/j.ultsonch.2018.01.022

11. Berry, S. L.; Walker, K.; Hoskins, C.; Telling, N. D.; Price, H. P. *Sci. Rep.* **2019,** *9,* 1059. doi:10.1038/s41598-018-37670-9

12. Kumar, R.; Pandey, K.; Sahoo, G. C.; Das, S.; Das, V. N. R.; Topno, R. K.; Das, P. *Mater. Sci. Eng., C* **2017,** *75,* 1465–1471. doi:10.1016/j.msec.2017.02.145

13. Zomorodian, K.; Veisi, H.; Mousavi, S. M.; Ataabadi, M. S.; Yazdanpanah, S.; Bagheri, J.; Mehr, A. P.; Hemmati, S.; Veisi, H. *Int. J. Nanomed.* **2018,** *13,* 3965–3973. doi:10.2147/ijn.s161002

14. Chang, E. H.; Harford, J. B.; Eaton, M. A. W.; Boisseau, P. M.; Dube, A.; Hayeshi, R.; Swai, H.; Lee, D. S. *Biochem. Biophys. Res. Commun.* **2015,** *468,* 511–517. doi:10.1016/j.bbrc.2015.10.136

15. Khatami, M.; Alijani, H.; Sharifi, I.; Sharifi, F.; Pourseyedi, S.; Kharazi, S.; Lima Nobre, M. A.; Khatami, M. *Sci. Pharm.* **2017,** *85,* 36. doi:10.3390/scipharm85040036

16. Lee, M. S.; Su, C.-M.; Yeh, J.-C.; Wu, P.-R.; Tsai, T.-Y.; Lou, S.-L. *Int. J. Nanomed.* **2016,** *11,* 4583–4594. doi:10.2147/ijn.s112415

17. Ranmadugala, D.; Ebrahiminezhad, A.; Manley-Harris, M.; Ghasemi, Y.; Berenjian, A. *Biotechnol. Lett.* **2018,** *40,* 237–248. doi:10.1007/s10529-017-2477-0

18. Yang, Y.; Wang, F.; Zheng, K.; Deng, L.; Yang, L.; Zhang, N.; Xu, C.; Ran, H.; Wang, Z.; Wang, Z.; Zheng, Y. *PLoS One* **2017,** *12,* e0177049. doi:10.1371/journal.pone.0177049

19. Flannery, A. R.; Renberg, R. L.; Andrews, N. W. *Curr. Opin. Microbiol.* **2013,** *16,* 716–721. doi:10.1016/j.mib.2013.07.018

20. Huynh, C.; Andrews, N. W. *Cell. Microbiol.* **2008,** *10,* 293–300. doi:10.1111/j.1462-5822.2007.01095.x

21. Mittra, B.; Andrews, N. W. *Trends Parasitol.* **2013,** *29,* 489–496. doi:10.1016/j.pt.2013.07.007

22. Verçoza, B. R. F.; Godinho, J. L. P.; de Macedo-Silva, S. T.; Huber, K.; Bracher, F.; de Souza, W.; Rodrigues, J. C. F. *Apoptosis* **2017,** *22,* 1169–1188. doi:10.1007/s10495-017-1397-8

23. Godinho, J. L. P.; Georgikopoulou, K.; Calogeropoulou, T.; de Souza, W.; Rodrigues, J. C. F. *Exp. Parasitol.* **2013,** *135,* 153–165. doi:10.1016/j.exppara.2013.06.015

24. Teixeira de Macedo Silva, S.; Visbal, G.; Lima Prado Godinho, J.;
Urbina, J. A.; de Souza, W.; Cola Fernandes Rodrigues, J.
J. Antimicrob. Chemother. **2018,** *73,* 2360–2373.
doi:10.1093/jac/dky229

25. de Azevedo-França, J. A.; Granado, R.; de Macedo Silva, S. T.;
dos Santos-Silva, G.; Scapin, S.; Borba-Santos, L. P.; Rozental, S.;
de Souza, W.; Martins-Duarte, É. S.; Barrias, E.; Rodrigues, J. C. F.;
Navarro, M. *Antimicrob. Agents Chemother.* **2020,** *64,* e01980-19.
doi:10.1128/aac.01980-19

26. Caldeira, L. R.; Fernandes, F. R.; Costa, D. F.; Frézard, F.;
Afonso, L. C. C.; Ferreira, L. A. M. *Eur. J. Pharm. Sci.* **2015,** *70,*
125–131. doi:10.1016/j.ejps.2015.01.015

27. Stroppa, P. H. F.; Antinarelli, L. M. R.; Carmo, A. M. L.; Gameiro, J.;
Coimbra, E. S.; da Silva, A. D. *Bioorg. Med. Chem.* **2017,** *25,*
3034–3045. doi:10.1016/j.bmc.2017.03.051

28. Emerit, J.; Beaumont, C.; Trivin, F. *Biomed. Pharmacother.* **2001,** *55,*
333–339. doi:10.1016/s0753-3322(01)00068-3

29. McCord, J. M. *Blood* **2004,** *11,* 3171S–3172S.
doi:10.1093/jn/134.11.3171s

30. Taylor, M. C.; Kelly, J. M. *Parasitology* **2010,** *137,* 899–917.
doi:10.1017/s0031182009991880

31. Vale-Costa, S.; Gomes-Pereira, S.; Teixeira, C. M.; Rosa, G.;
Rodrigues, P. N.; Tomás, A.; Appelberg, R.; Gomes, M. S.
PLoS Negl. Trop. Dis. **2013,** *7,* e2061.
doi:10.1371/journal.pntd.0002061

32. Bisti, S.; Konidou, G.; Papageorgiou, F.; Milon, G.; Boelaert, J. R.;
Soteriadou, K. *Eur. J. Immunol.* **2000,** *30,* 3732–3740.
doi:10.1002/1521-4141(200012)30:12<3732::aid-immu3732>3.0.co;2-d

33. Nafari, A.; Cheraghipour, K.; Sepahvand, M.; Shahrokhi, G.; Gabal, E.;
Mahmoudvand, H. *Parasite Epidemiol. Control* **2020,** *10,* e00156.
doi:10.1016/j.parepi.2020.e00156

34. Akbari, M.; Oryan, A.; Hatam, G. *Acta Trop.* **2017,** *172,* 86–90.
doi:10.1016/j.actatropica.2017.04.029

35. Della Pepa, M. E.; Martora, F.; Finamore, E.; Vitiello, M.; Galdiero, M.;
Franci, G. Role of Nanoparticles in Treatment of Human Parasites. In
Nanotechnology Applied to Pharmaceutical Technology; Rai, M.;
dos Santos, C. A., Eds.; Springer International Publishing: Cham,
Switzerland, 2017; pp 307–333. doi:10.1007/978-3-319-70299-5_13

36. Verçoza, B. R. F.; Bernardo, R. R.; Pentón-Madrigal, A.;
Sinnecker, J. P.; Rodrigues, J. C. F.; de Oliveira, L. A. S. Method for
the sustainable production of superparamagnetic iron oxide
nanoparticles. B.R. Pat. Appl. BR 10 2020 015814 7, Aug 3, 2020.

37. Martin, M. B.; Grimley, J. S.; Lewis, J. C.; Heath, H. T.; Bailey, B. N.;
Kendrick, H.; Yardley, V.; Caldera, A.; Lira, R.; Urbina, J. A.;
Moreno, S. N. J.; Docampo, R.; Croft, S. L.; Oldfield, E. *J. Med. Chem.*
2001, *44,* 909–916. doi:10.1021/jm0002578

Nanotechnological approaches in the treatment of schistosomiasis: an overview

Lucas Carvalho[1,2], Michelle Sarcinelli[*,‡2] and Beatriz Patrício[‡2,3]

Abstract

Schistosomiasis causes over 200,000 deaths annually. The current treatment option, praziquantel, presents limitations, including low bioavailability and resistance. In this context, nanoparticles have emerged as a promising option for improving schistosomiasis treatment. Several narrative reviews have been published on this topic. Unfortunately, the lack of clear methodologies presented in these reviews leads to the exclusion of many important studies without apparent justification. This integrative review aims to examine works published in this area with a precise and reproducible method. To achieve this, three databases (i.e., Pubmed, Web of Science, and Scopus) were searched from March 31, 2022, to March 31, 2023. The search results included only original research articles that used nanoparticles smaller than 1 µm in the treatment context. Additionally, a search was conducted in the references of the identified articles to retrieve works that could not be found solely using the original search formula. As a result, 65 articles that met the established criteria were identified. Inorganic and polymeric nanoparticles were the most prevalent nanosystems used. Gold was the primary material used to produce inorganic nanoparticles, while poly(lactic-*co*-glycolic acid) and chitosan were commonly used to produce polymeric nanoparticles. None of these identified works presented results in the clinical phase. Finally, based on our findings, the outlook appears favorable, as there is a significant diversity of new substances with schistosomicidal potential. However, financial efforts are required to advance these nanoformulations.

Introduction

Schistosomiasis is a disease common in tropical countries caused by trematodes from the genus Schistosoma. More than 220 million people are affected by this disease, in addition to 800 million at risk of infection [1,2]. Every year, 200 thousand deaths are caused by schistosomiasis, making it the third most devastating tropical disease in the world after malaria and

intestinal parasitosis [3]. After penetration of the skin by the larval form (cercariae), the schistosomes mature and migrate through the lung to the liver, gut, or bladder, depending on the species, where they elicit a marked immune response. The adult *Schistosoma mansoni* worms mate in the liver and lay eggs in the mesenteric venules of the intestine [4]. Nowadays, the only treatment available for this disease consists of praziquantel (PZQ) [5].

Praziquantel is a class II compound according to the biopharmaceutical classification system (BCS), so it has low solubility and high permeability in the gastrointestinal tract [6]. This drug is affected by the first-pass effect on the liver, which also impacts its bioavailability [6]. Unfortunately, this makes PZQ ineffective against young forms of *Schistosoma mansoni*, leading to concerns about the emergence of resistant strains. Indeed, reports of resistance have been documented worldwide, prompting research for alternative treatments or new approaches to improve the characteristics of PZQ [7]. Additionally, due to the first passage effect, high doses of PZQ are required, resulting in large tablet sizes, making its administration challenging for children, as no PZQ pediatric formulation is distributed by the World Health Organization (WHO). Consequently, people split adult PZQ tablets to treat children, but the bitter taste of PZQ makes it difficult for them to adhere to treatment [8]. Moreover, high dosages of PZQ have been associated with side effects such as abdominal pain, nausea, and allergy [9]. In this context, nanotechnological tools are being investigated as potential solutions to address all these issues related to PZQ and bring new treatment alternatives [10].

Nanotechnology involves the creation and use of materials and technologies at the nanoscale, while nanomedicine focuses on the application of nanotechnology to treat, monitor, and prevent diseases [11]. Nanomedicine uses nanocarriers to enhance drug delivery by ensuring that drugs are delivered in appropriate amounts to specific target areas and remains in the body for the necessary duration [12]. As a result, nanoparticles have been utilized mainly as drug delivery systems in various parasitic diseases, including schistosomiasis, to improve bioavailability, therapeutic efficacy, and decrease adverse effect profiles of the drugs used to treat such illnesses [13].

A few recent reviews provide a general overview of how nanotechnological tools are used in schistosomiasis treatment. However, most of these published works are narrative reviews limited to a specific drug or nanoparticle categories. For instance, some reviews only focus on PZQ [14], while others solely showcase nanosystems for drug delivery [15]. Nonetheless, recent literature reveals several works that employ various drugs and utilize nanoparticles not only as delivery systems but

also with intrinsic action. Moreover, some of the previous works were not so clear about the methodology followed to include and exclude articles in their narrative review.

That said, the purpose of this work is to produce an integrative review of the theme with a well-defined research methodology, highlighting the main nanoparticles and drugs used in the literature to treat schistosomiasis.

Results and Discussion

We found 65 available articles that met the requirements, 75% ($n = 49$) were found in databases, while the remaining 25% (16 articles) were found through reference scanning. Table S1 (Supporting Information File 1) summarizes all the articles found regarding the use of nanosystems and encapsulated drugs. In Figure 1, it is possible to observe that only 59% of the publications show effectiveness data solely in vivo. Also, most articles use nanoparticles as drug delivery systems (82%), and most of them encapsulated PZQ (Figure 2). Polymeric (23%) and inorganic (20%) nanoparticles were used in the majority of the studies (Figure 3). Most of the papers (78%) have not done toxicity tests, and the main route of administration was the oral route (Figure 4).

Figure 1: Percentage of articles that conducted effectiveness tests. The graph represents the number of articles out of the 65 found that conducted efficacy testing: solely in vitro, solely in vivo, both in vitro an in vivo, or none.
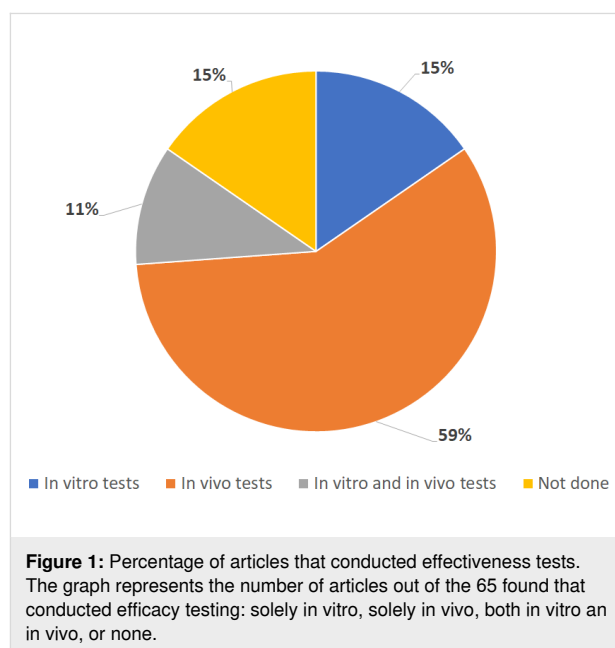
It is important to bring attention to the fact that from the 65 papers found using our research strategy, 25% (16 articles) were found using reference scanning in the previously selected papers, which shows the importance of this step in bibliographic research. That explains why our strategy was able to reunite a great number of articles, unlike previous reviews. Below, we discuss the main findings of these studies.

Figure 2: Percentage of compounds encapsulated among the selected articles. The graph considers a total of 53 articles that utilized nano-systems for drug delivery. It displays the percentage of these articles that used each drug category: praziquantel, plant-derived medicines, repositioned drugs, and other compounds.

Figure 4: Percentage of administration routes used in the 65 selected articles. The routes were: oral, subcutaneous, or intramuscular. In some cases, this information was unclear in the articles.

Nanosystems

Polymeric nanoparticles are nanoparticles composed of poly-meric materials which may be natural or synthetic [16]. They are generally produced by two strategies: the dispersion of preformed polymers or the polymerization of monomers [17].

The first one is more commonly describe in the literature, and the techniques usually employed to produce them include nano-precipitation, solvent evaporation, emulsification/solvent diffu-sion, and emulsification/reverse salting out [18,19]. The main advantages of using this type of nanoparticles as nanocarriers are their potential use for drug controlled release, the ability to

Figure 3: Percentage of types of nanosystems used in the selected articles. The graph considers a total of 65 articles found and displays the percent-age of them that utilizes the differents nanosystems: liposomes, lipid nanocapsules, nanosuspensions, nanocomposites, inorganic nanoparticles, nanostructure lipid carriers, nanoemulsions, nanocrystals, solid lipid nanoparticles, polymeric nanoparticles, noisomes, and others.

protect drugs and other molecules with biological activity against the environment, improvement of their bioavailability and therapeutic index [17].

These nanocarriers are divided into two types: nanocapsules and nanospheres [18]. Nanocapsules consist of reservoir systems with an oil or water core and an external polymeric shell. They are, overall, used to increase drug solubility [20]. Usually, once in the body, the encapsulated drug diffuses through the polymeric wall in a zero-order kinetic, that means, it constantly releases the encapsulated drug [17]. In opposition, nanospheres are matrix systems formed by polymers without a central core. During the administration, the matrix erodes and the drug diffuses, resulting in a first-order kinetic drug release, that is, an exponential drug release [17,20].

Our research found that many articles utilized poly(lactic-*co*-glycolic acid) (PLGA) and chitosan nanoparticles, especially because they are biocompatible polymers and present great biodegradability. The polymer PLGA is approved for clinical use by Food and Drug Administration since 1989 [21] and, although no human data attests to chitosan safety, many animal tests prove its safety [22]. Eudragit L 100 is another polymer commonly used in literature because of its biocompatibility [8]. Overall, it is used when a delayed release is required. It is derived from polyacid, and because of that, it is resistant to low pH values [23]. So, when nanoparticles with this material are orally administered, they resist against gastric secretions and release the drug in the intestine. This protects many drugs and increases their bioavailability [24].

Inorganic nanoparticles (IN) are derived from metals or silica [25]. The most common metal used in the production of IN found in this work was gold, even though it was also possible to observe a great amount of works using silver and zinc (Figure 5). While silica-derived nanoparticles are used in the treatment against schistosomiasis due to their characteristics as drug carriers [10], metal nanoparticles usually present intrinsic action even when not loaded with drugs. Works with other parasites suggest that metallic nanoparticles may affect enzyme activity necessary to the physiology and production of the tegument [26]. Therefore, metallic nanoparticles also have a curative role against schistosomiasis. A possible explanation for this action was suggested by Dkhil et al. in their work with gold nanoparticles [27]. They suggested that their curative effects are due to antioxidant properties which confer the ability to scavenge free radicals [27]. After that, many authors related a reduction in oxidative stress markers in vivo after metalic nanoparticle administration and/or amelioration in histopathological characteristics after infection, which corroborates the first hypothesis [27-34].

Figure 5: Percentage of material used to produce inorganic nanoparticles. The graph considers the 13 articles found that utilized inorganic nanoparticles and illustrates the type of material composing the nanoparticles used.
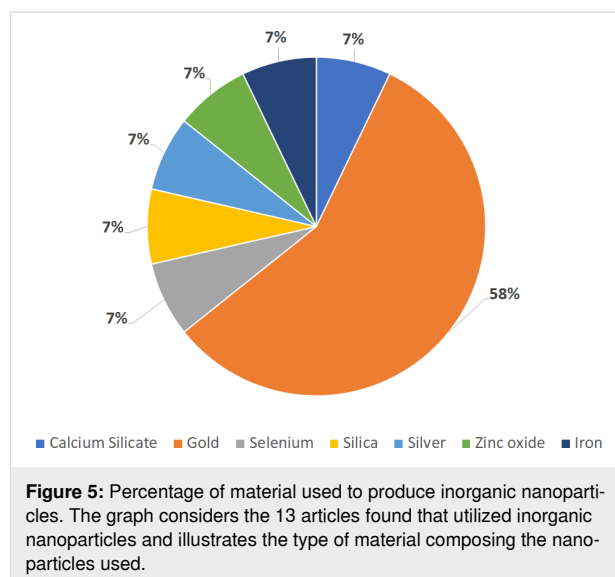
Solid lipid nanoparticles (SLN) are solid lipid matrices at room and body temperature [35]. Their advantages are similar to classic nanocarriers, such as protection of labile drugs from biodegradation process, excellent excipient tolerability, and prolonged release. In addition, some disadvantages of the classic nanocarriers are not present in SLN, such as lack of biocompatibility, difficulty to produce on a large scale, and high raw material cost [36]. Many methods are used to prepare SLN, and they are divided into (1) high-energy methods, for dispersion of the lipid phase (such as high-pressure homogenization); (2) low-energy methods, which requires the precipitation of nanoparticles from homogeneous systems (such as microemulsions); and (3) methods based on organic solvents (emulsification–diffusion method) [35].

Liposomes are vesicles composed of a phospholipid and cholesterol with an aqueous core. It can have one or multiple layers. Due to that, their size can range from 30 nm to the micrometer range [37]. As drug vehicles, they exhibit unique properties, such as protection of encapsulated compounds from physiological degradation, extended drug half-life, controlled release of the drug molecule, and excellent biocompatibility and safety [38]. Liposomes can also be modified to selectively deliver a drug to a specific site. This is very valuable because it can reduce potential side effects and increase the maximum tolerated dose, which improves therapeutic benefits [39]. For example, Adekiya et al. [40] produced PZQ encapsulated in nanoliposomes whose surface was modified with an antibody against calpain, a protein found in the tegument of the parasite and is upregulated in the regions where host–parasite interaction occurs [41]. The modified nanoparticles orally administered two or four weeks postinfection altered the drug release pattern in vitro, were more efficient in reducing worm burden and the

amount of eggs in the gut than PZQ alone, and altered the oogram pattern with the predominant presence of dead eggs. In addition, the nanoformulation showed no relevant toxicity in in vitro and in vivo models. Finally, the author discusses the possibility that the nanoformulation could be used to treat cases of schistosomiasis in the brain due to its smaller size [40]. Nevertheless, it is noteworthy that oral administration of biodegradable nanoparticles, such as conventional liposomes, exposes them to degradation by stomach acid, bile salts, and enzymes. Consequently, in in vivo models, intact liposomes may encounter challenges to reach the bloodstream owing to the adverse conditions of the stomach [42]. This elucidates why, in in vitro tests, the author exclusively assessed the release pattern of praziquantel by liposomes, omitting an examination of the impact of intact nanoparticles on the parasite, a facet explored by other researchers. Importantly, it is well known in the literature that modifications can be made to conventional liposomes to render these nanoparticles resistant to gastrointestinal barriers, representing another avenue of opportunity for the presented nanoformulation [42].

Niosomes are nanosystems similar to liposomes but formed using non-ionic surfactants like Span 60 [43]. They also could incorporate cholesterol in their structure beyond other lipids such as liposomes [44]. Therefore, they are able to be used as a carrier of amphiphilic or lipophilic drugs [45]. The main advantages of using this type of system are that they are osmotically active and stable and increase the stability of the entrapped drug. They could be used in oral, parenteral, and topical routes, and they are biodegradable, biocompatible, and non-immunogenic [45]. Moreover, they improve the therapeutic performance of the drug by protecting it from the biological environment and restricting effects to target cells, thereby reducing the clearance of the drug [45].

Drugs for treatment of schistosomiasis
Praziquantel
It is not surprising that praziquantel is the most encapsulated drug. It remains the only effective frontline medicine to treat the disease, and is currently characterized by its exclusive and extensive use as an important antischistosomal drug [46]. However, PZQ also brings disadvantages, such as occurrence of resistant strains, low bioavailability [47], and organoleptic characteristics such as bitter taste [29,48]. In the literature, it is described that nanoformulations approaches can overcome these drawbacks.

Most publications used nanotechnology to alter pharmacokinetics parameters. The nanoformulations were evaluated through efficacy criteria (e.g., parasite burden, egg counts, and granuloma diameter) or using traditional pharmacokinetics pa-

rameters (e.g., absorption rate or bioavailability). For example, Labib El Gendy et al. [49] showed that PZQ encapsulated in liposomes (500 mg/kg) could be more efficient than free PZQ treatment. Similar results have been shown in other works that also used liposome with PZQ in different concentrations [50-53]. In addition, Xie et al. [54] studied the pharmacokinetics of solid lipid nanoparticles composed of castor oil encapsulating PZQ. They observed that the drug took more than one week in vitro to be released. A pharmacokinetic study in vivo also showed that the PZQ concentration in the plasma was sustained for longer times when the nanoformulation was studied in mice. Thus, the results show that solid lipid nanoparticles increase bioavailability in all administration routes tested (oral, subcutaneous, and intramuscular). However, results showed that subcutaneous delivery was superior to oral and intramuscular, promoting the longest therapeutic concentration in the circulation (264h) and the highest bioavailability.

There is just one formulation of PZQ developed for pediatric use which is commercially available: Epiquantel (40 mg/kg), a liquid formulation produced by Eipico, an Egyptian pharmacy industry. However, this medicine is not distributed by WHO and, thus, few works tried to use nanotechnology to change the organoleptic properties of PZQ [8,48]. da Fonseca et al. [8] used poly(methyl methacrylate) nanoparticles loaded with PZQ produced by in situ mini emulsion polymerizations to mask the drug taste and develop an oral formulation. Although the taste was masked, the authors reported a gritty tongue sensation caused by the high solid content of the formulation. In vitro results were satisfactory and showed that the nanoformulation was effective against parasites, but in vivo results were inadequate due to fluctuations in the administered dose. Despite that, the work showed that this nanoformulation could be used in the future [8]. In another work, Gonzalez et al. [48] increased the dissolution of PZQ by producing nanocrystals through high-pressure homogenization, followed by drying through spray-drying. After that, they resuspended the powder in Oral plus® and Oral Sweet®, which are suspension vehicles known for their sweet taste and suitability for pediatric formulations [48].

Finally, few works tried to combine PZQ nanoformulations with other drugs/treatments [52,55]. Frezza et al. [52] tested PZQ-liposomes (oral route, 100 mg/kg) with hyperbaric oxygen and observed that it reduced the number of worms in mice. The combination also reduced the oviposition, changed the oogram pattern, and caused alteration in parasite tegument [52]. Eissa et al. [55] proved that a nanoformulation combining PZQ (250 mg/kg) and miltefosine (20 mg/kg) was efficient against all stages of the parasites, including juvenile forms. It was also noted alterations in parasite tegument and a reduction in granulomatous reactions in murine liver.

Although finding new forms to improve PZQ characteristics is essential, it would not solve the problem once only this drug is available to treat the disease and resistant strains are described. Therefore, finding new approaches with new drugs is crucial to raise treatment possibilities. Despite the fact that PZQ is the most encapsulated drug and most of the reviews about schistosomiasis only focus on it, we would like to bring to this review other drugs that are being studied.

Plant-derived drugs

After PZQ, most of the works in the literature involved plant-derived compounds. Guimarães et al. [56] tested the efficiency of epiisopiloturine in vitro and the best way to extract this molecule from leaves. Epiisopiloturine is an imidazole alkaloid found in jaborandi leaves (*Pilocarpus microphyllus*), which has known activity against adult, young, and egg forms of *Schistosoma mansoni* [57]. Since this is an apolar molecule with poor solubility, the author proposed a nanosystem using liposomes to make this molecule more useful in schistosomiasis therapy. The results showed that epiisopiloturine (300 µg/mL) has an effect in vitro, but it is not superior to PZQ. However, other nanotechnological approaches can potentialize the effect of the drug. Therefore, further studies should be made. Furthermore, the results showed that epiisopiloturine was not toxic to mice peritoneal cells, which is an encouraging prognosis for the development of future products [56].

Curcumin is a naturally yellow pigment obtained from the rhizomes of *Curcuma longa*. In the literature, many articles explore anti-inflammatory, antioxidant, antiviral, anti-infectious, and antitumoral properties of curcumin [58]. Mokbel et al. [59] showed that curcumin associated with a half-dose of PZQ and gold nanoparticles reduced the worm load in infected mice more than PZQ alone. This information is crucial since most side effects presented by patients who use PZQ could be avoided if there was a way to reduce the drug dose. Despite that, the combination could not reduce egg count more than that with PZQ alone. Nonetheless, the author affirms in the presentation of their results that the combination is more effective than the use of PZQ alone in this aspect [59].

Luz et al. [58] showed that curcumin encapsulated by polymeric nanoparticles could kill 100% of adult worms in vitro at a concentration of 100 µM. Lower concentrations reduced motility and caused tegumental alterations and couple separation [58]. However, curcumin has low bioavailability and poor water solubility. Thus, Aly et al. [60] tried to increase its solubility and permeability through the cellular membrane by making a nanoemulsion of *Curcuma longa* extract (i.e., the curcumin plant source). The nanoemulsion showed an effect against adults of *S. mansoni* in vitro (especially males). This is an inter-

esting finding because data from the literature reports that females are usually more susceptible to drug action than males. However, in this work, the death of females was only possible in a high concentration of the nanoformulation (100 µg/mL). Every dosage tested was also effective against young forms (esquistosomules) [60].

El-Menyawy et al. [61] used thymoquinone, a bioactive compound isolated from *Nigella sativa*, encapsulated in chitosan nanoparticles. The nanoformulation reduces the worm load in mice by 60% (predominantly female) and the number of couples found in vivo. Although the results showed a clear difference between control groups and the groups treated with nanoparticles, the author considered the results not good enough since other works showed a more prominent reduction [62]. Regarding egg counts in the liver and intestine, the nanoformulation was more efficient than blank particles which shows the relevance of nanoparticle for drug delivery. The histopathological exam also showed that nanoparticles could reduce the number and size of granulomas and diminish changes caused by infection. Although these results are very promising and interesting, the author does not mention the way in which the formulation was administered, which prevents a more critical analysis by the reader [61].

Elawamy et al. [63] also used *N. sativa* in their work, but instead of using one specific compound, they used the whole extract from this plant and encapsulated it in chitosan nanoparticles. The results showed that it is possible to diminish the worm load and change the oogram pattern in mice using the oral nanoformulation alone or with PZQ. Furthermore, the nanoparticle alone had a more significant effect than that for when the extract was administered with PZQ regarding granuloma formation, reducing the number and diameter of granulomas. Thus, *N. sativa* extract associated with chitosan nanoparticles may be a pharmacological strategy to replace PZQ or to help lower its dosage. However, the author admits in this work that no data proves the biological safety of using chitosan in a nanoformulation [63].

While on the subject, other extracts of vegetal sources were also studied to treat schistosomiasis by using a nanotechnological approach. A method using ultracentrifugation and ultrasonic dispersion produced ginger (*Zingiber officinale*) extract-derived nanoparticles which an average size of 238.3 nm [64]. The author justified his choice to use this kind of nanoparticles, claiming that they are less expensive than conventional ones, and in the literature, they were already used to treat inflammatory diseases [65,66]. Data proved that these nanoparticles orally administered in mice reduced the worm load, but not more than PZQ or mefloquine. However, when ginger-derived nanoparti-

cles were combined with a half-dose of mefloquine, the reduction in worm load was 100% even in a short time of infection (6 weeks). This combination also causes a reduction of 100% in hepatic and intestinal egg counts in the same period, in addition to showing a hepatoprotective effect conserving the typical tissue structure. Regarding granuloma formation, the combination was also efficient, although another combination using ginger-derived nanoparticles and PZQ caused a more significant effect than the total dose of PZQ. In addition to this, ginger-derived nanoparticles alone or combined with other drugs were able to cause alterations in parasite tegument [64].

Another work used carvacrol, a monoterpene present in essential oils derived from plants such as *Origanum vulgare*. Besides being commonly used as a flavoring agent in food and cosmetics, it shows antimicrobial activity. Xavier et al. [67] reported that nanoemulsions with carvacrol orally administered were able to reduce worm burden and eggs in feces more than PZQ in the prepatent period (21 days post-infection). This impressive result shows that this nanoformulation is more efficient in juvenile forms. The author also suggests that the mechanism by which the nanoemulsion could reduce the worm burden is its antimicrobial activity, connecting changes in microbiota with the response to parasites. However, the mechanism of action of carvacrol remains unknown [67].

Repositioned drugs

Works utilizing compounds repositioned from other diseases have also been found in our search. Miltefosine, for example, is a drug created to treat cutaneous metastasis from mammary carcinomas [68]. After that, it was also approved to treat leishmaniasis [69,70], and in 2011, Eissa et al. [71] verified that the drug has activity against different forms of *S. mansoni* in vivo. After that, the same group, in 2015, developed lipid nanocapsules positively charged (cationic) and tested them with and without oleic acid as a membrane permeabilizer in the composition. Both nanoformulations were able to reduce the whole treatment of schistosomiasis in mice to one single oral dose (20 mg/kg) [72]. In 2016, it was shown that despite both nanoformulations being effective, the formulation without oleic acid was more effective when administered on the first day of infection. On the other hand, oleic acid nanocapsules were more effective when administered 21 days after infection [73]. Late in 2020, while cationic lipid nanocapsules were hemolytic [72], the same group tested lipid nanocapsules with oleic acid on the membrane and miltefosine (20 mg/kg) alone or combined with PZQ. They reported that nanosystems containing miltefosine with or without PZQ were potent (when orally administered in mice) against all forms of *S. mansoni*, including juvenile forms. These nanosystems caused alterations in parasite tegument and reduced granulomatous reaction in the liver [55].

When administered by oral route in mice, celecoxib, a traditional non-steroidal inhibitor of cyclo-oxygenase used as an anti-inflammatory, analgesic, and antipyretic drug, was also effective against juvenile forms of *S. mansoni* when associated with solid lipid nanoparticles causing damage to parasite tegument [74].

Spironolactone is a diuretic drug mainly used to treat hypertension. Abd El Hady showed in vitro that polymeric nanoparticles were able to confer a sustained biphasic release pattern in comparison with that of spironolactone alone. Moreover, they proved in mice that orally administered nanoformulation was efficient against *S. mansoni* infection and induced significant reduction in spleen, liver indices, and total worm count, and it induced decline in the hepatic and small intestinal egg load. Finally, it also caused extensive damage to adult worms on tegument and suckers, leading to the death of the parasites in less time compared to that for the drug alone, and improve liver pathology [75].

Other compounds

Some of the selected works used new synthetic compounds in their formulation for schistosomiasis treatment. For example, 2-(butylamino)-1-phenyl-1-ethanethiosulfuric acid (BphEA) is a compound with poor solubility in water, which has demonstrated potential to be used in schistosomiasis treatment. Araújo et al. [76] developed a cationic nanoemulsion to increase solubility. This nanoemulsion increases efficiency in vitro, causing the death of female worms within three hours, alterations in tegument within 48 hours, and reduced male worm motility. A hypothesis suggested by the author is that the charge of nanoemulsion interacts with a negatively charged group in the tegument of parasites, facilitating drug delivery [76].

Articles utilizing synthetic drugs that were once used to treat schistosomiasis but, for safety reasons, were discontinued have also been found. Tartar emetic, for example, was part of the first class of compounds used to treat schistosomiasis [77]. However, due to their low therapeutic index and the rise of less toxic new drugs, it was discontinued. de Melo et al. [78] proved that pegylated liposomes could reduce toxicity and mortality of tartar emetic in mice even in high concentrations (27 mg Sb/kg). Although the mortality was reduced, drug efficiency remains unaltered, especially when the nanoformulation was intraperitoneally administered [78]. However, it is known that oral route adhesion is better than the others tested in this work (intraperitoneal and subcutaneous). Therefore, drug dosage forms with these characteristics may present compliance issues and problems with commercialization. Thus, an interesting pathway could be testing the same nanoformulations but using the oral route. After antimonials such as tartar emetic,

oxamniquine was released in the market, and with PZQ they remain as the drugs that can be used to treat schistosomiasis. However, signs of rising resistance to the drug slowed down the demand [78-82]. In 1997, Frézard and Melo [83] showed that liposomes with oxamniquine (10 mg/kg) subcutaneously applied efficiently reduce the worm load three to 14 days after infection (with a maximum reduction of 60%) in mice. These reports indicate that nanotechnological approaches may be a hope not only for PZQ or new compounds but also for bringing back improved versions of old medicines.

Amer et al. [43] used ubiquinol, a natural inhibitor of neutral magnesium-dependent sphingomyelinase, a key enzyme in sphingomyelin breakdown. This enzyme is essential because sphingomyelin is crucial in forming the outer leaflet of the tegumental lipid bilayer membrane in *Schistosoma mansoni* [43].

Araújo et al. [84] verified the activity of the sulfated polysaccharide α-D-glucan, a polysaccharide naturally found in extracts of lichen from *Ramalina celastri*. This work shows that liposomes with this carbohydrate could eliminate adult worms from infected mice 56 days post-infection when it was administered by the intraperitoneal route. The results also show that the nanoformulation reduced the number of eggs in feces of infected mice and hepatic granuloma in the liver. However, no difference between the nanoformulation and the controls was observed (sulfated polysaccharide α-D-glucan administered alone and empty liposomes). Furthermore, mice treated with sulfated polysaccharide α-D-glucan presented granulomas with histochemical markers, which could mean that this molecule stimulates the immunological system causing changes in membrane carbohydrates. Moreover, it raises the hypothesis that this change in the membrane molecule pattern is related to the reduction in granulomas. Finally, the author suggests that sulfated polysaccharide α-D-glucan could be used with other drugs with significantly higher effects against schistosomiasis, such as PZQ and oxamniquine, to stimulate the immunological system [83].

Oleic acid, a common unsaturated free fatty acid in the outer layer of human skin, is commonly used as a permeation promoter, inducing the disruption of the lipid structure of the membrane. de Oliveira et al. [85] showed in vitro that oleic acid encapsulated in polymeric nanoparticles could potentially be used in schistosomiasis treatment. Cytotoxicity assays confirm the compatibility of this fatty acid with biosystems, and in vitro results showed that nanoparticles reduced the time of action of free oleic acid in four to six hours. Oleic acid nanoparticles (50 μg/mL) caused 100% of mortality of adult worms in 24 hours, while neither empty nanoparticles nor raw oleic acid were able to yield the same mortality rate at the same time in

vitro. Doses lower than 50 μg/mL were able to cause worm separation and reduce motility. Doses higher than 25 μg/mL reduced oviposition when incubated for 24 hours. The results also show that even sublethal doses can cause alterations in parasite tegument [85].

Bee venom comprises various pharmacologically active components, including melittin (constituting more than 50% of total proteins) and a mixture of enzymes, cell-lytic peptides, proteases, and bioactive amines [86]. This mixture has antioxidant, anticoagulant, anti-bacterial, immunostimulatory, and hepatotoxic protection properties [87-89]. Because of that, it has been used in traditional medicine to treat inflammation and pain [90]. Mohamed et al. [91] reported that bee venom administered in infected mice reduces worm burden, ova count/liver, and granuloma diameter [91]. However, high concentrations of bee venom increase hepatic granuloma diameter. Thus, Badr et al. [92] tried to develop a nanoformulation approach to minimize the side effects of bee venom treatment. Polymeric nanoparticles created in their work allowed a sustained release and caused extreme changes in parasite tegument. In vivo, nanoparticles could reduce worm load and granuloma diameter and induce new biliary ducts. Nanoformulation was more effective in adult females than in juvenile forms and adult males [92].

Following the aforementioned studies, the majority of them (92%) utilized nanoformulations administered via the oral route. This outcome is unsurprising, as despite potential drawbacks such as first-pass metabolism, reduced bioavailability, and drug degradation throughout the digestive tract, the oral route is widely accepted and minimally invasive [93]. Consequently, releasing a new alternative to PZQ via a different route may not be the most advisable option, as it may not be well-received by patients, leading to potential commercialization challenges associated with a less familiar or less convenient delivery method.

Effectiveness tests

Effectiveness tests are important to demonstrate how powerful a drug is against the parasite. In previous sections it was detailed how certain studies demonstrated the effect of tested formulations. Overall, the parameters used to measure the in vitro efficacy of the treatment are reduction in mortality and mobility, couple separation, and tegument alterations. In vivo, the main criteria used is reducing worm burden, quantity and diameter of granuloma, eggs in feces, and oxidative stress markers (e.g., glutathione, nitrite/nitrate, and malondialdehyde).

Generally, articles that do not show effectiveness data use known drugs which have its effectivity attested, and aim to increase the dissolution of the drug in vitro [48,94]. Yang et al. [94] verified that PZQ nanocrystals had a more significant

dissolution rate than that of the conventional drug due to the particle size and, consequently, it also showed a bioavailability improvement. That is because bioavailability of orally administered drugs depends on their ability to be absorbed in the gastrointestinal tract. For class II drugs (e.g., PZQ) the absorption process is limited by drug dissolution rate in gastrointestinal media. Therefore, enhancement of the dissolution rate of these drugs will present improved bioavailability [95].

Other works do not show effectiveness tests because they are focused on evaluating pharmacokinetics. Cong et al. [96] showed that PZQ nanoemulsion has sustained drug release for a long time, both in vitro and in vivo. Mishra et al. [97] demonstrated similar conclusions using PZQ associated with solid lipid nanoparticles. Malhado et al. [98] concluded that PZQ associated with PMMA nanoparticles could not improve the pharmacokinetic curve. In fact, the absorption of the encapsulated drug was three times lower than that for conventional PZQ.

Other works do not address effectiveness tests because they evaluate the impact of nanosystems in physiological/pathological changes caused by *S. mansoni*. Dkhil et al. [32] showed that metallic nanoparticles could decrease all intestinal changes caused by the parasite. The nanoparticles avoided weight gain in infected mice, increased glutathione levels, and reduced the levels of oxidative stress markers. This work showed that selenium nanoparticles were even more effective than PZQ, reducing inflammation signs in jejunal tissue and tissue injury levels similarly to PZQ. El-Shorbagy et al. [34] showed that the treatment with gold nanoparticles decreased the granuloma index, but with less effectiveness in comparison to PZQ at concentrations of 2.5, and 1.25 µM/mL. Overall, the nanoparticles exhibited antioxidant effects in vitro.

Toxicity tests

Toxicity testing is essential to guarantee the safety of the treatment. Most articles have dealt with cytotoxicity testing in vitro or acute toxicity testing in vivo. Others deviated from traditional methods and used genotoxicity testing and mitochondrial metabolism evaluation to assess this. However, toxicity data were not reported in most of the articles. Although no explanation has been given in the articles regarding the absence of safety tests, there are possible reasons to explain why some tests are missing. Many articles use compounds that already have their safety stablished (e.g., PZQ or repurposed drugs) which have been approved before and their side effects are known. This was also the case in the Amer et al. [99] article in which ubiquinol, a natural compound approved as a dietary supplement, was used. Therefore, the safety tests were deemed unnecessary. Many papers that did not provide toxicity data concerning nanosystems referred to previous articles in which safety

testing was performed. However, it is important to highlight that even nanosystems that were tested before must be tested again if the study uses a different experimentation design (different drug concentrations, different methods to produce nanoparticles, or a different therapeutical scheme). Numerous articles in our research have substantiated this information. For instance, the study conducted by Amara et al. [100] in 2018 demonstrated that diverse compositions of lipid nanocapsules resulted in varying IC_{50} values. Additionally, this research revealed that the IC_{50} value of encapsulated PZQ was considerably higher than that of PZQ administered alone, underscoring the significance of conducting toxicity testing even for well-known drugs. That means that part of the articles selected in this review still must prove the safety of their nanoformulations. This is the only way for the product to advance to the next stages, such as clinical phase.

In fact, none of the papers in this work was in clinical trials, reflecting the small number of nanosystems that enter the clinical phase. This probably happens not only because many of these works do not present safety data, but also because of the high costs of clinical trials [101]. As a neglected disease, schistosomiasis does not have the investment necessary by the private sector. Nevertheless, schistosomiasis remains a disease with a big economic impact, especially in underdeveloped and developing nations. For example, in 2015, its impact costs US$ 41,7 million to Brazil [102].

Moreover, it is imperative to address the additional complexities associated with nanoparticle formulations. While it is evident that manufacturing nanoparticles incurs high costs, it is essential to highlight other intricacies related to these formulations. Despite none of the authors explicitly mentioning stability challenges as a concern in the nanoparticle manufacturing process, especially in tropical regions characterized by elevated temperatures and humidity, it is a critical aspect to consider. Such environmental conditions pose formidable obstacles to the effective deployment of these formulations [103]. Furthermore, upscaling presents a significant issue. As demonstrated in previous discussions, many of the articles employed production techniques that are challenging to scale up, with batch-to-batch variations further complicating the manufacturing process [104]. As a result, achieving a consistent and reproducible manufacturing process becomes a daunting task in the realm of nanoparticle formulations.

Thus, regardless of the reasons for the challenges in bringing nanoformulations to the market, the responsibility falls on the government to make concerted efforts and provide the necessary support to overcome economic and other barriers. This support is crucial for aiding research institutions in introducing

new products to the market, which can effectively mitigate the impact of the disease in those countries.
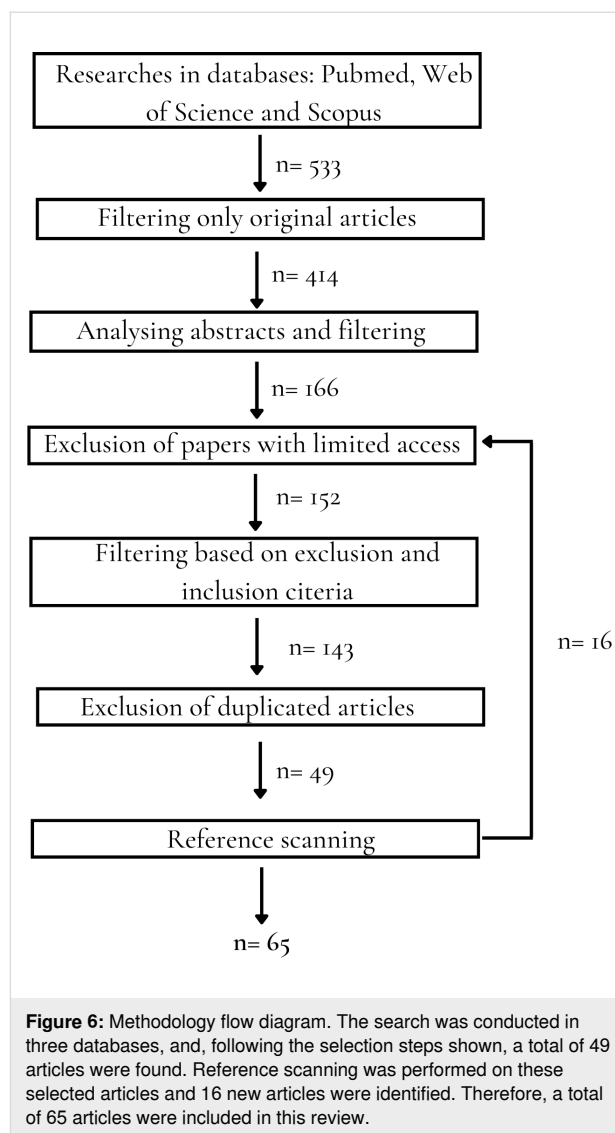
Conclusion

In this review, we selected 65 papers using three databases: Pubmed, Scopus, and Web of Science; and the reference within the selected papers. This is a great number since none of the recent reviews have brought this amount of articles on this topic [13,15,105] together. This is due to the methodology used in this paper, which included a reference scanning stage, responsible for 25% of the articles found. Moreover, our strategy allowed us to include articles not included in any of the previous reviews, proving that our method is more inclusive.

Inorganic and polymeric nanoparticles are among the most widely utilized nanotechnological systems. Most research articles utilized gold nanoparticle as inorganic nanoparticles, while PLGA and chitosan are commonly utilized to produce polymeric nanoparticles due to its biocompatibility reported in various animal studies. However, there is currently a lack of data to support the safety of chitosan formulations for human use.

Most of the articles reported superior results to PZQ in preclinical tests; however, no article was found in clinical phase. One of the reasons for that is the low financial support to treat schistosomiasis since it is a neglected disease. Nonetheless, there is big diversity of solutions with great potential to be superior to PZQ using nanotechnological resources. However, governmental investment is necessary for these nanomedicines to achieve full potential.

Experimental

Searches were done in Pubmed, Scopus, and Web of Science databases. These searches were conducted from March 31st, 2022, to March 31st, 2023, using the following search keywords: (nano* OR encapsul*) AND (treatment OR therap* OR activity OR chemotherapy) AND schistosomiasis. After obtaining the list of papers, a filter by type of article was applied, selecting only original research and excluding reviews. After that, the titles and abstracts were read, and articles unrelated to the theme were excluded. Afterward, it was checked if there was access to the remaining work. For those that could not be accessed, attempts were made to contact the authors and ask for a copy. The available articles were read entirely, and those unrelated to the theme were excluded. For exclusion, the criteria used were: (1) particle size over 999 nm; (2) articles that approach only prophylactic nanoformulations. After that, a search in the references of the selected papers was done to guarantee the maximal articles related to the theme in this review (Figure 6).

Figure 6: Methodology flow diagram. The search was conducted in three databases, and, following the selection steps shown, a total of 49 articles were found. Reference scanning was performed on these selected articles and 16 new articles were identified. Therefore, a total of 65 articles were included in this review.

Supporting Information

As supporting information we provide Table S1 cited in the results. This table shows the articles found using our methodology.

Supporting Information File 1
Nanosystems with their encapsulated drugs found in open access articles.
[https://www.beilstein-journals.org/bjnano/content/supplementary/2190-4286-15-2-S1.pdf]

ORCID® iDs

Lucas Carvalho - https://orcid.org/0000-0003-0504-7564

References

1. Kokaliaris, C.; Garba, A.; Matuska, M.; Bronzan, R. N.; Colley, D. G.; Dorkenoo, A. M.; Ekpo, U. F.; Fleming, F. M.; French, M. D.; Kabore, A.; Mbonigaba, J. B.; Midzi, N.; Mwinzi, P. N. M.; N'Goran, E. K.; Polo, M. R.; Sacko, M.; Tchuem Tchuenté, L.-A.; Tukahebwa, E. M.; Uvon, P. A.; Yang, G.; Wiesner, L.; Zhang, Y.; Utzinger, J.; Vounatsou, P. *Lancet Infect. Dis.* **2022,** *22,* 136–149. doi:10.1016/s1473-3099(21)00090-6

2. Hotez, P. J.; Alvarado, M.; Basáñez, M.-G.; Bolliger, I.; Bourne, R.; Boussinesq, M.; Brooker, S. J.; Brown, A. S.; Buckle, G.; Budke, C. M.; Carabin, H.; Coffeng, L. E.; Fèvre, E. M.; Fürst, T.; Halasa, Y. A.; Jasrasaria, R.; Johns, N. E.; Keiser, J.; King, C. H.; Lozano, R.; Murdoch, M. E.; O'Hanlon, S.; Pion, S. D. S.; Pullan, R. L.; Ramaiah, K. D.; Roberts, T.; Shepard, D. S.; Smith, J. L.; Stolk, W. A.; Undurraga, E. A.; Utzinger, J.; Wang, M.; Murray, C. J. L.; Naghavi, M. *PLoS Negl. Trop. Dis.* **2014,** *8,* e2865. doi:10.1371/journal.pntd.0002865

3. Verjee, M. A. *Res. Rep. Trop. Med.* **2019,** *10,* 153–163. doi:10.2147/rrtm.s204345

4. Crosby, A.; Jones, F. M.; Kolosionek, E.; Southwood, M.; Purvis, I.; Soon, E.; Butrous, G.; Dunne, D. W.; Morrell, N. W. *Am. J. Respir. Crit. Care Med.* **2011,** *184,* 467–473. doi:10.1164/rccm.201101-0146oc

5. Secor, W. E.; Montgomery, S. P. *Future Med. Chem.* **2015,** *7,* 681–684. doi:10.4155/fmc.15.9

6. Maragos, S.; Archontaki, H.; Macheras, P.; Valsami, G. *AAPS PharmSciTech* **2009,** *10,* 1444–1451. doi:10.1208/s12249-009-9346-7

7. Sanchez, M. C.; Cupit, P. M.; Bu, L.; Cunningham, C. *Mol. Biochem. Parasitol.* **2019,** *228,* 6–15. doi:10.1016/j.molbiopara.2018.12.005

8. da Fonseca, L. B.; Viçosa, A. L.; Mattos, A. C. A.; Coelho, P. M. Z.; Araújo, N.; Zamith, H. D. S.; Volpato, N. M.; Nele, M.; Pinto, J. C. C. S. *Vigil. Sanit. Debate* **2013,** *1,* 85–91. doi:10.3395/vd.v1i4.111en

9. Olliaro, P. L.; Vaillant, M. T.; Belizario, V. J.; Lwambo, N. J. S.; Ouldabdallahi, M.; Pieri, O. S.; Amarillo, M. L.; Kaatano, G. M.; Diaw, M.; Domingues, A. C.; Favre, T. C.; Lapujade, O.; Alves, F.; Chitsulo, L. *PLoS Negl. Trop. Dis.* **2011,** *5,* e1165. doi:10.1371/journal.pntd.0001165

10. Tawfeek, G. M.; Baki, M. H. A.; Ibrahim, A. N.; Mostafa, M. A. H.; Fathy, M. M.; Diab, M. S. E. D. M. *Parasitol. Res.* **2019,** *118,* 3519–3533. doi:10.1007/s00436-019-06475-8

11. Moniruzzaman, M.; Min, T. *Pharmaceutics* **2020,** *12,* 447. doi:10.3390/pharmaceutics12050447

12. Abaza, S. M. *Parasitol. United J.* **2016,** *9,* 1.

13. Adekiya, T. A.; Kondiah, P. P. D.; Choonara, Y. E.; Kumar, P.; Pillay, V. *Front. Bioeng. Biotechnol.* **2020,** *8,* 32. doi:10.3389/fbioe.2020.00032

14. Mengarda, A. C.; Iles, B.; Longo, J. P. F.; de Moraes, J. *Expert Opin. Drug Delivery* **2022,** *19,* 383–393. doi:10.1080/17425247.2022.2051477

15. Tomiotto-Pellissier, F.; Miranda-Sapla, M. M.; Machado, L. F.; Bortoleti, B. T. d. S.; Sahd, C. S.; Chagas, A. F.; Assolini, J. P.; Oliveira, F. J. d. A.; Pavanelli, W. R.; Conchon-Costa, I.; Costa, I. N.; Melanda, F. N. *Acta Trop.* **2017,** *174,* 64–71. doi:10.1016/j.actatropica.2017.06.025

16. Idrees, H.; Zaidi, S. Z. J.; Sabir, A.; Khan, R. U.; Zhang, X.; Hassan, S.-u. *Nanomaterials* **2020,** *10,* 1970. doi:10.3390/nano10101970

17. Zielińska, A.; Carreiró, F.; Oliveira, A. M.; Neves, A.; Pires, B.; Venkatesh, D. N.; Durazzo, A.; Lucarini, M.; Eder, P.; Silva, A. M.; Santini, A.; Souto, E. B. *Molecules* **2020,** *25,* 3731. doi:10.3390/molecules25163731

18. Patra, J. K.; Das, G.; Fraceto, L. F.; Campos, E. V. R.; Rodriguez-Torres, M. d. P.; Acosta-Torres, L. S.; Diaz-Torres, L. A.; Grillo, R.; Swamy, M. K.; Sharma, S.; Habtemariam, S.; Shin, H.-S. *J. Nanobiotechnol.* **2018,** *16,* 71. doi:10.1186/s12951-018-0392-8

19. Krishnamoorthy, K.; Mahalingam, M. *Adv. Pharm. Bull.* **2015,** *5,* 57–67.

20. Deng, S.; Gigliobianco, M. R.; Censi, R.; Di Martino, P. *Nanomaterials* **2020,** *10,* 847. doi:10.3390/nano10050847

21. Park, K.; Skidmore, S.; Hadar, J.; Garner, J.; Park, H.; Otte, A.; Soh, B. K.; Yoon, G.; Yu, D.; Yun, Y.; Lee, B. K.; Jiang, X.; Wang, Y. *J. Controlled Release* **2019,** *304,* 125–134. doi:10.1016/j.jconrel.2019.05.003

22. Mohammed, M. A.; Syeda, J. T.; Wasan, K. M.; Wasan, E. K. *Pharmaceutics* **2017,** *9,* 53. doi:10.3390/pharmaceutics9040053

23. dos Santos, J.; da Silva, G. S.; Velho, M. C.; Beck, R. C. R. *Pharmaceutics* **2021,** *13,* 1424. doi:10.3390/pharmaceutics13091424

24. de Oliveira, H. P.; Tavares, G. F.; Nogueiras, C.; Rieumont, J. *Int. J. Pharm.* **2009,** *380,* 55–61. doi:10.1016/j.ijpharm.2009.06.028

25. Nasirzadeh, K.; Nazarian, S.; Gheibi Hayat, S. M. *J. Appl. Biotechnol. Rep.* **2016,** *3,* 395–402. https://www.biotechrep.ir/article_69208.html

26. Kar, P. K.; Murmu, S.; Saha, S.; Tandon, V.; Acharya, K. *PLoS One* **2014,** *9,* e84693. doi:10.1371/journal.pone.0084693

27. Dkhil, M. A.; Bauomy, A. A.; Diab, M. S.; Al-Quraishy, S. *Int. J. Nanomed.* **2015,** *10,* 7467. doi:10.2147/ijn.s97622

28. Dkhil, M. A.; Bauomy, A. A.; Diab, M. S. M.; Wahab, R.; Delic, D.; Al-Quraishy, S. *Parasitol. Res.* **2015,** *114,* 3711–3719. doi:10.1007/s00436-015-4600-2

29. Dkhil, M. A.; Bauomy, A. A.; Diab, M. S.; Al-Quraishy, S. *Biomed. Res.* **2016,** *27,* 214–219.

30. Dkhil, M. A.; Khalil, M. F.; Bauomy, A. A.; Diab, M. S. M.; Al-Qura, S. *Biomed. Environ. Sci.* **2016,** *29,* 773–781. doi:10.3967/bes2016.104

31. Dkhil, M. A.; Khalil, M. F.; Diab, M. S. M.; Bauomy, A. A.; Al-Quraishy, S. *Saudi J. Biol. Sci.* **2017,** *24,* 1418–1423. doi:10.1016/j.sjbs.2016.12.017

32. Dkhil, M. A.; Khalil, M. F.; Diab, M. S. M.; Bauomy, A. A.; Santourlidis, S.; Al-Shaebi, E. M.; Al-Quraishy, S. *Saudi J. Biol. Sci.* **2019,** *26,* 1468–1472. doi:10.1016/j.sjbs.2018.02.008

33. Bauomy, A. A. *Environ. Sci. Pollut. Res.* **2020,** *27,* 18699–18707. doi:10.1007/s11356-020-08356-5

34. El-Shorbagy, A.; Gamil, I. S.; Mohey, M. A.; Nady, S. *Nanomed. J.* **2019,** *6,* 19–26. doi:10.22038/nmj.2019.06.003

35. Hernández-Esquivel, R.-A.; Navarro-Tovar, G.; Zárate-Hernández, E.; Aguirre-Bañuelos, P. Solid Lipid Nanoparticles (SLN). In *Nanocomposite Materials for Biomedical and Energy Storage Applications;* Sharma, S., Ed.; IntechOpen, 2022. doi:10.5772/intechopen.102536

36. Priyadarshani, A. *J. Nanomed. Biother. Discovery* **2022,** *12,* 173. https://www.longdom.org/open-access/advantages-and-disadvantages-of-solid-lipid-nanoparticles-96893.html

37. Mazur, F.; Bally, M.; Städler, B.; Chandrawati, R. *Adv. Colloid Interface Sci.* **2017,** *249,* 88–99. doi:10.1016/j.cis.2017.05.020

38. Niu, M.; Lu, Y.; Hovgaard, L.; Guan, P.; Tan, Y.; Lian, R.; Qi, J.; Wu, W. *Eur. J. Pharm. Biopharm.* **2012,** *81,* 265–272. doi:10.1016/j.ejpb.2012.02.009

39. Liu, P.; Chen, G.; Zhang, J. *Molecules* **2022,** *27,* 1372. doi:10.3390/molecules27041372

40. Adekiya, T. A.; Kumar, P.; Kondiah, P. P. D.; Choonara, Y. E. *Pharmaceutics* **2022,** *14,* 1531. doi:10.3390/pharmaceutics14081531

41. Siddiqui, A. A.; Zhou, Y.; Podesta, R. B.; Karcz, S. R.; Tognon, C. E.; Strejan, G. H.; Dekaban, G. A.; Clarke, M. W. *Biochim. Biophys. Acta, Mol. Basis Dis.* **1993,** *1181,* 37–44. doi:10.1016/0925-4439(93)90087-h

42. He, H.; Lu, Y.; Qi, J.; Zhu, Q.; Chen, Z.; Wu, W. *Acta Pharm. Sin. B* **2019,** *9,* 36–48. doi:10.1016/j.apsb.2018.06.005

43. Amer, E. I.; El-Azzouni, M. Z.; El-Bannan, R. T.; Shalaby, T. I.; El-Achy, S. N.; Gomaa, M. M. *Acta Trop.* **2022,** *226,* 106231. doi:10.1016/j.actatropica.2021.106231

44. Zoghroban, H. S.; El-Kowrany, S. I.; Aboul Asaad, I. A.; El Maghraby, G. M.; El-Nouby, K. A.; Abd Elazeem, M. A. *Parasitol. Res.* **2019,** *118,* 219–234. doi:10.1007/s00436-018-6132-z

45. Pola Chandu, V.; Arunachalam, A.; Jeganath, S.; Yamini, K.; Tharangini, K. *Int. J. Novel Trends Pharm. Sci.* **2012,** *2,* 25–31. https://scienztech.org/index.php/ijntps/article/view/58

46. Cioli, D.; Pica-Mattoccia, L.; Basso, A.; Guidi, A. *Mol. Biochem. Parasitol.* **2014,** *195,* 23–29. doi:10.1016/j.molbiopara.2014.06.002

47. Olliaro, P.; Delgado-Romero, P.; Keiser, J. *J. Antimicrob. Chemother.* **2014,** *69,* 863–870. doi:10.1093/jac/dkt491

48. Gonzalez, M. A.; Ramírez Rigo, M. V.; Gonzalez Vidal, N. L. *AAPS PharmSciTech* **2019,** *20,* 318. doi:10.1208/s12249-019-1548-z

49. Labib El Gendy, A. E. M.; Mohammed, F. A.; Abdel-Rahman, S. A.; Shalaby, T. I. A.; Fathy, G. M.; Mohammad, S. M.; El-Shafey, M. A.; Mohammed, N. A. *J. Parasit. Dis.* **2019,** *43,* 416–425. doi:10.1007/s12639-019-01106-6

50. Frezza, T. F.; Madi, R. R.; Banin, T. M.; Pinto, M. C.; de Souza, A. L. R.; Gremião, M. P. D.; Allegretti, S. M. *Rev. Cienc. Farm. Basica Apl.* **2007,** *28,* 209–214.

51. Frezza, T. F.; Gremião, M. P. D.; Zanotti-Magalhães, E. M.; Magalhães, L. A.; de Souza, A. L. R.; Allegretti, S. M. *Acta Trop.* **2013,** *128,* 70–75. doi:10.1016/j.actatropica.2013.06.011

52. Frezza, T. F.; de Souza, A. L. R.; Ribeiro Prado, C. C.; de Oliveira, C. N. F.; Gremião, M. P. D.; Giorgio, S.; Dolder, M. A. H.; Joazeiro, P. P.; Allegretti, S. M. *Acta Trop.* **2015,** *150,* 182–189. doi:10.1016/j.actatropica.2015.07.022

53. Mourão, S. C.; Costa, P. I.; Salgado, H. R. N.; Gremião, M. P. D. *Int. J. Pharm.* **2005,** *295,* 157–162. doi:10.1016/j.ijpharm.2005.02.009

54. Xie, S.; Pan, B.; Wang, M.; Zhu, L.; Wang, F.; Dong, Z.; Wang, X.; Zhou, W. *Nanomedicine (London, U. K.)* **2010,** *5,* 693–701. doi:10.2217/nnm.10.42

55. Eissa, M. M.; El-Azzouni, M. Z.; El-Khordagui, L. K.; Abdel Bary, A.; El-Moslemany, R. M.; Abdel Salam, S. A. *Parasites Vectors* **2020,** *13,* 474. doi:10.1186/s13071-020-04346-1

56. Guimarães, M. A.; Campelo, Y. D. M.; Véras, L. M. C.; Colhone, M. C.; Lima, D. F.; Ciancaglini, P.; Kuckelhaus, S. S.; Lima, F. C. A.; de Moraes, J.; de S. A. Leite, J. R. *J. Nanosci. Nanotechnol.* **2014,** *14,* 4519–4528. doi:10.1166/jnn.2014.8248

57. Veras, L. M.; Guimaraes, M. A.; Campelo, Y. D.; Vieira, M. M.; Nascimento, C.; Lima, D. F.; Vasconcelos, L.; Nakano, E.; Kuckelhaus, S. S.; Batista, M. C.; Leite, J. R.; Moraes, J. *Curr. Med. Chem.* **2012,** *19,* 2051–2058. doi:10.2174/092986712800167347

58. Luz, P. P.; Magalhães, L. G.; Pereira, A. C.; Cunha, W. R.; Rodrigues, V.; Andrade e Silva, M. L. *Parasitol. Res.* **2012,** *110,* 593–598. doi:10.1007/s00436-011-2527-9

59. Mokbel, K. E.-D. M.; Baiuomy, I. R.; Sabry, A. E.-H. A.; Mohammed, M. M.; El-Dardiry, M. A. *Sci. Rep.* **2020,** *10,* 15742. doi:10.1038/s41598-020-72901-y

60. Aly, N.; Husseein, A.; Emam, H.; Rashed, G. *Parasitol. United J.* **2017,** *10,* 44–51. doi:10.21608/puj.2017.4736

61. El-Menyawy, H. M.; Metwally, K. M.; Aly, I. R.; Abo Elqasem, A. A.; Youssef, A. A. *Egypt. J. Hosp. Med.* **2021,** *84,* 1818–1826. doi:10.21608/ejhm.2021.177604

62. Sadek, G. S.; Harba, N.; Elrefai, S. A.; Sharaf el-Deen, S. A.; Saleh, M. M. *J. Egypt. Soc. Parasitol.* **2018,** *48,* 629–638. doi:10.21608/jesp.2018.76578

63. Elawamy, W. E.; Mohram, A. F.; Naguib, M. M.; Ali, H. S.; Kishik, S. M.; Hendawi, F. F. *J. Med. Plants Res.* **2019,** *13,* 443–451. doi:10.5897/jmpr2019.6842

64. Abd El Wahab, W. M.; El-Badry, A. A.; Mahmoud, S. S.; El-Badry, Y. A.; El-Badry, M. A.; Hamdy, D. A. *PLoS Negl. Trop. Dis.* **2021,** *15,* e0009423. doi:10.1371/journal.pntd.0009423

65. Zhuang, X.; Deng, Z.-B.; Mu, J.; Zhang, L.; Yan, J.; Miller, D.; Feng, W.; McClain, C. J.; Zhang, H.-G. *J. Extracell. Vesicles* **2015,** *4,* 10.3402/jev.v4.28713. doi:10.3402/jev.v4.28713

66. Zhang, M.; Collins, J. F.; Merlin, D. *Nanomedicine (London, U. K.)* **2016,** *11,* 3035–3037. doi:10.2217/nnm-2016-0353

67. Xavier, E. S.; de Souza, R. L.; Rodrigues, V. C.; Melo, C. O.; Roquini, D. B.; Lemes, B. L.; Wilairatana, P.; Oliveira, E. E.; de Moraes, J. *Front. Pharmacol.* **2022,** 13. doi:10.3389/fphar.2022.917363

68. Hilgard, P.; Klenner, T.; Stekar, J.; Unger, C. *Cancer Chemother. Pharmacol.* **1993,** *32,* 90–95. doi:10.1007/bf00685608

69. Soto, J.; Toledo, J.; Gutierrez, P.; Nicholls, R. S.; Padilla, J.; Engel, J.; Fischer, C.; Voss, A.; Berman, J. *Clin. Infect. Dis.* **2001,** *33,* e57–e61. doi:10.1086/322689

70. Ganguly, N. K. Oral miltefosine may revolutionize treatment of visceral leishmaniasis. *TDR news;* W.H.O., 2002; Vol. 68:2.

71. Eissa, M. M.; El-Azzouni, M. Z.; Amer, E. I.; Baddour, N. M. *Int. J. Parasitol.* **2011,** *41,* 235–242. doi:10.1016/j.ijpara.2010.09.010

72. Eissa, M. M.; El-Moslemany, R. M.; Ramadan, A. A.; Amer, E. I.; El-Azzouni, M. Z.; El-Khordagui, L. K. *PLoS One* **2015,** *10,* e0141788. doi:10.1371/journal.pone.0141788

73. El-Moslemany, R. M.; Eissa, M. M.; Ramadan, A. A.; El-Khordagui, L. K.; El-Azzouni, M. Z. *Acta Trop.* **2016,** *159,* 142–148. doi:10.1016/j.actatropica.2016.03.038

74. Ibrahim, E. I.; Abou-El-Naga, I. F.; El-Temsahy, M. M.; Elsawy, E. S. A.; Makled, S.; Mogahed, N. M. F. H. *Acta Trop.* **2022,** *229,* 106342. doi:10.1016/j.actatropica.2022.106342

75. Abd El Hady, W. E.; El-Emam, G. A.; Saleh, N. E.; Hamouda, M. M.; Motawea, A. *Int. J. Nanomed.* **2023,** *18,* 987–1005. doi:10.2147/ijn.s389449

76. de Araújo, S. C.; de Mattos, A. C. A.; Teixeira, H. F.; Coelho, P. M. Z.; Nelson, D. L.; de Oliveira, M. C. *Int. J. Pharm.* **2007,** *337,* 307–315. doi:10.1016/j.ijpharm.2007.01.009

77. Cioli, D.; Pica-Mattoccia, L.; Archer, S. *Pharmacol. Ther.* **1995,** *68,* 35–85. doi:10.1016/0163-7258(95)00026-7

78. de Melo, A. L.; Silva-Barcellos, N. M.; Demicheli, C.; Frézard, F. *Int. J. Pharm.* **2003,** *255,* 227–230. doi:10.1016/s0378-5173(03)00125-x

79. Cioli, D.; Pica-Mattoccia, L.; Archer, S. *Parasitol. Today* **1993,** *9,* 162–166. doi:10.1016/0169-4758(93)90138-6

80. Fallon, P. G.; Doenhoff, M. J. *Am. J. Trop. Med. Hyg.* **1994,** *51,* 83–88. doi:10.4269/ajtmh.1994.51.83

81. Bonesso-Sabadini, P. I. P.; Dias, L. C. d. S. *Mem. Inst. Oswaldo Cruz* **2002,** *97,* 381–385. doi:10.1590/s0074-02762002000300019

82. Sturrock, R. F. *Mem. Inst. Oswaldo Cruz* **2001,** *96,* 17–27. doi:10.1590/s0074-02762001000900003

83. Frézard, F.; de Melo, A. L. *Rev. Inst. Med. Trop. Sao Paulo* **1997,** *39,* 97–100. doi:10.1590/s0036-46651997000200006

84. Araújo, R. V. S.; Melo-Júnior, M. R.; Beltrão, E. I. C.; Mello, L. A.; Iacomini, M.; Carneiro-Leão, A. M. A.; Carvalho, L. B., Jr.; Santos-Magalhães, N. S. *Braz. J. Med. Biol. Res.* **2011,** *44,* 311–318. doi:10.1590/s0100-879x2011007500014

85. de Oliveira, R. N.; Campos, P. M.; Pinto, R. M. C.; Mioduski, J.; Santos, R. D.; Justus, B.; de Paula, J. d. F. P.; Klein, T.; Boscardin, P. M. D.; Corrêa, S. d. A. P.; Allegretti, S. M.; Ferrari, P. C. *J. Drug Delivery Sci. Technol.* **2021,** *63,* 102429. doi:10.1016/j.jddst.2021.102429

86. Saleh, A.; Badr, A.; Mahmoud, S.; Mahana, N.; Abo Dena, A. *Int. J. Vet. Sci.* **2020,** *9,* 473–475.

87. Zhang, S. F.; Shi, W. J.; Cheng, J. A.; Zhang, C. X. *Acta Genet. Sin.* **2003,** *30,* 861–866.

88. Gauldie, J.; Hanson, J. M.; Rumjanek, F. D.; Shipolini, R. A.; Vernon, C. A. *Eur. J. Biochem.* **1976,** *61,* 369–376. doi:10.1111/j.1432-1033.1976.tb10030.x

89. Habermann, E. *Science* **1972,** *177,* 314–322. doi:10.1126/science.177.4046.314

90. Doo, A.-R.; Kim, S.-T.; Kim, S.-N.; Moon, W.; Yin, C. S.; Chae, Y.; Park, H.-K.; Lee, H.; Park, H.-J. *Neurol. Res.* **2010,** *32,* 88–91. doi:10.1179/016164109x12537002794282

91. Mohamed, A. H.; Hassab El-Nabi, S. E.; Bayomi, A. E.; Abdelaal, A. A. *J. Parasit. Dis.* **2016,** *40,* 390–400. doi:10.1007/s12639-014-0516-5

92. Badr, A. M.; Saleh, A. H.; Mahmoud, S. S.; Mousa, M. R.; Mahana, N. A.; Abo Dena, A. S. *J. Drug Delivery Sci. Technol.* **2022,** *71,* 103344. doi:10.1016/j.jddst.2022.103344

93. Alqahtani, M. S.; Kazi, M.; Alsenaidy, M. A.; Ahmad, M. Z. *Front. Pharmacol.* **2021,** *12,* 618411. doi:10.3389/fphar.2021.618411

94. Yang, R.; Zhang, T.; Yu, J.; Liu, Y.; Wang, Y.; He, Z. *Asian J. Pharm. Sci.* **2019,** *14,* 321–328. doi:10.1016/j.ajps.2018.06.001

95. Dizaj, S. M.; Vazifehasl, Z.; Salatin, S.; Adibkia, K.; Javadzadeh, Y. *Res. Pharm. Sci.* **2015,** *10,* 95–108.

96. Cong, Z.; Shi, Y.; Peng, X.; Wei, B.; Wang, Y.; Li, J.; Li, J.; Li, J. *Drug Dev. Ind. Pharm.* **2017,** *43,* 558–573. doi:10.1080/03639045.2016.1270960

97. Mishra, A.; Vuddanda, P. R.; Singh, S. *J. Nanotechnol.* **2014,** *2014,* 351693. doi:10.1155/2014/351693

98. Malhado, M.; Pinto, D. P.; Silva, A. C. A.; Silveira, G. P. E.; Pereira, H. M.; Santos, J. G. F., Jr.; Guilarducci-Ferraz, C. V. V.; Viçosa, A. L.; Nele, M.; Fonseca, L. B.; Pinto, J. C. C. S.; Calil-Elias, S. *J. Pharm. Biomed. Anal.* **2016,** *117,* 405–412. doi:10.1016/j.jpba.2015.09.023

99. Amer, E. I.; Abou-El-Naga, I. F.; Boulos, L. M.; Ramadan, H. S.; Younis, S. S. *Biomédica* **2022,** *42,* 67–84. doi:10.7705/biomedica.5913

100. Amara, R. O.; Ramadan, A. A.; El-Moslemany, R. M.; Eissa, M. M.; El-Azzouni, M. Z.; El-Khordagui, L. K. *Int. J. Nanomed.* **2018,** *13,* 4493. doi:10.2147/ijn.s167285

101. Sertkaya, A.; Wong, H.-H.; Jessup, A.; Beleche, T. *Clin. Trials* **2016,** *13,* 117–126. doi:10.1177/1740774515625964

102. Nascimento, G. L.; Pegado, H. M.; Domingues, A. L. C.; Ximenes, R. A. d. A.; Itria, A.; Cruz, L. N.; Oliveira, M. R. F. d. *Mem. Inst. Oswaldo Cruz* **2019,** *114,* S0074-02762019000100304. doi:10.1590/0074-02760180347

103. Bott, R. F.; Oliveira, W. P. *Drug Dev. Ind. Pharm.* **2007,** *33,* 393–401. doi:10.1080/03639040600975022

104. Metselaar, J. M.; Lammers, T. *Drug Delivery Transl. Res.* **2020,** *10,* 721–725. doi:10.1007/s13346-020-00740-5

105. Islan, G. A.; Durán, M.; Cacicedo, M. L.; Nakazato, G.; Kobayashi, R. K. T.; Martinez, D. S. T.; Castro, G. R.; Durán, N. *Acta Trop.* **2017,** *170,* 16–42. doi:10.1016/j.actatropica.2017.02.019

License and Terms

Curcumin-loaded nanostructured systems for treatment of leishmaniasis: a review

Douglas Dourado[*1], Thayse Silva Medeiros[2], Éverton do Nascimento Alencar[3], Edijane Matos Sales[4] and Fábio Rocha Formiga[*1,5]

Address:
[1]Department of Immunology, Aggeu Magalhães Institute (IAM), Oswaldo Cruz Foundation (FIOCRUZ), 50670-420 Recife, PE, Brazil, [2]Department of Pharmacy, Federal University of Rio Grande do Norte (UFRN), 59010180, Natal, RN, Brazil, [3]College of Pharmaceutical Sciences, Food and Nutrition. Federal University of Mato Grosso do Sul (UFMS), 79070-900, Campo Grande, MS, Brazil, [4]University Ruy Barbosa (UniRuy), 41720-200, Salvador, BA, Brazil and [5]Faculty of Medical Sciences (FCM), University of Pernambuco (UPE), 50100-130, Recife, PE, Brazil

Email:
Douglas Dourado[*] - ddourado.science@gmail.com;
Fábio Rocha Formiga[*] - fabio.formiga@fiocruz.br

* Corresponding author

Abstract

Leishmaniasis is a neglected tropical disease that has affected more than 350 million people worldwide and can manifest itself in three different forms: cutaneous, mucocutaneous, or visceral. Furthermore, the current treatment options have drawbacks which compromise efficacy and patient compliance. To face this global health concern, new alternatives for the treatment of leishmaniasis have been explored. Curcumin, a polyphenol obtained from the rhizome of turmeric, exhibits leishmanicidal activity against different species of *Leishmania* spp. Although its mechanism of action has not yet been fully elucidated, its leishmanicidal potential may be associated with its antioxidant and anti-inflammatory properties. However, it has limitations that compromise its clinical use. Conversely, nanotechnology has been used as a tool for solving biopharmaceutical challenges associated with drugs, such as curcumin. From a drug delivery standpoint, nanocarriers (1–1000 nm) can improve stability, increase solubility, promote intracellular delivery, and increase biological activity. Thus, this review offers a deep look into curcumin-loaded nanocarriers intended for the treatment of leishmaniasis.

Introduction

Neglected tropical diseases (NTDs) comprise a group of 20 diseases that are caused, in most cases, by viruses, fungi, bacteria, or parasites, such as helminths and protozoa. They affect mainly women and children from impoverished communities. Leishmaniasis is a NTD that has affected more than 350 million people worldwide, with worrisome 700,000 to one million new cases annually [1,2].

This tropical disease is caused by a vector-borne protozoan parasite of the genus *Leishmania* which is transmitted by the bite of female sandflies. Different species of *Leishmania* spp. can cause specific clinical manifestations. These are (i) cutaneous leishmaniasis, which can be the localized type when the lesions are limited to certain areas of the skin, or diffuse when several lesions occur over an extensive area of skin tissue [3]; (ii) mucocutaneous leishmaniasis, which causes total or partial degeneration of the mucous membranes of the nose, mouth, and throat [4], and (iii) visceral leishmaniasis (also known as kala-azar), can cause systemic infection affecting the liver, spleen, hematogenous and lymphatic systems [5,6].

For the treatment of these infections, therapies based on pentavalent antimony (first-line drug treatment), amphotericin B, miltefosine, and paromomycin have been employed [7]. Despite being effective, these drugs cause cardiotoxicity, renal, pancreatic, and liver toxicity, and teratogenicity. Furthermore, cases of drug resistance are already well reported for antileishmanial drugs, such as the pentavalent antimonial salts [8].

Therefore, finding new therapeutic alternatives for this neglected tropical disease continues to be of utmost importance [9]. Current studies have highlighted curcumin as a promising antiparasitic alternative [10]. Curcumin (diferuloylmethane) is a yellow polyphenol extracted from the rhizome of *Curcuma longa*, popularly known as turmeric [11-13]. This molecule presents a high tolerance profile, and it has shown *in vitro* and *in vivo* leishmanicidal properties against different species of *Leishmania* spp. [11,14].

Despite its pharmacological potential, curcumin has some physicochemical and biopharmaceutical limitations that should be highlighted, such as: (i) low aqueous solubility, (ii) poor gastrointestinal absorption, (iii) high rates of metabolism, (iv) inactivity of metabolic products, and (v) rapid elimination and clearance [15,16].

To get around these several limitations, nanotechnological systems such as nanoemulsions [17], microemulsions [18], self-nanoemulsifying systems [19], nanoparticles [20], nanolipo-somes [21], micelles [22], and nanocrystals [23] have been utilized. These systems can promote (i) protection of the drug against degradation in physiological media, (ii) increase in drug solubility, and (iii) modification/targeting of the drug enabling transport through biological membranes [13,24].

Therefore, this review focuses on mapping the nanotechnologies used to load curcumin and discussing the increase in the leishmanicidal properties of this drug according to its nanostructured vehicles.

Review
Leishmaniasis: general aspects

Leishmaniasis is a neglected tropical disease caused by a flagellated protozoa of the genus *Leishmania*. The genus belongs to the Trypanosomatidae family, and it is transmitted by insect vectors of the genus Phlebotomus (in the Old World) or Lutzomyia (in the New World) [25]. The disease is present in several countries and it has affected more than 350 million people worldwide. Its incidence has increased more than 40-fold in the last 20 years, making it the second most prevalent parasitic disease in the world after malaria [2,26,27].

The disease can manifest in three different forms: cutaneous leishmaniasis (CL), which is the most abundant form; mucocutaneous leishmaniasis (MCL); and visceral leishmaniasis (VL), which is the severe and lethal form of the disease, with a mortality rate above 95% [28]. The form in which the disease manifests itself in the patient is determined mainly by immunological aspects and general health conditions of the host and by the species of the parasite. In general, CL and MCL are caused by *L. tropica*, *L. major*, *L. amazonensis,* and *L. brasiliensis*. Meanwhile, VL is caused by *L. donovani*, *L. infantum,* and *L. chagasi*. However, there are reports of cutaneous leishmaniasis caused by the *L. donovani* and *L. infantum* complex. This is due to advances in the molecular detection of these species worldwide [29-31].

The *Leishmania* spp. life cycle is mainly divided into two evolutionary stages: (i) extracellular promastigote, which is the flagellate form and is in the intestine of the invertebrate host; (ii) intracellular amastigote, a spherical form that is found in cells of the vertebrate host. Infected sandflies inject blood with the parasite in promastigote form into the vertebrate host, which causes macrophages or other cells of the mononuclear phagocytic system to phagocytose the promastigotes. The *leishmania* spp. cells then differentiate into amastigotes inside the phagocytic cells, multiply by binary fission until the host cell breaks down and releases the parasites to infect other cells and tissues [2,32,33].

The Food Drug Administration (FDA) recommends five drugs for the treatment of leishmaniasis: pentavalent antimonials, amphotericin B, pentamidine, paromomycin, and miltefosine. Among these drugs, only the pentavalent antimonials were designed for leishmaniasis, while the other four were initially approved to treat other diseases. Although used in different treatment protocols, most are only capable of controlling the infection and relieving symptoms, while displaying concerning toxicity and numerous therapeutic limitations [34-36].

Furthermore, treatment abandonment and failure due to drug resistance are two of the problems encountered with the usual treatments. Thus, seeking therapeutic alternatives to those currently available, many natural or synthetic molecules have been studied and evaluated for their antileishmanial potential, among which curcumin may be featured [4].

Curcumin and its antileishmanial properties

Curcumin (curc) is a polyphenol (Figure 1) obtained from the rhizome of *Curcuma longa* and is the main curcuminoid present in this plant [11,12]. Due to its good tolerance profile and safety
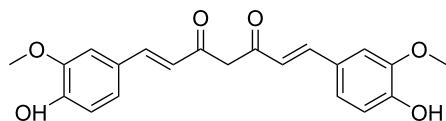
Figure 1: Chemical structure of curcumin.

even at high doses (12 g/day), curc has been extensively studied as a therapeutic agent [11,14]. Numerous preclinical and clinical trials have concluded that curc has great potential for the treatment of various diseases in humans [37-39].

Among the diverse biological potential of this molecule, its antiparasitic properties against different diseases have attracted considerable attention in recent decades [10,40,41]. Among such, the potential of curc against cutaneous and visceral leishmaniasis has been explored [42]. *In vitro* and *in vivo* studies have revealed that curc displays leishmanicidal activity against amastigotes and promastigotes of the species *Leishmania amazonensis* [43]*, Leishmania braziliensis* [44]*, Leishmania donavani* [45]*, Leishmania infantum* [46]*, Leishmania major* [46,47]*,* and *Leishmania tropica* [46,48].

Although proposed mechanisms of action are not fully elucidated, curc has been shown to have antileishmanial effects through its anti-inflammatory and antioxidant properties [42,47,49,50]. Figure 2 reveals the possible mechanisms of action of this drug against leishmaniasis.

Curc inhibits the activation of nuclear factor-κB (NFκB); the production of TNFα, IFNγ, and nitric oxide; and gene expression of inducible nitric oxide synthase (iNOS) [49,51]. These pro-inflammatory factors are related to the parasitic infection of leishmaniasis. Additionally, this molecule produces reactive oxygen species (ROS) and elevates cytosolic calcium. These occur in the exposure of phosphatidylserine to the outer plasma
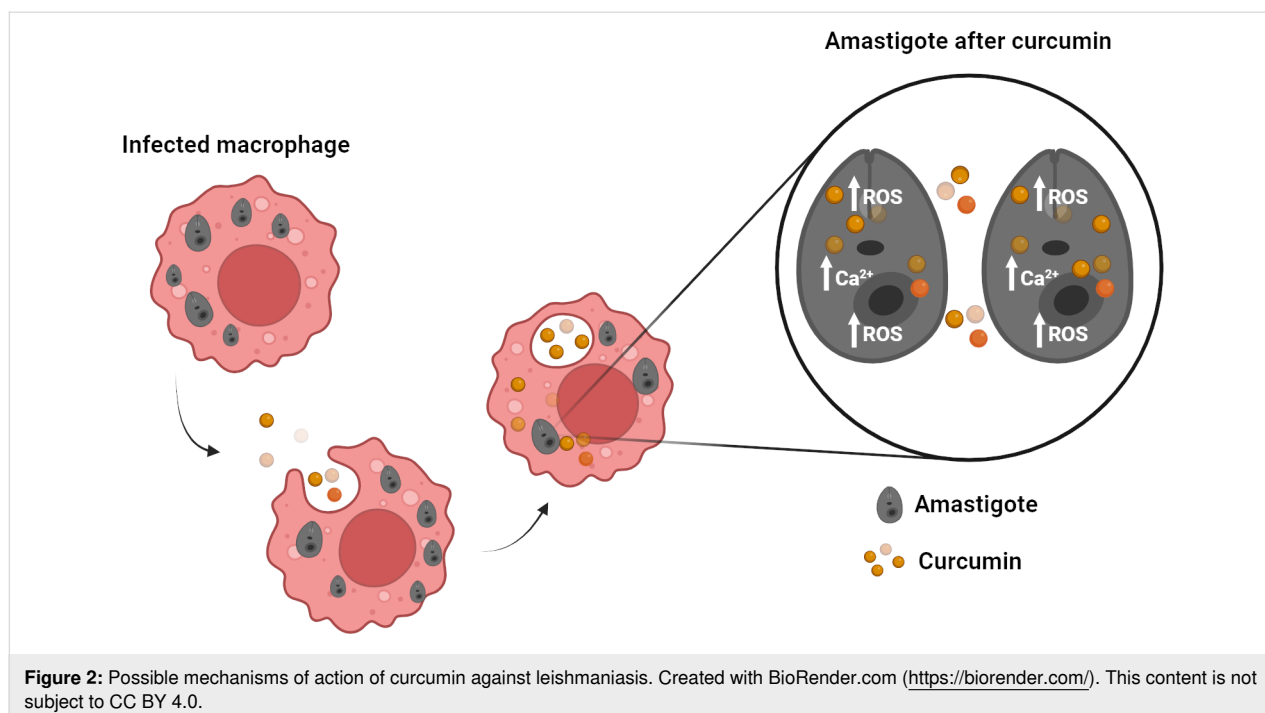
Figure 2: Possible mechanisms of action of curcumin against leishmaniasis. Created with BioRender.com (https://biorender.com/). This content is not subject to CC BY 4.0.

membrane leaflet and DNA fragmentation, causing the death of the leishmaniasis parasite [47,52].

Despite its promising antileishmanial potential, curc has several drawbacks, such as: (i) low aqueous solubility, (ii) rapid clearance, (iii) low tissue absorption, and (iv) notable chemical degradation (neutral and alkaline pH), which severely reduces its bioavailability and hinder its clinical use [18,53,54]. Given this scenario, approaches such as carrying curc in nanostructures have been used to overcome such drawbacks.

Nanostructured systems for the treatment of leishmaniasis

The existing treatments for leishmaniasis (cutaneous, mucocutaneous, or visceral) are still insufficient or frequently ineffective. This is due to several limitations of the drugs used, such as (i) high levels of toxicity and prolonged treatment time, which leads patients to discontinue treatment, (ii) high cost of treatment and parasite resistance to drugs, which is a major issue and occurs as a result of genetic mutations that reduce the response of the parasite towards a given drug through decreased uptake of the drug by macrophages [55-57].

Thus, nanotechnology-based systems are a promising alternative for drug delivery and vectorization in the treatment of leishmaniasis as they present several advantages. One could mention decreased side effects, modified drug release, prevention of rapid metabolization, protection of photosensitive molecules, the ability to deliver multiple antileishmanial drugs that can have a synergistic effect, and increased solubility, which results in increased bioavailability. These advantages are determined by the physicochemical properties of the systems, and by the release and targeting features of the loaded nanosystems, rather than by the drug properties themselves [58-62].

The intracellular amastigote form of *Leishmania* spp. allocates in macrophage phagolysosomes from infected individuals [63]. However, the intracellular uptake of bioactive molecules is especially hindered for hydrophobic molecules [64], making it difficult for the drug to reach the parasite. On the other hand, nanocarriers can target the interior of macrophages residing in the spleen, liver, and bone marrow, effectively delivering antileishmanial drugs to such sites. Overall, drug targeting results in increased treatment efficacy and reduced toxicity, mostly by reducing drug doses and preventing its interaction with unwanted receptors [30,65].

In this scenario, active targeting happens by the functionalization of nanocarriers, making drug delivery specific to macrophage targets, such as D-mannose, phosphatidylserine, or lactoferrin. This may reduce the drug resistance of the parasite in the

long term. Furthermore, the surface charge of nanostructures may influence internalization since positive charges favor electrostatic interactions of these carriers with the macrophage membrane. As a result, the macrophages uptake the drug-loaded nanocarrier by phagocytosis, where they will directly act on the parasites [65-67].

Several types of nanosystems have been studied for carrying antileishmanial drugs, such as polymeric nanoparticles, lipid nanoparticles, nano- and microemulsions, liposomes, or metallic nanoparticles [68]. Costa-Lima and colleagues incorporated bisnaphthalimidopropyldiaminooctane (BNIPDaoct) into PLGA polymeric nanoparticles and obtained particles with sizes around 150 nm, with encapsulation efficiency around 90% [69]. BNIPDaoct is a bisnaphthalimidopropyl derivative, which acts on the life cycle of *Leishmania infantum*. Therefore, the authors evaluated the antileishmanial potential of the formulations and the free molecule in amastigote forms of *Leishmania infantum*. The study showed an eight- to ten-fold decrease in macrophage cytotoxicity of the nanoencapsulated molecule when compared to its free form. In addition, the uptake of these nanoparticles by macrophages was higher than that by fibroblasts, with an IC_{50} approximately two times lower than that of the free drug, and a selectivity index 20 times higher. *In vivo* studies demonstrated that the nanoformulations were more effective in reducing parasitemia in the spleen, with results equivalent to the group treated with amphotericin B.

Das and collaborators, on the other hand, addressed the development of nanostructured lipid carriers (NLC) with ursolic acid (UA) functionalized with *N*-octyl chitosan. The NLC were approximately 143 nm of the hydrodynamic diameter. The authors also found encapsulation and drug-load efficiencies of $88.63 \pm 2.70\%$ and $12.05 \pm 0.54\%$, respectively [70]. They evaluated the antileishmanial potential of the nanosystems against resistant strains of *Leishmania donovani*, which resulted in a 15-fold improvement in drug activity when into NLC, with a selectivity index for the intracellular model in macrophages almost three times higher than that of the free drug. *In vivo* studies showed that the suppression of parasite load in the spleen of mice was around 60% for free-UA and close to 90% for NLC-UA. Confocal microscopy images proved the cell uptake of NLC into macrophages.

Metal nanoparticles are also excellent alternatives for carrying antileishmanial drugs [71]. Almayouf et al. produced silver nanoparticles (Ag-NP) with sizes ≈100 nm by green synthesis using extracts of *Ficus carica* Linn and *Olea europaea* L., which are rich in phenolic compounds. The authors also evaluated the antileishmanial potential of the nanosystems regarding concurrent treatment or pretreatment against *Leishmania major*

cutaneous infection in female Balb/c mice [72]. The results of the study showed an improvement in skin lesions of groups treated with Ag-NP both before and after infection. The group treated after infection displayed a significant decrease in lesion size starting in the second week of treatment, with complete healing after 21 days, while the group treated with Pentostan healed after 28 days.

Moraes and colleagues prepared nanoemulsions (NE) of andiroba oil (*Carapa guianensis* Aublet, anoandi) and copaiba oil (*Copaifera sp*. Linnaeus, nanocopa) and tested their effects against *L. infantum* and *L. amazonensis* promastigotes and intracellular amastigotes, as well as the effects of oral administration of the formulations in infected mice [73]. The droplet size of the NEs was 76 and 88 nm for nanocopa and nanoandi, respectively. The authors observed a significant decrease in parasite load for both investigated species when treated by both nanoandi and nanocopa. Moreover, there was a decrease in lesion size and parasite load from the liver and spleen of mice treated with NE. In ultrastructural analysis performed by scanning electron microscopy, it was possible to observe morphological changes, oval aspect, and disappearance of the flagellum in the promastigote parasites treated with doses of NE above the IC_{50}.

Peixoto and collaborators developed epoxy-α-lapachone-loaded microemulsions (ME). They assessed the ME *in vivo* performance against *L. amazonensis* in infected BALB/c mice. The ME droplet size was smaller than 120.4 ± 7.7 nm and displayed a good stability profile over 73 days. The *in vivo* studies demonstrated that after two weeks of treatment, BALB/c mice infected with *L. amazonensis* showed a decrease in paw lesions (about two-fold) in response to microemulsion, compared to the untreated group. Additionally, the amount of parasites in the lymph nodes (31.5%) and footpad (60.3%) decreased [57].

Another nanostructured platform explored for the delivery of leishmanicidal drugs is the liposomal platform [74]. Artemisinin-loaded nanoliposomes smaller than 100 nm were obtained and evaluated in a murine model infected with *L. donovani*. Artemisinin-NPs reduced the number of *ex vivo* infected macrophages and the intracellular infection of *Leishmania donovani* amastigotes (IC_{50} of 6.0 ± 1.4 μg/mL and 5.1 ± 0.9 μg/mL, respectively). Artemisinin-NPs showed better efficacy than free artemisinin after therapy in a mouse model of visceral leishmaniasis. Percentages of inhibition in the liver and spleen were 82.4 ± 3.8% and 77.6 ± 5.5%, respectively [75].

The results of the studies highlighted in this topic confirm the relevance of the use of nanostructured formulations for the delivery of bioactive compounds and uptake by macrophages,

promoting an increase in antileishmanial efficacy, a decrease of toxicity, and, as a result, an increase in the selectivity index of these compounds. The same rationale is applied to the incorporation of curc in nanostructured systems, which will be discussed in the following topics.

Nanostructured systems with curcumin for the treatment of leishmaniasis

Different nanostructured systems with curc intended for the treatment of leishmaniasis have been developed (Figure 3). The articles included in this work approach the following nanosystems: (i) self-nanoemulsifying drug-delivery systems (SNEDDSs), (ii) nanoliposomes, (iii) nanostructured lipid carriers, (iv) polymeric, and (v) metallic nanoparticles. Different performances of nanostructured systems containing curc are discussed in the section below.

Figure 3: Overall scheme demonstrating curcumin-loaded nanostructured systems that have been assayed in vitro and/or in vivo against different *Leishmania* species for the treatment of leishmaniasis. Created with BioRender.com (https://biorender.com/). This content is not subject to CC BY 4.0.
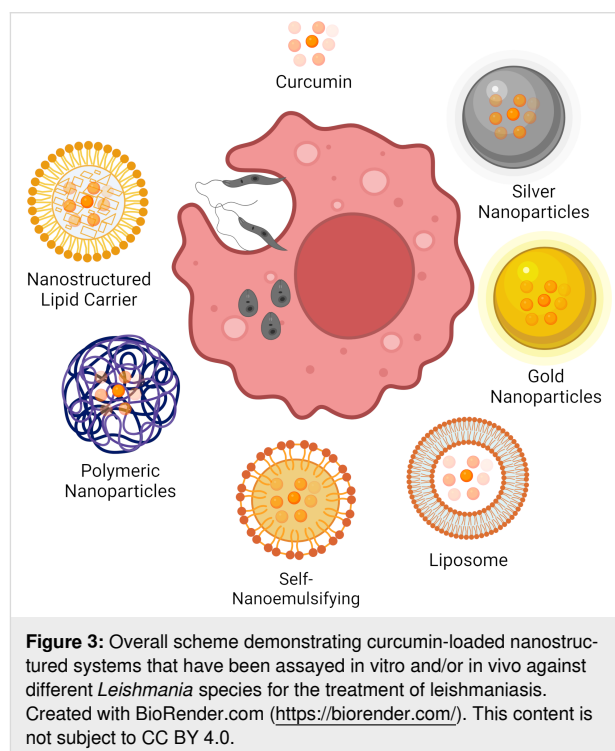
Self-nanoemulsifying drug-delivery systems

The SNEDDSs are lipid-based drug-delivery systems made of an isotropic blend of oils, surfactants, and co-surfactants or co-solvents [76]. These spontaneously form O/W nanoemulsions (≤200 nm) in aqueous media (generally in a physiological media) [77,78]. The SNEDDSs have been successfully used to carry molecules with biopharmaceutical limitations, improving their physicochemical and leishmanicidal properties [79,80].

In this context, curcumin-loaded SNEDDSs intended for the treatment of leishmaniasis were developed. Khan and collabora-

tors developed curcumin-loaded self-emulsifying drug delivery systems (curc-SNEDDSs) for topical administration in cutaneous and mucocutaneous leishmaniasis [81]. The systems were produced by homogenization using a vortex mixer. The authors obtained two nanoformulations, which showed droplet size between 26–29 nm, polydispersity index (PdI) lower than 0.2, and zeta potential between −3.6 and −4.4 mV. The curc-SNEDDSs (1% of curc) promoted an increase in antileishmanial (*in vitro*) activity (IC_{50}: 0.13–0.18 μg/mL and 0.25–0.27 μg/mL) when compared to curc in its free form (IC_{50}: 22.50–24.60 μg/mL) against promastigote and amastigote forms of *Leishmania tropica*, respectively. The nanoformulations were able to kill the intracellular amastigotes in macrophages. Moreover, the authors developed a further study wherein seven nanoformulations with different mixtures of oils, surfactants, and co-surfactants were reported [48]. The obtained SNEDDSs showed droplet size between 30–80 nm and IC_{50} values of 0.26–0.36 μg/mL and 0.23–0.37 μg/mL against promastigotes and amastigotes of *Leishmania tropica*, respectively. However, in this study, they did not perform intracellular studies on infected macrophages. Nevertheless, both studies containing curcumin-loaded SNEDDSs promoted an increase in leishmanicidal activity.

Differently, Khan and collaborators also developed SNEDDSs for the entrapment of amphotericin B against *Leishmania tropica*. The authors also observed low IC_{50} values promoted by the nanosystems (two different SNEDDSs) against amastigote (IC_{50} values for SNEDDSs A and B, 0.025 and 0.056 μg/mL, respectively) and promastigote forms (IC_{50} values for SNEDDSs A and B, 0.017 and 0.031, respectively). These results evidenced the effectiveness of different SNEDDSs when compared to that of the control AmB-liposome AmBisome, which demonstrated IC_{50} values 10 times higher for amastigotes and promastigotes [79]. Although this nanostructured system is a promising carrier, further *in vitro* and *in vivo* studies are necessary to evaluate such improvements for curc or other leishmanicidal drugs.

Nanoliposomes

Nanoliposomes are nanoscale lipid bilayer vesicles mainly composed of phospholipids. These systems (small liposomes: 20–100 nm and large liposomes: >100 nm) are capable of loading both hydrophilic and lipophilic drugs [82,83]. Leishmanial drugs, such as miltefosine [84], buparvaquone [85], nitazoxanide [86], artemisinin [75], berberine [87], and paromomycin [88] have already been successfully loaded into nanoliposomes promoting increased antiparasitic activity.

Recently, Bafghi and collaborators produced nanoliposomes for curc delivery as a new alternative for leishmaniasis treatment [89]. Briefly, the nanoliposomes were prepared by thin-film

hydration, resulting in spherical vesicles with 176.5 nm of diameter, PdI <0.2, zeta potential of + 35 mV, and an entrapment efficiency of 92%. Curcumin-entrapped nanoliposomes showed leishmanicidal activity (*in vitro*) against the promastigotes of *Leishmania major*, whose IC_{50} values were 6.41, 3.80, and 2.33 μg/mL for the incubation times of 24, 48, and 72 h, respectively. Additionally, this nanosystem proved to be biocompatible with skin fibroblasts (*in vitro*). However, neither the cell viability of this system in healthy macrophages nor models of parasite infection in this cell type were evaluated. Considering that the nanoscale platform approved by the FDA and currently used in the treatment of leishmaniasis is liposomal amphotericin-B (IC_{50}: 0.18 μg/mL) [90], this liposomal formulation containing curc should receive greater attention. In addition, more complex efficacy and safety studies (*in vivo*) must be conducted so that they could be transferred to the market following the Ambisome® path.

Nanostructured lipid carriers

Nanostructured lipid carriers (NLCs) are lipid-based formulations with a solid matrix at room temperature that differ from solid lipid nanoparticles when it comes to their matrix organizational level. Nanostructured lipid carriers offer advantages such as enhanced stability, low toxicity, increased shelf life, improved drug loading capacity, and biocompatibility over other conventional lipid-based nanocarriers, such as nanoemulsions and solid lipid nanoparticles [91]. Due to their properties, the use of NLCs has been a successful strategy for entrapping drugs with leishmanicidal activity [92-95]. Accordingly, Riaz and collaborators entrapped curc into NLCs to evaluate their activity in the treatment of cutaneous leishmaniasis (*L. tropica*) [96]. The authors obtained the NLCs by hot homogenization, resulting in structures with a hydrodynamic mean particle size of 312 ± 1.89 nm, PdI of 0.305 ± 0.17 and zeta potential of −38 ± 0.93 mV. These particles were able to entrap 88% of curc due to the irregular lipid crystal structure of NLCs [53]. The NLCs proved to be safe for macrophages, which promptly internalized the nanostructures, as proven by the strong intracellular fluorescence levels. Furthermore, NLCs increased the *in vitro* leishmanicidal activity of curc (IC_{50}: 105.49 ± 3.71 μg/mL) when compared to curc-free NLCs (IC_{50}: 165.06 ± 4.64 μg/mL). Similar performance occurred *in vivo* in axenic amastigotes, (IC_{50} of the curc-NLC: 190.3 ± 3.19 and IC_{50} value of the curc-free: 243.56 ± 2.89 μg/mL) corroborating the improvements in the leishmanicidal response after entrapment of curc in the nanostructure.

This biological performance was also observed in artemether-NLC against *L. infantum*. Nanostructured lipid carriers conferred an increase in the leishmanicidal activity of the drug. Artemether-NLCs presented IC_{50} values of *L. infantum*

promastigote and amastigotes of 16.43 and 15.42 µg/mL, respectively. On the other hand, free artemether IC_{50} values were 2-fold higher (i.e., 37.12 and 32.10 µg/Ml). Finally, the nanostructured system revealed the lowest cytotoxicity against J774 macrophages [97].

Amphotericin B-loaded NLCs were also developed for the treatment of leishmaniasis. Free amphotericin B (AmB) and AmB-NLCs (250 nm) were evaluated for their leishmanicidal performance against the amastigote form and host cells. Unlike curc-NLCs, which revealed an increase in activity, AmB-NLCs obtained IC_{50} with efficacy equivalent to AmB-free against the amastigote form of *L. braziliensis* (11.7 ± 1.73 and 5.3 ± 0.55 ng/mL respectively). However, NLCs greatly increased drug selectivity (1046 versus 813), as macrophages revealed smaller toxicity indicators, without evidence of nitric oxide or TNFα production [95].

In this perspective, NLCs have been a nanoscale platform with promising results aimed at encapsulating anti-leishmanial drugs. This encourages further studies to better understand how NLCs might affect the mechanisms of action of curc when delivered via these nanostructured systems.

Polymeric nanoparticles

Polymeric nanoparticles (PNPs) are colloidal systems made of natural or synthetic polymers [98]. These systems can encapsulate or adsorb active pharmaceutical ingredients (APIs) and macromolecules [99-101]. In addition, PNPs can impact specific drug release kinetics and increase biocompatibility [60]. Different biodegradable polymers have been used for the development of targeted PNPs for the treatment of leishmaniasis [102].

In this scenario, chitosan is an interesting polymer for NP synthesis due to its positive charge, which favors adsorption by negatively charged cell membranes [103]. Additionally, studies have revealed antileishmanial properties of this polymer against Leishmania parasites, making it attractive for the synthesis of NPs intended for this treatment [56,104].

Therefore, Chaubey and colleagues developed mannose-conjugated curcumin–chitosan nanoparticles (curc-MCNPs) intended for visceral leishmaniasis [50]. The selected nanoparticles (curc-MCNPs) presented spherical morphology, hydrodynamic mean particle size of 215 nm, PdI of 0.381, zeta potential of +24.37 mV, and entrapment efficiency of 82.12%. Curc-MCNPs showed a more effective uptake and pronounced *in vitro* leishmanicidal activity (curc-MCNPs, median effective dose (ED_{50}): 0.518 ± 0.01 µg/mL) against *L. donovani* amastigotes than curc-chitosan nanoparticles (curc-CNPs, ED_{50}: 1.87 ± 0.075 µg/mL) and free curc (ED_{50}: 2.8 ± 0.03 µg/mL).

Furthermore, the *in vivo* uptake study indicated that the endocytosis of the NPs effectively occurred within macrophages of the reticuloendothelial system. Moreover, in another work of the research group, the authors evaluated the *in vitro* and *in vivo* leishmanicidal efficacy and toxicity of these nanoparticles [105]. *In vivo* antileishmanial activity in hamsters demonstrated significantly greater suppression of parasite replication in the spleen with Cur-MCNPs compared to that of Cur-CNPs. In addition, no cytotoxic profile was observed *in vitro* in macrophages (J774A.1), which was also confirmed by the minimal cytotoxicity observed in *in vivo* studies.

Hence, chitosan-based nanoparticles are a good strategy for drug delivery intended to treat leishmaniasis. This polymer can stimulate macrophages to produce pro-inflammatory cytokines, as they bind to receptors present in the cells of the immune system [106]. In this way, there is an internalization of the NPs containing this polymer and delivery of the drug for leishmanicidal activity. Additionally, the conjugation of the nanoparticles with sugars, such as mannose, makes drug delivery targeted and specific to the macrophage receptor, increasing the uptake by the system and consequently the intracellular leishmanicidal activity [50,105].

Poly(lactic-co-glycolic) acid (PLGA) is another polymer used for the development of nanoparticles for the treatment of leishmaniasis [107,108]. PLGA is an FDA-approved polymer that is commonly used in the synthesis of nanoparticles due to its special features such as biocompatibility, biodegradability, low toxicity, and adjuvanticity [109,110]. Given these properties, Tiwari and co-workers produced curcumin-loaded Eudragit-PLGA-nanoparticles (curc-E-PLGA-NPs) and evaluated their leishmanicidal activity with miltefosine combination therapy. The authors functionalized the surface of PLGA-NPs with Eudragit L30D, a polymer that provides pH-dependent drug release and significantly improved targeted action, thus increasing the efficacy of the drug [45].

Curc-E-PLGA-NPs showed spherical morphology, with a hydrodynamic mean diameter of 182.3 ± 7.4 nm, PdI of 0.281 ± 0.015, zeta potential of −12.7 ± 0.141 mV, and entrapment efficiency of 93.2 ± 3.9 %. Curc-E-PLGA-NPs exhibited IC_{50} values *in vitro* of 1.34 ± 0.045 and 1.61 ± 0.032 µg/mL for promastigotes and amastigotes of *L. donovani*, respectively. Furthermore, the association of curc-E-PLGA-NPs with miltefosine revealed synergism in both promastigotes and amastigotes. In the *in vivo* hamster model, curc-E-PLGA-NPs also showed leishmanicidal activity, individually or associated with miltefosine. The synergy evidenced between these drugs (i) increased the production of toxic reactive oxygen/nitrogen metabolites, (ii) increased phagocytic activity, and (iii) in-

creased lymphocyte proliferation [45]. Furthermore, curc-E-PLGA-NPs proved to be effective as an adjuvant in the therapy against leishmaniasis.

Like curc, other leishmanicidal drugs have been encapsulated into polymeric nanoparticles and shown promising results. Ghosh and collaborators encapsulated amphotericin B in PLGA-NPs by modifying its surface with mannose. As with curc nanoparticles functionalized with mannose, an increase in leishmanicidal activity was observed. AmB-free, AmB-PLGA-NPs, and mannose-PLGA-NPs presented IC_{50} values of 0.15 ± 0.08, 0.09 ± 0.07, and 0.07 ± 0.04 µM and selectivity index (SI) of 80, 255, and 314, respectively. In addition to the influence of the nanostructure, sugar promotes greater internalization of these nanoparticles due to the mannose receptors on the surface of macrophages [111].

Pentamidine-loaded nanoparticles also showed great results due to the nanostructure. Free pentamidine and Pentamidine-NPs were administered orally in an *in vivo* experimental model of mice infected with visceral leishmaniasis. Only the nanoencapsulated drug showed a significant reduction in the relative weight of organs such as the spleen and liver, commonly increased in visceral leishmaniasis [112]. Thus, polymeric nanoparticles have proven themselves as suitable for increasing the antileishmanial potential of compounds known to be used against *Leishmania*. Further, they are versatile and safe nanostructured systems that promote increased leishmanicidal activity and can encapsulate curc as a therapeutic alternative for the treatment of leishmaniasis.

Metallic nanoparticles

Metallic nanoparticles (MNPs) are versatile nanostructures due to their tunability in shape, composition, size, structure, assembly, and optical properties [113]. These nanoformulations can be synthesized through chemical, physical, or biological processes and are solely generated from metal precursors such as silver and gold [114,115]. In addition, MNPs have been widely used in therapy, drug delivery, targeting, and imaging [116,117]. Current studies have directed the use of metallic nanoparticles such as silver and gold nanoparticles against *Leishmania* sp. [118]. As silver and gold nanoparticles can produce reactive oxygen species (ROS) and Leishmania is known to be extremely sensitive to these compounds, these have been promising nanoformulations in the treatment of leishmaniasis [118-121].

Given these properties, the synergistic activity of MNPs and leishmanicidal drugs has been evaluated, highlighting an increase in antileishmanial efficacy [122,123]. Accordingly, Badirzadeh and collaborators synthesized curc-coated silver

nanoparticles (curc-AgNPs) for the treatment of cutaneous leishmaniasis [124]. Curc-AgNPs presented a spherical shape, 32 nm of diameter, and a zeta potential of −19.8 mV. This nanoformulation prevented the *in vitro* growth of *L. major* promastigotes and inhibited their viability (IC_{50}: 58.99 µg/mL). In addition, it eliminated amastigotes inside macrophages (EC_{50}: 57.14 µg/mL), which remained viable above 50% at concentrations below 307.16 µg/mL. Further, the authors carried out *in vivo* assays with BALB/c mice containing lesions caused by *L. major* infection. The treatment was carried out for 50 days with different concentrations of curc-AgNPs (20–60 µg/kg). The results indicated a decrease in lesions when compared to the negative control. Furthermore, a significant decline in *L. major* load was observed in 4 weeks.

A different study evaluated the leishmanicidal performance of curc-coated gold nanoparticles (curc-AuNPs) against *L. major* [125]. The NPs showed spherical morphology, particle size of 22 nm, and adequate polydispersity. Curc-AuNPs revealed IC_{50} values against *L. major* promastigotes of 64.79 µg/mL and 29.89 µg/mL in 24 h and 48 h, respectively. Additionally, they inhibited and eliminated amastigotes inside macrophages (IC_{50}: 63.29 µg/mL on 24 h and 54.04 µg/mL on 48 h). *In vivo* treatment (BALB/c mice for 50 days) with curc-AuNPs (20–60 µg/kg) reduced lesions caused by *L. major* promastigotes after four weeks. The parasite burden of the paws and lymph nodes of mice infected with *L. major* was also significantly reduced compared to the negative control.

Hence, it is noteworthy that both MNPs had an impact on cutaneous leishmaniasis infections. However, there was no influence of metal (Ag or Au) particles on the leishmanicidal activity of the systems. In these studies, the found activity may be mostly attributed to curc-coated NPs. The same behavior was observed in Miltefosine-AgNPs developed by Kalangi and collaborators. Silver nanoparticles alone (50 µM) did not demonstrate an antileishmanial effect on the promastigote stage of the *Leishmania* parasite. However, when AgNPs were combined with miltefosine (12.5 µM and 25 µM) the leishmanicidal effect of the drug doubled [122]. Therefore, combining leishmanicidal drugs, such as curc, with metallic particles can be an effective strategy against the leishmania parasite.

The formulations described in Section 1.4 are summarized in Table 1, which also describes their physicochemical characteristics and performance *in vitro* and *in vivo*.

General discussion and final considerations

This study discussed that curcumin is a polyphenol with diverse biological properties, including a potent leishmanicidal activity. Despite the promising activity, this molecule shows poor water

Table 1: Summary of the curcumin-loaded nanoformulations intended for the treatment of leishmaniasis.

Nanoformulation	Composition	Size/ PdI/ ZP/ EE/ DL	Parasite	*In vitro* and *in vivo* outcomes
SNEDDSs [81]	Captex® 355, Crem EL®, Crem RH® 40, Tween® 80, PEG 200, PEG 300, caprylic acid and curc	≈29 nm/ 0.2/ −3.6 to −4.4 mV/ −/ −	*L. tropica*	IC_{50} decreased by 125 times and more than 90 times compared to free curcumin against promastigotes and amastigotes, respectively.
SNEDDSs [48]	Captex® 355, Crem EL®, Crem RH® 40, Tween® 80, PEG 200, PEG 300, caprylic acid and curc	30–80 nm/ ≈0.2/ −1.5 to −4.8 mV/ −/ −	*L. tropica*	IC_{50} decreased by more than 86 times and more than 66 times compared to free curc against promastigotes and amastigotes, respectively.
nanoliposomes [89]	phosphatidylcholine, cholesterol, curc	176.5 nm/ ≈0.2/ +35 mV/ 92%/ −	*L. major*	IC_{50} values decreased as the incubation time increased, from 24 h to 72 h.
NLC [96]	glyceryl monostearate, soy phosphatidylcholine, curc	≈312 nm/ ≈0.3/ −38mV/ 88%/ 1.07%	*L. tropica*	NLCs increased the leishmanicidal activity of curc in 1.55 times *in vitro* and 1.28 times *in vivo*.
polymeric NPs [50]	chitosan, mannose, curc	215 nm/ ≈0.3/ +24.73 mV/ 82.12%/ −	*L. donovani*	curc-CNPs and curc-MCNPs showed *in vitro* IC_{50} values (1.5 and 4.5 times, respectively) lower than that of free curcumin. The *in vivo* uptake study showed the endocytosis of NPs by macrophages.
polymeric NPs [105]	chitosan, mannose, curc	215 nm/ ≈0.3/ +24.73 mV/ 82%/ −	*L. donovani*	*In vivo* antileishmanial study showed greater suppression of parasite replication in the spleen by curc-MCNPs compared to curc-CNPs.
polymeric NPs [45]	PLGA, Eudragit® L30D, curc, miltefosine	≈182 nm/ ≈0.2/ −12.7 mV/ ≈93%/ ≈18%	*L. donovani*	Association of curc-E-PLGA-NPs with miltefosine revealed synergism in promastigote and amastigote forms.
metallic NPs [124]	silver nitrate, curc	32 nm/ −/ −19.8 mV/ −/ −	*L. major*	curc-AgNPs (i) prevented the *in vitro* growth of *L. major* promastigotes, and (ii) inhibited their viability; (iii) eliminated amastigotes inside macrophages, and (iv) decreased cutaneous lesions *in vivo*.
metallic NPs [125]	Au, curc	22 nm/ −/ −/ −/ −	*L. major*	curc-AuNPs IC_{50} values decreased as the incubation time increased (24 to 48 h). *In vivo* treatment demonstrated curc-AuNPs reduced cutaneous lesions after four weeks.

Ag: silver; Au: gold; C: chitosan; curc: curcumin; DL: drug load; EE: encapsulation efficiency; M: mannose; MNPs: metallic nanoparticles; NPs; nanoparticles; NLC: nanostructured lipid carriers; SNEDDSs: self-nanoemulsifying drug-delivery systems; PdI: polydispersity Index; PLGA: poly(lactic-*co*-glycolic acid); ZP: zeta potential.

solubility, high metabolism, and fast elimination impair, which results in low systemic bioavailability and poor *in vivo* pharmacological effect. In this context, molecules with similar limitations have been combined with nanotechnology tools to allow their clinical use. In recent years, different nanostructured systems have been explored, such as lipid nanoparticles, metallic nanoparticles, polymeric nanoparticles, nanovesicles, and self-emulsifying nanosystems. These can promote increased solubility, permeability, protection against degradation in biological media, and a controlled release profile. Additionally, nanostructures, especially those smaller than 200 nanometers, are susceptible to uptake by the cells infected with the etio-

logical agent of leishmaniasis. This ability allows an expressive increase in the leishmanicidal activity of curcumin against the parasite.

Despite its versatility, several studies stop at the development of nanostructures containing curc and fail to further assess their activity in the parasites, which slows down the path to a future product. Therefore, only a few studies have evidenced *in vitro* and *in vivo* proof-of-concept that curc nanostructured systems might be promising for the treatment of leishmaniasis. Overall, alternative therapeutic nanostructured systems have been presented. They are nanoliposomes, SNEDDSS, NLCs, poly-

meric and metallic nanoparticles. These nanostructured systems have different compositions, sizes, charges, and modified surfaces which improves the leishmanicidal activity of curc and other control drugs.

To date, only three *in vivo* studies in mice using nanostructured curc have been carried out. These were all based on polymers and metallic nanostructures. Despite the conducted investigations, there are still gaps regarding a better understanding of the mechanisms of action of curc against leishmaniasis parasites. This review demonstrated that the known aspects related to curc leishmanicidal activity involve the increased production of ROS and intra-amastigote release of Ca^{2+}. In this context, we could observe that the studies failed to correlate consecutive intra-macrophage and intra-amastigote cellular uptake kinetics, once it appears to greatly interfere with the proposed biochemical triggers of *Leishmania* spp. cell death.

In addition, the work could also summarize that lipid-based nanostructures are great alternatives. However, the lack of *in vivo* studies on this matter limits their fair comparison to polymeric formulations. Overall, all assessed studies could prove that nanostructures improve curc dispersion in aqueous media (increase in apparent solubility). Altogether, we could also observe a general decrease in IC_{50} when compared to free curc, which was mainly attributed to the cell uptake of these structures. Indeed, studies that functionalized nanostructures with mannose for an increase in macrophage phagocytosis evidenced that functionalized nanoparticles decreased IC_{50} when compared to non-functionalized nanostructures and the free drug. These results take us in the direction of avoiding furtive conditions when developing further nanostructures for leishmaniasis.

Hence, based on the biological potential of curcumin and known safety/tolerability, and based on the existing proof of concept that nanostructured systems are more effective than conventional medicines, reduce the duration of treatment and the frequency of administration, there is an urgent need for industrial innovation towards new treatments for leishmaniasis.

Conclusion
Given that leishmaniasis is a neglected tropical disease, treatment is still poorly funded. Although the disease is spread in countries with large populations, such as Brazil and India, there are insufficient worldwide investments and not enough priority to prevent this disease from spreading, which makes it deadly to a large part of the population. Due to resistance to many drugs, several research works have focused on optimizing the use of amphotericin B nanoformulations (e.g., AmBisome®, Abelcet®,

and Anforicin B®), which is an antifungal and now widely used for leishmaniasis. However, this potent drug is not selective enough to be used in all cases. Present research and future works might still focus on this effective, traditional, and toxic molecule, once there are already different products on the market. However, due to the fast increase in drug resistance, alternatives must be taken into consideration and there is room for new medicines with drugs that are not only effective but less toxic.

This work showed that many nanostructures are being developed and assessed for leishmaniasis on a research level. However, policies and investments that fast-track the development of a nanostructured product from the bench to the market might be key in the future. Although promising, biopharmaceutical limitations still should be regarded and might limit the current studies on nanostructures containing curcumin. Therefore, efforts, time, and resources could be saved by optimizing a single nanostructure for different administration routes, which takes into consideration the biological barriers involved in the treatment of different forms of leishmaniasis (VL, CL, and MCL). This rationale is based on the lack of information observed in the studies regarding skin permeability on lesioned and healed skin, and gastric stability of nanostructured curc *in vivo*.

Also, clinical studies that prove the efficacy and safety of nanostructured curc must be conducted to encourage the transfer of these formulations to the therapeutic scenario. Based on the findings, polymeric nanoparticles reveal themselves to be a step ahead in the game, once more *in vivo* information is available and current medicines based on nanoparticles provide insights for fast-tracking this system from the technological and regulatory point of view.

Abbreviations
Table 2 lists the in this article used abbreviations and their explanations.

Table 2: Explanation of abbreviations.

Abbreviation	Explanation
NTDs	neglected tropical diseases
Curc	curcumin
NLCs	nanostructured lipid carriers
PdI	polydispersity index
SNEDDSs	self-nanoemulsifying drug-delivery systems
NE	nanoemulsions
ME	microemulsions
PNPs	polymeric nanoparticles

Table 2: Explanation of abbreviations. (continued)

APIs	active pharmaceutical ingredients
ED_{50}	median effective dose
IC_{50}	inhibitory concentration
ZP	zeta potential
NPs	nanoparticles
SI	selectivity index
VL	visceral leishmaniasis
CL	cutaneous leishmaniasis
MCL	mucocutaneous leishmaniasis
DL	drug load
EE	encapsulation efficiency
FDA	Food Drug Administration

Acknowledgements

Funding

Author Contributions

Douglas Dourado: conceptualization, methodology, formal analysis, investigation, original draft writing. Thayse Medeiros: formal analysis, investigation, writing. Éverton do Nascimento Alencar: formal analysis, investigation, writing – review & editing, visualization. Edijane Matos Sales: formal analysis, investigation, writing. Fábio Rocha Formiga: writing – review & editing, visualization, supervision, project administration, funding acquisition. All authors have read and agreed to the published version of the manuscript.

Conflict of Interest

The authors declare that they have no known competing financial interests or personal relationships that could have appeared to influence the work reported in this paper.

ORCID® iDs

Douglas Dourado - https://orcid.org/0000-0003-3445-5217
Thayse Silva Medeiros - https://orcid.org/0000-0002-8069-5871
Éverton do Nascimento Alencar - https://orcid.org/0000-0002-6148-6804
Edijane Matos Sales - https://orcid.org/0000-0002-8868-5176

References

1. Torres-Guerrero, E.; Quintanilla-Cedillo, M. R.; Ruiz-Esmenjaud, J.; Arenas, R. *F1000Research* **2017,** *6,* 750. doi:10.12688/f1000research.11120.1
2. WHO Word Heath Organization. Leishmaniasis. https://www.who.int/news-room/fact-sheets/detail/leishmaniasis (accessed June 7, 2023).
3. Madusanka, R. K.; Silva, H.; Karunaweera, N. D. *Infect. Dis. Ther.* **2022,** *11,* 695–711. doi:10.1007/s40121-022-00602-2
4. Gopu, B.; Kour, P.; Pandian, R.; Singh, K. *Int. Immunopharmacol.* **2023,** *114,* 109591. doi:10.1016/j.intimp.2022.109591
5. Abadías-Granado, I.; Diago, A.; Cerro, P. A.; Palma-Ruiz, A. M.; Gilaberte, Y. *Actas Dermo-Sifiliogr.* **2021,** *112,* 601–618. doi:10.1016/j.ad.2021.02.008
6. Mann, S.; Frasca, K.; Scherrer, S.; Henao-Martínez, A. F.; Newman, S.; Ramanan, P.; Suarez, J. A. *Curr. Trop. Med. Rep.* **2021,** *8,* 121–132. doi:10.1007/s40475-021-00232-7
7. *EBioMedicine* **2023,** *87,* 104440. doi:10.1016/j.ebiom.2023.104440
8. Pradhan, S.; Schwartz, R. A.; Patil, A.; Grabbe, S.; Goldust, M. *Clin. Exp. Dermatol.* **2022,** *47,* 516–521. doi:10.1111/ced.14919
9. Sundar, S.; Singh, B. *Expert Opin. Ther. Targets* **2018,** *22,* 467–486. doi:10.1080/14728222.2018.1472241
10. Shahiduzzaman, M.; Daugschies, A. Curcumin: A natural herb extract with antiparasitic properties. In *Nature Helps...: How plants and other organisms vontribute to solve health problems;* Mehlhorn, H., Ed.; Springer: Berlin, Heidelberg, 2011; pp 141–152. doi:10.1007/978-3-642-19382-8_6
11. Goel, A.; Kunnumakkara, A. B.; Aggarwal, B. B. *Biochem. Pharmacol.* **2008,** *75,* 787–809. doi:10.1016/j.bcp.2007.08.016
12. Dourado, D.; Freire, D. T.; Pereira, D. T.; Amaral-Machado, L.; Alencar, É. N.; de Barros, A. L. B.; Egito, E. S. T. *Biomed. Pharmacother.* **2021,** *139,* 111578. doi:10.1016/j.biopha.2021.111578
13. Singh, R.; Kumari, P.; Kumar, S. Nanotechnology for enhanced bioactivity of bioactive phytomolecules. In *Nutrient Delivery;* Grumezescu, A. M., Ed.; Academic Press: London, UK, 2017; pp 413–456. doi:10.1016/b978-0-12-804304-2.00011-1
14. Kunnumakkara, A. B.; Hegde, M.; Parama, D.; Girisa, S.; Kumar, A.; Daimary, U. D.; Garodia, P.; Yenisetti, S. C.; Oommen, O. V.; Aggarwal, B. B. *ACS Pharmacol. Transl. Sci.* **2023,** *6,* 447–518. doi:10.1021/acsptsci.2c00012
15. Wiggers, H. J.; Zaioncz, S.; Cheleski, J.; Mainardes, R. M.; Khalil, N. M. Curcumin, a multitarget phytochemical: Challenges and perspectives. In *Studies in Natural Products Chemistry;* Atta ur, R., Ed.; Elsevier: Amsterdam, Netherlands, 2017; Vol. 53, pp 243–276. doi:10.1016/b978-0-444-63930-1.00007-7
16. El-Saadony, M. T.; Yang, T.; Korma, S. A.; Sitohy, M.; Abd El-Mageed, T. A.; Selim, S.; Al Jaouni, S. K.; Salem, H. M.; Mahmmod, Y.; Soliman, S. M.; Mo'men, S. A. A.; Mosa, W. F. A.; El-Wafai, N. A.; Abou-Aly, H. E.; Sitohy, B.; Abd El-Hack, M. E.; El-Tarabily, K. A.; Saad, A. M. *Front. Nutr.* **2023,** *9,* 1040259. doi:10.3389/fnut.2022.1040259
17. Gonçalves, R. F. S.; Martins, J. T.; Abrunhosa, L.; Vicente, A. A.; Pinheiro, A. C. *Nanomaterials* **2021,** *11,* 815. doi:10.3390/nano11030815
18. Dourado, D.; Oliveira, M. C. d.; Araujo, G. R. S. d.; Amaral-Machado, L.; Porto, D. L.; Aragão, C. F. S.; Alencar, E. d. N.; Egito, E. S. T. d. *Colloids Surf., A* **2022,** *652,* 129720. doi:10.1016/j.colsurfa.2022.129720

19. Józsa, L.; Vasvári, G.; Sinka, D.; Nemes, D.; Ujhelyi, Z.;
Vecsernyés, M.; Váradi, J.; Fenyvesi, F.; Lekli, I.; Gyöngyösi, A.;
Bácskay, I.; Fehér, P. *Molecules* **2022,** *27,* 6652.
doi:10.3390/molecules27196652

20. Kabiriyel, J.; Jeyanthi, R.; Jayakumar, K.; Amalraj, A.; Arjun, P.;
Shanmugarathinam, A.; Vignesh, G.; Mohan, C. R.
Carbohydr. Polym. Technol. Appl. **2023,** *5,* 100260.
doi:10.1016/j.carpta.2022.100260

21. Arab-Tehrany, E.; Elkhoury, K.; Francius, G.; Jierry, L.; Mano, J. F.;
Kahn, C.; Linder, M. *Int. J. Mol. Sci.* **2020,** *21,* 7276.
doi:10.3390/ijms21197276

22. Bagheri, M.; Fens, M. H.; Kleijn, T. G.; Capomaccio, R. B.; Mehn, D.;
Krawczyk, P. M.; Scutigliani, E. M.; Gurinov, A.; Baldus, M.;
van Kronenburg, N. C. H.; Kok, R. J.; Heger, M.; van Nostrum, C. F.;
Hennink, W. E. *Mol. Pharmaceutics* **2021,** *18,* 1247–1263.
doi:10.1021/acs.molpharmaceut.0c01114

23. Kotian, V.; Koland, M.; Mutalik, S. *Crystals* **2022,** *12,* 1565.
doi:10.3390/cryst12111565

24. Pires, P. C.; Santos, A. O. *J. Controlled Release* **2018,** *270,* 89–100.
doi:10.1016/j.jconrel.2017.11.047

25. El-SayedAzab, M. Leishmaniasis. In *Textbook of Parasitic Zoonoses;*
Parija, S. C.; Chaudhury, A., Eds.; Springer Nature: Singapore, 2022;
pp 107–124. doi:10.1007/978-981-16-7204-0_11

26. Islan, G. A.; Durán, M.; Cacicedo, M. L.; Nakazato, G.;
Kobayashi, R. K. T.; Martinez, D. S. T.; Castro, G. R.; Durán, N.
Acta Trop. **2017,** *170,* 16–42. doi:10.1016/j.actatropica.2017.02.019

27. Ahmad, A.; Ullah, S.; Syed, F.; Tahir, K.; Khan, A. U.; Yuan, Q.
Nanomedicine (London, U. K.) **2020,** *15,* 809–828.
doi:10.2217/nnm-2019-0413

28. Jones, C. M.; Welburn, S. C. *Front. Vet. Sci.* **2021,** *8,* 618766.
doi:10.3389/fvets.2021.618766

29. Singh, O. P.; Gedda, M. R.; Mudavath, S. L.; Srivastava, O. N.;
Sundar, S. *Nanomedicine (London, U. K.)* **2019,** *14,* 1911–1927.
doi:10.2217/nnm-2018-0448

30. Kammona, O.; Tsanaktsidou, E. *Int. J. Pharm.* **2021,** *605,* 120761.
doi:10.1016/j.ijpharm.2021.120761

31. de Vries, H. J. C.; Schallig, H. D. *Am. J. Clin. Dermatol.* **2022,** *23,*
823–840. doi:10.1007/s40257-022-00726-8

32. Santos-Valle, A. B. C.; Souza, G. R. R.; Paes, C. Q.; Miyazaki, T.;
Silva, A. H.; Altube, M. J.; Morilla, M. J.; Romero, E. L.;
Creczynski-Pasa, T. B.; Cabral, H.; Pittella, F. *Annu. Rev. Control*
2019, *48,* 423–441. doi:10.1016/j.arcontrol.2019.08.001

33. Borghi, S. M.; Fattori, V.; Conchon-Costa, I.; Pinge-Filho, P.;
Pavanelli, W. R.; Verri, W. A., Jr. *Parasitol. Res.* **2017,** *116,* 465–475.
doi:10.1007/s00436-016-5340-7

34. Frézard, F.; Demicheli, C.; Ribeiro, R. R. *Molecules* **2009,** *14,*
2317–2336. doi:10.3390/molecules14072317

35. Sangshetti, J. N.; Kalam Khan, F. A.; Kulkarni, A. A.; Arote, R.;
Patil, R. H. *RSC Adv.* **2015,** *5,* 32376–32415. doi:10.1039/c5ra02669e

36. Tiwari, N.; Gedda, M. R.; Tiwari, V. K.; Singh, S. P.; Singh, R. K.
Mini-Rev. Med. Chem. **2018,** *18,* 26–41.
doi:10.2174/1389557517666170425105129

37. Aggarwal, B. B.; Harikumar, K. B. *Int. J. Biochem. Cell Biol.* **2010,** *41,*
40–59. doi:10.1016/j.biocel.2008.06.010

38. Zhou, H.; Beevers, C. S.; Huang, S. *Curr. Drug Targets* **2011,** *12,*
332–347. doi:10.2174/138945011794815356

39. Celani, L. M. S.; Egito, E. S. T.; Azevedo, Í. M.; Oliveira, C. N.;
Dourado, D.; Medeiros, A. C. *Acta Cir. Bras.* **2022,** *37,* e370602.
doi:10.1590/acb370602

40. Haddad, M.; Sauvain, M.; Deharo, E. *Planta Med.* **2011,** *77,* 672–678.
doi:10.1055/s-0030-1250549

41. Rai, M.; Ingle, A. P.; Pandit, R.; Paralikar, P.; Anasane, N.;
Santos, C. A. D. *Expert Rev. Anti-Infect. Ther.* **2020,** *18,* 367–379.
doi:10.1080/14787210.2020.1730815

42. Albalawi, A. E.; Alanazi, A. D.; Sharifi, I.; Ezzatkhah, F. *Acta Parasitol.*
2021, *66,* 797–811. doi:10.1007/s11686-021-00351-1

43. Alonso, L.; Dorta, M. L.; Alonso, A.
Biochim. Biophys. Acta, Biomembr. **2022,** *1864,* 183977.
doi:10.1016/j.bbamem.2022.183977

44. Pereira, A. H. C.; Marcolino, L. M. C.; Pinto, J. G.; Ferreira-Strixino, J.
Antibiotics (Basel, Switz.) **2021,** *10,* 634.
doi:10.3390/antibiotics10060634

45. Tiwari, B.; Pahuja, R.; Kumar, P.; Rath, S. K.; Gupta, K. C.; Goyal, N.
Antimicrob. Agents Chemother. **2017,** *61,* e01169-16.
doi:10.1128/aac.01169-16

46. Saleheen, D.; Ali, S. A.; Ashfaq, K.; Siddiqui, A. A.; Agha, A.;
Yasinzai, M. M. *Biol. Pharm. Bull.* **2002,** *25,* 386–389.
doi:10.1248/bpb.25.386

47. Elamin, M.; Al-Olayan, E.; Abdel-Gaber, R.; Yehia, R. S.
Rev. Argent. Microbiol. **2021,** *53,* 240–247.
doi:10.1016/j.ram.2020.08.004

48. Khan, M.; Ali, M.; Shah, W.; Shah, A.; Yasinzai, M. M.
Appl. Microbiol. Biotechnol. **2019,** *103,* 7481–7490.
doi:10.1007/s00253-019-09990-x

49. Adapala, N.; Chan, M. M. *Lab. Invest.* **2008,** *88,* 1329–1339.
doi:10.1038/labinvest.2008.90

50. Chaubey, P.; Mishra, B.; Mudavath, S. L.; Patel, R. R.; Chaurasia, S.;
Sundar, S.; Suvarna, V.; Monteiro, M. *Int. J. Biol. Macromol.* **2018,**
111, 109–120. doi:10.1016/j.ijbiomac.2017.12.143

51. Chan, M. M.-Y.; Huang, H.-I.; Mattiacci, J. A.; Fong, D. Modulation of
Cytokine Gene Expression by Curcumin. *Food Factors in Health
Promotion and Disease Prevention;* ACS Symposium Series, Vol.
851; American Chemical Society: Washington, DC, USA, 2003;
pp 88–99. doi:10.1021/bk-2003-0851.ch008

52. Das, R.; Roy, A.; Dutta, N.; Majumder, H. K. *Apoptosis* **2008,** *13,*
867–882. doi:10.1007/s10495-008-0224-7

53. Agrawal, N.; Jaiswal, M. *Eur. J. Med. Chem. Rep.* **2022,** *6,* 100081.
doi:10.1016/j.ejmcr.2022.100081

54. Paolino, D.; Vero, A.; Cosco, D.; Pecora, T. M. G.; Cianciolo, S.;
Fresta, M.; Pignatello, R. *Front. Pharmacol.* **2016,** *7,* 485.
doi:10.3389/fphar.2016.00485

55. Amato, V. S.; Tuon, F. F.; Bacha, H. A.; Neto, V. A.; Nicodemo, A. C.
Acta Trop. **2008,** *105,* 1–9. doi:10.1016/j.actatropica.2007.08.003

56. Goonoo, N.; Laetitia Huët, M. A.; Chummun, I.; Karuri, N.; Badu, K.;
Gimié, F.; Bergrath, J.; Schulze, M.; Müller, M.; Bhaw-Luximon, A.
R. Soc. Open Sci. **2022,** *9,* 220058. doi:10.1098/rsos.220058

57. Peixoto, J. F.; Gonçalves-Oliveira, L. F.; Souza-Silva, F.;
Côrtes, L. M. d. C.; Dias-Lopes, G.; Cardoso, F. d. O.;
Santos, R. d. O.; Patricio, B. F. d. C.; Nicoletti, C. D.;
Lima, C. G. d. S.; Calabrese, K. d. S.; Moreira, D. d. L.;
Rocha, H. V. A.; da Silva, F. d. C.; Ferreira, V. F.; Alves, C. R.
Int. J. Pharm. **2023,** *636,* 122864. doi:10.1016/j.ijpharm.2023.122864

58. Khalil, N. M.; de Mattos, A. C.; Moraes Moreira Carraro, T. C.;
Ludwig, D. B.; Mainardes, R. M. *Curr. Pharm. Des.* **2013,** *19,*
7316–7329. doi:10.2174/13816128194113121919135458

59. Varma, D. M.; Redding, E. A.; Bachelder, E. M.; Ainslie, K. M.
ACS Biomater. Sci. Eng. **2021,** *7,* 1725–1741.
doi:10.1021/acsbiomaterials.0c01132

60. de Souza, A.; Marins, D. S. S.; Mathias, S. L.; Monteiro, L. M.; Yukuyama, M. N.; Scarim, C. B.; Löbenberg, R.; Bou-Chacra, N. A. *Int. J. Pharm.* **2018,** *547,* 421–431. doi:10.1016/j.ijpharm.2018.06.018

61. Pires, V. C.; Magalhães, C. P.; Ferrante, M.; Rebouças, J. d. S.; Nguewa, P.; Severino, P.; Barral, A.; Veras, P. S. T.; Formiga, F. R. *Acta Trop.* **2020,** *211,* 105595. doi:10.1016/j.actatropica.2020.105595

62. Verçoza, B. R. F.; Bernardo, R. R.; de Oliveira, L. A. S.; Rodrigues, J. C. F. *Beilstein J. Nanotechnol.* **2023,** *14,* 893–903. doi:10.3762/bjnano.14.73

63. Abpeikar, Z.; Safaei, M.; Akbar Alizadeh, A.; Goodarzi, A.; Hatam, G. *Int. J. Pharm.* **2023,** *633,* 122615. doi:10.1016/j.ijpharm.2023.122615

64. Kalepu, S.; Nekkanti, V. *Acta Pharm. Sin. B* **2015,** *5,* 442–453. doi:10.1016/j.apsb.2015.07.003

65. Owais, M.; Gupta, C. M. *Curr. Drug Delivery* **2005,** *2,* 311–318. doi:10.2174/156720105774370177

66. Saleem, K.; Khursheed, Z.; Hano, C.; Anjum, I.; Anjum, S. *Nanomaterials* **2019,** *9,* 1749. doi:10.3390/nano9121749

67. Loo, C.-Y.; Siew, E. L.; Young, P. M.; Traini, D.; Lee, W.-H. *Food Chem. Toxicol.* **2022,** *163,* 112976. doi:10.1016/j.fct.2022.112976

68. Santana, É. S. d.; Belmiro, V. B. d. S.; de Siqueira, L. B. d. O.; do Nascimento, T.; Santos-Oliveira, R.; dos Santos Matos, A. P.; Ricci-Junior, E. *J. Drug Delivery Sci. Technol.* **2022,** *75,* 103622. doi:10.1016/j.jddst.2022.103622

69. Costa Lima, S. A.; Resende, M.; Silvestre, R.; Tavares, J.; Ouaissi, A.; Lin, P. K. T.; Cordeiro-da-Silva, A. *Nanomedicine (London, U. K.)* **2012,** *7,* 1839–1849. doi:10.2217/nnm.12.74

70. Das, A.; Kamran, M.; Ali, N. *Front. Cell. Infect. Microbiol.* **2021,** *11,* 694470. doi:10.3389/fcimb.2021.694470

71. Caballero, A.; Salas, J.; Sánchez-Moreno, M. Metal-based therapeutics for Leishmaniasis. In *Leishmaniasis - Trends in Epidemiology, Diagnosis and Treatment;* Claborn, D. M., Ed.; InTechOpen: Rijeka, Croatia, 2014. doi:10.5772/57376

72. Almayouf, M. A.; El-khadragy, M.; Awad, M. A.; Alolayan, E. M. *Biosci. Rep.* **2020,** *40,* BSR20202672. doi:10.1042/bsr20202672

73. Dhorm Pimentel de Moraes, A. R.; Tavares, G. D.; Soares Rocha, F. J.; de Paula, E.; Giorgio, S. *Exp. Parasitol.* **2018,** *187,* 12–21. doi:10.1016/j.exppara.2018.03.005

74. Tuon, F. F.; Dantas, L. R.; de Souza, R. M.; Ribeiro, V. S. T.; Amato, V. S. *Parasitol. Res.* **2022,** *121,* 3073–3082. doi:10.1007/s00436-022-07659-5

75. Want, M. Y.; Islammudin, M.; Chouhan, G.; Ozbak, H. A.; Hemeg, H. A.; Chattopadhyay, A. P.; Afrin, F. *Int. J. Nanomed.* **2017,** *12,* 2189–2204. doi:10.2147/ijn.s106548

76. Siqueira Jørgensen, S. D.; Al Sawaf, M.; Graeser, K.; Mu, H.; Müllertz, A.; Rades, T. *Eur. J. Pharm. Biopharm.* **2018,** *124,* 116–124. doi:10.1016/j.ejpb.2017.12.014

77. Buya, A. B.; Beloqui, A.; Memvanga, P. B.; Préat, V. *Pharmaceutics* **2020,** *12,* 1194. doi:10.3390/pharmaceutics12121194

78. Thomas, N.; Holm, R.; Müllertz, A.; Rades, T. *J. Controlled Release* **2012,** *160,* 25–32. doi:10.1016/j.jconrel.2012.02.027

79. Khan, M.; Nadhman, A.; Shah, W.; Khan, I.; Yasinzai, M. *IET Nanobiotechnol.* **2019,** *13,* 477–483. doi:10.1049/iet-nbt.2018.5281

80. Smith, L.; Serrano, D. R.; Mauger, M.; Bolás-Fernández, F.; Dea-Ayuela, M. A.; Lalatsa, A. *Mol. Pharmaceutics* **2018,** *15,* 2570–2583. doi:10.1021/acs.molpharmaceut.8b00097

81. Khan, M.; Nadhman, A.; Sehgal, S. A.; Siraj, S.; Yasinzai, M. M. *Curr. Top. Med. Chem.* **2018,** *18,* 1603–1609. doi:10.2174/1568026618666181025104818

82. Mozafari, M. R. Nanoliposomes: Preparation and Analysis. In *Methods in Molecular Biology;* Weissig, V., Ed.; Humana Press: New York, NY, USA, 2010; Vol. 605, pp 29–50. doi:10.1007/978-1-60327-360-2_2

83. Aguilar-Pérez, K. M.; Avilés-Castrillo, J. I.; Medina, D. I.; Parra-Saldivar, R.; Iqbal, H. M. N. *Front. Bioeng. Biotechnol.* **2020,** *8,* 579536. doi:10.3389/fbioe.2020.579536

84. Najafian, H. R.; Mohebali, M.; Rezayat, S. M.; Partoazar, A. R.; Esmaili, J.; Elikaee, S.; Nahavandi, K. H.; Jaafari, M. R.; Mahmoodi, M.; Shirzadi, M. R.; Mortazavi, H. *Int. J. Pharm. Res. Allied Sci.* **2016,** *5,* 97–107. https://ijpras.com/article/nanoliposomal-miltefosine-for-the-treatment-of-cutaneous-leishmaniasis-caused-by-leishmania-major-mrhoir75er-the-drug-preparation-and-in-vitro-study

85. da Costa-Silva, T. A.; Galisteo, A. J., Jr.; Lindoso, J. A. L.; Barbosa, L. R. S.; Tempone, A. G. *Antimicrob. Agents Chemother.* **2017,** *61,* e02297-16. doi:10.1128/aac.02297-16

86. Pinto, E. G.; Barbosa, L. R. S.; Mortara, R. A.; Tempone, A. G. *Chem.-Biol. Interact.* **2020,** *332,* 109296. doi:10.1016/j.cbi.2020.109296

87. Bafghi, A. F.; Mirzaei, F.; Norouzi, R.; Haghirosadat, F.; Pournasir, S.; Pournasir, F.; Siyadatpanah, A. *Ann. Parasitol.* **2021,** *67,* 637–646. doi:10.17420/ap6704.380

88. Kalantari, H.; Hemmati, A. A.; Bavarsad, N.; Rezaie, A.; Ahmadi, S. *Jundishapur J. Nat. Pharm. Prod.* **2014,** *9,* e17565. doi:10.17795/jjnpp-17565

89. Bafghi, A. F.; Haghirosadat, B. F.; Yazdian, F.; Mirzaei, F.; Pourmadadi, M.; Pournasir, F.; Hemati, M.; Pournasir, S. *Prep. Biochem. Biotechnol.* **2021,** *51,* 990–997. doi:10.1080/10826068.2021.1885045

90. Singodia, D.; Verma, A.; Khare, P.; Dube, A.; Mitra, K.; Mishra, P. R. *J. Liposome Res.* **2012,** *22,* 8–17. doi:10.3109/08982104.2011.584317

91. Garg, J.; Pathania, K.; Sah, S. P.; Pawar, S. V. *Future J. Pharm. Sci.* **2022,** *8,* 25. doi:10.1186/s43094-022-00414-8

92. Monteiro, L. M.; Löbenberg, R.; Barbosa, E. J.; de Araujo, G. L. B.; Sato, P. K.; Kanashiro, E.; de Araujo Eliodoro, R. H.; Rocha, M.; de Freitas, V. L. T.; Fotaki, N.; Bou-Chacra, N. A. *Eur. J. Pharm. Sci.* **2022,** *169,* 106097. doi:10.1016/j.ejps.2021.106097

93. Ferreira, M. A.; de Almeida Júnior, R. F.; Onofre, T. S.; Casadei, B. R.; Farias, K. J. S.; Severino, P.; de Oliveira Franco, C. F.; Raffin, F. N.; de Lima e Moura, T. F. A.; de Melo Barbosa, R. *Pharmaceutics* **2021,** *13,* 1912. doi:10.3390/pharmaceutics13111912

94. Rahnama, V.; Motazedian, M. H.; Mohammadi-Samani, S.; Asgari, Q.; Ghasemiyeh, P.; Khazaei, M. *Res. Pharm. Sci.* **2021,** *16,* 623–633. doi:10.4103/1735-5362.327508

95. Rebouças-Silva, J.; Tadini, M. C.; Devequi-Nunes, D.; Mansur, A. L.; Silveira-Mattos, P. S.; de Oliveira, C. I.; Formiga, F. R.; Berretta, A. A.; Marquele-Oliveira, F.; Borges, V. M. *Int. J. Nanomed.* **2020,** *15,* 8659–8672. doi:10.2147/ijn.s262642

96. Riaz, A.; Ahmed, N.; Khan, M. I.; Haq, I.-u.; Rehman, A. u.; Khan, G. M. *J. Drug Delivery Sci. Technol.* **2019,** *54,* 101232. doi:10.1016/j.jddst.2019.101232

97. Khazaei, M.; Rahnama, V.; Motazedian, M. H.; Samani, S. M.; Hatam, G. *J. Parasit. Dis.* **2021,** *45,* 964–971. doi:10.1007/s12639-021-01373-2

98. Gagliardi, A.; Giuliano, E.; Venkateswararao, E.; Fresta, M.; Bulotta, S.; Awasthi, V.; Cosco, D. *Front. Pharmacol.* **2021,** *12,* 601626. doi:10.3389/fphar.2021.601626

99. Mehanna, M. M.; Mohyeldin, S. M.; Elgindy, N. A. *J. Controlled Release* **2014,** *187,* 183–197. doi:10.1016/j.jconrel.2014.05.038

100. Kreuter, J. *Adv. Drug Delivery Rev.* **2014,** *71,* 2–14. doi:10.1016/j.addr.2013.08.008

101. Zielińska, A.; Carreiró, F.; Oliveira, A. M.; Neves, A.; Pires, B.; Venkatesh, D. N.; Durazzo, A.; Lucarini, M.; Eder, P.; Silva, A. M.; Santini, A.; Souto, E. B. *Molecules* **2020,** *25,* 3731. doi:10.3390/molecules25163731

102. Banik, B. L.; Fattahi, P.; Brown, J. L. *Wiley Interdiscip. Rev.: Nanomed. Nanobiotechnol.* **2016,** *8,* 271–299. doi:10.1002/wnan.1364

103. Rajitha, P.; Gopinath, D.; Biswas, R.; Sabitha, M.; Jayakumar, R. *Expert Opin. Drug Delivery* **2016,** *13,* 1177–1194. doi:10.1080/17425247.2016.1178232

104. Esboei, B. R.; Mohebali, M.; Mousavi, P.; Fakhar, M.; Akhoundi, B. *J. Vector Borne Dis.* **2018,** *52,* 111–115.

105. Chaubey, P.; Patel, R. R.; Mishra, B. *Expert Opin. Drug Delivery* **2014,** *11,* 1163–1181. doi:10.1517/17425247.2014.917076

106. de Santana, N. S.; de Oliveira de Siqueira, L. B.; do Nascimento, T.; Santos-Oliveira, R.; dos Santos Matos, A. P.; Ricci-Júnior, E. *J. Nanopart. Res.* **2023,** *25,* 24. doi:10.1007/s11051-023-05676-8

107. Cruz, K. P.; Patricio, B. F. C.; Pires, V. C.; Amorim, M. F.; Pinho, A. G. S. F.; Quadros, H. C.; Dantas, D. A. S.; Chaves, M. H. C.; Formiga, F. R.; Rocha, H. V. A.; Veras, P. S. T. *Front. Chem. (Lausanne, Switz.)* **2021,** *9,* 644827. doi:10.3389/fchem.2021.644827

108. Tosyali, O. A.; Allahverdiyev, A.; Bagirova, M.; Abamor, E. S.; Aydogdu, M.; Dinparvar, S.; Acar, T.; Mustafaeva, Z.; Derman, S. *Mater. Sci. Eng., C* **2021,** *120,* 111684. doi:10.1016/j.msec.2020.111684

109. Malyala, P.; Singh, M. Micro/nanoparticle adjuvants: Preparation and formulation with antigens. In *Vaccine Adjuvants: Methods and Protocols;* Davies, G., Ed.; Humana Press: Totowa, NJ, USA, 2010; pp 91–101. doi:10.1007/978-1-60761-585-9_7

110. Silva, A. L.; Soema, P. C.; Slütter, B.; Ossendorp, F.; Jiskoot, W. *Hum. Vaccines Immunother.* **2016,** *12,* 1056–1069. doi:10.1080/21645515.2015.1117714

111. Ghosh, S.; Das, S.; De, A. K.; Kar, N.; Bera, T. *RSC Adv.* **2017,** *7,* 29575–29590. doi:10.1039/c7ra04951j

112. Valle, I. V.; Machado, M. E.; Araújo, C. d. C. B.; da Cunha-Junior, E. F.; da Silva Pacheco, J.; Torres-Santos, E. C.; da Silva, L. C. R. P.; Cabral, L. M.; do Carmo, F. A.; Sathler, P. C. *Nanotechnology* **2019,** *30,* 455102. doi:10.1088/1361-6528/ab373e

113. Thakur, M.; Sharma, A.; Chandel, M.; Pathania, D. Modern applications and current status of green nanotechnology in environmental industry. In *Green Functionalized Nanomaterials for Environmental Applications;* Shanker, U.; Hussain, C. M.; Rani, M., Eds.; Elsevier: Amsterdam, Netherlands, 2022; pp 259–281. doi:10.1016/b978-0-12-823137-1.00010-5

114. Bhardwaj, P.; Singh, B.; Behera, S. P. Green approaches for nanoparticle synthesis: emerging trends. In *Nanomaterials;* Kumar, R. P.; Bharathiraja, B., Eds.; Academic Press: London, UK, 2021; pp 167–193. doi:10.1016/b978-0-12-822401-4.00015-5

115. Yaqoob, S. B.; Adnan, R.; Rameez Khan, R. M.; Rashid, M. *Front. Chem. (Lausanne, Switz.)* **2020,** *8,* 376. doi:10.3389/fchem.2020.00376

116. Kong, F.-Y.; Zhang, J.-W.; Li, R.-F.; Wang, Z.-X.; Wang, W.-J.; Wang, W. *Molecules* **2017,** *22,* 1445. doi:10.3390/molecules22091445

117. Want, M. Y.; Yadav, P.; Khan, R.; Chouhan, G.; Islamuddin, M.; Aloyouni, S. Y.; Chattopadhyay, A. P.; AlOmar, S. Y.; Afrin, F. *Int. J. Nanomed.* **2021,** *16,* 7285–7295. doi:10.2147/ijn.s268548

118. Sasidharan, S.; Saudagar, P. *Acta Trop.* **2022,** *231,* 106448. doi:10.1016/j.actatropica.2022.106448

119. Morones, J. R.; Elechiguerra, J. L.; Camacho, A.; Holt, K.; Kouri, J. B.; Ramírez, J. T.; Yacaman, M. J. *Nanotechnology* **2005,** *16,* 2346–2353. doi:10.1088/0957-4484/16/10/059

120. Holt, K. B.; Bard, A. J. *Biochemistry* **2005,** *44,* 13214–13223. doi:10.1021/bi0508542

121. Chamakura, K.; Perez-Ballestero, R.; Luo, Z.; Bashir, S.; Liu, J. *Colloids Surf., B* **2011,** *84,* 88–96. doi:10.1016/j.colsurfb.2010.12.020

122. Kalangi, S. K.; Dayakar, A.; Gangappa, D.; Sathyavathi, R.; Maurya, R. S.; Narayana Rao, D. *Exp. Parasitol.* **2016,** *170,* 184–192. doi:10.1016/j.exppara.2016.09.002

123. Das, S.; Roy, P.; Mondal, S.; Bera, T.; Mukherjee, A. *Colloids Surf., B* **2013,** *107,* 27–34. doi:10.1016/j.colsurfb.2013.01.061

124. Badirzadeh, A.; Alipour, M.; Najm, M.; Vosoogh, A.; Vosoogh, M.; Samadian, H.; Hashemi, A. S.; Farsangi, Z. J.; Amini, S. M. *J. Drug Delivery Sci. Technol.* **2022,** *74,* 103576. doi:10.1016/j.jddst.2022.103576

125. Amini, S. M.; Hadighi, R.; Najm, M.; Alipour, M.; Hasanpour, H.; Vosoogh, M.; Vosough, A.; Hajizadeh, M.; Badirzadeh, A. *Curr. Microbiol.* **2023,** *80,* 104. doi:10.1007/s00284-022-03172-1

Development and characterization of potential larvicidal nanoemulsions against *Aedes aegypti*

Jonatas L. Duarte[*1], Leonardo Delello Di Filippo[1],

Anna Eliza Maciel de Faria Mota Oliveira[2], Rafael Miguel Sábio[1], Gabriel Davi Marena[1,3],

Tais Maria Bauab[3], Cristiane Duque[4], Vincent Corbel[5,6] and Marlus Chorilli[*1]

Full Research Paper

Address:
[1]Department of Drugs and Medicines, School of Pharmaceutical Sciences, São Paulo State University (UNESP), Araraquara, São Paulo, Brazil, [2]Departamento de Ciências Biológicas e da Saúde, Universidade Federal do Amapá, Macapá, AP, Brazil, [3]Department of Biological Sciences, São Paulo State University (UNESP), School of Pharmaceutical Sciences, Campus Araraquara, São Paulo, Brazil, [4]Department of Preventive and Restorative Dentistry, Araçatuba Dental School - São Paulo State University (UNESP), Araçatuba, SP, Brazil, [5]Institut de Recherche pour le Développement (IRD), MIVEGEC, Univ. Montpellier, CNRS, IRD, 911 Av Agropolis, 34 394 Montpellier, France and [6]Fundação Oswaldo Cruz (FIOCRUZ), Instituto Oswaldo Cruz (IOC), Laboratório de Fisiologia e Controle de Artrópodes Vetores (Laficave). Avenida Brasil, 4365 Manguinhos, Rio de Janeiro – RJ, CEP: 21040-360, Brazil

Email:
Jonatas L. Duarte[*] - jl.duarte@unesp.br; Marlus Chorilli[*] - marlus.chorilli@unesp.br

* Corresponding author

Keywords:
colloidal stability; drug delivery system; hydrophile–lipophile balance; monoterpenes

Abstract

Plant-based insecticides offer advantages such as negligible residual effects, reduced risks to both humans and the environment, and immunity to resistance issues that plague conventional chemicals. However, the practical use of monoterpenes in insect control has been hampered by challenges including their poor solubility and stability in aqueous environments. In recent years, the application of nanotechnology-based formulations, specifically nanoemulsions, has emerged as a prospective strategy to surmount these obstacles. In this study, we developed and characterized nanoemulsions based on cymene and myrcene and assessed their toxicity both in vitro using human keratinocytes (HaCAT) cells and in an in vivo model involving *Galleria mellonella* larvae. Additionally, we investigated the insecticidal efficacy of monoterpenes against the mosquito *Aedes aegypti*, the primary dengue vector, via larval bioassay. Employing a low-energy approach, we successfully generated nanoemulsions. The cymene-based nanoemulsion exhibited a hydrodynamic diameter of approximately 98 nm and a zeta potential of −25 mV. The myrcene-based nanoemulsion displayed a hydrodynamic diameter of 118 nm and a zeta potential of −20 mV. Notably, both nanoemulsions demonstrated stability over

60 days, accompanied by controlled release properties and low toxicity towards HaCAT cells and *Galleria mellonella* larvae. Moreover, the nanoemulsions exhibited significant lethality against third-instar *Aedes aegypti* larvae at a concentration of 50 mg/L. In conclusion, the utilization of nanoemulsions encapsulating cymene and myrcene presents a promising avenue for overcoming the limitations associated with poor solubility and stability of monoterpenes. This study sheds light on the potential of the nanoemulsions as effective and environmentally friendly insecticides in the ongoing battle against mosquito-borne diseases.

Introduction

Aedes aegypti (Linnaeus, 1762) is a mosquito species that is cosmopolitan and well adapted to anthropized and peridomestic environments. It is an important vector of arboviruses, including dengue, chikungunya fever, zika, and urban yellow fever and can cause alarming socio-economic impacts in the affected regions [1]. The World Health Organization (WHO) considers dengue, zika, and chikungunya as neglected and emerging tropical diseases transmitted by mosquitoes and as one of the main concerns in developing countries, which may become a major public health problem worldwide. This problem is evidenced by recent cases of Zika virus infection in Brazil and their relationship with microcephaly in newborns [2]. In the case of dengue, the most prevalent viral infection transmitted by *Aedes* mosquitoes with clinical forms ranging from asymptomatic to fatal cases, around 3.9 billion people in more than 129 countries are at risk [3]. The continuous and indiscriminate use of synthetic insecticides for the control of the *Aedes aegypti* mosquito (Linnaeus) has been responsible for the emergence of insecticide-resistant mosquitoes [4,5]. Therefore, it becomes urgent to search for safer and more effective vector control agents to prevent vector-borne diseases [6].

Bioinsecticides from plant derivatives, which degrade rapidly in the environment and have less toxicity in non-target organisms, are a promising option for vector control [7]. Terpenes are the largest group of secondary plant metabolites and have shown promising health benefits as antioxidant and anti-inflammatory agents in many animal studies [8,9]. The compound *p*-cymene, also known as *p*-cymol or *p*-isopropyltoluene, is a monocyclic hydrocarbonated monoterpene naturally occurring in essential oils (EOs) of various aromatic plants, including the genera *Artemisia*, *Protium*, *Origanum*, and *Thymus*. Myrcene is an acyclic monoterpene found in hops, lemongrass, basil, and mangos [10].

Some intrinsic characteristics of monoterpenes, mainly poor water solubility and high volatility, make their formulation a true challenge. In this regard, nanoemulsions (NEs), which are dispersions of two immiscible liquids with one of them dispersed as small droplets [11,12], stand out as new delivery vehicles for these bioactive compounds. They are especially important to enhance the water availability of poorly water-soluble compounds, which is achieved when the oil constitutes the internal phase. In this case, oil-in-water nanoemulsions or aqueous nanoemulsions are obtained. The main advantage of NEs is their better kinetic stability compared to macro-emulsions. Also, the NEs protect the EO constituents from oxidation, in addition to promoting better sensorial properties [13]. Moreover, the development of aqueous nanoemulsions would enable a better dispersion of vector control agents, inducing a controlled release and a possibly higher effectiveness in eliminating immature stages of mosquitoes [14].

NEs can be obtained through two general approaches, that is, high-energy methods and low-energy methods. The high-energy methods are characterized by using equipment such as sonicators, high-speed homogenizers, and high-pressure homogenizers, which provide high energy input during processing, leading to the generation of dispersed material on a nanoscale [15]. The low-energy methods are characterized by the use and control of the chemical energy of the system in the formation of droplets on the nanoscale. A crucial point is that these systems can be obtained at low cost and with eco-friendly techniques [16,17].

Griffin established the hydrophile–lipophile balance (HLB) as a tool for classifying and selecting non-ionic emulsifiers [18]. The determination of the required HLB (rHLB) of essential oils appears as a critical step for the development of stable emulsions [19]. Determining the required HLB, one can obtain the nanoemulsion with the smallest droplet size, leading to more stable formulations [20]. The rHLB is usually determined by preparing NEs with different ratios of surfactant blends and choosing the most stable formulation to determine the rHLB of the oil phase [21].

Biocompatibility assessment is an essential aspect of the development of NEs, particularly for biomedical and cosmetic applications, as it determines the safety and efficacy of the formulations. The assessment involves evaluating the potential cytotoxicity and genotoxicity of the NEs on different cell types and determining the effect on the immune response in vivo. In vitro cytotoxicity assays are an important tool for evaluating the safety of NEs. HaCaT cells are a widely used human keratinocyte cell line that exhibits several characteristics of

normal human epidermal keratinocytes, making them an excellent model for evaluating cytotoxicity [22].

In vivo toxicity studies are also crucial for evaluating the safety of NEs. *Galleria mellonella* larvae have emerged as an alternative to mammalian models for in vivo studies of acute toxicity because of their low maintenance cost, easy handling, and high similarity in immune response with mammals. Furthermore, *G. mellonella* larvae have been successfully used to evaluate the acute toxicity of various nanoparticles and drugs [23]. The immune response of *G. mellonella* larvae can be evaluated by monitoring their survival rate and melanization response [24].

The aim of the present work was (i) to develop stable oil-in-water nanoemulsions containing myrcene or cymene as the dispersed phase, (ii) to determine the required rHLB values for emulsion stability, (iii) to assess the biocompatibility via in vitro and in vivo assays, and (iv) to evaluate the bioefficacy of the NE against *Aedes aegypti* mosquito larvae.

Results and Discussion
Preparation and characterization of the nanoemulsions
The determination of the required HLB (rHLB) is an important step in the development of NEs containing volatile oils [19,25]. From the determination of the rHLB, it is possible to determine the best ratio between two surfactants, one more lipophilic and one more hydrophilic, which will be necessary to obtain a stable NE [18]. The rHLB of myrcene and cymene was determined using a mixture of Span 80 (lipophilic) and Tween 20 (surfactant). At a time of 24 h after preparation, formulations containing cymene with HLB values of 10–13 showed a yellowish layer on the surface, which may be an indication of phase separation (Figure S1, Supporting Information File 1). Formulations

with HLB values of 16 and 16.7 showed a milky appearance and slight creaming, which may be indicative of Ostwald maturation, a very important mechanism when it comes to the instability of NEs. It is related to the difference between the droplet sizes in the formulation, with the smaller droplets having greater chemical potential and, thus, diffusing to the larger ones [26]. Formulations with HLB values of 14 and 15 were the ones that presented the best visual characteristics, in addition to a bluish appearance, a characteristic of NEs [27,28]. Thus, the formulations with HLB values of 14 and 15 were selected for analysis by DLS.

After 24 h (D1), the formulation with HLB 14 had a droplet size of 116 ± 0.40 nm, and after 21 days there was no significant change in particle size, nor in polydispersity index (PdI) and zeta potential. The formulation with HLB 15 exhibited smaller particle size and lower PdI and zeta potential than the HLB 14 formulation. Also, there was no significant variation in these parameters throughout the analyzed period (60 days) (Table 1). For this reason, the formulation with HLB 15 was the formulation chosen as the rHLB of cymene.

After 24 h, the myrcene formulations with lower HLB values (10–11), that is, a greater amount of the surfactant (Tween 20) plus lipophilic (Span 80), showed classic signs of instability (i.e., creaming) (Figure S2, Supporting Information File 1). Formulations with HLB values of 12–14 and 16.7 showed a milky appearance and a more viscous appearance, characteristic of emulsions with droplets on the micrometric scale. It is important to mention that these formulations also showed signs of instability after 21 days. The formulations with HLB 15 and 16 were the ones that presented the best visual appearance, such as a bluish appearance characteristic of nanoemulsions, and maintained these characteristics over time. Thus, these formulations were selected for DLS.

Table 1: Hydrodynamic diameter, PdI, and zeta potential of Cym-NEs.[a]

Time	HLB 14			HLB 15		
	Size (nm)	PdI	Zeta potential (mV)	Size (nm)	PdI	Zeta potential (mV)
D1	116.0 ± 0.40	0.322 ± 0.024	−34.7 ± 1.1	98.46 ± 0.83	0.209 ± 0.002	−25.9 ± 0.43
D7	111.2 ± 1.58	0.285 ± 0.007	−36.1 ± 0.7	96.74 ± 1.00	0.226 ± 0.006	−24.3 ± 0.80
D14	107.6 ± 1.59	0.331 ± 0.023	−26.8 ± 0.4	95.43 ± 1.20	0.204 ± 0.006	−25.4 ± 1.45
D21	106.5 ± 0.73	0.350 ± 0.003	−34.5 ± 0.8	98.7 ± 1.508	0.216 ± 0.004	−25.5 ± 0.68
D30	—	—	—	96.09 ± 0.61	0.218 ± 0.009	−23.3 ± 0.45
D45	—	—	—	97.69 ± 0.20	0.205 ± 0.013	−25.5 ± 1.14
D60	—	—	—	89.70 ± 0.17	0.240 ± 0.004	−25.9 ± 0.35

[a]The data are expressed as mean ± standard deviation, *n* = 3.

The droplet size and PdI of the formulation with HLB 16 were slightly smaller than those of the formulation with HLB 15 (Table 2). Over time, there was no significant variation in the size for both formulations. Unlike the formulation containing cymene, the best formulation with myrcene was the one with HLB 16, which has in its composition a greater amount of Tween 20, the more hydrophilic surfactant.

It has been shown that a significant difference of the headgroup size of the surfactants has a synergistic effect on emulsion stabilization. Furthermore, the use of mixed surfactants enhances the properties of the interfacial film, leading to improved adsorption between the oil and water phases and enhancing the stability of nanoemulsions [29].

Previous studies have reported similar findings regarding NEs containing terpenes. Polydispersity index values comparable to those observed in our study were obtained, indicating the formation of stable and suitable NEs for larvicidal applications [30]. It is noteworthy that several studies have utilized essential oils containing chemical components structurally analogous to terpenes, thus, achieving table formulations using the same surfactants and active ingredient concentration (5%) [26-28]. However, there is only a limited number of studies that focus specifically on the production and characterization of nanoemulsions incorporating cymene or myrcene. Nevertheless, it has been demonstrated that a high-energy method can yield a nanoemulsion comprising 5% *p*-cymene stabilized with 1% Tween 80, with droplet sizes measuring approximately 150 nm, which maintained its stability for 60 days [31].

The zeta potential is used to predict the stability of dispersions, and its value depends on the physicochemical properties of active ingredients, polymers, vehicles, and the presence of electrolytes and their adsorption [32]. The zeta potential values found for the NEs obtained remained stable in the analyzed period, which indicates the stability of the formulation to avoid Ostwald maturation and coalescence of the droplets. Similar zeta potential characteristics, between 20 and 30 mV, have been described in other studies about nanoemulsions containing terpenes suitable for larvicidal applications [30,33,34].

Regarding the physical characterization, the bluish reflex is characteristic of this type of colloidal system, and it is attributed to the Tyndall effect, making it a valuable macroscopic indicator of nanodroplet generation [16]. In addition, Forgiarini et al. indicated that a suitable nanoemulsion should have small drops of the dispersed phase (average below 300 nm) [35]. Izquierdo et al. stated that polydispersion index values close to 0.2 are an indication of kinetic stability with an almost monomodal distribution [36]. Thus, considering that in this study the stable formulations had similar size distribution profiles and low polydispersity index, the present study on cymene and myrcene nanoemulsions may be considered promising.

Nanoparticle tracking analysis

From the two results obtained above, the HLB 15 formulation containing cymene and the HLB 16 formulation containing myrcene underwent nanoparticle tracking analysis (NTA). NTA is a technique for direct and real-time visualization, sizing, and counting of nanometric materials suspended in aqueous media [37]. According to NTA measurements, the Cym-NE particle size was 145.7 ± 7.7 nm, while the Myr-NE particle size was 126.4 ± 5.6 nm, confirming the nanometric droplet size.

Cryogenic transmission electron microscopy

Cryogenic transmission electron microscopy (cryo-TEM) is one of the most useful techniques for the investigation of NEs, since it provides detailed information about the internal structure of colloidal systems observed in their native state [38]. In cryo-TEM, it was possible to observe spherical droplets (Figure 1).

Table 2: Hydrodynamic diameter, PdI and zeta potential of Myr-NEs.[a]

	HLB 15			HLB 16		
Time	Size (nm)	PdI	Zeta potential (mV)	Size (nm)	PdI	Zeta potential (mV)
1D	123.9 ± 1.15	0.369 ± 0.02	−17.4 ± 0.0	118.8 ±1.2	0.241 ± 0.01	−21.1 ± 0.3
7 D	113.5 ± 1.45	0.352 ± 0.05	−20.7 ± 0.3	118.0 ± 3.7	0.227 ± 0.006	−21.5 ± 0.5
14 D	112.0 ± 0.51	0.364 ± 0.01	−26.8 ± 0.4	110.8 ± 3.4	0.235 ± 0.007	−22.6 ± 2.3
21 D	115.4 ± 0.45	0.240 ± 0.02	−24.3 ± 0.5	104.5 ± 0.4	0.255 ± 0.005	−25.5 ± 0.6
D30	—	—	—	105.5 ± 0.7	0.227 ± 0.009	−25.3 ± 1.63
D45	—	—	—	99.93 ± 1.45	0.246 ± 0.012	−21.0 ± 2.47
D60	—	—	—	84.50 ± 0.82	0.217 ± 0.008	−20.7 ± 0.95

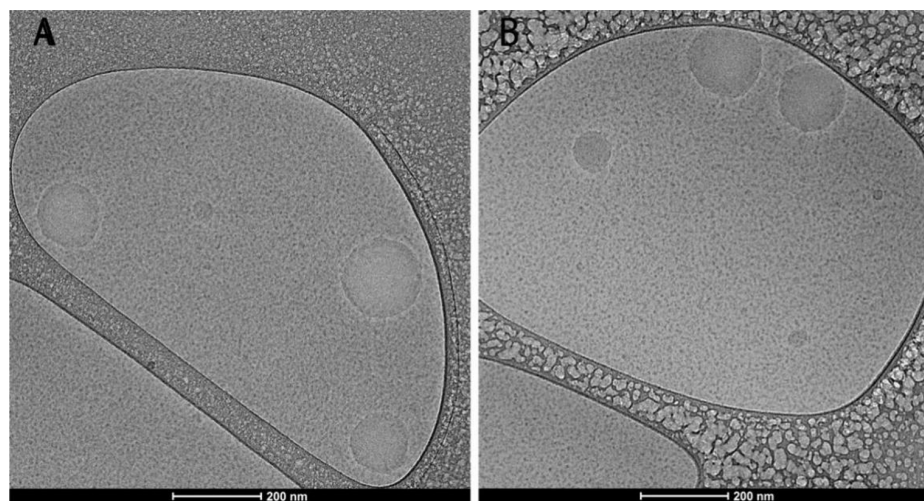[a]The data are expressed as mean ± standard deviation, *n* = 3.

Figure 1: Cryogenic transmission electron microscopy of (A) Cym-NE and (B) Myr-NE.

Similar results of spherical droplets smaller than 180 nm were observed with cryo-TEM [39]. This technique is widely used to characterize the morphology of nanoemulsions and faithfully confirms the results obtained with other techniques [40].

In vitro drug release

One potential advantage of using NEs is their ability to enhance drug solubility and bioavailability. NEs have been shown to increase the solubility of poorly soluble drugs, such as monoterpenes, which can improve drug delivery and efficacy. The cumulative release of both free terpenes was lower than the cumulative release of nanoemulsions (Figure 2).
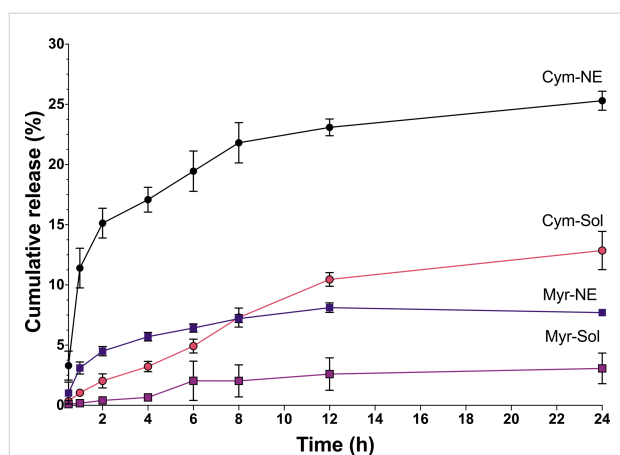

Figure 2: The in vitro drug release of nanoemulsions (Cym-NE, Myr-NE) and free terpenes (Cym-Sol and Myr-Sol).

The observed differences in the release of terpenes can be attributed to their specific chemical characteristics. Cymene has a lower log P value than myrcene, indicating higher water solu-

bility. This greater solubility in water may contribute to its higher release rate when compared to myrcene. Additionally, cymene has a lower molar volume than myrcene, which could also enhance its release rate (Table 3).

Table 3: In silico molecular/physicochemical properties of cymene and myrcene.

Compound	log P	Molar volume (cm^3)	Water solubility (mg/L)
cymene	4.02	155.8 ± 3.0	27.88
myrcene	4.58	177.0 ± 3.0	6.923

Previous research supports the fact that monoterpenes exhibit slower release than other drugs from delivery nanosystems [41]. This phenomenon can be explained by the higher surfactant/oil solubility, which leads to a stronger affinity to the oil–surfactant core–shell structure within the micelles. Consequently, a lower amount of monoterpenes is released into the surrounding medium [42].

Among the mathematical models used to study drug kinetics, the Korsmeyer–Peppas release model proved to be the most suitable for our formulations (Table 4). Our results show that Cym-NE has a k value of 10.4, while Myr-NE has a k value of 3.3. A higher k value indicates faster drug release, while a lower k value indicates slower transport kinetics and, consequently, poor drug release from nanocarriers [43].

Furthermore, both Cym-NE and Myr-NE demonstrated a transport exponent value (n) of 0.3, indicating a release mechanism primarily driven by Fickian diffusion [44]. The free terpenes

Table 4: Mathematical release kinetics models for nanoemulsions (Cym-NE, Myr-NE) and free terpenes (Cym-Sol and Myr-Sol).

	Model	Zeroth order	First order	Higuchi	Hixson–Crowel	Korsmeyer–Peppas
Cym-Sol	k	0.0001	0.0069	24.783	0.0023	1.5587
	R^2	0.8946	0.881	0.8993	0.8729	0.9534
	n	—	—	—	—	0.6865
Cym-NE	k	0.0008	0.0191	6.5154	0.0059	10.465
	R^2	0.6729	0	0.6161	0	0.8776
	n	—	—	—	—	0.3005
Myr-Sol	k	0	0.0017	0.6424	0.0006	0.4836
	R^2	0.857	0.7223	0.8576	0.7195	0.8813
	n	—	—	—	—	0.6152
Myr-NE	k	0	0.0053	2.1477	0.0017	3.3949
	R^2	0.6317	0	0.6145	0	0.8419
	n	—	—	—	—	0.3079

exhibited a value of 0.6, suggesting an anomalous transport mechanism for drug release. This mechanism involves a combination of diffusion and dissolution processes for drug release [45].

These results indicate that the use of NEs may be an effective strategy to improve the control of the release rate of terpenes for more durable and effective control of immature stages of pest vectors.

Larvicidal properties of NEs against *Aedes aegypti*

The potential larvicidal activity of free monoterpenes and nanoemulsions was assessed using third-instar *Aedes aegypti* larvae. The negative control group was treated with surfactant solutions (Span 80 and Tween 20) at the same concentrations as in the nanoemulsions. Mortality of mosquito larvae was recorded after 24 h of exposition according to the WHO protocol [55].

Free cymene exhibited a concentration-dependent larvicidal activity. At 5 mg/L, mortality was 20% ± 4%, rising to 83% ± 2.3% at 25 mg/L and peaking at 98.6% ± 2.3% at 50 mg/L. Surprisingly, the cymene NE displayed a slightly reduced efficacy at lower concentrations (5 mg/L and 25 mg/L) compared to free cymene. This suggests that the encapsulation influences the bioactivity, potentially because of improved dispersion and controlled release of cymene.

Similarly, free myrcene exhibited a concentration-dependent efficacy. Myrcene NEs consistently outperformed free myrcene at all concentrations, indicating a better dispersion of the nanoemulsions in aqueous media. This was most prominent at lower concentrations, resulting in mortality rates of 10.6% ± 2.3% at 5 mg/L and up to 100% at 50 mg/L (Table 5).

Table 5: Average mortality of *Aedes aegypti* larvae after 24 h of exposure to the free monoterpenes and their nanoemulsion.

	Average mortality (%) after 24 h		
	5 mg/L	25 mg/L	50 mg/L
Cym-free	20 ± 4	83 ± 2.3	98.6 ± 2.3
Cym-NE	14.6 ± 2.3	78.6 ± 4.6	100 ± 0
Myr-free	13.3 ± 2.3	81.3 ± 4.6	98.6 ± 2.3
Myr-NE	10.6 ± 2.3	94.6 ± 2.3	100 ± 0

Cytotoxicity of NEs in human keratinocytes

The evaluation of the biocompatibility in human cells is an important step in the development and commercialization of any drug [46]. Here, the toxicity of the terpene-based formulations was evaluated in the HaCAT cell line (Table 6). The results show that the IC_{50} values of the free terpenes were lower those of the nanoemulsions, suggesting that the nanoemulsification reduces the cytotoxicity of terpenes. It is important to note that the surfactant solutions presented the highest IC_{50} values, which indicates that the composition of the nanoemulsion may influence its ability to decrease terpene toxicity. These results are in line with the existing literature, which indicates that monoterpenes exert low cytotoxicity on keratinocyte cells, either free [47-49] or in nanoemulsions [50,51]. It is important to highlight that the excipients used in the formulation are within the maximum concentration recommended by the FDA (7% for Span 80 and 5% for Tween 20) [52].

Acute toxicity of LNCs in alternative in vivo model using *Galleria mellonella*

The in vivo acute toxicity of the NEs was assessed against *G. mellonella* larvae. No mortality was observed at concentra-

Table 6: Inhibitory concentrations 50 (IC_{50}) of the NEs (Cym-NE and Myr-NE), free terpenes (Cym-free and Myr-free), and surfactants solution (B-Cym and B-Myr) in human keratinocytes.

	IC_{50} (mg/mL)
Cym-free	6.43 ± 0.56
Myr-free	1.86 ± 0.15
B-Cym	16.98 ± 0.90
B-Myr	22.37 ± 0.32
Cym-NE	14.95 ± 0.64
Myr-NE	2.37 ± 0.33

tions ranging from 250 to 1000 mg/kg, indicating that the NEs did not cause acute toxicity (Figure 3). However, irritation was observed on day 0, as the larvae exhibited abnormal movements, such as repetitive jumping, after injection of the NEs. This behavior was not constant and ceased after 10 min. On day 1, the larvae treated with both free drugs produced a web of oily/sticky nature, particularly at higher concentrations, which persisted up to day 2. The absence of acute toxicity of nanoparticles on *G. mellonella* larvae is consistent with previous observations [53,54]. Overall, the results suggest that the NEs are not toxic to the larvae at the tested concentrations.

Conclusion

The rHLB values for cymene and myrcene were 15 and 16, respectively. These formulations demonstrated good colloidal stability over 60 days with stable values of size, PdI, and zeta

potential. In vitro release studies demonstrated that the encapsulation of myrcene or cymene in nanoemulsions led to a sustained release of the compounds, suggesting that they could potentially provide a more efficient method for delivering these compounds compared to free solutions.
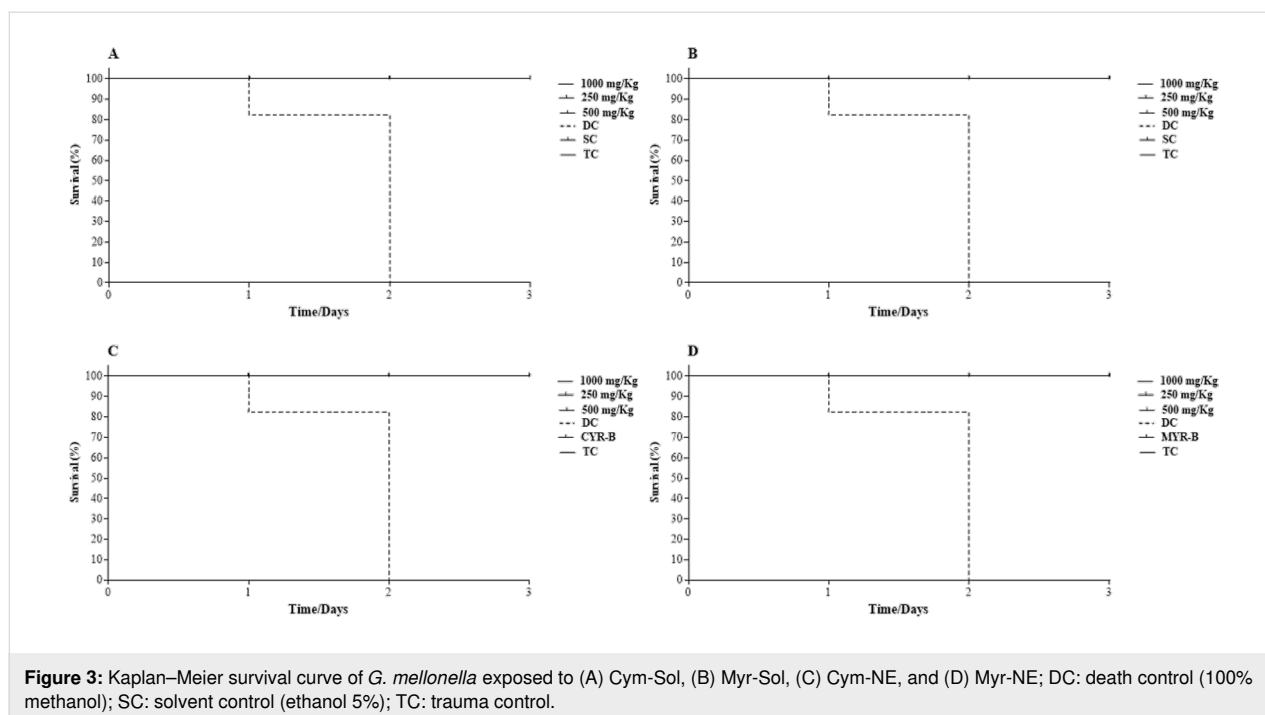
Furthermore, the study showed that the nanoemulsification process reduced the cytotoxicity of terpenes, as evidenced by the lower IC_{50} values of free terpenes compared to the nanoemulsions containing monoterpenes. The in vivo acute toxicity assessment in *G. mellonella* larvae indicated that the nanoemulsions exhibit a good toxicological profile. Finally, bioassays showed that terpene nanoemulsions had equal or greater insecticidal properties than free terpenes and they might facilitate their dispersion in an aqueous environment.

The larvicidal effect of the nanoemulsions, together with their safety and sustained release attributes, holds significant promise for environmentally friendly and effective pest control. Subsequent investigations should further optimize these formulations to unlock their full potential as part of integrated pest management.

Experimental
Preparation of terpene nanoemulsions

Cymene (Cym-NE) and myrcene (Myr-NE) nanoemulsions were obtained by a low-energy method. Briefly, an oil phase composed of the terpene (cymene or myrcene) (5% w/w) was mixed with the surfactants (Span 80/Tween 20) (5% w/w) using

Figure 3: Kaplan–Meier survival curve of *G. mellonella* exposed to (A) Cym-Sol, (B) Myr-Sol, (C) Cym-NE, and (D) Myr-NE; DC: death control (100% methanol); SC: solvent control (ethanol 5%); TC: trauma control.

a magnetic stirrer. After homogenization, the aqueous phase of ultrapure water (90% w/w) was added dropwise. The terpenes were obtained commercially from Sigma-Aldrich.

Determination of the rHLB of the terpenes

The rHLB values of cymene and myrcene were determined by mixing different proportions of a lipophilic (sorbitan monooleate, Span 80, HLB 4.3) and a hydrophilic surfactant (polysorbate 20, Tween 20, HLB 16.7). Different formulations were prepared in a HLB range of 10.0–16.7, and the rHLB was the one in which the formulation had the best colloidal stability (Table S1, Supporting Information File 1).

Characterization of the nanoemulsions
Visual appearance

The formulations obtained were maintained at room temperature and evaluated visually 24 h and 7, 14, and 21 days after preparation. Signs of instability such as creaming, sedimentation, and phase separation were recorded, as well as physical aspects such as color, transparency, and fluidity.

Dynamic light scattering analysis

The average hydrodynamic diameter and polydispersity index (PdI) of the NEs were evaluated over a period of 60 days using dynamic light scattering, and the zeta potential was determined via electrophoretic mobility in a Zetasizer 3000 HSA (Malvern Instruments) device, using a 10 mW HeNe laser operated at 633 nm with a detection angle of incidence of 173° at 25 °C. Data analysis was performed in automatic mode. The NEs were diluted in deionized water (1:25) before the analysis.

Nanoparticle tracking analysis

Nanoparticle tracking analysis was performed in a NanoSight NS300 (Malvern Instruments, United Kingdom) apparatus equipped with a sample chamber and a 638 nm laser. The samples were diluted (1:1000 v/v) in ultrapure water. The NEs were injected into the sample chamber with sterile syringes until the liquid extended to the tip of the injector. The measurements were performed in triplicate at room temperature (25 °C) and the data were represented as mean ± standard deviation.

Cryogenic transmission electron microscopy

The nanoemulsions were mounted onto a copper grid with lacy carbon film (300 mesh). The acquisition was carried out with a MET Talos Arctica G2 apparatus.

In vitro terpene release profile

The in vitro release assays were conducted assuring sink conditions. Modified Franz cells, equipped with a polyethersulfone membrane (Sigma-Aldrich) and with a diffusion area of 1.77 cm^2 were used in the assays. A Microette (Hanson

Research, USA) was used. The receptor compartment was filled with 7.0 mL of a receptor solution composed of 0.1 M phosphate buffer and ethanol (50:50 v/v), pH 5.5. 1 mL of the formulations was used, as allowed by the Franz cell.

The acceptor solution was constantly agitated at 300 rpm using mini-magnetic agitators. The temperature was maintained at 37 ± 2 °C by utilizing a circulating heating bath in the jacketed cells.

The evaluation of the release of cymene and myrcene from the nanoemulsions was performed at specific time intervals: 30 min and 1, 2, 4, 6, 8, 12, and 24 h. Each measurement was repeated six times to ensure reliability. The released compounds were quantified by high-performance liquid chromatography, following a previously validated method.

In silico molecular and physicochemical properties of the monoterpenes

The ACD/Labs Percepta Platform, particularly the PhysChem Module, was employed to forecast molecular and physicochemical data. The ChemSpider tool facilitated the acquisition of these properties [56,57].

Preliminary larvicidal assay

The protocol involved exposing III–IV-instar larvae to terpenes and terpene-based nanoemulsions; the mortality was recorded after 24 h. The laboratory-susceptible reference strain (Bora) from French Polynesia was utilized. The experimental protocol adhered to WHO guidelines with certain modifications [55]. Each experiment was conducted in triplicate, involving 25 third-instar larvae within each sample. Nanoemulsions diluted in distilled water at concentrations of 5, 25, and 50 mg/L were employed. For the negative control, a surfactant solution was utilized at the highest concentration of the tested samples.

Cytotoxicity in human keratinocytes (HaCAT)

The HaCat cell line (code 341; Rio de Janeiro Cell Bank, Rio de Janeiro, Brazil) is a line of non-tumorigenic human epithelial keratinocytes. These cells were cultured in Dulbecco's modified Eagle's medium (DMEM) supplemented with 10% bovine fetal serum and 100 µg/mL of penicillin G/streptomycin. Maintained at 37 °C with 5% CO_2, the cells were grown until they reached a subconfluent density. To detach the cells, a 5 min trypsin treatment with TrypLE™ Express at 37 °C was performed, followed by inactivation using 0.3 mg/mL trypsin inhibitor. The cells were then centrifuged at 500g for 5 min, resuspended in DMEM, and placed overnight in 96-well microplates (200 µL/well, 1×10^6 cells/mL) at 37 °C with 5% CO_2. After incubation, nanoemulsions, free terpenes, and surfactant solutions were administered at concentrations from 0.1 to

250 mg/mL to the cells for 24 h at 37 °C with 5% CO_2. Cell viability was assessed using a colorimetric MTT assay. Cells were exposed to a 10 μL MTT stock solution (5 mg/mL in PBS) and incubated at 37 °C for 2 h. After incubation, the culture medium was replaced with 100 μL of DMSO. The optical density at 570 nm was measured using a microplate reader. Cell viability was determined by comparing the absorbance of each product concentration to untreated cells, with the negative control (DMEM) representing 100% cellular metabolism. The analysis utilized average values.

In vivo toxicity evaluation
The experiment used larvae of the *G. mellonella* species, as described by Allegra et al. and Marena et al. with modifications [54,58]. A minimum of ten larvae per group (*n* = 10) were used, which were fed and raised at 25 °C until they weighed more than 0.2 mg. Larvae between 0.2 and 0.3 mg were used for the experiment, and the samples were administered (10 μL/larva) on the left side of the last proleg using a 10 μL Hamilton syringe. The larvae were then kept in the dark at room temperature and observed after 24, 48, and 72 h to evaluate their behavior, including physical aspects such as color, melanization, or loss of mobility, in response to the treatment. Death was considered when there was no physical reaction after stimulation. The samples were tested at concentrations of 250, 500, and 1000 mg/kg, with controls including trauma control (puncture only, TC), death control (100% methanol, DC), solvent control (5% ethanol, SC), and NE control (Cym-B and Myr-B).

Supporting Information

Supporting Information File 1
Additional details on experimental methods and results.
[https://www.beilstein-journals.org/bjnano/content/supplementary/2190-4286-15-10-S1.pdf]

ORCID® iDs
Jonatas L. Duarte - https://orcid.org/0000-0002-7276-3686
Anna Eliza Maciel de Faria Mota Oliveira -
https://orcid.org/0000-0001-9337-4519
Rafael Miguel Sábio - https://orcid.org/0000-0002-3852-2184
Gabriel Davi Marena - https://orcid.org/0000-0002-4573-5743
Tais Maria Bauab - https://orcid.org/0000-0002-1929-6003
Marlus Chorilli - https://orcid.org/0000-0002-6698-0545

Data Availability Statement
The data that supports the findings of this study is available from the corresponding author upon reasonable request.

References
1. Duarte, J. L.; Di Filippo, L. D.; Araujo, V. H. S.; de Faria Mota Oliveira, A. E. M.; de Araújo, J. T. C.; da Rocha Silva, F. B.; Pinto, M. C.; Chorilli, M. *Acta Trop.* **2021,** *216,* 105848. doi:10.1016/j.actatropica.2021.105848
2. Brady, O. J.; Osgood-Zimmerman, A.; Kassebaum, N. J.; Ray, S. E.; de Araújo, V. E. M.; da Nóbrega, A. A.; Frutuoso, L. C. V.; Lecca, R. C. R.; Stevens, A.; Zoca de Oliveira, B.; de Lima, J. M.; Bogoch, I. I.; Mayaud, P.; Jaenisch, T.; Mokdad, A. H.; Murray, C. J. L.; Hay, S. I.; Reiner, R. C.; Marinho, F. *PLoS Med.* **2019,** *16,* e1002755. doi:10.1371/journal.pmed.1002755
3. Vector-borne diseases. https://www.who.int/news-room/fact-sheets/detail/vector-borne-diseases (accessed Dec 15, 2023).
4. Moyes, C. L.; Vontas, J.; Martins, A. J.; Ng, L. C.; Koou, S. Y.; Dusfour, I.; Raghavendra, K.; Pinto, J.; Corbel, V.; David, J.-P.; Weetman, D. *PLoS Negl. Trop. Dis.* **2017,** *11,* e0005625. doi:10.1371/journal.pntd.0005625
5. Al-Amin, H. M.; Gyawali, N.; Graham, M.; Alam, M. S.; Lenhart, A.; Hugo, L. E.; Rašić, G.; Beebe, N. W.; Devine, G. J. *Pest Manage. Sci.* **2023,** *79,* 2846–2861. doi:10.1002/ps.7462
6. Pereira Filho, A. A.; Pessoa, G. C. D.; Yamaguchi, L. F.; Stanton, M. A.; Serravite, A. M.; Pereira, R. H. M.; Neves, W. S.; Kato, M. J. *Front. Plant Sci.* **2021,** *12,* 685864. doi:10.3389/fpls.2021.685864
7. Oliveira, A. E. M. F. M.; Duarte, J. L.; Cruz, R. A. S.; Souto, R. N. P.; Ferreira, R. M. A.; Peniche, T.; da Conceição, E. C.; de Oliveira, L. A. R.; Faustino, S. M. M.; Florentino, A. C.; Carvalho, J. C. T.; Fernandes, C. P. *J. Nanobiotechnol.* **2017,** *15,* 2. doi:10.1186/s12951-016-0234-5
8. Surendran, S.; Qassadi, F.; Surendran, G.; Lilley, D.; Heinrich, M. *Front. Nutr.* **2021,** *8,* 699666. doi:10.3389/fnut.2021.699666
9. Balahbib, A.; El Omari, N.; El Hachlafi, N.; Lakhdar, F.; El Menyiy, N.; Salhi, N.; Mrabti, H. N.; Bakrim, S.; Zengin, G.; Bouyahya, A. *Food Chem. Toxicol.* **2021,** *153,* 112259. doi:10.1016/j.fct.2021.112259

10. Richter, G.; Hazzah, T.; Hartsel, J. A.; Eades, J.; Hickory, B.; Makriyannis, A. Cannabis Sativa: An Overview. In *Nutraceuticals;* Gupta, R. C.; Lall, R.; Srivastava, A., Eds.; Academic Press: London, UK, 2021; pp 603–624. doi:10.1016/b978-0-12-821038-3.00038-0

11. McClements, D. J. *Soft Matter* **2011,** *7,* 2297–2316. doi:10.1039/c0sm00549e

12. Fryd, M. M.; Mason, T. G. *Annu. Rev. Phys. Chem.* **2012,** *63,* 493–518. doi:10.1146/annurev-physchem-032210-103436

13. da Silva, B. D.; do Rosário, D. K. A.; Weitz, D. A.; Conte-Junior, C. A. *Trends Food Sci. Technol.* **2022,** *121,* 1–13. doi:10.1016/j.tifs.2022.01.026

14. Folly, D.; Machado, F. P.; Esteves, R.; Duarte, J. L.; Cruz, R. A. S.; Oliveira, A. E. M. F. M.; Ferreira, R. M. A.; Souto, R. N. P.; Santos, M. G.; Carvalho, J. C. T.; Ruppelt, B. M.; Fernandes, C. P.; Rocha, L. *J. Essent. Oil Res.* **2021,** *33,* 559–566. doi:10.1080/10412905.2021.1966847

15. Kumar, M.; Bishnoi, R. S.; Shukla, A. K.; Jain, C. P. *Prev. Nutr. Food Sci.* **2019,** *24,* 225–234. doi:10.3746/pnf.2019.24.3.225

16. Solans, C.; Solé, I. *Curr. Opin. Colloid Interface Sci.* **2012,** *17,* 246–254. doi:10.1016/j.cocis.2012.07.003

17. Solans, C.; Morales, D.; Homs, M. *Curr. Opin. Colloid Interface Sci.* **2016,** *22,* 88–93. doi:10.1016/j.cocis.2016.03.002

18. Griffin, W. C. *J. Soc. Cosmet. Chem.* **1949,** *1,* 311–326.

19. Fernandes, C. P.; Mascarenhas, M. P.; Zibetti, F. M.; Lima, B. G.; Oliveira, R. P. R. F.; Rocha, L.; Falcão, D. Q. *Rev. Bras. Farmacogn.* **2013,** *23,* 108–114. doi:10.1590/s0102-695x2012005000127

20. Somala, N.; Laosinwattana, C.; Teerarak, M. *Sci. Rep.* **2022,** *12,* 10280. doi:10.1038/s41598-022-14591-2

21. Hong, I. K.; Kim, S. I.; Lee, S. B. *J. Ind. Eng. Chem. (Amsterdam, Neth.)* **2018,** *67,* 123–131. doi:10.1016/j.jiec.2018.06.022

22. Kyadarkunte, A.; Patole, M.; Pokharkar, V. *Cosmetics* **2014,** *1,* 159–170. doi:10.3390/cosmetics1030159

23. Moya-Andérico, L.; Vukomanovic, M.; del Mar Cendra, M.; Segura-Feliu, M.; Gil, V.; del Río, J. A.; Torrents, E. *Chemosphere* **2021,** *266,* 129235. doi:10.1016/j.chemosphere.2020.129235

24. Wojda, I. *Insect Sci.* **2017,** *24,* 342–357. doi:10.1111/1744-7917.12325

25. Orafidiya, L. O.; Oladimeji, F. A. *Int. J. Pharm.* **2002,** *237,* 241–249. doi:10.1016/s0378-5173(02)00051-0

26. Nazarzadeh, E.; Anthonypillai, T.; Sajjadi, S. *J. Colloid Interface Sci.* **2013,** *397,* 154–162. doi:10.1016/j.jcis.2012.12.018

27. Ortiz-Zamora, L.; Bezerra, D. C.; de Oliveira, H. N. S.; Duarte, J. L.; Guisado-Bourzac, F.; Chil-Núñez, I.; da Conceição, E. C.; Barroso, A.; Mourão, R. H. V.; de Faria Mota Oliveira, A. E. M.; Cruz, R. A. S.; Carvalho, J. C. T.; Solans, C.; Fernandes, C. P. *Ind. Crops Prod.* **2020,** *158,* 112989. doi:10.1016/j.indcrop.2020.112989

28. McClements, D. J. *Soft Matter* **2012,** *8,* 1719–1729. doi:10.1039/c2sm06903b

29. Chong, W.-T.; Tan, C.-P.; Cheah, Y.-K.; Lajis, A. F. B.; Habi Mat Dian, N. L.; Kanagaratnam, S.; Lai, O.-M. *PLoS One* **2018,** *13,* e0202771. doi:10.1371/journal.pone.0202771

30. Duarte, J. L.; Amado, J. R. R.; Oliveira, A. E. M. F. M.; Cruz, R. A. S.; Ferreira, A. M.; Souto, R. N. P.; Falcão, D. Q.; Carvalho, J. C. T.; Fernandes, C. P. *Rev. Bras. Farmacogn.* **2015,** *25,* 189–192. doi:10.1016/j.bjp.2015.02.010

31. Qi, X.; Zhong, S.; Schwarz, P.; Chen, B.; Rao, J. *Ind. Crops Prod.* **2023,** *197,* 116575. doi:10.1016/j.indcrop.2023.116575

32. Gurpret, K.; Singh, S. K. *Indian J. Pharm. Sci.* **2018,** *80,* 781–789.

33. Khumpirapang, N.; Pikulkaew, S.; Müllertz, A.; Rades, T.; Okonogi, S. *PLoS One* **2017,** *12,* e0188848. doi:10.1371/journal.pone.0188848

34. Sundararajan, B.; Ranjitha Kumari, B. D. *J. Trace Elem. Med. Biol.* **2017,** *43,* 187–196. doi:10.1016/j.jtemb.2017.03.008

35. Forgiarini, A.; Esquena, J.; González, C.; Solans, C. Studies of the relation between phase behavior and emulsification methods with nanoemulsion formation. In *Trends in Colloid and Interface Science XIV;* Buckin, V., Ed.; Progress in Colloid and Polymer Science, Vol. 115; Springer: Berlin, Heidelberg, 2000; pp 36–39. doi:10.1007/3-540-46545-6_8

36. Izquierdo, P.; Feng, J.; Esquena, J.; Tadros, T. F.; Dederen, J. C.; Garcia, M. J.; Azemar, N.; Solans, C. *J. Colloid Interface Sci.* **2005,** *285,* 388–394. doi:10.1016/j.jcis.2004.10.047

37. Hou, J.; Ci, H.; Wang, P.; Wang, C.; Lv, B.; Miao, L.; You, G. *J. Hazard. Mater.* **2018,** *360,* 319–328. doi:10.1016/j.jhazmat.2018.08.010

38. Klang, V.; Matsko, N. B.; Valenta, C.; Hofer, F. *Micron* **2012,** *43,* 85–103. doi:10.1016/j.micron.2011.07.014

39. Kawakami, M. Y. M.; Zamora, L. O.; Araújo, R. S.; Fernandes, C. P.; Ricotta, T. Q. N.; de Oliveira, L. G.; Queiroz-Junior, C. M.; Fernandes, A. P.; da Conceição, E. C.; Ferreira, L. A. M.; Barros, A. L. B.; Aguiar, M. G.; Oliveira, A. E. M. F. M. *Biomed. Pharmacother.* **2021,** *134,* 111109. doi:10.1016/j.biopha.2020.111109

40. Nain, A.; Tripathy, D. B.; Gupta, A.; Dubey, R.; Kuldeep; Singh, A. Nanoemulsions: Nanotechnological approach in food quality monitoring. In *Nanotechnology Applications for Food Safety and Quality Monitoring;* Sharma, A.; Vijayakumar, P. S.; Pramod, E.; Prabhakar, K.; Kumar, R., Eds.; Academic Press: London, UK, 2023; pp 223–238. doi:10.1016/b978-0-323-85791-8.00020-3

41. Zielińska, A.; Ferreira, N. R.; Feliczak-Guzik, A.; Nowak, I.; Souto, E. B. *Pharm. Dev. Technol.* **2020,** *25,* 832–844. doi:10.1080/10837450.2020.1744008

42. Miastkowska, M.; Śliwa, P. *Molecules* **2020,** *25,* 2747. doi:10.3390/molecules25122747

43. Wu, I. Y.; Bala, S.; Škalko-Basnet, N.; di Cagno, M. P. *Eur. J. Pharm. Sci.* **2019,** *138,* 105026. doi:10.1016/j.ejps.2019.105026

44. Gao, Y.; Zuo, J.; Bou-Chacra, N.; Pinto, T. d. J. A.; Clas, S.-D.; Walker, R. B.; Löbenberg, R. *BioMed Res. Int.* **2013,** 136590. doi:10.1155/2013/136590

45. Malekjani, N.; Jafari, S. M. *Compr. Rev. Food Sci. Food Saf.* **2021,** *20,* 3–47. doi:10.1111/1541-4337.12660

46. Spinozzi, E.; Pavela, R.; Bonacucina, G.; Perinelli, D. R.; Cespi, M.; Petrelli, R.; Cappellacci, L.; Fiorini, D.; Scortichini, S.; Garzoli, S.; Angeloni, C.; Freschi, M.; Hrelia, S.; Quassinti, L.; Bramucci, M.; Lupidi, G.; Sut, S.; Dall'Acqua, S.; Benelli, G.; Canale, A.; Drenaggi, E.; Maggi, F. *Ind. Crops Prod.* **2021,** *172,* 114027. doi:10.1016/j.indcrop.2021.114027

47. Rodrigues, V.; Cabral, C.; Évora, L.; Ferreira, I.; Cavaleiro, C.; Cruz, M. T.; Salgueiro, L. *Arabian J. Chem.* **2019,** *12,* 3236–3243. doi:10.1016/j.arabjc.2015.08.026

48. Xanthis, V.; Fitsiou, E.; Voulgaridou, G.-P.; Bogadakis, A.; Chlichlia, K.; Galanis, A.; Pappa, A. *Antioxidants* **2021,** *10,* 127. doi:10.3390/antiox10010127

49. Cabral, C.; Francisco, V.; Cavaleiro, C.; Gonçalves, M. J.; Cruz, M. T.; Sales, F.; Batista, M. T.; Salgueiro, L. *Phytother. Res.* **2012,** *26,* 1352–1357. doi:10.1002/ptr.3730

50. Vater, C.; Bosch, L.; Mitter, A.; Göls, T.; Seiser, S.; Heiss, E.;
    Elbe-Bürger, A.; Wirth, M.; Valenta, C.; Klang, V.
    Eur. J. Pharm. Biopharm. **2022,** *170,* 1–9.
    doi:10.1016/j.ejpb.2021.11.004
51. Alqarni, M. H.; Foudah, A. I.; Aodah, A. H.; Alkholifi, F. K.;
    Salkini, M. A.; Alam, A. *Gels* **2023,** *9,* 193. doi:10.3390/gels9030193
52. FDA/Center for Drug Evaluation and Research. Inactive Ingredient
    Search for Approved Drug Products.
    https://www.accessdata.fda.gov/scripts/cder/iig/index.cfm (accessed
    Dec 25, 2022).
53. Lopes Rocha Correa, V.; Assis Martins, J.; Ribeiro de Souza, T.;
    de Castro Nunes Rincon, G.; Pacheco Miguel, M.;
    Borges de Menezes, L.; Correa Amaral, A. *Int. J. Biol. Macromol.* **2020,**
    162, 1465–1475. doi:10.1016/j.ijbiomac.2020.08.027
54. Marena, G. D.; Ramos, M. A. D. S.; Lima, L. C.; Chorilli, M.;
    Bauab, T. M. *Sci. Total Environ.* **2022,** *807,* 151023.
    doi:10.1016/j.scitotenv.2021.151023
55. Guidelines for laboratory and field testing of long-lasting insecticidal
    mosquito nets.
    https://www.who.int/publications/i/item/who-cds-whopes-gcdpp-2005.14
    (accessed Dec 15, 2023).
56. Rao, J.; McClements, D. J. *Food Chem.* **2012,** *134,* 749–757.
    doi:10.1016/j.foodchem.2012.02.174
57. Duarte, J. L.; Bezerra, D. C.; da Conceição, E. C.; Mourão, R. H. V.;
    Fernandes, C. P. *Colloid Interface Sci. Commun.* **2020,** *34,* 100225.
    doi:10.1016/j.colcom.2019.100225
58. Allegra, E.; Titball, R. W.; Carter, J.; Champion, O. L. *Chemosphere*
    2018, *198,* 469–472. doi:10.1016/j.chemosphere.2018.01.175

Nanomedicines against Chagas disease: a critical review

Maria Jose Morilla[1], Kajal Ghosal[2] and Eder Lilia Romero[*1]

Abstract

Chagas disease (CD) is the most important endemic parasitosis in South America and represents a great socioeconomic burden for the chronically ill and their families. The only currently available treatment against CD is based on the oral administration of benznidazole, an agent, developed in 1971, of controversial effectiveness on chronically ill patients and toxic to adults. So far, conventional pharmacological approaches have failed to offer more effective and less toxic alternatives to benznidazole. Nanomedicines reduce toxicity and increase the effectiveness of current oncological therapies. Could nanomedicines improve the treatment of the neglected CD? This question will be addressed in this review, first by critically discussing selected reports on the performance of benznidazole and other molecules formulated as nanomedicines in *in vitro* and *in vivo* CD models. Taking into consideration the developmental barriers for nanomedicines and the degree of current technical preclinical efforts, a prospect of developing nanomedicines against CD will be provided. Not surprisingly, we conclude that structurally simpler formulations with minimal production cost, such as oral nanocrystals and/or parenteral nano-immunostimulants, have the highest chances of making it to the market to treat CD. Nonetheless, substantive political and economic decisions, key to facing technological challenges, are still required regarding a realistic use of nanomedicines effective against CD.

Introduction

Nanomedicines are used to solve the problems posed by poor solubility and/or permeability and high toxicity of drugs with low molecular weight [1,2]. Different 2-nitroimidazole-based nanomedicines against Chagas disease (CD) to reduce the toxic-

ity and increase the effectiveness of benznidazole (BNZ) treatment have been preclinically screened in the last two decades (see the recently reviewed BNZ-based preclinical anti-CD nanomedicines [3]). But how realistic is thinking of nanomedi-

cines to treat CD? To answer this elemental question, selected preclinical reports will be thoroughly discussed in this review. Then, by addressing current contexts and directions of nanomedical advances, the idea of using nanomedicines against CD will be critically analyzed.

Review
Chagas disease, a threat no longer limited to developing countries

Chagas disease is a parasitic, systemic, chronic, and often fatal infection caused by the protozoan *Trypanosoma cruzi* [4]. The World Health Organization classifies CD as the most prevalent of poverty-promoting neglected tropical diseases, and the most important parasitic one. Also known as American trypanosomiasis, CD is the third most infectious disease in Latin America; it is endemic in 21 countries and constitutes a global public health issue affecting six to eight million people [5]. Globally, CD creates an annual burden exceeding 800,000 disability-adjusted life years and $600,000,000 in healthcare costs [6]. Classically, the infectious cycle in the human host begins as an acute phase, asymptomatic except in children, where trypomastigotes circulate in the blood and intracellular amastigotes are usually found in hepatic macrophages. Amastigotes multiply and differentiate into trypomastigotes, which are released back to the blood after cell rupture. The acute phase is followed by an indeterminate, asymptomatic phase. Ten to thirty years after the acute phase, 30%–40% of patients will develop a chronic phase. This phase presents typical denervation and fibrosis of cardiac or digestive muscles, with scarcer intracellular forms. The subsequent cardiac arrhythmias or progressive heart failure and sudden death are the highest attributable cost of the disease [7,8]. With 75 million people at risk, 30,000 new cases each year, and 12,000 deaths in 2019, less than 30% of infected people are diagnosed [5]. Currently, because of emigration, CD is becoming increasingly important in North America, Europe, Japan, and Australia [9,10]. Nearly 300,000 individuals in the United States are calculated to have CD, with up to 45,000 having cardiomyopathies [11].

The infection is treated with benznidazole, first manufactured by Roche (Roche 7-501, Rochagan, *N*-benzyl-2-(2-nitro-1*H*-imidazol-1-yl)acetamide). BNZ is currently available in the United States after being approved by the US Food and Drug Administration in 2018. Since the early 70s, patients received the same BNZ-based treatment, which is long, toxic to adults, effective in recently infected people, and controversially effective in the chronic phase [12]. A recommended course of 5–10 mg BNZ/kg orally, is divided into two daily doses for 60 days after meals [13].

On BNZ metabolization, doses, and toxicity

BNZ is a prodrug that requires activation by oxygen-insensitive NADH-dependent trypanosomal type-I nitroreductase (NTRI), found in some protozoan parasites, but not in humans [14]. This activation produces hydroxy and hydroxylamine intermediates in a two-step, two-electron transfer reaction, culminating in 4,5-dihydro-4,5-dihydroxyimidazole, whose breakdown releases the reactive dialdehyde glyoxal, which, in the presence of guanosine, generates guanosine–glyoxal adducts. These reactive metabolites are toxic to the parasite, resulting in its fast killing. Lately, it was suggested that the major metabolic impact of BNZ is on the glutathione (and trypanothione) pathway so that covalent binding of BNZ with low-molecular-weight thiols and with protein thiols is the drug's primary mode of action against *T. cruzi* [15].

In mammalian cells, BNZ is reduced by oxygen-sensitive nitroreductases. During its anaerobic nitro reduction, primarily in the hepatic microsomal fraction, BNZ generates reactive metabolites that bind to the host's DNA, proteins, and lipids. The nitro reduction also occurs in fecal matter, with an intensity that increases with age. The toxicity of these products on rodent adrenals, colon, and esophagus has been extensively studied by Castro's group in Argentina. The same group reported that BNZ also inhibits the metabolism of several xenobiotics transformed by the cytochrome P450 system and their metabolites react with fetal components *in vivo* [16-18]. The consumption of glutathione resulting from its reaction with BNZ metabolites would later lead to oxidative stress processes. One of the main disadvantages of BNZ pharmacotherapy is the high doses administered, thought to be responsible for the pronounced idiosyncratic adverse drug reactions (ADRs), caused by BNZ reduction products, which are maximal in adults and lead to treatment discontinuation [19]. Typical ADRs include headache, anorexia, weakness and/or lack of energy, skin rash, gastrointestinal complaints, and mild, peripheral neurological effects [20].

The dosage of BNZ has been reported to be inadequate [21]. In children, markedly lower plasma BNZ concentrations than those previously reported in adults treated with comparable BNZ milligram per kilogram doses (possibly due to a higher clearance/bioavailability), but still retaining a high therapeutic response, were detected [22]. This finding led to the assumption that in adults the BNZ treatment could be overdosed. Unlike adults, children show few ADRs; therefore, the existence of a potential direct correlation between drug concentration and the incidence of ADRs was suggested. Data from simulations showed that reducing the cumulative dose from 2.5 mg/kg/12 h to 2.5 mg/kg/24 h rendered BNZ plasma concentrations within the accepted therapeutic range of 3 to 6 mg/L

[22]. This is an important point: When BNZ toxicity is attributed to overdosing, it could be simply reduced by reducing its dose. The implementation of shorter treatments has also been proposed [23,24].

Other reports suggest, nonetheless, that the overdosage of BNZ as the origin of ADRs is debatable. Studies implemented with adult patients not only failed to connect the manifestation of ADRs with the BNZ plasma levels but also opened the theory of genetic background or immunological profile in addition to hypersensitivity reactions to BNZ [25,26]. Accordingly, reducing BNZ doses to decrease its plasma levels would not have an impact on its toxicity [27].

Oral BNZ-based nanomedicines aimed to increase BNZ solubility

Besides uncertainties about BNZ dose, its biopharmaceutical classification differs according to the data source and interpretation. In the early 1980s, BNZ was reported to be readily absorbed, highly lipophilic, and extensively metabolized, with only 5% of the dose excreted unchanged in the urine [28]. Since poorly soluble drugs are those whose solubility is below 1 mg/mL over the physiological pH range and the BNZ solubility in distilled water or simulated gastric and enteric fluids oscillates between 0.2 and 0.4 mg/mL [29,30], BNZ is considered a poorly soluble drug. Some authors classify BNZ as a class-II drug, according to the Biopharmaceutical Classification System (BCS) [31], which means that it is a poorly soluble but permeable molecule. The limitation in the absorption of class-II drugs is due to their rate of dissolution, except at very high doses. Their bioavailability is variable but can be increased by augmenting their dissolution rate, and *in vitro–in vivo* correlation is normally applied [31]. These drugs are suitable for sustained release and controlled release formulations that provide more stable and predictable plasma levels. Drug solubility can be increased by employing strategies from classical pharmaceutical technology such as lyophilization, micrometerization, microemulsion, the inclusion of surfactants, solid dispersion, and the use of complexing agents such as cyclodextrins, Zer-Os tablet innovation, soft gels, and triglas [32]. Nanomedicines can also be used to increase the oral bioavailability of BNZ, and their contribution is examined below.

The *in vitro* performance of BNZ loaded into nanoparticles (Nps) is shown in Table 1. In many of these reports, formulations were tested on different parasite stages (epimastigote, trypomastigote, and amastigote), and their cytotoxicity was assessed on mammalian cells [33-38]. However, orally administered nanomedicines do not cross the intact gastrointestinal epithelium and would never be uptaken by target cells, except enterocytes. During gastrointestinal transit, biodegradable nano-

particles are degraded or not absorbed, leaving only released BNZ available for absorption [39,40]. Other studies determined the release profile of BNZ in different media [41-44] and its permeability across Caco-2 cells [43,44].

Between 2012 and 2018 the BERENICE (BEnznidazol and triazol REsearch group for Nanomedicine and Innovation on Chagas diseasE) consortium, aiming for a new, cheaper, more effective, better-tolerated solutions for chronic Chagas patients, was constituted [45]. The consortium, financed by the Seventh Framework Programme, was coordinated by the Institut Catala De La Salut and included ten researchers from Spain, endemic countries' institutions (Brazil and Argentina), and private pharmaceutical companies. The project started proposing a sublingual formulation of BNZ within liposomes or lipid nanoparticles, assuming the intact formulations could reach the blood, avoid the hepatic first-pass metabolism, and reduce the toxicity of BNZ. The project, however, failed in its attempt to incorporate BNZ into liposomes, while lipid nanoparticles could not be formulated into sublingual tablets. The project changed to formulate BNZ/hydroxypropyl-β-cyclodextrin complexes. These complexes were prepared on a scale seven times larger than in the laboratory and showed a comparable *in vitro* activity to free BNZ [33]. Formulated as oral tablets containing a reduced dose of BNZ/cyclodextrin (50% loading of BNZ (% BNZ/total mass)) and administered to a murine model, BNZ/cyclodextrin did not overcome the efficacy of free BNZ during the acute phase of the infection. The project eventually gave up on its attempts to formulate BNZ in nanomedicines and focused on clinical trials of reduced BNZ doses for the treatment of the chronic phase [23].

In parallel to the BERENICE project, several reports showed the *in vivo* performance of different nanomedicines capable of increasing the solubility of BNZ (Table 2). Trypomastigotes are known to display high resistance to the trypanocidal effect of BNZ [46,47]; replicative epimastigote and amastigote forms of the parasite, instead, would be sensitive to cumulative doses of BNZ. Arguing that a reduction in the cumulative dose of BNZ would reduce its toxicity without losing effectiveness [48], BNZ has recently been formulated as nanocrystals (NCs). The solubility of BNZ formulated as nanocrystals prepared by nanoprecipitation using the non-ionic surfactant poloxamer 188 as a stabilizer (BNZ-NC) was increased 10-fold (from 0.4 mg/mL for bulk BNZ to 3.99 mg/mL for BNZ-NC) [49]. After oral administration of BNZ-NC to an acute murine model infected with the Nicaragua strain of *T. cruzi* at 300 mg/kg total dose (TD) (30 days treatment) and 375 mg/kg TD (15 days treatment), which was about half of the 750 mg/kg free BNZ TD administered at 50 mg/kg/day over 15 days, both BNZ-NC and free BNZ showed 100% survival at 50 days post-infection (dpi)

Table 1: *In vitro* performance of BNZ-based nanomedicines.[a]

Type of nanomedicine/ composition	Physicochemical properties	*In vitro* assays	Outcome	Ref.
vesicles, SLN, NLC and cyclodextrins (CDs)	vesicles: ≈200 nm CDs: 5–10 μm SLN: ≈170 nm, –21 mV ζ-potential NLC: ≈200 nm, –26 mV ζ-potential	cytotoxicity on L-929 cells and HepG2 cells activity on epimastiotes, trypomastigotes, and amastigotes of CL strain, clone B5	SLN less active than BNZ, NLC less active and more toxic than CD vesicles low EE CDs best-balanced anti-trypanosoma activity /toxicity, (less cytotoxicity of BNZ-CDs than BNZ without reduction of trypanocidal activity)	[33]
CaCO$_3$ Nps	42 ± 8 nm	cytotoxicity on LLC-MK2 cells activity on epimastigotes, trypomastigotes, and amastigote of Y strain	less toxicity and higher selectivity, with anti-trypanosoma activity at 25 times lower concentrations of BNZ	[34]
mesoporous silica Nps (MCM-41) chitosan succinate covalently attached	–11.5 ± 0.5 mV ζ-potential	activity on epimastigotes of CL Brener strain	the same anti-trypanosomal effect as that of BNZ-MCM-41 at 30 times lower BNZ concentration	[35]
Nps based on Eudragit® RS PO and Eudragit® RL PO	200–300 nm; 24–36 mV ζ-potential; EE: 78% DL: 18% w/w	*in vitro* release in 0.1 N HCl (pH 1.2)	increased dissolution rate of drug from Nps	[41]
zeolitic imidazolate framework ZIF-8 (BNZ@ZIF-8)		*in vitro* release at pH 4.5 and 7.6	at pH 4.5, BNZ@ZIF-8 showed a faster release with a burst effect, while, at pH 7.6, it showed prolonged and controlled release	[42]
nanocrystals		*in vitro* release in FaSSGF, FeSSIF, and FaSSIF integrity of tight junction dynamics and permeability on Caco-2	safety and increased permeation through the Caco-2 cells with minimal interactions with mucin glycoproteins	[43]
lipid nanocapsules Lipoid S 100, Kolliphor® HS 15 and Labrafac® WL 1349 oil phase at three oil/surfactant ratios	30, 50, and 100 nm; PDI < 0.07; –1.59 to –0.96 mV ζ-potential	release in FaSSGF, FeSSIF, and FaSSIF with pancreatic enzymes permeability on Caco-2	NCPs protected BNZ in simulated gastric fluid and provided sustained release in a simulated intestinal fluid improved BNZ permeability	[44]
NLC myristyl myristate/crodamol oil/poloxamer 188	150 nm; –13 mV ζ-potential; EE: 80%	release at pH 6.8 haemolysis cytotoxicity on CHO and Vero cells activity on trypomastigotes and amastigotes of strain K98	biphasic drug release profile with an initial burst release followed by a prolonged phase trypanocidal activity similar to that of free BNZ, with lower cytotoxicity to mammalian cells	[36]
NLC compritol, crodamol, Tween 80 and poloxamer 407 (P407)	110 nm; PDI: 0.19 –18 mV ζ-potential; EE: 83%; DL: 1.64	haemolysis cytotoxicity on L929 cells activity on epimastigotes of Colombian strain	NLC-BNZ had higher trypanocidal activity than free BNZ with low cytotoxicity to mammalian cells	[38]
Polymeric Nps cashew phthalate gum		activity on epimastigotes and trypomastigotes cytotoxicity on macrophages	Nps enhanced trypanocidal activity, and reduced cytotoxicity	[37]

[a]Abbreviations: DL – drug loading; EE – encapsulation efficiency; FaSSGF – fasted-state simulated gastric fluid; FaSSIF – fasted-state simulated intestinal fluid; FeSSIF – fed-state simulated intestinal fluid; NLC – nanostructured lipid carriers; PDI – polydispersity index; SLN – solid lipid nanoparticles.

Table 2: *In vivo* performance of oral BNZ-based nanomedicines.[a]

Type nanomedicine/ composition	Physicochemical properties	*In vivo* assays	Outcome	Ref.
nanocrystals (BNZ-NC) BNZ dispersed in poloxamer 188	63.3 ± 2.82 nm; PDI: 3.35 ± 0.1; −18.30 ± 1.0 mV ζ-potential BNZ-NC dispersed in olive oil for administration	acute model, C3H/HeN mice, Nicaragua strain BNZ: 50 mg/kg/day for 15 days (750 mg/kg TD) BNZ-NC: 50, 25, and 10 mg/kg/day for 30 days (1500, 750, and 300 mg/kg TD, respectively) and 50 and 25 mg/kg/day for 15 days (750 and 375 mg/kg TD, respectively)	without treatment 15% survival at 50 dpi with BNZ and BNZ-NC 100% survival	[50]
BNZ-NC same formulation as in [50]		acute model, C3H/HeN mice, Nicaragua strain infected + immunosuppression (60 dpi) BNZ: 50 mg/kg/day for 30 days (1500 mg/kg TD) BNZ-NC:10, 25, and 50 mg/kg/day for 30 days (300, 750, and 1500 mg/kg TD, respectively) starting 2 dpi.	without treatment 15% survival BNZ and BNZ-NC survived until 92 dpi	[49]
BNZ-NC same formulation as in [50]		chronic model, C57BL/6J mice, Nicaragua strain BNZ: 50 and 75 mg/kg/day for 30 days (1500 and 2250 mg/kg TD, respectively) or 13 times one dose every seven days (it) of 75 or 100 mg/kg (975 and 1300 mg/kg TD, respectively) BNZ-NC: 25 and 50 mg/kg/day for 30 days (750 and 1500 mg/kg TD, respectively) or 13 times one dose every seven days (it) of 50 and 75 mg/kg/day (650 and 975 mg/kg TD, respectively) starting 90 dpi	All infected mice survived (210 dpi). Untreated mice median parasite load 8.9 Eq/mL BNZ (75 mg/kg × 30 days) and BNZ (it) 100, showed 80% and 75% without parasitaemia, respectively BNZ-NC (it) 50, 80% negative qPCR no parasite load could be detected in any other BNZ-NC group	[51]
BNZ-SNEDDSs Miglyol®810N, Capryol 90®, Lipoid S75, Labrasol®, *N*-methyl pyrrolidone (30:15:20:15:20 v/v)	25 mg/mL BNZ; 500 nm	acute model, BALB/c mice, Y strain 100 mg/kg/day starting 4 dpi for 20 days	57% cure for both free-BNZ and BNZ-SEDDSs groups	[52]
BNZ-NFX-SNEDDSs Labrasol, Labrafil 1944CS, Capryol 90 50.00:10.12:39.88 (w/w)	132 ± 7 nm; PDI: 0.610 ± 0.056; 33.1 ± 2.4 mV ζ-potential	acute model, BALB/c mice, Y strain. NFX (50 mg/kg/day) or BNZ (50 mg/kg/day) orally daily for 5 days NFX-BNZ-SNEDDSs (25 and 50 mg/kg/day), BNZ-SNEDDSs (50 and 100 mg/kg/day) administered orally once a day for five consecutive days starting 5 dpi	without treatment 15–17.5 days survival NFX and BNZ increase survival to 30 dpi	[53]
NCP Eudragit L100 (0.25 g), BNZ (0.025 g), sorbitan monooleate (0.19 g), medium-chain triglycerides (413 μL), ethanol (67 mL), and aqueous phase (polysorbate 80 (0.19 g) and water))	146 ± 0.6 nm; PDI: 0.15 ± 0.01; −12.8 ± 0.87 mV ζ-potential; EE: 96%	acute model, Swiss mice, Y strain BNZ-NCP 5, 10, 15, and 20 mg/kg/day starting 2 dpi for eight days	BNZ (100 mg/kg/day) reduced parasitemia and 100% survival after 30 days	[54]

[a]Abbreviations: NCP – nanocapsules, IV – intravenous, it – intermittent.

[50]. In a model of immunosuppressed chronic phase, 750 mg/kg BNZ-NC TD showed the same efficacy as 1500 mg/kg free BNZ. Immunosuppressed mice treated with BNZ-NC exhibited 40% of PCR negative samples; 50% of the mice showed negative IgG titers after 3 months, and 100% after 6 months. In contrast, parasites were detected in blood from mice treated with free BNZ, and *T. cruzi* antibodies were detected for up to 6 months. BNZ-NC decreases parasite burden, heart inflammation, and lesions [49]. The intermittent administration of BNZ-NC at 75 mg/kg (975 mg/kg TD) to a chronic murine model was also tested; it was as equally effective (parasite load, *T. cruzi*-specific antibodies levels, degree of fibrosis, frequency of IFN-γ producing cells, and improvement of electrocardiographic alteration) as intermittent free BNZ at 100 mg/kg (1300 mg/kg TD). BNZ-NC induced a 57% reduction in cardiac inflammation but failed to overcome the more significant reduction provided with intermittent free BNZ [51]. Overall, employing intermittent and lower cumulative doses of BNZ-NC, the authors showed comparable therapeutic effects to conventional treatment with free BNZ. These studies, however, did not compare the plasma levels of BNZ resulting from administering nanocrystals to rodents with identical doses of free BNZ.

Other authors have recently reported the formulation of BNZ into self-nanoemulsified drug delivery systems (SNEDDSs). SNEEDSs provide a pediatric liquid formulation of BNZ, which is only marketed as solid tablets. SNEDDSs are isotropic mixtures of oil, surfactants, and co-surfactants that form submicrometer-droplet emulsions under agitation in water or gastrointestinal fluids. BNZ-SNEDDSs resulted in the same percentage of cure (57%) as free BNZ in an acute murine model infected with the Y strain of *T. cruzi* [52]. In a subsequent report, BNZ and nifurtimox (NFX) were loaded in a solid formulation of SNEDDSs, and their administration at 25 and 50 mg/kg/day (BNZ and NFX, respectively) over 5 days ensured 30 dpi survival in two-thirds of treated animals [53]. BNZ was also loaded in Eudragit L-100 nanocapsules (BNZ-NCP). Their administration at 20 mg/kg/day for 8 days yielded reduced parasitemia, and 50% of treated mice survived 30 dpi [54].

Intravenous BNZ-based nanomedicines

According to other authors, BNZ is a class-III drug, that is, a soluble and poorly permeable molecule. The classification is based on BNZ's dose number (which for BNZ is 1; dose numbers ≤ 1 correspond to highly soluble drugs) and on its calculated partition coefficient value clogP, a lipophilicity indicator and the most critical parameter predictor of passive membrane permeability (which for BNZ is 0.9; a clogP value below 1.35 is indicative of low permeability) [29,55]. In contrast, others consider BNZ as a class-IV drug, this is, a poorly soluble and poorly permeable molecule [30] with low tissue distributions in healthy mice [56].

By loading into intravenously administered nanomedicines, the biodistribution of poorly permeable and poorly soluble drugs could be controlled, and their activity against selected targets improved. For BNZ, the avoidance of healthy tissues and the reduction of hepatic first-pass metabolism is expected to minimize its toxicity [57,58]. Except on immediately accessible targets such as epithelia, however, controlled biodistribution of nanomedicines requires intravenous injection [59,60]. A fraction of injected nanomedicines would passively accumulate in inflamed tissues and could be delivered to amastigotes after being endocytosed by infected cells. In addition, since endocytosis occurs with cellular energy expenditure, the internalization of BNZ would be independent of its permeability and dose. In this way, very small doses of BNZ could be site-specifically concentrated in areas of infection.

Intravenously administered nanomedicines can deliver minute drug amounts and mediate shorter, less toxic, and more effective treatments than conventional medicines. The effectivity of low liposomal amphotericin B doses used to treat lethal visceral leishmaniasis implemented in India in the mid-1990s is an excellent example [61,62]. Amphotericin B binds to parasite ergosterol precursors, such as lanosterol, disrupting the parasite membrane. Since protozoan trypanosomatids such as Leishmania and Trypanosoma present ergosterol as a component of their membranes [63], short doses of liposomal amphotericin B were expected to act effectively against CD. Unfortunately, the trials did not exceed the preclinical phase. Liposomal amphotericin B cleared blood trypomastigotes and improved survival but did not cure mice [64,65]. All animals treated with liposomal amphotericin B relapsed after immunosuppression with cyclophosphamide, or amastigotes remained in tissues of all mice, particularly in the heart and brain after treating a chronic model of infection with *T. cruzi* CL strain [66]. The failure of liposomal amphotericin B was likely because therapeutic targets in CD are less accessible than in leishmaniasis, where only macrophages are infected.

The first report on BNZ-based nanomedicines intravenously administered to rats and mice dates back to 2004 [67] with disappointing results. An intravenous bolus of 0.7% w/w BNZ/lipid multilamellar liposomes administered two times a week over three weeks, at 0.4 mg BNZ/kg (2.4 mg/kg TD), increased blood BNZ levels and caused a transient and threefold higher accumulation of BNZ in the liver, which was insufficient to defeat the infection of an acute murine model infected with *T. cruzi* RA strain.

More recently, BNZ was formulated into polymersomes of poly(ethylene glycol)-*block*-poly(propylene sulfide) (BNZ-PS, 114.3 ± 4.1 nm; PDI: 0.11 ± 0.02; 4.92 ± 1.93 mV ζ-potential; DL: 1%) [68]. Only two injections of BNZ-PS (3 mg/kg TD) were highly potent in treating *T. cruzi*-infected mice (acute model; BALB/c mice; Y strain; 466-fold lower dose than oral free BNZ with 1400 mg/kg TD), caused no detectable hepatotoxicity, and completely abrogated the weight loss. BNZ-PS, but not free BNZ, significantly reduced the number of parasites in the heart and the inflammation.

In 2005, ultra-low doses of pH-sensitive nanoliposomes of etanidazole (a soluble 2-nitroimidazole; 0.63 mg etanidazole/kg/day in nine total doses, three doses per week over three weeks: 5.67 mg etanidazole/kg TD) reduced trypomastigotes in blood of an acute murine model infected with *T. cruzi* RA strain [69], to the same extent as orally administered BNZ at a 353-fold higher dose (100 mg/kg/day over 20 days: 2000 mg/kg TD [52]).

The study of the effect of pH-sensitive liposomes for etanidazole delivery to CD models was discontinued, but along with BNZ-polymersomes both showed that ultralow doses of the antiparasitic drug could reduce infection and increase survival. Nonetheless, the efficacy of these few experiments is uncertain, since their effect on chronic and immunosuppressed models, as well as the potential toxicity, remain unknown.

Non-approved drugs-based nanomedicines

The *in vivo* activity of non-approved drugs loaded into lipid and polymeric nanoparticles orally and intravenously administered has also been tested (Table 3). For example, oral solid lipid nanoparticles loaded with a poorly bioavailable lipophilic cyclic compound derived from dithiocarbazate, effectively reduced parasitemia, diminished inflammation and lesions of the liver and heart, and resulted in 100% survival of an acute murine model [70].

Either orally or intravenously administered to acute and chronic murine models, poly(D,L-lactide)-*block*-polyethylene glycol nanocapsules loaded with lychnopholide (LYC-PLA-PEG NCs), a lipophilic sesquiterpene lactone isolated from *Lychnophora trichocarpha* of poor solubility, which is degraded at extreme pH values, showed improved efficacy against *T. cruzi* infection. The most relevant results in the acute model were that equal cure rates were obtained for oral LYC-PLA-PEG-NCs and BNZ (62.5%). In contrast, intravenous LYC-PLA-PEG NCs caused 100% [determined by parasitological, fresh blood examination, haemoculture, peripheric blood PCR, and serological (ELISA) methods] cure rate compared to 75% for BNZ, while free LYC reduced parasitemia and improved

mice survival but did not lead to a cure [71]. The most relevant results in the chronic model were that oral LYC-PLA-PEG-NCs yielded a 55.6% cure rate vs 0% for BNZ and free LYC. Intravenous LYC-PLA-PEG-NCs yielded a 50.0% cure rate vs 0% for free LYC and BNZ [72]. Intravenous LYC-PLA-PEG NCs increased 16-fold the body exposure, 26-fold the plasma half-life, and reduced 17-fold the plasma clearance in comparison with free LYC [73], protecting the host against the cardiotoxicity of LYC [74]. Higher doses (12 mg/kg/day) of oral LYC-PLA-PEG-NCs cured 75% of animals in the acute phase and 88% of those in the chronic phase of murine models [75].

Orally administered to acute and chronic murine models, PLGA Nps (PLGA-CUR Nps) loaded with curcumin (the most active polyphenolic flavonoid constituent of Curcuma longa rhizomes with low bioavailability) and free BNZ, induced anti-inflammatory effects and cardiac protection. A low BNZ dose (750 mg/kg TD) plus PLGA-CUR Nps, reduced cardiac hypertrophy and parasite load, chronic inflammation, fibrosis, and the levels and activities of cardiopathogenic biomarker enzymes and cytokines/chemokines (IL-1β, TNF-α, IL-6, and CCL5), matrix metalloproteinases (MMP-2 and MMP-9), and inducible enzymes (cyclooxygenase and nitric oxide synthase) implicated in leukocyte recruitment and cardiac remodelling [76]. More recently, Theracurmin® (a natural product of Theravalues, Tokyo, Japan, that enhances the curcumin bioavailability 30-fold compared with curcumin powder [77,78]) showed immunomodulatory (reduced CCL2 in cardiac tissue, IL-15 in cardiac and skeletal tissue, plasma creatine kinase, and tissue leukocyte infiltration) and trypanocidal effects (reduction of parasitemia) in an acute murine model [79]. A complementary use of Theracurmin® with BNZ therapy is suggested.

Intravenous polycaprolactone Nps loaded with ursolic acid (UR-PCL), a natural pentacyclic triterpene of low bioavailability and poor aqueous solubility used as a dietary supplement, was found to reduce twofold parasitemia, compared with a 3.5-fold reduction of BNZ, in an acute murine model [80]. However, while BNZ caused liver toxicity, UR-PCL was not toxic to liver and kidney.

Which diseases has nanomedicine focused on in the last 28 years?

There are currently between 50 [81] and 60 [82] nanomedicines on the market, and nearly 560 in clinical trials, most of them in clinical phase I (33%) and phase II (21%) [83]. 15% of marketed nanomedicines are antibody–drug conjugates, such as Loncastuximab tesirine, launched in 2021 to treat B-cell lymphoma [84]. Nearly 10% are polymer–drug/protein conjugates such as polyethylene glycol-L-asparaginase (Calaspargase pegol, Asparlas), launched in 2019 in the USA to treat acute

Table 3: *In vivo* performance of nanomedicines based on non-approved drugs.

Administration route/drug/type of nanomedicine	Composition/properties	*In vivo* studies	Ref.
oral H2bdtc[a] SLN	Na taurodeoxycholate, stearic acid, soya lecithin, and H2bdtc (0.12, 0.95, 0.48, and 0.02% w/v, respectively) 127 ± 0.130 nm; PDI < 0.3; –56.1 ± 4.40 mV ζ-potential	acute model, Swiss mice, Y strain BNZ 1 mg/kg/day H2bdtc and H2bdtc-SLN 1.4 mg/kg/day starting 5 dpi oral for 10 days	[70]
IV LYC polymeric NCs	PLA-PEG NC: 1:1 PLA-PEG and Resomer 203 (1.2% w/v), Epikuron 170 (0.4% w/v), Miglyol 810N (2.5% v/v) 105.3 ± 2.3 nm; PDI < 0.3	acute model, Swiss mice, Y strain 4th dpi for up to 20 consecutive days at 2 mg/kg/day	[71]
oral LYC polymeric NCs	same formulations as in [71]	acute and chronic models, Swiss mice, Y strain acute: from 4 dpi for up to 20 consecutive days 5 mg/kg/day; BNZ 100 mg/kg/day chronic: stating on 90 dpi for 20 days 2 mg/kg/day; BNZ 50 mg/kg/day	[72]
oral LYC polymeric NCs	PLA-PEG NC 107 ± 8 nm; PDI < 0.3; –31 ± 8 mV ζ-potential	acute and chronic models, Swiss mice, VL-10 strain (100% resistant to BNZ and NFX). free LYC and LYC-PLA-PEG-NC 8 or 12 mg/kg/day by oral gavage from 9 dpi for acute and from 90 dpi for chronic administered for 20 days	[75]
oral BNZ + curcumin polymeric Nps	PLGA (50:50) Nps	chronic model, C57BL/6 mice, Brazil strain BNZ (25 mg/kg/day) + Np PLGA CUR (200 mg/kg/day) for 30 days from 60 dpi	[76]
oral curcumin nanodispersion	Theracurmin 10 w/w% of curcumin, 2% of other curcuminoids, 46% of glycerin, 4% of gum ghatti, and 38% of water 190 nm	acute model, Swiss mice, Colombian strain 30 mg/kg day theracurmin for 30 days	[79]
IV ursolic acid polymeric Nps	PLC and poloxamer 407 173.2 ± 7.28 nm; PDI 0.09 ± 0.03; –36 ± 3.34 mV ζ-potential	acute model, C57BL/6 mice, Y strain starting 48 h post-infection for 7 days	[80]

[a]H2bdtc: 5-hydroxy-3-methyl-5-phenylpyrazoline-1-(*S*-benzyl dithiocarbazate).

lymphoblastic leukemia [85]. Another 10% are protein-based nanoparticles including Abraxane, the first formulation based on protein nanotechnology launched in 2005 [86]. Nearly 10% are inorganic nanoparticles such as the radiosensitizer Hensify, which in 2019 obtained CE Mark approval in the European Union for the treatment of locally advanced soft tissue sarcoma. This category also includes cancer imaging and diagnosis such as the MRI imaging agent Resovist, carboxydextran-coated superparamagnetic iron oxide nanoparticles approved for liver contrast-enhanced MRI102 [87]. Another 10% are nanocrystals, such as Tricor (approved in 2004) or Triglide (approved in 2005), used to improve the bioavailability of the anti-hypercholesterolemic fenofibrate [88,89].

Polymeric nanoparticles and cell-derived vehicles such as exosomes have not entered the market yet because of issues regarding quality control, large-scale repeatable preparation, effectiveness, and safety [90].

The remaining nearly 45% are lipid-based nanoparticles, constituting the most prevalent category of nanomedicines accessible in the market [91]. These include uni- or multilamellar liposomes (vesicles formed by bilayers of amphiphilic lipids), and lipid nanoparticles. The introduction of new preparation techniques on the industrial scale, such as microfluidic devices, contributes to their successful clinical translation and reduces the production cost to relatively affordable prices [92-94].

The main proportion of lipid-based nanoparticles are liposomes. These are used for the delivery of antitumoral drugs with low molecular weight, such as Doxil® (for delivery of doxorubicin) launched in 1995, DoceAqualip® (for delivery of docetaxel, devoid of polysorbate-80 and ethanol) launched in 2014, Onivyde® (for delivery of irinotecan) launched in 2015, and Vyxeos® (for synchronous delivery of cytarabine and daunorubicin) launched in 2017. These liposomes act mainly by passive targeting mechanisms upon intravenous administration.

Parenteral liposomes employing the DepoFoam technology are used in clinical analgesia, that is, DepoDur™ and Expare®, approved in 2004 and 2018, respectively.

The above summary shows that until now, most nanomedicines have been marketed to solve two big problems, namely (i) the low bioavailability and/or (ii) the high toxicity of drugs with low molecular weight. The most representative examples of the first group of nanomedicines are nanocrystals, carrier-free colloidal systems in the nanometer range (100–1000 nm), with a theoretical drug loading of 100%. They consist of pure drugs, usually in a solid amorphous state, with a minimal quantity of surface-active agents for stabilization. Nanocrystals are superior to microsuspensions at increasing the oral bioavailability of class-II drugs with low solubility, or low or irregular bioavailability, and promoting adhesion to the gastrointestinal wall [95]. The small size of the crystals is associated with a large surface area, which increases interactions with the dissolving medium and accelerates the dissolution rate. The latest marketed nanocrystals are for intramuscular injection and provide long-time delivery of drugs such as paliperidone palmitate, an atypical antipsychotic, or antiretrovirals. Excluding the anti-fungal griseofulvin (not a nanocrystal, but a micrometer-sized crystal), and anti-retrovirals, the remaining drugs formulated in nanocrystals are used to treat noncommunicable diseases (anti-emetic, immunosuppressant, antiarrhythmic, anti-chronic pain, anti-angina, anti-inflammatory and anti-hypercholesterolemic agents, appetite stimulants, and bronchial dilatators). The other big group of nanomedicines [89] are liposomes aimed to reduce the toxicity of oncological drugs by changing their biodistribution and pharmacodynamics, requiring intravenous administration. The success rate from phase 1 to approval, of antitumor nanomedicines is 6%, compared with 3.4% for classical oncological drugs [96].

The newest nanomedicines not only improve the pharmacokinetics and safety profile of classical medicines but also display higher effectiveness [97].

This portfolio of liposomal nanomedicines is now broadening to include other than oncological drugs, such as those to prevent deadly infections or treat chronic diseases [81]. Nanocort for instance, is a novel liposomal platform for intravenous administration of prednisolone to patients with chronic inflammatory diseases, such as ulcerative colitis, inflammatory bowel diseases, rheumatoid arthritis, and multiple sclerosis, in phase-II/III clinical trials sponsored by Enceladus Pharmaceuticals BV™ [98].

Newly available nanomedicines are not limited to the delivery of small drugs. Several anti-infective nanoparticulate vaccines, most of them for non-viral gene delivery have recently hit the market. Examples are these constituted by lipid nanoparticles made of phospholipids, cholesterol, polyethylene glycol (PEG) lipids, and ionizable synthetic lipids (ALC-0315 from BioNTech-Pfizer and SM-102 from Moderna Therapeutics) for enhanced delivery of messenger RNA (mRNA) encoding the spike protein of the SARS-COV-2 virus to antigen-presenting cells [82]. These vaccines were approved by the FDA, Pfizer-BioNTech COVID-19 in 2021 [99] and Moderna COVID-19 Vaccine in 2022 [100], after the approval in 2018 of Onpattro (Patisiran) [101], the first gene therapy based on lipid nanoparticles containing RNA interference, for the treatment of hereditary transthyretin-mediated amyloidosis. Vaccines made of lipid-based nanoparticles for delivery of mRNA are currently being investigated to protect against other viral diseases such as Zika, influenza, human immunodeficiency virus (HIV), respiratory syncytial virus cytomegalovirus, and bacterial diseases such as tuberculosis [102]. Another example of nanoparticulate vaccine is the anti-malarial Mosquirix™ (RTS, S/AS01), recommended by the World Health Organization in four doses for children in 2021. Mosquirix™ employs a liposome-based adjuvant, AS01 (GlaxoSmithKline) [103] that contains 3-*O*-desacyl-monophosphoryl lipid A and QS-21, a water-soluble triterpene glycoside (saponin) [104]. Although the vaccine has low efficacy, it has considerable advantages regarding general health: Four doses of the vaccine would avoid 116,480 instances of malarial infection and 484 fatalities per 100,000 immunized children.

There are good reasons to predict a bright commercial future for the abovementioned groups of nanomedicines. Currently, the approval of anti-tumor nanomedicines and the recruitment of nanomedicines for clinical trials related to infectious diseases are gaining momentum [82]. Moreover, economic forecast reports predict an additional 12.8% growth by the year 2025 driven by the evolution of vaccines against COVID-19 based on nanomedicines and the projected huge global demand for these products [105]. However, the clinical translatability of nanomedicines is still complex. Consider, for instance, the liposomal formulation of the antifungal amphotericin B AmBisome®, with significantly lower nephrotoxic effects compared to amphotericin B deoxycholate and launched in 1990 [106,107]. Remarkably, despite being used to combat visceral leishmaniasis [62], AmBisome® was not made to treat a neglected disease, but to fight systemic mycoses resulting from immunosuppression caused by oncological treatments [108]. The big picture shows that nanomedicines, specifically the drug delivery field, are (and probably will be) focused on diseases that exclude parasitic diseases, regardless of their socioeconomic burden. In the next two sections, we will examine the general and particular factors leading to this situation.

General barriers to the development of nanomedicines

Typical challenges in pharmaceutical development result from low efficiency and high attrition rate [109]. Unfortunately, these challenges are magnified in nanomedicine development [1,82,110], and the reasons can be summarized as follows:

Difficult scale-up, structural characterization, and conservation: The structure of nanomedicines is much more complex than that of drugs with low molecular weight. Because of that, nanomedicines are considered as non-biological complex drugs (NBCDs). NBCDs present heterogeneous molecular nature, difficult to be precisely controlled, and cannot be fully characterized by physicochemical analysis; nanoparticles are not a mere excipient, but the entire complex is the active pharmaceutical ingredient [111]. The transition from small laboratory batch sizes to large industrial volumes is the most challenging step in nanomedicine product development [112]. Slight structural changes induced during the industrial-scale production may modify pharmacokinetics, biodistribution, and pharmacodynamics of nanomedicines and alter their therapeutic properties and toxic profile [113,114]. The industrial quality control is much more complex than that of conventional pharmaceuticals, focused mainly on the properties of the low-molecular-weight drug constituting the active pharmaceutical ingredient [115-117]. Given their structural complexity and high surface area, nanomedicines are highly susceptible to aggregation, hygroscopicity, contamination, phase transition, amorphous-to-crystalline transitions, and degradation. It is critical to maintain batch-to-batch reproducibility (in terms of mean size, polydispersity, ζ-potential, and drug loading) not only during large-scale manufacturing [118] but also during storage. These characteristics reduce the affordability of nanomedicines in developing and low-income countries [119,120].

Changes in current pharmacological paradigms: The four paradigms are (i) the choice of right administration route, (ii) the need for analytical techniques different from those used in classical pharmaceutical technology, (iii) new toxicological assays, and (iv) suitable animal models: (i) Most nanomedicines, except nanocrystals/nanosuspensions, should be injected into the blood circulation. This is not convenient for many patients compared to oral or other non-invasive routes [121]. (ii) Drugs with low molecular weight diffuse readily across biological barriers and their concentration in blood is in equilibrium and related to achievable target tissue levels. The blood concentration of drugs loaded in nanomedicines, instead, is not indicative of the drug's bioavailability. Because of their huge size, nanomedicines in the blood cannot escape from vascular confinement and are not readily able to extravasate across the endothelium. Moreover, ne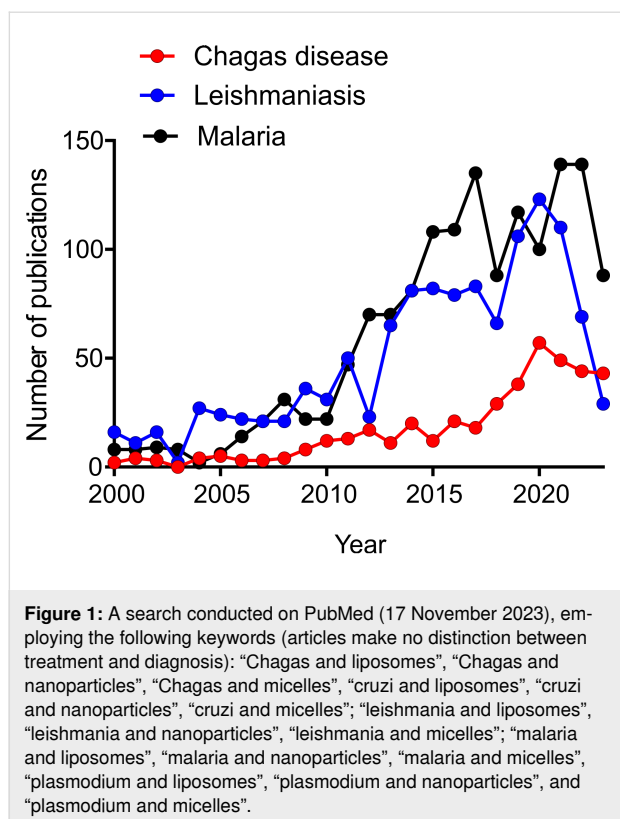ither their extravasation in areas of high vascular permeability, nor their accumulation in the vicinity of target cells, signify they are bioavailable unless the drug is released or the nanomedicine is endocytosed. These factors make it difficult to determine the pharmacokinetics and biodistribution of nanomedicines. (iii) In the blood circulation, nanomedicines tend to aggregate, adsorb plasma proteins, and prematurely release their cargos; also, they are phagocytosed by circulating monocytes or tissue macrophages to be degraded. This gives rise to the emergence of new modes of toxicity, including hemolysis, inflammation, oxidative stress, and impaired lysosomal or mitochondrial function. In the case of BNZ, it is important to note that the potential toxicity of oral BNZ-loaded nanomedicines would result from absorbed free BNZ. The toxicity of intravenous nanomedicines (e.g., pH-sensitive liposomes or polymersomes) instead, would be caused by the interaction of the nanomedicine structure with blood components, and its nature may completely differ from that raised of free BNZ (or other 2-nitroimidazole compounds). (iv) Potential acute toxicity of intravenous nanomedicines cannot be observed in rodents, which are not suitable predictive models for potentially lethal reactions such as the complement activation-related pseudo-allergy effect [122]. Investigation of chronic toxicity is time-consuming, and analyzing chronic toxicity data is more demanding [123].

Complex regulatory aspects: The regulatory decisions on nanomedicines can only be made based on individual assessments of benefits and risks [123]. The lack of universal regulatory protocols for good manufacturing practices of nanomedicines makes their quality control aspects overly complex [110,124]. In addition, the regulatory framework for a given nanomedicine will change according to the country, thereby hindering approval and regulation [125-127].

High cost: The prohibitive costs of the raw materials, intensive research, and complicated production steps make nanomedicines expensive, discouraging the interest of pharmaceutical companies. For those reasons, the clinical therapeutic effect of nanomedicines must be much higher than that of conventional therapeutics [128-130]. Besides, the sophisticated nature of nanomedicines leads to complex issues related to patenting and the determination of intellectual properties [124].

Status of current preclinical nanomedicines against CD and challenges ahead

While the reports published over the last 20 years on treatments against CD and leishmaniasis are comparable in number, those against malaria (a parasitosis endemic to Asian countries) are more than fourfold higher. According to a search that includes diagnosis and treatment (Figure 1), the reports on anti-CD nanomedicines in the last 20 years are no more than a few

Figure 1: A search conducted on PubMed (17 November 2023), employing the following keywords (articles make no distinction between treatment and diagnosis): "Chagas and liposomes", "Chagas and nanoparticles", "Chagas and micelles", "cruzi and liposomes", "cruzi and nanoparticles", "cruzi and micelles"; "leishmania and liposomes", "leishmania and nanoparticles", "leishmania and micelles"; "malaria and liposomes", "malaria and nanoparticles", "malaria and micelles", "plasmodium and liposomes", "plasmodium and nanoparticles", and "plasmodium and micelles".

hundred. This means that despite its high burden for developing countries, CD is neglected not only by pharmaceutical companies and governments but also by the academic [131] community, including nanomedical researchers.

The failure of the only large-scale multinational project aiming for cheap nanomedicines against CD was a missed unique opportunity since the original idea of bypassing liver metabolism was reasonable for a toxic drug such as BNZ. This project, gathering pharmaceutical companies, state institutions, and scientists, was sufficiently funded to lay the groundwork for a potential future commercial product. Seeking to increase the solubility of BNZ is a reasonable strategy if BNZ is considered a class-II drug. In this regard, most contemporaneous *in vitro* reports on BNZ-based nanomedicines aimed to increase BNZ solubility dismissed the fact that oral nanomedicines are not absorbed into the blood circulation. Since the recently discovered non-replicative state of parasites seems to be less susceptible to BNZ-induced damage, *in vitro* models of dormant parasites may be useful to explore the effect of endocytosed nanomedicines on these forms. The results would be suitable, however, only for intravenous nanomedicines. The much scarcer reports on the *in vivo* activity of oral BNZ-based nanomedicines, show trypanocide effects on acute/chronic and even immunocompromised mouse models, suggesting a cure. In these studies, the plasma levels of BNZ remain to be deter-

mined. This is important given, for example, the significant increase in the drug's bioavailability provided by nanocrystals, and the potential toxic effects observed in humans, which some authors have linked to high BNZ plasma levels. While BNZ-based nanomedicines such as BNZ-NC are advantageous because of the extraordinarily high BNZ loading, unexplored issues may arise from its huge specific surface area and interfacial free energy. Nanocrystals are thermodynamically unstable, with a tendency to aggregate, undergoing Oswald ripening and changes in the crystal polymorph, inducing potential tissue irritation [132,133]. Also, if ADRs were associated with an intrinsic susceptibility of patients, reducing BNZ plasma levels would not be helpful. Hence, what type of nanomedicines could solve the problem of BNZ-based medication? Targeting BNZ to diseased tissues while avoiding healthy ones, for instance, could alleviate the problem. However, for controlled biodistribution, nanomedicines must be intravenously administered. This fact, as discussed previously, raises the complexity of the therapeutic strategy to limits that may impair its implementation in developing countries. Unfortunately, early attempts to treat CD with intravenously administered nanomedicines failed or were discontinued.

The assessment of pharmacokinetics and biodistribution of nanomedicines is complicated since many aspects of human disease cannot be modeled in animals [134]. With respect to standardized models needed for predictive preclinical evaluation of novel therapies against CD [135], issues regarding assay design and endpoint definitions persist [136]. Moreover, vessel diameters, irregular permeability, and microenvironments of diseased tissues from animal models are hardly comparable to those of healthy or diseased humans. This constitutes a problem for the development of predictive preclinical models. In addition, alternatives such as "Replacing, Reducing, and Refining" the use of animals in research (3R concept) [137] toward the more predictive and less cruel use of 3D human cell cultures and microfluidics, are still too costly for routine research in developing countries [138,139]. The therapeutic performance of intravenous nanomedicines strongly depends on the anatomical pathological context, mainly on the extent of inflammation or retention permeation effect, and the extracellular matrix tightness of target tissues. This aspect, practically overlooked in animal models of Chagas disease, could distort the biodistribution of nanomedicines, yielding falsely promising preclinical results, as occurred with anti-tumor nanomedicines administered to xenografts tumor models [140].

Finally, to successfully develop nanomedicines, disease-led rather than formulation-led design is essential [141]. In treatments performed with intravenous nanomedicines, hydrody-

namic diameter (much larger than that of a low-molecular-weight drug) and surface nature, are critical to maximize the access to target sites. The extracellular or intracellular character of the targets must be known beforehand, as well as the diseased tissue's location, the presence of acidity, oxidative stress, or associated inflammation. The pathophysiology and the nature of targets in CD, however, seem not to be completely defined yet. Our limited understanding of the infection process, pathology progress, and its long-term nature makes it difficult to find new drugs for better treatments, or vaccines to prevent or treat CD [142]. It has been suggested, for example, that the classical view of the infective cycle is superficial and that the process in mammalian hosts is certainly more complex. Acceptable formulations for the treatment of the chronic phase [136], for example, should reach intracellular targets. But what is the nature of these targets and how feasible for nanomedicines is it to access them? Recently, the presence of intracellular epimastigote-like forms, named zoids (cells with kinetoplast but no nucleus, which quickly die and are degraded by the host cell) and of metabolically quiescent or dormant amastigotes, have been described. Dormant amastigotes can reside over long periods of time in chronically infected tissues and can spontaneously restart the infection, even after treatment, accounting for drug resistance in CD. An adaptive difference between *T. cruzi* strains to induce dormancy has also been suggested. Infected muscle or tissue macrophages can only be targeted by intravenous nanomedicines if local inflammation is manifested [39]. In the absence of inflammation, cells hosting dormant parasites could be inaccessible to nanomedicine extravasation. Determining the presence of inflammation is critical to predicting the success of intravenous nanomedicine-based treatment. Also, if BNZ is not effective against quiescent forms, a treatment with BNZ-based nanomedicines will not be of use to solve the problem.

The preclinical data gathered to date tells us that we are far from determining whether the efficacy and reduced toxicity of BNZ or 2-nitroimidazole-based nanomedicines would outperform the current oral BNZ-based treatment.

Drugs are not developed because of social or humanitarian reasons. The cost of drug development and the risks are high, and the times are long [143,144]. In the end, there must be certainty of making profit, and it is the pharmaceutical companies that take that risk. Investment in nanomedicines, thus, is of high risk and must yield a high reward. This magnification of cost deepens the challenge of developing drugs against endemic infections affecting millions of people in poor or developing countries. Even relatively high anticipated sales volumes may provide insufficient incentives if the expected pricing is low [145].

In this scenario, it can be predicted that *de novo* development of nanomedicines exclusively aimed at increasing bioavailability, reducing toxicity, or for targeted delivery of drugs such as the relatively well-known BNZ is not an impossible, but an expensive, enterprise. Much more expensive and riskier will be developing nanomedicines for the delivery of non-approved molecules.

In 2021, the effect of a subcutaneous immunostimulant with imiquimod loaded in nanoarchaeosomes (a type of lipid vesicles, nanoarc-imq) on an acute model of CD was reported. The lipids from nanoarc-imq showed extraordinary resistance to factors that normally reduce the structural stability of nanoparticulate material. The treatment not only reduced parasitemia but also eliminated inflammation and cardiac fibrosis more efficiently than BNZ [146]. These preliminary results, based on immunostimulation in the absence of antigens, matched those achieved with intravenous administration of liposomal amphotericin B in acute mice models of CD. Structurally simple formulations like that made of lipid nanovesicles, the same as nanocrystals, are examples of nanomedicines that, because of their easy industrial scale-up, structural assessment, and cheaper production (compared to that required for drug delivery or vaccination), could make it to the market against CD. Consider the development of Mosquirix™, which took nearly 35 years, for instance. In comparison, the factors that made the rapid appearance of nanomedical anti-infective vaccines possible were long-term investments in research infrastructure and major government interventions, which absorbed much of the risk from research and development. None of these elements exist in most countries where CD is endemic. Repurposing nanomedicines already available, as happened with liposomal amphotericin B and leishmaniasis could be a possibility. However, today there are no prospects in sight for nanomedicines with potential anti-CD activity on the market.

Conclusion

Overall, the main difficulty for developing anti-CD nanomedicines would not lie in the complexity of the pathology itself, but in the neglected character of CD [147]. The challenge of improving the treatment of the chronic phase of CD has been posed for decades, and the classic pharmaceutical industry has not been able or interested to face it. Will nanomedicine be able to do it? The answer is more political than technical.

ORCID® iDs

Maria Jose Morilla - https://orcid.org/0000-0003-3706-9207
Kajal Ghosal - https://orcid.org/0000-0001-6392-2182
Eder Lilia Romero - https://orcid.org/0000-0003-3020-1746

Data Availability Statement
Data sharing is not applicable as no new data was generated or analyzed in this study.

References

1. Bhardwaj, V.; Kaushik, A.; Khatib, Z. M.; Nair, M.; McGoron, A. J. *Front. Pharmacol.* **2019,** *10,* 1369. doi:10.3389/fphar.2019.01369

2. Crommelin, D. J. A.; van Hoogevest, P.; Storm, G. *J. Controlled Release* **2020,** *318,* 256–263. doi:10.1016/j.jconrel.2019.12.023

3. Gomes, D. C.; Medeiros, T. S.; Alves Pereira, E. L.; da Silva, J. F. O.; de Freitas Oliveira, J. W.; Fernandes-Pedrosa, M. de F.; de Sousa da Silva, M.; da Silva-Júnior, A. A. *Int. J. Mol. Sci.* **2023,** *24,* 13778. doi:10.3390/ijms241813778

4. Lidani, K. C. F.; Andrade, F. A.; Bavia, L.; Damasceno, F. S.; Beltrame, M. H.; Messias-Reason, I. J.; Sandri, T. L. *Front. Public Health* **2019,** *7,* 166. doi:10.3389/fpubh.2019.00166

5. Chagas disease (also known as American trypanosomiasis). https://www.who.int/news-room/fact-sheets/detail/chagas-disease-%28American-trypanosomiasis%29 (accessed Nov 14, 2023).

6. Lee, B. Y.; Bacon, K. M.; Bottazzi, M. E.; Hotez, P. J. *Lancet Infect. Dis.* **2013,** *13,* 342–348. doi:10.1016/s1473-3099(13)70002-1

7. Chagas Disease: What U.S. Clinicians Need to Know - Lesson 1: Page: 3. https://www.cdc.gov/parasites/cme/chagas/lesson_1/3.html (accessed Nov 14, 2023).

8. Pérez-Molina, J. A.; Molina, I. *Lancet* **2018,** *391,* 82–94. doi:10.1016/s0140-6736(17)31612-4

9. Navarro, M.; Reguero, L.; Subirà, C.; Blázquez-Pérez, A.; Requena-Méndez, A. *Travel Med. Infect. Dis.* **2022,** *47,* 102284. doi:10.1016/j.tmaid.2022.102284

10. Enfermedad de Chagas. DNDi América Latina. https://dndial.org/es/doencas/doenca-de-chagas#datos/ (accessed Nov 15, 2023).

11. Bern, C.; Kjos, S.; Yabsley, M. J.; Montgomery, S. P. *Clin. Microbiol. Rev.* **2011,** *24,* 655–681. doi:10.1128/cmr.00005-11

12. Fabbro, D. L.; Streiger, M. L.; Arias, E. D.; Bizai, M. L.; del Barco, M.; Amicone, N. A. *Rev. Soc. Bras. Med. Trop.* **2007,** *40,* 1–10. doi:10.1590/s0037-86822007000100001

13. Banco de Recursos de Comunicación del Ministerio de Salud de la Nación. Guías para la atención al paciente infectado con Trypanosoma cruzi (Enfermedad de Chagas). https://bancos.salud.gob.ar/recurso/guias-para-la-atencion-al-paciente-infectado-con-trypanosoma-cruzi-enfermedad-de-chagas (accessed Nov 15, 2023).

14. Hall, B. S.; Wilkinson, S. R. *Antimicrob. Agents Chemother.* **2012,** *56,* 115–123. doi:10.1128/aac.05135-11

15. Trochine, A.; Creek, D. J.; Faral-Tello, P.; Barrett, M. P.; Robello, C. *PLoS Negl. Trop. Dis.* **2014,** *8,* e2844. doi:10.1371/journal.pntd.0002844

16. Castro, J. A.; Diaz de Toranzo, E. G. *Biomed. Environ. Sci.* **1988,** *1,* 19–33.

17. Castro, J. A.; deMecca, M. M.; Bartel, L. C. *Hum. Exp. Toxicol.* **2006,** *25,* 471–479. doi:10.1191/0960327106het653oa

18. Castro, J. A.; Montalto de Mecca, M.; Díaz Gómez, M. I.; Castro, G. D. *Acta Bioquim. Clin. Latinoam.* **2015,** *49,* 73–82.

19. Ferraz, L. R. de M.; Alves, A. É. G.; Nascimento, D. D. S. da S.; Amariz, I. A. e.; Ferreira, A. S.; Costa, S. P. M.; Rolim, L. A.; Lima, Á. A. N. de; Rolim Neto, P. J. *Acta Trop.* **2018,** *185,* 127–132. doi:10.1016/j.actatropica.2018.02.008

20. Aldasoro, E.; Posada, E.; Requena-Méndez, A.; Calvo-Cano, A.; Serret, N.; Casellas, A.; Sanz, S.; Soy, D.; Pinazo, M. J.; Gascon, J. *J. Antimicrob. Chemother.* **2018,** *73,* 1060–1067. doi:10.1093/jac/dkx516

21. Soy, D.; Aldasoro, E.; Guerrero, L.; Posada, E.; Serret, N.; Mejía, T.; Urbina, J. A.; Gascón, J. *Antimicrob. Agents Chemother.* **2015,** *59,* 3342–3349. doi:10.1128/aac.05018-14

22. Altcheh, J.; Moscatelli, G.; Mastrantonio, G.; Moroni, S.; Giglio, N.; Marson, M. E.; Ballering, G.; Bisio, M.; Koren, G.; García-Bournissen, F. *PLoS Negl. Trop. Dis.* **2014,** *8,* e2907. doi:10.1371/journal.pntd.0002907

23. Molina-Morant, D.; Fernández, M. L.; Bosch-Nicolau, P.; Sulleiro, E.; Bangher, M.; Salvador, F.; Sanchez-Montalva, A.; Ribeiro, A. L. P.; de Paula, A. M. B.; Eloi, S.; Correa-Oliveira, R.; Villar, J. C.; Sosa-Estani, S.; Molina, I. *Trials* **2020,** *21,* 328. doi:10.1186/s13063-020-4226-2

24. Álvarez, M. G.; Ramírez, J. C.; Bertocchi, G.; Fernández, M.; Hernández, Y.; Lococo, B.; Lopez-Albizu, C.; Schijman, A.; Cura, C.; Abril, M.; Laucella, S.; Tarleton, R. L.; Natale, M. A.; Castro Eiro, M.; Sosa-Estani, S.; Viotti, R. *Antimicrob. Agents Chemother.* **2020,** *64,* 10.1128/AAC.00439-20. doi:10.1128/aac.00439-20

25. Pinazo, M.-J.; Guerrero, L.; Posada, E.; Rodríguez, E.; Soy, D.; Gascon, J. *Antimicrob. Agents Chemother.* **2013,** *57,* 390–395. doi:10.1128/aac.01401-12

26. Salvador, F.; Sánchez-Montalvá, A.; Martínez-Gallo, M.; Sala-Cunill, A.; Viñas, L.; García-Prat, M.; Aparicio, G.; Sao Avilés, A.; Artaza, M. Á.; Ferrer, B.; Molina, I. *Clin. Infect. Dis.* **2015,** *61,* 1688–1694. doi:10.1093/cid/civ690

27. Keenan, M.; Chaplin, J. H. *Prog. Med. Chem.* **2015,** *54,* 185–230. doi:10.1016/bs.pmch.2014.12.001

28. Workman, P.; White, R. A.; Walton, M. I.; Owen, L. N.; Twentyman, P. R. *Br. J. Cancer* **1984,** *50,* 291–303. doi:10.1038/bjc.1984.176

29. Kasim, N. A.; Whitehouse, M.; Ramachandran, C.; Bermejo, M.; Lennernäs, H.; Hussain, A. S.; Junginger, H. E.; Stavchansky, S. A.; Midha, K. K.; Shah, V. P.; Amidon, G. L. *Mol. Pharmaceutics* **2004,** *1,* 85–96. doi:10.1021/mp034006h

30. Maximiano, F. P.; Costa, G. H. Y.; De Souza, J.; Da Cunha-Filho, M. S. S. *Quim. Nova* **2010,** *33,* 1714–1719. doi:10.1590/s0100-40422010000800018

31. Amidon, G. L.; Lennernäs, H.; Shah, V. P.; Crison, J. R. *Pharm. Res.* **1995,** *12,* 413–420. doi:10.1023/a:1016212804288

32. Singh, A.; Worku, Z. A.; Van den Mooter, G. *Expert Opin. Drug Delivery* **2011,** *8,* 1361–1378. doi:10.1517/17425247.2011.606808

33. Vinuesa, T.; Herr, R.; Oliver, L.; Elizondo, E.; Acarregui, A.; Esquisabel, A.; Pedraz, J. L.; Ventosa, N.; Veciana, J.; Viñas, M. *Am. J. Trop. Med. Hyg.* **2017,** *97,* 1469–1476. doi:10.4269/ajtmh.17-0044

34. Tessarolo, L. D.; de Menezes, R. R. P. P. B.; Mello, C. P.; Lima, D. B.; Magalhães, E. P.; Bezerra, E. M.; Sales, F. A. M.; Barroso Neto, I. L.; Oliveira, M. d. F.; dos Santos, R. P.; Albuquerque, E. L.; Freire, V. N.; Martins, A. M. *Parasitology* **2018,** *145,* 1191–1198. doi:10.1017/s0031182018000197

35. Nhavene, E. P. F.; da Silva, W. M.; Trivelato Junior, R. R.; Gastelois, P. L.; Venâncio, T.; Nascimento, R.; Batista, R. J. C; Machado, C. R.; Macedo, W. A. de A.; Sousa, E. M. B. de. *Microporous Mesoporous Mater.* **2018,** *272,* 265–275. doi:10.1016/j.micromeso.2018.06.035

36. Muraca, G.; Ruiz, M. E.; Gambaro, R. C.; Scioli-Montoto, S.; Sbaraglini, M. L.; Padula, G.; Cisneros, J. S.; Chain, C. Y.; Álvarez, V. A.; Huck-Iriart, C.; Castro, G. R.; Piñero, M. B.; Marchetto, M. I.; Alba Soto, C.; Islan, G. A.; Talevi, A. *Beilstein J. Nanotechnol.* **2023,** *14,* 804–818. doi:10.3762/bjnano.14.66

37. Oliveira, A. C. d. J.; Silva, E. B.; Oliveira, T. C. d.; Ribeiro, F. d. O. S.; Nadvorny, D.; Oliveira, J. W. d. F.; Borrego-Sánchez, A.; Rodrigues, K. A. d. F.; Silva, M. S.; Rolim-Neto, P. J.; Viseras, C.; Silva-Filho, E. C.; Silva, D. A. d.; Chaves, L. L.; Soares, M. F. d. L. R.; Soares-Sobrinho, J. L. *Int. J. Biol. Macromol.* **2023,** *230,* 123272. doi:10.1016/j.ijbiomac.2023.123272

38. da Silva, F. L. O.; Marques, M. B. de F.; Yoshida, M. I.; Mussel, W. da N.; da Silveira, J. V. W.; Barroso, P. R.; Kato, K. C.; Martins, H. R.; Carneiro, G. *Braz. J. Pharm. Sci.* **2023,** *59,* e22111. doi:10.1590/s2175-97902023e22111

39. Lebreton, V.; Legeay, S.; Saulnier, P.; Lagarce, F. *Drug Discovery Today* **2021,** *26,* 2259–2268. doi:10.1016/j.drudis.2021.04.017

40. He, H.; Lu, Y.; Qi, J.; Zhu, Q.; Chen, Z.; Wu, W. *Acta Pharm. Sin. B* **2019,** *9,* 36–48. doi:10.1016/j.apsb.2018.06.005

41. Seremeta, K. P.; Arrúa, E. C.; Okulik, N. B.; Salomon, C. J. *Colloids Surf., B* **2019,** *177,* 169–177. doi:10.1016/j.colsurfb.2019.01.039

42. de Moura Ferraz, L. R.; Tabosa, A. É. G. A.; da Silva Nascimento, D. D. S.; Ferreira, A. S.; Silva, J. Y. R.; Junior, S. A.; Rolim, L. A.; Rolim-Neto, P. J. *J. Mater. Sci.: Mater. Med.* **2021,** *32,* 59. doi:10.1007/s10856-021-06530-w

43. Arrua, E. C.; Hartwig, O.; Loretz, B.; Goicoechea, H.; Murgia, X.; Lehr, C.-M.; Salomon, C. J. *Colloids Surf., B* **2022,** *217,* 112678. doi:10.1016/j.colsurfb.2022.112678

44. Arrua, E. C.; Hartwig, O.; Loretz, B.; Murgia, X.; Ho, D.-K.; Bastiat, G.; Lehr, C.-M.; Salomon, C. J. *Int. J. Pharm.* **2023,** *642,* 123120. doi:10.1016/j.ijpharm.2023.123120

45. Benznidazol and Triazol REsearch group for Nanomedicine and Innovation on Chagas diseasE | BERENICE | Project | Fact sheet | FP7 | CORDIS. European Commission https://cordis.europa.eu/project/id/305937 (accessed Nov 15, 2023).

46. Moraes, C. B.; Giardini, M. A.; Kim, H.; Franco, C. H.; Araujo-Junior, A. M.; Schenkman, S.; Chatelain, E.; Freitas-Junior, L. H. *Sci. Rep.* **2014,** *4,* 4703. doi:10.1038/srep04703

47. MacLean, L. M.; Thomas, J.; Lewis, M. D.; Cotillo, I.; Gray, D. W.; De Rycker, M. *PLoS Negl. Trop. Dis.* **2018,** *12,* e0006612. doi:10.1371/journal.pntd.0006612

48. Viotti, R.; Vigliano, C.; Lococo, B.; Alvarez, M. G.; Petti, M.; Bertocchi, G.; Armenti, A. *Expert Rev. Anti-Infect. Ther.* **2009,** *7,* 157–163. doi:10.1586/14787210.7.2.157

49. Rial, M. S.; Scalise, M. L.; Arrúa, E. C.; Esteva, M. I.; Salomon, C. J.; Fichera, L. E. *PLoS Negl. Trop. Dis.* **2017,** *11,* e0006119. doi:10.1371/journal.pntd.0006119

50. Scalise, M. L.; Esteva, M. I.; Rial, M. S.; Fichera, L. E.; Arrúa, E. C.; Salomon, C. J. *Am. J. Trop. Med. Hyg.* **2016,** *95,* 388–393. doi:10.4269/ajtmh.15-0889

51. Rial, M. S.; Arrúa, E. C.; Natale, M. A.; Bua, J.; Esteva, M. I.; Prado, N. G.; Laucella, S. A.; Salomon, C. J.; Fichera, L. E. *J. Antimicrob. Chemother.* **2020,** *75,* 1906–1916. doi:10.1093/jac/dkaa101

52. Mazzeti, A. L.; Oliveira, L. T.; Gonçalves, K. R.; Schaun, G. C.; Mosqueira, V. C. F.; Bahia, M. T. *Eur. J. Pharm. Sci.* **2020,** *145,* 105234. doi:10.1016/j.ejps.2020.105234

53. Rolon, M.; Hanna, E.; Vega, C.; Coronel, C.; Dea-Ayuela, M. A.; Serrano, D. R.; Lalatsa, A. *Pharmaceutics* **2022,** *14,* 1822. doi:10.3390/pharmaceutics14091822

54. Dutra da Silva, A.; Fracasso, M.; Bottari, N. B.; Gundel, S.; Ourique, A. F.; Assmann, C. E.; Ferreira, D. A. S. P.; Castro, M. F. V.; Reichert, K. P.; de Souza, L. A. F.; da Veiga, M. L.; da Rocha, M. I. U. M.; Monteiro, S. G.; Morsch, V. M.; Chitolina Schetinger, M. R.; da Silva, A. S. *Exp. Parasitol.* **2023,** *249,* 108520. doi:10.1016/j.exppara.2023.108520

55. Bennion, B. J.; Be, N. A.; McNerney, M. W.; Lao, V.; Carlson, E. M.; Valdez, C. A.; Malfatti, M. A.; Enright, H. A.; Nguyen, T. H.; Lightstone, F. C.; Carpenter, T. S. *J. Phys. Chem. B* **2017,** *121,* 5228–5237. doi:10.1021/acs.jpcb.7b02914

56. Perin, L.; Pinto, L.; Balthazar Nardotto, G. H.; da Silva Fonseca, K.; Oliveira Paiva, B.; Fernanda Rodrigues Bastos Mendes, T.; Molina, I.; Correa-Oliveira, R.; Melo de Abreu Vieira, P.; Martins Carneiro, C. *J. Antimicrob. Chemother.* **2020,** *75,* 2213–2221. doi:10.1093/jac/dkaa130

57. Romero, E. L.; Morilla, M. J. *Adv. Drug Delivery Rev.* **2010,** *62,* 576–588. doi:10.1016/j.addr.2009.11.025

58. Morilla, M. J.; Romero, E. L. *Nanomedicine (London, U. K.)* **2015,** *10,* 465–481. doi:10.2217/nnm.14.185

59. Ashford, M. *Drug Delivery Transl. Res.* **2020,** *10,* 1888–1894. doi:10.1007/s13346-020-00858-6

60. Morgan, P.; Brown, D. G.; Lennard, S.; Anderton, M. J.; Barrett, J. C.; Eriksson, U.; Fidock, M.; Hamrén, B.; Johnson, A.; March, R. E.; Matcham, J.; Mettetal, J.; Nicholls, D. J.; Platz, S.; Rees, S.; Snowden, M. A.; Pangalos, M. N. *Nat. Rev. Drug Discovery* **2018,** *17,* 167–181. doi:10.1038/nrd.2017.244

61. Bern, C.; Adler-Moore, J.; Berenguer, J.; Boelaert, M.; Boer, M. d.; Davidson, R. N.; Figueras, C.; Gradoni, L.; Kafetzis, D. A.; Ritmeijer, K.; Rosenthal, E.; Royce, C.; Russo, R.; Sundar, S.; Alvar, J. *Clin. Infect. Dis.* **2006,** *43,* 917–924. doi:10.1086/507530

62. Thakur, C. P.; Pandey, A. K.; Sinha, G. P.; Roy, S.; Behbehani, K.; Olliaro, P. *Trans. R. Soc. Trop. Med. Hyg.* **1996,** *90,* 319–322. doi:10.1016/s0035-9203(96)90271-0

63. Roberts, C. W.; McLeod, R.; Rice, D. W.; Ginger, M.; Chance, M. L.; Goad, L. J. *Mol. Biochem. Parasitol.* **2003,** *126,* 129–142. doi:10.1016/s0166-6851(02)00280-3

64. Yardley, V.; Croft, S. L. *Am. J. Trop. Med. Hyg.* **1999,** *61,* 193–197. doi:10.4269/ajtmh.1999.61.193

65. Cencig, S.; Coltel, N.; Truyens, C.; Carlier, Y. *PLoS Negl. Trop. Dis.* **2011,** *5,* e1216. doi:10.1371/journal.pntd.0001216

66. Clemons, K. V.; Sobel, R. A.; Martinez, M.; Correa-Oliveira, R.; Stevens, D. A. *Am. J. Trop. Med. Hyg.* **2017,** *97,* 1141–1146. doi:10.4269/ajtmh.16-0975

67. Morilla, M. J.; Montanari, J. A.; Prieto, M. J.; Lopez, M. O.; Petray, P. B.; Romero, E. L. *Int. J. Pharm.* **2004,** *278,* 311–318. doi:10.1016/j.ijpharm.2004.03.025

68. Li, X.; Yi, S.; Scariot, D. B.; Martinez, S. J.; Falk, B. A.; Olson, C. L.; Romano, P. S.; Scott, E. A.; Engman, D. M. *JCI Insight* **2021,** *6,* e145523. doi:10.1172/jci.insight.145523

69. Morilla, M. J.; Montanari, J.; Frank, F.; Malchiodi, E.; Corral, R.; Petray, P.; Romero, E. L. *J. Controlled Release* **2005,** *103,* 599–607. doi:10.1016/j.jconrel.2004.12.012

70. Carneiro, Z. A.; Pedro, P. I.; Sesti-Costa, R.; Lopes, C. D.; Pereira, T. A.; Milanezi, C. M.; da Silva, M. A. P.; Lopez, R. F. V.; Silva, J. S.; Deflon, V. M. *PLoS Negl. Trop. Dis.* **2014,** *8,* e0003524. doi:10.1371/journal.pntd.0002847

71. Branquinho, R. T.; Mosqueira, V. C. F.; de Oliveira-Silva, J. C. V.; Simões-Silva, M. R.; Saúde-Guimarães, D. A.; de Lana, M. *Antimicrob. Agents Chemother.* **2014,** *58,* 2067–2075. doi:10.1128/aac.00617-13

72. de Mello, C. G. C.; Branquinho, R. T.; Oliveira, M. T.; Milagre, M. M.; Saúde-Guimarães, D. A.; Mosqueira, V. C. F.; de Lana, M. *Antimicrob. Agents Chemother.* **2016,** *60,* 5215–5222. doi:10.1128/aac.00178-16

73. Tupinambá Branquinho, R.; Pound-Lana, G.; Marques Milagre, M.; Saúde-Guimarães, D. A.; Vilela, J. M. C.; Spangler Andrade, M.; de Lana, M.; Mosqueira, V. C. F. *Sci. Rep.* **2017,** *7,* 8429. doi:10.1038/s41598-017-08469-x

74. Branquinho, R. T.; Roy, J.; Farah, C.; Garcia, G. M.; Aimond, F.; Le Guennec, J.-Y.; Saude-Guimarães, D. A.; Grabe-Guimaraes, A.; Mosqueira, V. C. F.; de Lana, M.; Richard, S. *Sci. Rep.* **2017,** *7,* 44998. doi:10.1038/srep44998

75. Branquinho, R. T.; De Mello, C. G. C.; Oliveira, M. T.; Soares Reis, L. E.; De Abreu Vieira, P. M.; Saúde-Guimarães, D. A.; Furtado Mosqueira, V. C.; De Lana, M. *Antimicrob. Agents Chemother.* **2020,** *64,* 10.1128/aac.01937-19. doi:10.1128/aac.01937-19

76. Hernández, M.; Wicz, S.; Pérez Caballero, E.; Santamaría, M. H.; Corral, R. S. *Parasitol. Int.* **2021,** *81,* 102248. doi:10.1016/j.parint.2020.102248

77. Sasaki, H.; Sunagawa, Y.; Takahashi, K.; Imaizumi, A.; Fukuda, H.; Hashimoto, T.; Wada, H.; Katanasaka, Y.; Kakeya, H.; Fujita, M.; Hasegawa, K.; Morimoto, T. *Biol. Pharm. Bull.* **2011,** *34,* 660–665. doi:10.1248/bpb.34.660

78. Chung, H.; Yoon, S. H.; Cho, J.-Y.; Yeo, H. K.; Shin, D.; Park, J.-Y. *Int. J. Clin. Pharmacol. Ther.* **2021,** *59,* 684–690. doi:10.5414/cp204058

79. Louise, V.; Machado, B. A. A.; Pontes, W. M.; Menezes, T. P.; Dias, F. C. R.; Ervilhas, L. O. G.; Pinto, K. M. de C.; Talvani, A. *Trop. Med. Infect. Dis.* **2023,** *8,* 343. doi:10.3390/tropicalmed8070343

80. Abriata, J. P.; Eloy, J. O.; Riul, T. B.; Campos, P. M.; Baruffi, M. D.; Marchetti, J. M. *Mater. Sci. Eng., C* **2017,** *77,* 1196–1203. doi:10.1016/j.msec.2017.03.266

81. Germain, M.; Caputo, F.; Metcalfe, S.; Tosi, G.; Spring, K.; Åslund, A. K. O.; Pottier, A.; Schiffelers, R.; Ceccaldi, A.; Schmid, R. *J. Controlled Release* **2020,** *326,* 164–171. doi:10.1016/j.jconrel.2020.07.007

82. Younis, M. A.; Tawfeek, H. M.; Abdellatif, A. A. H.; Abdel-Aleem, J. A.; Harashima, H. *Adv. Drug Delivery Rev.* **2022,** *181,* 114083. doi:10.1016/j.addr.2021.114083

83. Shan, X.; Gong, X.; Li, J.; Wen, J.; Li, Y.; Zhang, Z. *Acta Pharm. Sin. B* **2022,** *12,* 3028–3048. doi:10.1016/j.apsb.2022.02.025

84. Calabretta, E.; Hamadani, M.; Zinzani, P. L.; Caimi, P.; Carlo-Stella, C. *Blood* **2022,** *140,* 303–308. doi:10.1182/blood.2021014663

85. Radadiya, A.; Zhu, W.; Coricello, A.; Alcaro, S.; Richards, N. G. J. *Biochemistry* **2020,** *59,* 3193–3200. doi:10.1021/acs.biochem.0c00354

86. Sofias, A. M.; Dunne, M.; Storm, G.; Allen, C. *Adv. Drug Delivery Rev.* **2017,** *122,* 20–30. doi:10.1016/j.addr.2017.02.003

87. Wang, Y.-X. J. *World J. Gastroenterol.* **2015,** *21,* 13400–13402. doi:10.3748/wjg.v21.i47.13400

88. Fontana, F.; Figueiredo, P.; Zhang, P.; Hirvonen, J. T.; Liu, D.; Santos, H. A. *Adv. Drug Delivery Rev.* **2018,** *131,* 3–21. doi:10.1016/j.addr.2018.05.002

89. Lu, L.; Xu, Q.; Wang, J.; Wu, S.; Luo, Z.; Lu, W. *Pharmaceutics* **2022,** *14,* 797. doi:10.3390/pharmaceutics14040797

90. Operti, M. C.; Bernhardt, A.; Sincari, V.; Jager, E.; Grimm, S.; Engel, A.; Hruby, M.; Figdor, C. G.; Tagit, O. *Pharmaceutics* **2022,** *14,* 276. doi:10.3390/pharmaceutics14020276

91. Giordani, S.; Marassi, V.; Zattoni, A.; Roda, B.; Reschiglian, P. *J. Pharm. Biomed. Anal.* **2023,** *236,* 115751. doi:10.1016/j.jpba.2023.115751

92. Khalil, I. A.; Younis, M. A.; Kimura, S.; Harashima, H. *Biol. Pharm. Bull.* **2020,** *43,* 584–595. doi:10.1248/bpb.b19-00743

93. Hou, X.; Zaks, T.; Langer, R.; Dong, Y. *Nat. Rev. Mater.* **2021,** *6,* 1078–1094. doi:10.1038/s41578-021-00358-0

94. Schoenmaker, L.; Witzigmann, D.; Kulkarni, J. A.; Verbeke, R.; Kersten, G.; Jiskoot, W.; Crommelin, D. J. A. *Int. J. Pharm.* **2021,** *601,* 120586. doi:10.1016/j.ijpharm.2021.120586

95. Gigliobianco, M. R.; Casadidio, C.; Censi, R.; Di Martino, P. *Pharmaceutics* **2018,** *10,* 134. doi:10.3390/pharmaceutics10030134

96. Wong, C. H.; Siah, K. W.; Lo, A. W. *Biostatistics* **2019,** *20,* 273–286. doi:10.1093/biostatistics/kxx069

97. Bhatia, S. N.; Chen, X.; Dobrovolskaia, M. A.; Lammers, T. *Nat. Rev. Cancer* **2022,** *22,* 550–556. doi:10.1038/s41568-022-00496-9

98. Metselaar, J. M.; Middelink, L. M.; Wortel, C. H.; Bos, R.; van Laar, J. M.; Vonkeman, H. E.; Westhovens, R.; Lammers, T.; Yao, S.-L.; Kothekar, M.; Raut, A.; Bijlsma, J. W. J. *J. Controlled Release* **2022,** *341,* 548–554. doi:10.1016/j.jconrel.2021.12.007

99. FDA Approves First COVID-19 Vaccine. FDA https://www.fda.gov/news-events/press-announcements/fda-approves-first-covid-19-vaccine (accessed Nov 16, 2023).

100. Coronavirus (COVID-19) Update: FDA Takes Key Action by Approving Second COVID-19 Vaccine. FDA https://www.fda.gov/news-events/press-announcements/coronavirus-covid-19-update-fda-takes-key-action-approving-second-covid-19-vaccine (accessed Nov 16, 2023).

101. FDA approves first-of-its kind targeted RNA-based therapy to treat a rare disease. FDA https://www.fda.gov/news-events/press-announcements/fda-approves-first-its-kind-targeted-rna-based-therapy-treat-rare-disease (accessed Nov 16, 2023).

102. Hajiaghapour Asr, M.; Dayani, F.; Saedi Segherloo, F.; Kamedi, A.; Neill, A. O.; MacLoughlin, R.; Doroudian, M. *Pharmaceutics* **2023,** *15,* 1127. doi:10.3390/pharmaceutics15041127

103. Nadeem, A. Y.; Shehzad, A.; Islam, S. U.; Al-Suhaimi, E. A.; Lee, Y. S. *Vaccines (Basel, Switz.)* **2022,** *10,* 713. doi:10.3390/vaccines10050713

104. Didierlaurent, A. M.; Laupèze, B.; Di Pasquale, A.; Hergli, N.; Collignon, C.; Garçon, N. *Expert Rev. Vaccines* **2017,** *16,* 55–63. doi:10.1080/14760584.2016.1213632

105. Nanomedicine Market Size, Share, Growth Report 2023 to 2028. https://www.marketdataforecast.com/market-reports/nanomedicine-market (accessed Nov 16, 2023).

106. Adler-Moore, J. *Bone Marrow Transplant.* **1994,** *14* (Suppl. 5), S3–S7.

107. Anselmo, A. C.; Mitragotri, S. *Bioeng. Transl. Med.* **2019,** *4,* e10143. doi:10.1002/btm2.10143

108. Kotani, T.; Takeuchi, T.; Makino, S.; Hata, K.; Yoshida, S.; Nagai, K.; Wakura, D.; Isoda, K.; Hanafusa, T. *J. Infect. Chemother.* **2013,** *19,* 691–697. doi:10.1007/s10156-012-0545-x

109. Scannell, J. W.; Blanckley, A.; Boldon, H.; Warrington, B. *Nat. Rev. Drug Discovery* **2012,** *11,* 191–200. doi:10.1038/nrd3681

110. Đorđević, S.; Gonzalez, M. M.; Conejos-Sánchez, I.; Carreira, B.; Pozzi, S.; Acúrcio, R. C.; Satchi-Fainaro, R.; Florindo, H. F.; Vicent, M. J. *Drug Delivery Transl. Res.* **2022,** *12,* 500–525. doi:10.1007/s13346-021-01024-2

111. Gaspar, R. S.; Silva-Lima, B.; Magro, F.; Alcobia, A.; da Costa, F. L.; Feio, J. *Front. Med.* **2020,** *7,* 590527. doi:10.3389/fmed.2020.590527

112. Eaton, M. A. W.; Levy, L.; Fontaine, O. M. A. *Nanomedicine (N. Y., NY, U. S.)* **2015,** *11,* 983–992. doi:10.1016/j.nano.2015.02.004

113. Feng, S.-S.; Mu, L.; Win, K.; Huang, G. *Curr. Med. Chem.* **2004,** *11,* 413–424. doi:10.2174/0929867043455909

114. Muthu, M. S.; Wilson, B. *Nanomedicine (London, U. K.)* **2012,** *7,* 307–309. doi:10.2217/nnm.12.3

115. Paliwal, R.; Babu, R. J.; Palakurthi, S. *AAPS PharmSciTech* **2014,** *15,* 1527–1534. doi:10.1208/s12249-014-0177-9

116. Atia, N. N.; Tawfeek, H. M.; Rageh, A. H.; El-Zahry, M. R.; Abdelfattah, A.; Younis, M. A. *Saudi Pharm. J.* **2019,** *27,* 540–549. doi:10.1016/j.jsps.2019.02.001

117. Dormont, F.; Rouquette, M.; Mahatsekake, C.; Gobeaux, F.; Peramo, A.; Brusini, R.; Calet, S.; Testard, F.; Lepetre-Mouelhi, S.; Desmaële, D.; Varna, M.; Couvreur, P. *J. Controlled Release* **2019,** *307,* 302–314. doi:10.1016/j.jconrel.2019.06.040

118. Zamboni, W. C.; Torchilin, V.; Patri, A. K.; Hrkach, J.; Stern, S.; Lee, R.; Nel, A.; Panaro, N. J.; Grodzinski, P. *Clin. Cancer Res.* **2012,** *18,* 3229–3241. doi:10.1158/1078-0432.ccr-11-2938

119. Doane, T. L.; Burda, C. *Chem. Soc. Rev.* **2012,** *41,* 2885–2911. doi:10.1039/c2cs15260f

120. Wicki, A.; Witzigmann, D.; Balasubramanian, V.; Huwyler, J. *J. Controlled Release* **2015,** *200,* 138–157. doi:10.1016/j.jconrel.2014.12.030

121. Wu, L.-P.; Wang, D.; Li, Z. *Mater. Sci. Eng., C* **2020,** *106,* 110302. doi:10.1016/j.msec.2019.110302

122. Bedőcs, P.; Szebeni, J. *Front. Immunol.* **2020,** *11,* 584966. doi:10.3389/fimmu.2020.584966

123. Desai, N. *AAPS J.* **2012,** *14,* 282–295. doi:10.1208/s12248-012-9339-4

124. Hua, S.; de Matos, M. B. C.; Metselaar, J. M.; Storm, G. *Front. Pharmacol.* **2018,** *9,* 10.3389/fphar.2018.00790. doi:10.3389/fphar.2018.00790

125. Mühlebach, S. *Adv. Drug Delivery Rev.* **2018,** *131,* 122–131. doi:10.1016/j.addr.2018.06.024

126. Soares, S.; Sousa, J.; Pais, A.; Vitorino, C. *Front. Chem. (Lausanne, Switz.)* **2018,** *6,* 10.3389/fchem.2018.00360. doi:10.3389/fchem.2018.00360

127. Foulkes, R.; Man, E.; Thind, J.; Yeung, S.; Joy, A.; Hoskins, C. *Biomater. Sci.* **2020,** *8,* 4653–4664. doi:10.1039/d0bm00558d

128. Resnik, D. B.; Tinkle, S. S. *Nanomedicine (London, U. K.)* **2007,** *2,* 345–350. doi:10.2217/17435889.2.3.345

129. Allen, T. M.; Cullis, P. R. *Adv. Drug Delivery Rev.* **2013,** *65,* 36–48. doi:10.1016/j.addr.2012.09.037

130. Bosetti, R.; Jones, S. L. *Nanomedicine (London, U. K.)* **2019,** *14,* 1367–1370. doi:10.2217/nnm-2019-0130

131. Mueller-Langer, F. *Health Econ., Policy Law* **2013,** *8,* 185–208. doi:10.1017/s1744133112000321

132. Lu, Y.; Qi, J.; Dong, X.; Zhao, W.; Wu, W. *Drug Discovery Today* **2017,** *22,* 744–750. doi:10.1016/j.drudis.2017.01.003

133. Jarvis, M.; Krishnan, V.; Mitragotri, S. *Bioeng. Transl. Med.* **2019,** *4,* 5–16. doi:10.1002/btm2.10122

134. Akhtar, A. *Cambridge Q. Healthcare Ethics* **2015,** *24,* 407–419. doi:10.1017/s0963180115000079

135. Chatelain, E.; Konar, N. *Drug Des., Dev. Ther.* **2015,** *9,* 4807. doi:10.2147/dddt.s90208

136. Chatelain, E.; Scandale, I. *Expert Opin. Drug Discovery* **2020,** *15,* 1381–1402. doi:10.1080/17460441.2020.1806233

137. Burgdorf, T.; Piersma, A. H.; Landsiedel, R.; Clewell, R.; Kleinstreuer, N.; Oelgeschläger, M.; Desprez, B.; Kienhuis, A.; Bos, P.; de Vries, R.; de Wit, L.; Seidle, T.; Scheel, J.; Schönfelder, G.; van Benthem, J.; Vinggaard, A. M.; Eskes, C.; Ezendam, J. *Toxicol. In Vitro* **2019,** *59,* 1–11. doi:10.1016/j.tiv.2019.03.039

138. Zuppinger, C. *Front. Cardiovasc. Med.* **2019,** *6,* 10.3389/fcvm.2019.00087. doi:10.3389/fcvm.2019.00087

139. Limongi, T.; Guzzi, F.; Parrotta, E.; Candeloro, P.; Scalise, S.; Lucchino, V.; Gentile, F.; Tirinato, L.; Coluccio, M. L.; Torre, B.; Allione, M.; Marini, M.; Susa, F.; Di Fabrizio, E.; Cuda, G.; Perozziello, G. *Cells* **2022,** *11,* 1699. doi:10.3390/cells11101699

140. Sun, D.; Zhou, S.; Gao, W. *ACS Nano* **2020,** *14,* 12281–12290. doi:10.1021/acsnano.9b09713

141. Hare, J. I.; Lammers, T.; Ashford, M. B.; Puri, S.; Storm, G.; Barry, S. T. *Adv. Drug Delivery Rev.* **2017,** *108,* 25–38. doi:10.1016/j.addr.2016.04.025

142. Martín-Escolano, J.; Marín, C.; Rosales, M. J.; Tsaousis, A. D.; Medina-Carmona, E.; Martín-Escolano, R. *ACS Infect. Dis.* **2022,** *8,* 1107–1115. doi:10.1021/acsinfecdis.2c00123

143. Hwang, T. J.; Carpenter, D.; Lauffenburger, J. C.; Wang, B.; Franklin, J. M.; Kesselheim, A. S. *JAMA Intern. Med.* **2016,** *176,* 1826–1833. doi:10.1001/jamainternmed.2016.6008

144. Prasad, V.; Mailankody, S. *JAMA Intern. Med.* **2017,** *177,* 1569–1575. doi:10.1001/jamainternmed.2017.3601

145. Roope, L. S. J. *J. Controlled Release* **2022,** *345,* 275–277. doi:10.1016/j.jconrel.2022.03.023

146. Parra, F. L.; Frank, F. M.; Alliani, B. F.; Romero, E. L.; Petray, P. B. *Colloids Surf., B* **2020,** *189,* 110850. doi:10.1016/j.colsurfb.2020.110850

147. Neglected tropical diseases. https://www.who.int/news-room/questions-and-answers/item/neglected-tropical-diseases (accessed Nov 16, 2023).

Green synthesis of silver nanoparticles derived from algae and their larvicidal properties to control *Aedes aegypti*

Matheus Alves Siqueira de Assunção[1], Douglas Dourado[1],
Daiane Rodrigues dos Santos[1], Gabriel Bezerra Faierstein[1], Mara Elga Medeiros Braga[2],
Severino Alves Junior[3], Rosângela Maria Rodrigues Barbosa[1],
Herminio José Cipriano de Sousa[2] and Fábio Rocha Formiga[*1,4]

Review

Address:
[1]Aggeu Magalhães Institute (IAM), Oswaldo Cruz Foundation (FIOCRUZ), 50670-420, Recife, PE, Brazil, [2]Chemical Process Engineering and Forest Products Research Centre (CIEPQPF), Department of Chemical Engineering, University of Coimbra, 3030-790, Coimbra, Portugal, [3]Department of Fundamental Chemistry (DQF), Federal University of Pernambuco (UFPE), 50740-560, Recife, PE, Brazil and [4]Faculty of Medical Sciences, University of Pernambuco (UPE), 52171-011, Recife, PE, Brazil

Email:
Fábio Rocha Formiga[*] - fabio.formiga@fiocruz.br

* Corresponding author

Abstract

Mosquito vectors such as *Aedes spp.* are responsible for the transmission of arboviruses that have a major impact on public health. Therefore, it is necessary to search for ways to control these insects, avoiding the use of conventional chemical insecticides that are proven to be toxic to nature. In the last years, there has been growing evidence for the potential of silver nanoparticles (AgNPs) to be ecologically benign alternatives to the commercially available chemical insecticides against vector-borne diseases. Natural seaweed extracts contain metabolites such as polyphenols, terpenoids, and alkaloids. These compounds act as reducing agents and stabilizers to synthesize biogenic AgNPs. The green synthesis of AgNPs has advantages over other methods, such as low cost and sustainable biosynthesis. In the perspective of using AgNPs in the development of novel insecticides for vector control, this review deals with the eco-friendly synthesis of AgNPs through seaweed extracts as reducing and stabilizing agents. In addition, assessment of toxicity of these nanomaterials in non-target species is discussed.

Introduction

Arboviroses are diseases caused by the pathogens transmitted by arthropods, and their transmission to humans occurs through the bite of hematophagous arthropods. Mosquitoes are the most important vectors of arboviroses [1], although many are maintained by ticks [2], phlebotomines [3], and other arthropods [4]. Arboviroses represent a major public health concern in tropical and sub-tropical regions of the world [5]. *Aedes aegypti* (Stegomyia) Linnaeus (1762) (Diptera: Culicidae), known as the dengue mosquito, is a vector of important arboviroses, including Dengue, Zika, Chikungunya, and Yellow Fever [6].

Since there are no specific antiviral treatments for arboviruses and the endemicity of these diseases is determined by the presence of the vector, approaches for the control of arthropod-borne diseases involve strategies focused on the vector. These may include the application of synthetic insecticides or the implementation of treatments targeted at patients [7,8]. An emerging strategy for controlling arboviral vectors are nanomaterials or nanomaterial-based formulations as so-called nanopesticides, providing new, modern, and low-cost formulations [9,10] with the ability to penetrate through the exoskeleton into mosquito cells, causing mortality after binding to proteins or DNA [11]. Nanomaterials provide characteristics such as greater absorption capacity, greater bioavailability, controlled release of active ingredients, improved solubility of hydrophobic substances in water, and good kinetic stability [12-14].

Metallic nanoparticles have been investigated as a promising approach for vector control. The chemical reduction of metal ions through biological compounds can be used to synthesize non-toxic and environmentally safe "green" insecticide alternatives in the form of metal-based nanoparticles [15]. A promising option are silver nanoparticles (AgNPs) obtained through synthesis from natural extracts containing secondary metabolites that act as reducing and stabilizing agents. Among these metabolites, alkanes, aromatics, phenols, ethers, amines, and amides stand out for their role in the reduction, stabilization, and capping of silver nanoparticles [11,16-19]. Compounds of natural origin are generally preferred in vector control because of a less deleterious effect on non-target organisms and their inherent biodegradability. The development of sustainable pest control tools is a challenge for researchers and public health authorities [20]. Seaweed extracts are composed of bioactive agents such as phenols, ascorbic acid, flavonoids, polyphenolics, alkaloids, and terpenes, which could act as reducing agents [21].

This review focuses on AgNPs produced in a green and sustainable way through the use of natural products as reducing agents, namely seaweed extracts. The activity of AgNPs upon *A. aegypti* and their potential role for the control and prevention of arboviruses are presented. Finally, ecotoxicity and environmental risk assessment of AgNPs are further discussed.

Review
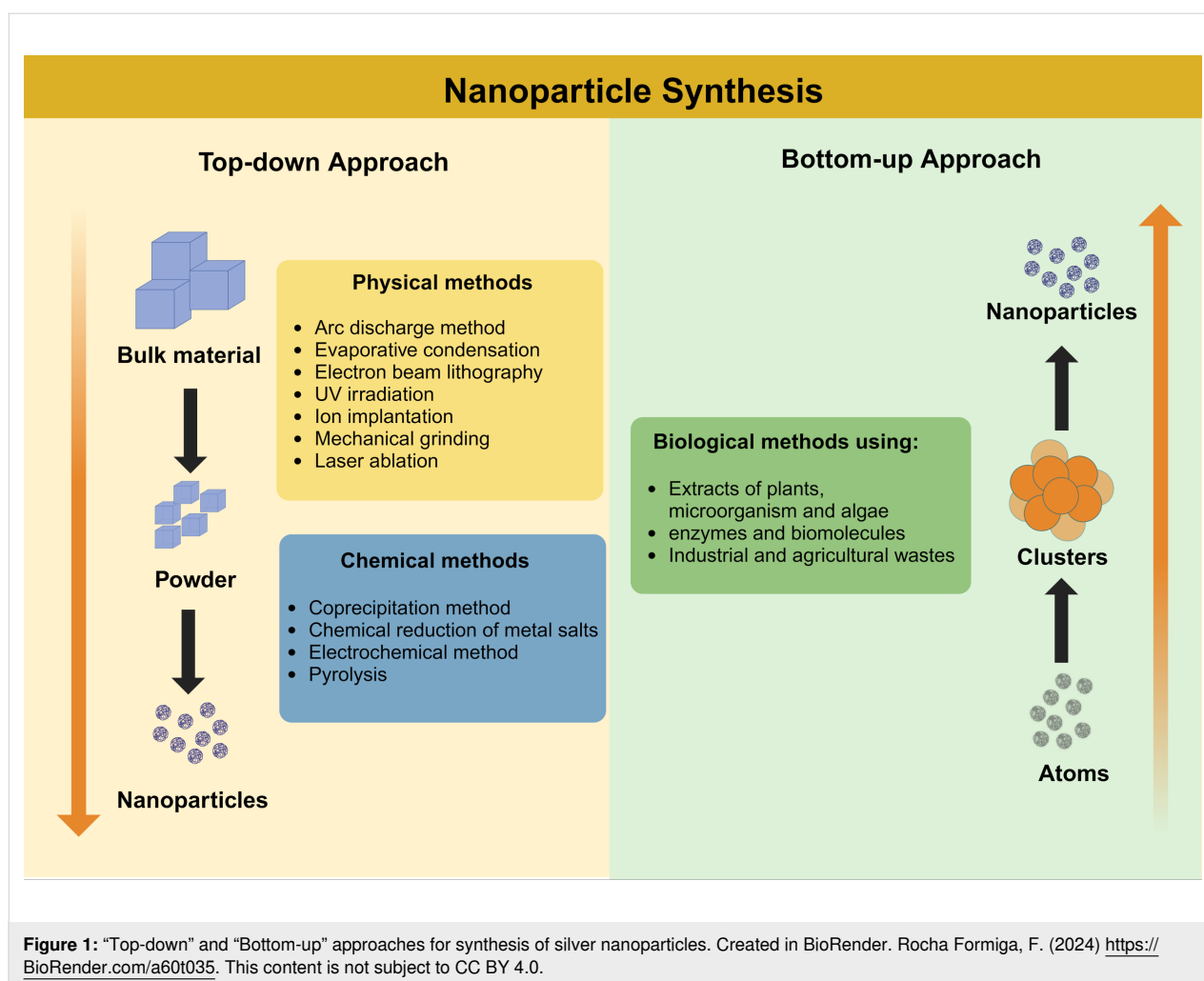### Synthesis of silver nanoparticles

AgNPs are metallic nanoparticles in a size range between 1 and 100 nm with unique electrical, optical, and magnetic properties for a wide range of applications [22,23]. They can be synthesized by different procedures based on "top-down" or "bottom-up" approaches [24] (Figure 1). Top-down synthesized silver nanoparticles can be obtained by lithography, attrition, milling, and other processes that involve reducing the size of bulk silver materials to the atomic size of the AgNPs [25]. Bottom-up AgNPs are synthesized via precursor salt reactions that lead to the formation of AgNPs [26] including condensation, precipitation, and pyrolysis [27].

AgNPs can be synthesized using physical, chemical, or biological methods [28]. Chemical AgNPs synthesis can require toxic substances such as polyvinylpyrrolidone, polyvinyl alcohol, and polyacrylonitrile as stabilizing agents and sodium borohydride, hydrazine, and hydroxylamine as reducing agents [29]. These may generate more toxic chemical residues in the environment [30]. Physical methods include laser ablation, UV irradiation, evaporation condensation, aerosol methods, and lithography. High cost, high energy consumption, and expensive equipment make these techniques uneconomical [31].

Because of these disadvantages, synthesis methods based on naturally occurring biomaterials have been used as an alternative to obtain metallic nanoparticles [32,33]. These do not involve any toxic chemicals and require less energy and synthesis time. Simple protocols have been used involving the reduction of metal ions using biological extracts as reducing agent [34]. In this way, the green synthesis of nanoparticles has expanded in nanoscience and nanotechnology [35].

Synthesis of silver nanoparticles using algae

Green nanoparticle synthesis is the design and development of strategies for the production of nanoparticles to reduce the use or formation of substances harmful to human health and the environment [36,37]. It has many advantages compared to chemical and physical methods, that is, it is non-toxic, pollution-free, ecological and economical, and more sustainable [38,39]. There is a variety of natural resources for the green synthesis of silver nanoparticles (yeasts, plants, fungi, algae, and bacteria), which are capable of reducing inorganic metal ions to metallic nanoparticles quickly [40,41]. Among these, algae have been highlighted because of their immense bioac-

Figure 1: "Top-down" and "Bottom-up" approaches for synthesis of silver nanoparticles. Created in BioRender. Rocha Formiga, F. (2024) https://BioRender.com/a60t035. This content is not subject to CC BY 4.0.

tive potential of compounds such as accessory pigments, proteins, sulfated polysaccharides and other biomolecules. The latter include flavonoids, alkaloids, steroids, phenols, and saponins with hydroxy, carboxyl, and amino functional groups, which are effective agents in metal reduction and also provide a robust coating on the metallic nanoparticles in a single step [42-46].

These bioactive compounds associated with metallic nanoparticles increase the specific delivery of drugs to the target and, thus, reduce the required amount of active compounds [47]. In addition, the control of particle size and morphology is essential for applications in biotechnology, and the biological approach has the ability to better control the particle size than chemical and physical synthesis methods of metallic NPs [48,49]. Thus, different species of algae have been used in the green synthesis of silver nanoparticles. In this review, species of brown algae (*Sargassum polycystum*, *Sargassum natans*, *Padina gymnospora*), red algae (*Hypnea musciformis*, *Centroceras clavulatum*, *Amphiroa rígida*, *Gracilaria firma*),

blue algae (*Oscillatoria sancta*), and green algae (*Ulva lactuta*) are reported as biomass for the green synthesis of AgNPs (Table 1).

Murugan and collaborators, in their study on the development of silver nanoparticles from aqueous extracts of *C. clavulatum* leaves, assessed that silver ions were reduced to form AgNPs. They indicated that the functional groups potentially involved in the reduction of silver ions were the amide and carbonyl groups of terpenoids and flavonoids [50].

Vinoth and colleagues also prepared AgNPs using brown seaweed, that is, the seaweed *S. polycystum* [51]. Initially, the authors prepared an aqueous extract (50 g of seaweed/500 mL H_2O) via boiling for 30 min followed by cooling and filtration. The NPs were prepared from 10 mL of the aqueous extract filtrate with 90 mL of $AgNO_3$ (1 mM). To increase the yield of silver nanoparticles, the sample was placed under magnetic stirring varying the heating temperatures (37–80 °C). The formation of NPs was verified from the color change in the solution to

Table 1: Data from studies on the green synthesis of silver nanoparticles.

Algae extract	Synthesis conditions	Particle characteristics	Reference
aqueous extract of *Sargassum polycystum*	AgNO$_3$ concentration – 1 mM reaction period – 3 h reaction temperature – 37–80 °C	SPR[a] – 418 nm size – 20–88 nm shape – cubical	[51]
ethanol extract of *Hypnea musciformis*	AgNO$_3$ concentration – 1 mM reaction period – 120 min reaction temperature – room temperature	SPR[a] – 420 nm size – 40–65 nm shape – spherical	[52]
ethyl alcohol extract of *Sargassum natans*	AgNO$_3$ concentration – 100 mM reaction period – 24 h reaction temperature – room temperature	SPR[a] – 340 nm size – 50 nm shape – ND[b]	[53]
aqueous extract of *Centroceras clavulatum*	AgNO$_3$ concentration – 1 mM reaction period – ND[b] reaction temperature – room temperature	SPR[a] – 410 nm size – 35–65 nm shape – spherical and cubic	[50]
aqueous extract of *Amphiroa rigida*	AgNO$_3$ concentration – 1 mM reaction period – 30 min reaction temperature – 37 °C	SPR[a] – 420 nm size – 20–30 nm shape – spherical	[54]
aqueous extract of *Oscillatoria sancta*	AgNO$_3$ concentration – 1 mM reaction period – 60 min reaction temperature – 28 °C	SPR[a] – 450 nm size – 25–50 nm shape – cubical and hexagonal	[55]
aqueous extract of *Gracilaria firma*	AgNO$_3$ concentration – 1 mM reaction period – ND[b] reaction temperature – room temperature	SPR[a] – 440 nm size – 12–200 nm shape – spherical	[32]
aqueous extract of *Ulva lactuca*	AgNO$_3$ concentration – 1 mM reaction period – ND[b] reaction temperature – ND[b]	SPR[a] – 453 nm size – 20–50 nm shape – ND[b]	[56]

[a]SPR: surface plasmon resonance; [b]ND: not defined.

reddish brown. The possible chemical compounds evaluated as potential reducing agents in the biosynthesis of AgNPs were the secondary amines, aromatic primary amines, carboxylates, amides, alkenes, and aromatic compounds.

Roni and collaborators prepared AgNPs from red algae [52]. An aqueous extract of *H. musciformis* was obtained (10 g of seaweed leaves/100 mL of purified water) by heating the mixture for 5 min and decanting for 1 h. After this process, the mixture was filtered and stored for 5 days at 15 °C. Finally, the filtered solution was treated with an aqueous solution of AgNO$_3$ (1 mM) and incubated at room temperature. The chemical compounds found were amino acid residues, aromatic rings, geminal methyls, ether linkages, flavones, terpenoids, aliphatic amines, and alcohols/phenols.

AgNPs were synthesized from an extract of the brown alga *S. natans* [53]. The extract was obtained via hot Soxhlet extraction of crushed leaves (40 °C) using ethanol, concentrated in a rotary vacuum evaporator, and finally stored at refrigerator temperature. A hydroalcoholic extract was produced by adding 1 mL of *S. natans* extract to 99 mL of purified water and 0.5 mL of Triton®. This extract was treated with AgNO$_3$ (100 mM; 99:1) and conditioned at room temperature until the color changed to brown, indicative of the formation of AgNPs.

Chemical analysis of the AgNPs demonstrated the presence of alcoholic compounds, phenolic compounds, aliphatic compounds, and carbonyl groups.

Green algae were also used to obtain AgNPs. Aziz et al., synthesized AgNPs from *U. lactuca* extract [56]. Initially, 10 g of the extract powder was extracted using a Soxhlet extractor (ethanol, 78 °C for 8 h) and concentrated in a rotary vacuum evaporator (40 °C). 100 mL of the extract was treated with AgNO$_3$ solution (1 mM), showing the formation of NPs by the yellowish color. The authors did not report on the proportion volume ratio between extract and AgNO$_3$ solution, nor the used part of the alga under study.

The red seaweed *G. firma* was used for the green synthesis of AgNPs [32]. The extract was prepared from ground seaweed. 10 g of the powder was added to purified water (100 mL) under boiling for 5 min. The filtrate was treated with aqueous AgNO$_3$ solution (1 mM; the ratio of aqueous solution to AgNO$_3$ solution was not mentioned) and incubated at room temperature. Finally, a yellowish-brown solution was observed, indicating the formation of AgNPs. Chemical analysis of the AgNPs demonstrated the presence of carbonyl groups from polyphenols such as catechin gallate, epicatechin gallate, epigallocatechin, epigallocatechin gallate, gallocatechin gallate, and flavin,

amide groups, ethylene systems, and aliphatic amines/alcohols/phenols (polyphenols).

Gopu et al. also synthesized AgNPs from red algae [54]. *A. rigida* seaweed extract was prepared by adding pulverized seaweed (10 g) to 500 mL of purified water. The mixture was heated to a temperature of 80 °C under magnetic stirring for 20 min. Finally, the extract was filtered and centrifuged (12298*g* for 10 min). The NPs were obtained by mixing 10 mL of the extract supernatant with 90 mL of AgNO₃ solution (1 mM) at a temperature of 37 °C, until a color change from colorless to reddish brown was observed. The chemical analysis of AgNPs demonstrated the presence of phenolic compounds, ether groups, and polysaccharides.

Also, blue algae were used to obtain silver nanoparticles. Elumalai et al. synthesized AgNPs from the aqueous extract of *O. sancta* [55]. A mixture of crushed seaweed (8 g) with purified water (100 mL) was heated to 60 °C for 20 min. The mixture was filtered to obtain the final extract, which was treated with AgNO₃ (1 mM; 15:85 ratio) and incubated at 28 °C for 60 min.

Composition of algae species, metal concentration, agitation, reaction time and temperature can impact the characteristics of AgNPs [57]. Thus, such systems must be well characterized, as

discussed in the next section. Different chemical compounds are involved in the reduction of AgNO₃ and the stabilization of AgNPs. Chemical analysis of AgNPs demonstrated the presence of alcohols, phenols, alkynes, aromatic compounds, long-chain fatty acids, secondary amides, and terpenoids. The predominance of phenolic compounds was evident in all species. These compounds act by reducing Ag^+ ions to Ag^0 and stabilize nanoparticles by capping [58] (Figure 2).

Larvicidal activity of AgNPs against *Aedes aegypti*

Aedes aegypti, also known as the dengue mosquito, is a vector of important arboviruses, including Dengue, Zika, Chikungunya and Yellow Fever [6,59]. Among them, dengue fever is highlighted as this disease is endemic in more than 100 countries, proving to be an important public health problem. Its incidence has grown dramatically worldwide in recent decades, with cases reported to the WHO rising from 505,430 in 2000 to 5.2 million in 2019 [60]. Additionally, it is predicted that about 60 percent of the global population will be at risk of dengue in 2080 [61].

Therefore, it is imperative to developed more advanced and efficient strategies for the control of mosquitoes and mosquito-borne diseases. Increased attention has been placed on using nanoparticles in controlling vector mosquitoes [62]. AgNPs
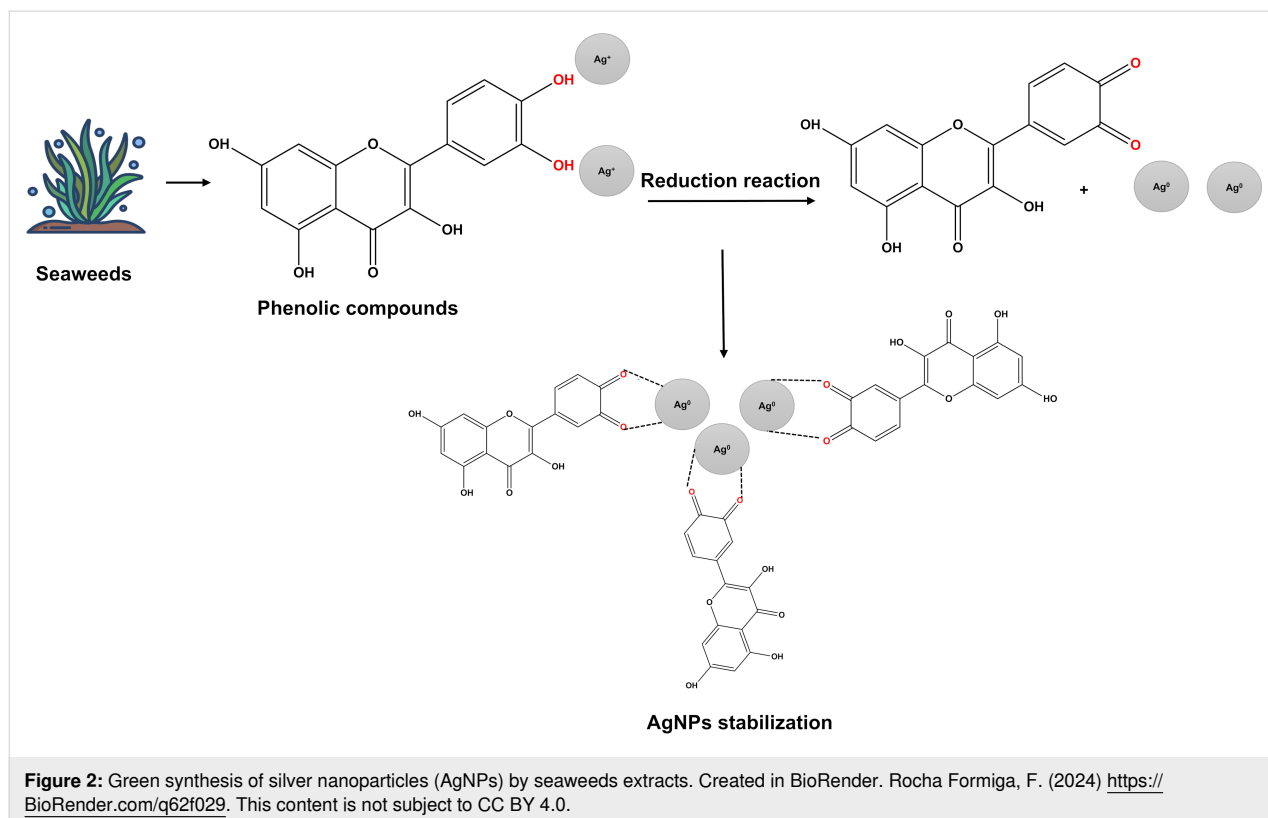

Figure 2: Green synthesis of silver nanoparticles (AgNPs) by seaweeds extracts. Created in BioRender. Rocha Formiga, F. (2024) https://BioRender.com/q62f029. This content is not subject to CC BY 4.0.

Table 2: Larvicidal activity of silver nanoparticles synthesized from seaweed against *Aedes aegypti*.

Algae	Exposure period (h)	Larval stage	LC$_{50}$[a] (μg/mL)	LC$_{90}$[b] (μg/mL)	References
Sargassum polycystum	24	L4	0.30	85.81	[51]
	48		0.06	12.74	
	72		0.03	1.98	
Hypnea musciformis	24	L1–L3	ND[c]	ND[c]	[52]
Sargassum natans	ND[c]	L4	16.47	310.76	[53]
Centroceras clavulatum	ND[c]	L1–L4	21.460, 29.155	46.103–58.39	[50]
Amphiroa rigida	24	L3–L4	ND[c]	ND[c]	[54]
Oscillatoria sancta	24	L4	3.98	8.90	[55]
Gracilaria firma	24	ND[c]	ND[c]	ND[c]	[32]
	48				
	72				
Ulva lactura	ND[c]	L4	80.51	226.9	[56]

[a]Lethal concentration responsible for the mortality of 50% of individuals; [b]lethal concentration responsible for the mortality of 90%; [c]not defined.

synthesized from seaweed have been investigated as a vector control strategy based on their larvicidal properties. Table 2 summarizes data from bioassays with AgNPs synthesized from different species of seaweed against *A. aegypti* larvae. The mechanism of toxicity of AgNPs in mosquito larvae has recently been reported (Figure 3).

The small size of AgNPs is linked to two pathways of action. First, AgNPs can pass through the insect cuticle and penetrate individual cells. The second way is the ingestion of AgNPs by larvae through their generalist eating habits. For both pathways, damage to the midgut, epithelial cells, and cortex in mosquito larvae can be observed, resulting in physiological changes such
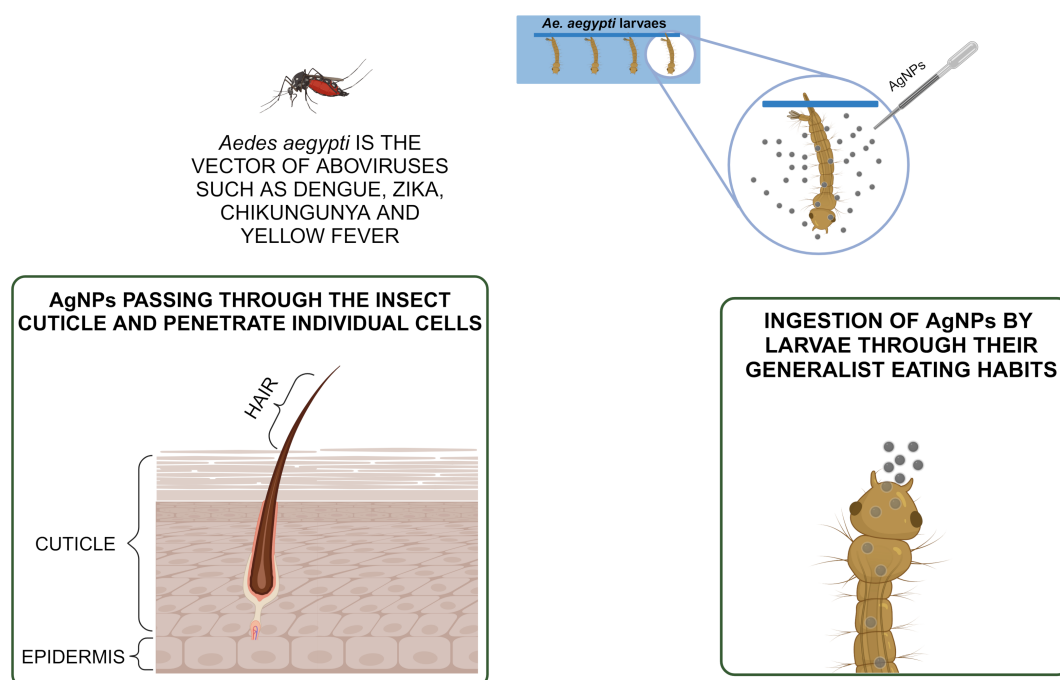

Figure 3: Potential of silver nanoparticles to be used in vector control against *Aedes aegypti*, according to [63]. Created in BioRender. Rocha Formiga, F. (2024) https://BioRender.com/y89s911. This content is not subject to CC BY 4.0.

as shrinkage in the abdominal region, change in the shape of the thorax and loss of lateral hairs, oral brushes, and anal gills. These processes lead to oxidation and degradation of enzymes and organelles in the intracellular space of cells, affecting cellular physiological processes, leading to large-scale apoptosis and, consequently, larval death.

Vinoth, et al. [51] evaluated the larvicidal activity of AgNPs from *S. polycystum* seaweed extract against *A. aegypti* larvae. The L4 larvae were treated with 1 mL of NPs in 249 mL of distilled water. An increasing mortality was observed after periods of 24, 48, and 72 h, yielding the lowest LC_{50} value after a period of 72 h (Table 2). The response of the free extract against the larvae was not evaluated by the authors.

Similar results were observed in AgNPs developed by Roni and collaborators [52]. The authors evaluated the larvicidal activity after 24 h of exposure (25 larvae per 250 mL water) at different larval stages (L1–L4) of both the extract of *H. musciformis* (100–500 μg/mL) and the synthesized nanoparticles (10–50 μg/mL). The extract presented LC_{50} values ten times higher than the LC_{50} of NPs under the same conditions, showing the enhancement of larvicidal activity.

Another study presented data that corroborates the increase in larvicidal activity in AgNPs compared to the algae used for its synthesis. In this investigation, larvae (L4) were treated with the extract of the seaweed of *S. natans* (100–900 μg/mL) and with the synthesized NPs (100–300 μg/mL) [53]. The seaweed extract of *S. natans* showed an LC_{50} value of 299 μg/mL, while the derived AgNPs showed an LC_{50} value of 167 μg/mL. It is noteworthy that the treatment exposure time was not described by the authors.

Murugan et al. [50] were also able to obtain AgNPs with larvicidal activity derived from algae. The authors evaluated the larvicidal activity of seaweed extract of *C. clavulatums* (100–500 μg/mL) and the corresponding NPs (10–50 μg/mL) against *A. aegypti* larvae (L1–L4). The aqueous seaweed extract showed LC_{50} values of 269 μg/mL (L1), 310 μg/mL (L2), 348 μg/mL (L3), and 388 μg/mL (L4), while *C. clavulatum*-synthesized AgNPs were highly toxic against *A. aegypti,* revealing LC_{50} values of 21 μg/mL (L1), 24 μg/mL (L2), 26 μg/mL (L3), and 29 μg/mL (4). The treatment exposure time was not described by the authors.

Gopu, et al. synthesized and investigated the larvicidal potential of AgNPs from the seaweed extract *Amphiroa rigida* [54]. *Aedes aegypti* larvae at stages L3 and L4 were treated with *A. rigida* AgNPs (5–80 μg/mL). After 24 h of exposure, mortality of the larvae was observed above concentrations of

20 μg/mL (L3) and 40 μg/mL (L4). In this study, the LC_{50} values were not calculated; however, according to the mortality values presented, the LC_{50} values are in the range of 5–10 μg/mL for both larval stages. Furthermore, only the NPs were evaluated, and there is no mention of the larvicidal activity of the algae extract under study.

Elumai and colleagues evaluated the larvicidal activity of AgNPs derived from *Oscillatoria sancta* against larvae of *A. aegypti* [55]. Larvae in stages L3 and L4 were treated with the aqueous extract of the seaweed *Oscillatoria sancta* (10–100 μg/mL) and with AgNPs derived from *Oscillatoria sancta* (2–10 μg/mL); 24 h after treatment, the mortality of the larvae was evaluated. The NPs had a higher larvicidal activity than the seaweed aqueous extract, as also observed in other studies.

An increase in larvicidal activity was also observed in studies by Aziz [56]. An aqueous extract of the seaweed (100–900 μg/mL) and AgNPs (50–250 μg/mL) were applied to larvae in stage L4. The aqueous extract revealed LC_{50} values two times higher than those of NPs, demonstrating the enhancement of larvicidal activity. The authors did not highlight the period of time after which mortality was evaluated.

The formation of AgNPs after mixing the extracts with silver nitrate can be due to the synergy of biomolecules with reducing activity present in the extracts binding to the surface of the particles [64]. Despite the evident higher larvicidal activity of silver nanoparticles compared to algae extracts, there are significant variations in the results that must be considered. Larvicidal studies require standardization. Factors such as water volume, number of larvae, exposure time, larval stage, and mention of the presence or absence of larvae feeding must be established for better reliability of larvicidal studies. Furthermore, although the studies included did not carry out toxicity studies on non-target species, it is important to highlight the need for studies such as phytotoxicity, in vitro studies in cells, and in vivo models such as *Danio rerio* (zebrafish).

Conclusion

Nanotechnology has great potential in current medicinal and agricultural systems, where pests and disease vectors are controlled by chemical pesticides that are toxic to non-target species and harmful to soil fertility and ecosystems. The biofabrication of metallic nanoparticles using marine resources has gained an exponential increase in attention over recent years. It is a promising area in nanoscience and nanotechnology that uses eco-friendly "green" methods. Silver nanoparticles (AgNPs) are known to have the benefits of being economical, energy efficient, and environmentally friendly.

The use of AgNPs synthesized from extracts of seaweed species against *Aedes aegypti* may be a viable option for replacing commercially available synthetic chemical insecticides, being able to surpass them in terms of larvicidal activity with lower toxicity to non-target organisms. Among the biogenic compounds of natural origin for green synthesis are flavonoids, tannins, terpenoids, saponins, phenols, and their derivatives. These compounds are responsible for the reduction and stabilization of silver nanoparticles.

The present review suggests that the green synthesis of nanomaterials from seaweed extracts is an environmentally friendly option for the control and prevention of vector-borne diseases. These nanomaterials are potential candidates for replacing commercially available toxic chemicals. Despite the proven formation of silver nanoparticles via green synthesis and their larvicidal activity against *A. aegypti*, some challenges still persist. Aspects such as the mechanism of action of AgNPs in the different stages of *A. aegypti*, resistance of mosquitoes to larvicides, and the long-term effects of NPs on non-target organisms still need to be elucidated to obtain a better understanding of their efficacy and safety.

Funding

Acknowledgements

Conflict of Interest

The authors declare that they have no known competing financial interests or personal relationships that could have appeared to influence the work reported in this paper.

Author Contributions

Matheus Alves Siqueira de Assunção: conceptualization; formal analysis; investigation; methodology; writing – original draft; writing – review & editing. Douglas Dourado: formal analysis; investigation; visualization; writing – review & editing. Daiane Rodrigues dos Santos: formal analysis; investigation; writing – original draft. Gabriel Bezerra Faierstein: visualization; writing – review & editing. Mara Elga Medeiros Braga: supervision; visualization; writing – review & editing. Severino Alves Junior: supervision; visualization; writing – review & editing. Rosângela Maria Rodrigues Barbosa: supervision; visualization; writing – review & editing. Herminio José Cipriano de Sousa: visualization; writing – review & editing. Fábio Rocha Formiga: conceptualization; formal analysis; funding acquisition; methodology; project administration; resources; supervision; writing – review & editing.

ORCID® iDs

Matheus Alves Siqueira de Assunção - https://orcid.org/0000-0002-6365-5464
Douglas Dourado - https://orcid.org/0000-0003-3445-5217
Daiane Rodrigues dos Santos - https://orcid.org/0000-0003-1767-9892
Mara Elga Medeiros Braga - https://orcid.org/0000-0003-4142-4021
Rosângela Maria Rodrigues Barbosa - https://orcid.org/0000-0002-1171-598X
Herminio José Cipriano de Sousa - https://orcid.org/0000-0002-2629-7805
Fábio Rocha Formiga - https://orcid.org/0000-0003-1553-0533

Data Availability Statement

Data sharing is not applicable as no new data was generated or analyzed in this study.

References

1. Conway, M. J.; Colpitts, T. M.; Fikrig, E. *Annu. Rev. Virol.* **2014,** *1,* 71–88. doi:10.1146/annurev-virology-031413-085513
2. Mansfield, K. L.; Jizhou, L.; Phipps, L. P.; Johnson, N. *Front. Cell. Infect. Microbiol.* **2017,** *7,* 298. doi:10.3389/fcimb.2017.00298
3. Alkan, C.; Bichaud, L.; de Lamballerie, X.; Alten, B.; Gould, E. A.; Charrel, R. N. *Antiviral Res.* **2013,** *100,* 54–74. doi:10.1016/j.antiviral.2013.07.005
4. Carpenter, S.; Groschup, M. H.; Garros, C.; Felippe-Bauer, M. L.; Purse, B. V. *Antiviral Res.* **2013,** *100,* 102–113. doi:10.1016/j.antiviral.2013.07.020
5. Gomes, H.; de Jesus, A. G.; Quaresma, J. A. S. *One Health* **2023,** *16,* 100499. doi:10.1016/j.onehlt.2023.100499
6. de Santana Silva, L. L.; Silva, S. C. C.; de Oliveira, A. P. S.; da Silva Nascimento, J.; de Oliveira Silva, E.; Coelho, L. C. B. B.; Neto, P. J. R.; do Amaral Ferraz Navarro, D. M.; Napoleão, T. H.; Paiva, P. M. G. *Acta Trop.* **2021,** *214,* 105789. doi:10.1016/j.actatropica.2020.105789
7. Roiz, D.; Wilson, A. L.; Scott, T. W.; Fonseca, D. M.; Jourdain, F.; Müller, P.; Velayudhan, R.; Corbel, V. *PLoS Negl. Trop. Dis.* **2018,** *12,* e0006845. doi:10.1371/journal.pntd.0006845
8. Oliveros-Díaz, A. F.; Pájaro-González, Y.; Cabrera-Barraza, J.; Hill, C.; Quiñones-Fletcher, W.; Olivero-Verbel, J.; Díaz Castillo, F. *Arabian J. Chem.* **2022,** *15,* 104365. doi:10.1016/j.arabjc.2022.104365
9. Deka, B.; Babu, A.; Baruah, C.; Barthakur, M. *Front. Nutr.* **2021,** *8,* 686131. doi:10.3389/fnut.2021.686131
10. Bosly, H. A. E.-K.; Salah, N.; Salama, S. A.; Pashameah, R. A.; Saeed, A. *Acta Trop.* **2023,** *237,* 106735. doi:10.1016/j.actatropica.2022.106735

11. Nasir, S.; Walters, K. F. A.; Pereira, R. M.; Waris, M.; Ali Chatha, A.; Hayat, M.; Batool, M. *J. Asia-Pac. Entomol.* **2022,** *25,* 101937. doi:10.1016/j.aspen.2022.101937

12. Porto, A. S.; de Almeida, I. V.; Vicentini, V. E. P. *Rev. Fitos* **2020,** *14,* 513–527. doi:10.32712/2446-4775.2020.1060

13. Vuitika, L.; Prates-Syed, W. A.; Silva, J. D. Q.; Crema, K. P.; Côrtes, N.; Lira, A.; Lima, J. B. M.; Camara, N. O. S.; Schimke, L. F.; Cabral-Marques, O.; Sadraeian, M.; Chaves, L. C. S.; Cabral-Miranda, G. *Vaccines (Basel, Switz.)* **2022,** *10,* 1385. doi:10.3390/vaccines10091385

14. Viana, V. C. R.; Machado, F. P.; Esteves, R.; Duarte, J. A. D.; Enríquez, J. J. S.; Campaz, M. L. M.; Oliveira, E. E.; Santos, M. G.; Ricci-Junior, E.; Ruppelt, B. M.; Rocha, L. *Sustainable Chem. Pharm.* **2023,** *32,* 100992. doi:10.1016/j.scp.2023.100992

15. Chithiga, A.; Manimegalai, K. *Exp. Parasitol.* **2023,** *249,* 108513. doi:10.1016/j.exppara.2023.108513

16. Athanassiou, C. G.; Kavallieratos, N. G.; Benelli, G.; Losic, D.; Usha Rani, P.; Desneux, N. *J. Pest Sci.* **2018,** *91,* 1–15. doi:10.1007/s10340-017-0898-0

17. Benelli, G.; Caselli, A.; Canale, A. *J. King Saud Univ., Sci.* **2017,** *29,* 424–435. doi:10.1016/j.jksus.2016.08.006

18. Mikaili, P.; Maadirad, S.; Moloudizargari, M.; Aghajanshakeri, S.; Sarahroodi, S. *Iran. J. Basic Med. Sci.* **2013,** *16,* 1031.

19. Shaalan, E. A.-S.; Canyon, D.; Younes, M. W. F.; Abdel-Wahab, H.; Mansour, A.-H. *Environ. Int.* **2005,** *31,* 1149–1166. doi:10.1016/j.envint.2005.03.003

20. Burin, G. R. M.; Formiga, F. R.; Pires, V. C.; Miranda, J. C.; Barral, A.; Cabral-Albuquerque, E. C. M.; Vieira de Melo, S. A. B.; Braga, M. E. M.; de Sousa, H. C. *J. Supercrit. Fluids* **2022,** *186,* 105607. doi:10.1016/j.supflu.2022.105607

21. Santhoshkumar, J.; Rajeshkumar, S.; Venkat Kumar, S. *Biochem. Biophys. Rep.* **2017,** *11,* 46–57. doi:10.1016/j.bbrep.2017.06.004

22. Klaus, T.; Joerger, R.; Olsson, E.; Granqvist, C.-G. *Proc. Natl. Acad. Sci. U. S. A.* **1999,** *96,* 13611–13614. doi:10.1073/pnas.96.24.13611

23. Galatage, S. T.; Hebalkar, A. S.; Dhobale, S. V.; Mali, O. R.; Kumbhar, P. S.; Nikade, S. V.; Killedar, S. G. Silver Nanoparticles: Properties, Synthesis, Characterization, Applications and Future Trends. In *Silver Micro-Nanoparticles - Properties, Synthesis, Characterization, and Applications;* Kumar, S., Ed.; IntechOpen: London, United Kingdom, 2021. doi:10.5772/intechopen.99173

24. Samuel, M. S.; Ravikumar, M.; John J., A.; Selvarajan, E.; Patel, H.; Chander, P. S.; Soundarya, J.; Vuppala, S.; Balaji, R.; Chandrasekar, N. *Catalysts* **2022,** *12,* 459. doi:10.3390/catal12050459

25. Ju-Nam, Y.; Lead, J. R. *Sci. Total Environ.* **2008,** *400,* 396–414. doi:10.1016/j.scitotenv.2008.06.042

26. Bapat, M. S.; Singh, H.; Shukla, S. K.; Singh, P. P.; Vo, D.-V. N.; Yadav, A.; Goyal, A.; Sharma, A.; Kumar, D. *Chemosphere* **2022,** *286,* 131761. doi:10.1016/j.chemosphere.2021.131761

27. Khan, M.; Khan, M. S. A.; Borah, K. K.; Goswami, Y.; Hakeem, K. R.; Chakrabartty, I. *Environ. Adv.* **2021,** *6,* 100128. doi:10.1016/j.envadv.2021.100128

28. Lazov, L.; Singh Ghalot, R.; Teirumnieks, E. Silver Nanoparticles - Preparation Methods and Anti-Bacterial/Viral Remedy Impacts against COVID 19. In *Silver Micro-Nanoparticles - Properties, Synthesis, Characterization, and Applications;* Samir, K.; Prabhat, K.; Chandra Shakher, P., Eds.; IntechOpen: London, United Kingdom, 2021. doi:10.5772/intechopen.99368

29. Leema, M.; Sreekumar, G.; Sivan, A.; Pillai, Z. S. *Mater. Today: Proc.* **2019,** *18,* 4724–4728. doi:10.1016/j.matpr.2019.07.459

30. Hassan, A. I.; Samir, A.; Youssef, H. F.; Mohamed, S. S.; Asker, M. S.; Mahmoud, M. G. *J. Pharm. Pharmacol. (Chichester, U. K.)* **2021,** *73,* 1503–1512. doi:10.1093/jpp/rgab037

31. Sri Ramkumar, S. R.; Sivakumar, N.; Selvakumar, G.; Selvankumar, T.; Sudhakar, C.; Ashokkumar, B.; Karthi, S. *RSC Adv.* **2017,** *7,* 34548–34555. doi:10.1039/c6ra28328d

32. Kalimuthu, K.; Panneerselvam, C.; Chou, C.; Lin, S.-M.; Tseng, L.-C.; Tsai, K.-H.; Murugan, K.; Hwang, J.-S. *Hydrobiologia* **2017,** *785,* 359–372. doi:10.1007/s10750-016-2943-z

33. Kalimuthu, K.; Cha, B. S.; Kim, S.; Park, K. S. *Microchem. J.* **2020,** *152,* 104296. doi:10.1016/j.microc.2019.104296

34. Asmathunisha, N.; Kathiresan, K. *Colloids Surf., B* **2013,** *103,* 283–287. doi:10.1016/j.colsurfb.2012.10.030

35. Moorthi, P. V.; Balasubramanian, C.; Mohan, S. *Appl. Biochem. Biotechnol.* **2015,** *175,* 135–140. doi:10.1007/s12010-014-1264-9

36. Tamuly, C.; Hazarika, M.; Borah, S. C.; Das, M. R.; Boruah, M. P. *Colloids Surf., B* **2013,** *102,* 627–634. doi:10.1016/j.colsurfb.2012.09.007

37. Hamedi, S.; Shojaosadati, S. A. *Polyhedron* **2019,** *171,* 172–180. doi:10.1016/j.poly.2019.07.010

38. Sajadi, S. M.; Nasrollahzadeh, M.; Maham, M. *J. Colloid Interface Sci.* **2016,** *469,* 93–98. doi:10.1016/j.jcis.2016.02.009

39. Devi, H. S.; Boda, M. A.; Shah, M. A.; Parveen, S.; Wani, A. H. *Green Process. Synth.* **2019,** *8,* 38–45. doi:10.1515/gps-2017-0145

40. Ponnuchamy, K.; Jacob, J. A. *Nanotechnol. Rev.* **2016,** *5,* 589–600. doi:10.1515/ntrev-2016-0010

41. Javan bakht Dalir, S.; Djahaniani, H.; Nabati, F.; Hekmati, M. *Heliyon* **2020,** *6,* e03624. doi:10.1016/j.heliyon.2020.e03624

42. Abdel-Raouf, N.; Al-Enazi, N. M.; Ibraheem, I. B. M. *Arabian J. Chem.* **2017,** *10,* S3029–S3039. doi:10.1016/j.arabjc.2013.11.044

43. Abdel-Raouf, N.; Al-Enazi, N. M.; Ibraheem, I. B. M.; Alharbi, R. M.; Alkhulaifi, M. M. *Saudi J. Biol. Sci.* **2019,** *26,* 1207–1215. doi:10.1016/j.sjbs.2018.01.007

44. Roseline, T. A.; Murugan, M.; Sudhakar, M. P.; Arunkumar, K. *Environ. Technol. Innovation* **2019,** *13,* 82–93. doi:10.1016/j.eti.2018.10.005

45. Gnanadesigan, M.; Anand, M.; Ravikumar, S.; Maruthupandy, M.; Syed Ali, M.; Vijayakumar, V.; Kumaraguru, A. K. *Appl. Nanosci.* **2012,** *2,* 143–147. doi:10.1007/s13204-011-0048-6

46. Davis, T. A.; Volesky, B.; Mucci, A. *Water Res.* **2003,** *37,* 4311–4330. doi:10.1016/s0043-1354(03)00293-8

47. Selvaraj, P.; Neethu, E.; Rathika, P.; Jayaseeli, J. P. R.; Jermy, B. R.; AbdulAzeez, S.; Borgio, J. F.; Dhas, T. S. *Biocatal. Agric. Biotechnol.* **2020,** *28,* 101719. doi:10.1016/j.bcab.2020.101719

48. Gurunathan, S.; Raman, J.; Abd Malek, S. N.; John, P. A.; Vikineswary, S. *Int. J. Nanomed.* **2013,** *8,* 4399–4413. doi:10.2147/ijn.s51881

49. Dadashpour, M.; Firouzi-Amandi, A.; Pourhassan-Moghaddam, M.; Maleki, M. J.; Soozangar, N.; Jeddi, F.; Nouri, M.; Zarghami, N.; Pilehvar-Soltanahmadi, Y. *Mater. Sci. Eng., C* **2018,** *92,* 902–912. doi:10.1016/j.msec.2018.07.053

50. Murugan, K.; Aruna, P.; Panneerselvam, C.; Madhiyazhagan, P.; Paulpandi, M.; Subramaniam, J.; Rajaganesh, R.; Wei, H.; Alsalhi, M. S.; Devanesan, S.; Nicoletti, M.; Syuhei, B.; Canale, A.; Benelli, G. *Parasitol. Res.* **2016,** *115,* 651–662. doi:10.1007/s00436-015-4783-6

51. Vinoth, S.; Shankar, S. G.; Gurusaravanan, P.; Janani, B.; Devi, J. K.
J. Cluster Sci. **2019**, *30,* 171–180. doi:10.1007/s10876-018-1473-4

52. Roni, M.; Murugan, K.; Panneerselvam, C.; Subramaniam, J.;
Nicoletti, M.; Madhiyazhagan, P.; Dinesh, D.; Suresh, U.; Khater, H. F.;
Wei, H.; Canale, A.; Alarfaj, A. A.; Munusamy, M. A.; Higuchi, A.;
Benelli, G. *Ecotoxicol. Environ. Saf.* **2015**, *121,* 31–38.
doi:10.1016/j.ecoenv.2015.07.005

53. Barnawi, A.; Tariq SAlghamdi, T.; Mahyoub, J.; Al-Ghamdi, K. J.
Entomol. Zool. Stud. **2019**, *7,* 333–337.

54. Gopu, M.; Kumar, P.; Selvankumar, T.; Senthilkumar, B.; Sudhakar, C.;
Govarthanan, M.; Selva Kumar, R.; Selvam, K.
Bioprocess Biosyst. Eng. **2021**, *44,* 217–223.
doi:10.1007/s00449-020-02426-1

55. Elumalai, D.; Hemavathi, M.; Rekha, G. S.; Pushpalatha, M.;
Leelavathy, R.; Vignesh, A.; Ashok, K.; Babu, M. *Sens. Bio-Sens. Res.*
2021, *34,* 100457. doi:10.1016/j.sbsr.2021.100457

56. Aziz, A. T. *IET Nanobiotechnol.* **2022**, *16,* 145–157.
doi:10.1049/nbt2.12082

57. Srikar, S. K.; Giri, D. D.; Pal, D. B.; Mishra, P. K.; Upadhyay, S. N.
Green Sustainable Chem. **2016**, *06,* 34–56.
doi:10.4236/gsc.2016.61004

58. Omidi, S.; Sedaghat, S.; Tahvildari, K.; Derakhshi, P.; Motiee, F.
Green Chem. Lett. Rev. **2018**, *11,* 544–551.
doi:10.1080/17518253.2018.1546410

59. Liu, Y.; Lillepold, K.; Semenza, J. C.; Tozan, Y.; Quam, M. B. M.;
Rocklöv, J. *Environ. Res.* **2020**, *182,* 109114.
doi:10.1016/j.envres.2020.109114

60. WHO World Health Organization. *Dengue And Severe Dengue*.
https://www.who.int/news-room/fact-sheets/detail/dengue-and-severe-d
engue.

61. Messina, J. P.; Brady, O. J.; Golding, N.; Kraemer, M. U. G.;
Wint, G. R. W.; Ray, S. E.; Pigott, D. M.; Shearer, F. M.; Johnson, K.;
Earl, L.; Marczak, L. B.; Shirude, S.; Davis Weaver, N.; Gilbert, M.;
Velayudhan, R.; Jones, P.; Jaenisch, T.; Scott, T. W.; Reiner, R. C., Jr.;
Hay, S. I. *Nat. Microbiol.* **2019**, *4,* 1508–1515.
doi:10.1038/s41564-019-0476-8

62. Gunathilaka, U. M. T. M.; de Silva, W. A. P. P.; Dunuweera, S. P.;
Rajapakse, R. M. G. *RSC Adv.* **2021**, *11,* 8857–8866.
doi:10.1039/d1ra00014d

63. Rodrigues dos Santos, D.; Lopes Chaves, L.; Couto Pires, V.;
Soares Rodrigues, J.; Alves Siqueira de Assunção, M.;
Bezerra Faierstein, G.; Gomes Barbosa Neto, A.;
de Souza Rebouças, J.;
Christine de Magalhães Cabral Albuquerque, E.;
Alexandre Beisl Vieira de Melo, S.; Costa Gaspar, M.;
Maria Rodrigues Barbosa, R.; Elga Medeiros Braga, M.;
Cipriano de Sousa, H.; Rocha Formiga, F. *Int. J. Pharm.* **2023**, *643,*
123221. doi:10.1016/j.ijpharm.2023.123221

64. Borase, H. P.; Patil, C. D.; Salunkhe, R. B.; Narkhede, C. P.;
Salunke, B. K.; Patil, S. V. *J. Nanomed. Biother. Discovery* **2013**, *3,*
111. doi:10.4172/2155-983x.1000111